

# INSTRUMENTATION IN SMALL LOW ENERGY MACHINES

U. Raich, AB Dep. CERN, Geneva, Switzerland

## Abstract

Low energy particle accelerators are used either as injectors for higher energy machines or as dedicated machines for special purposes. These may be industrial, medical or prototype machines for testing new accelerating schemes. Low energy beams open measurement possibilities not available at higher energies due to the low magnetic rigidity of the particles, due to their small penetration depth and due to rather big beam spot sizes. On the other hand these beams also represent special challenges due to their high energy deposition in matter, space charge problems etc. which are not seen at higher energies. Measurement principles typical for small accelerators will be presented and explained with the help of example implementations.

## INTRODUCTION: THE LHC

The Large Hadron Collider (LHC) is without any doubt CERN's biggest project and one of the most gigantic scientific endeavours ever undertaken in high energy physics. For this reason all eyes of the physics world are focused on it. But... what has the LHC to do with instrumentation in small and low energy machines? The quality factor for a collider is its luminosity  $L$ :

$$L \propto \frac{k_b N^2}{\epsilon_n}$$

where  $k_b$  is the number of bunches,  $N$  the number of particles per bunch and  $\epsilon_n$  the normalised emittance.

In electron-positron colliders like LEP the synchrotron radiation emitted by electrons at high energy inhibits the move to even higher energies but it is also responsible for Landau damping of the beam emittance. The beam quality is to a good fraction determined by the highest energy machine. In hadron machines however, due to the much higher mass of hadrons, synchrotron radiation is very much suppressed and the beam brightness is essentially determined in the injector chain.

This shows the importance of being capable to measure the beam characteristics in the low energy machines well enough.

Acceleration of ions, foreseen for LHC, poses additional constraints. At low energies ions are only partially ionised and they further ionise through stripping when interacting with an intercepting sensor. In addition energy deposition in matter is at a maximum.

Small machines are however not only used as injectors. There are many industrial applications (e.g. material tests) and medical applications (cancer therapy) which need accelerated particles of rather low energy.

## INTENSITY MEASUREMENTS AT LOW ENERGIES

### FARADAY CUPS

At energies of up to a few MeV and low intensities Faraday cups are used for intensity measurements. Figure 1 shows a very simple cup design [1]. The sensor itself (2) consists of a stainless steel cone which is connected to a vacuum feed-through. Another feed-through is used for the supply of a polarisation voltage to a cylindrical repeller electrode (1) pushing secondary electrons, created when the beam touches the sensor surface, back into the cup.

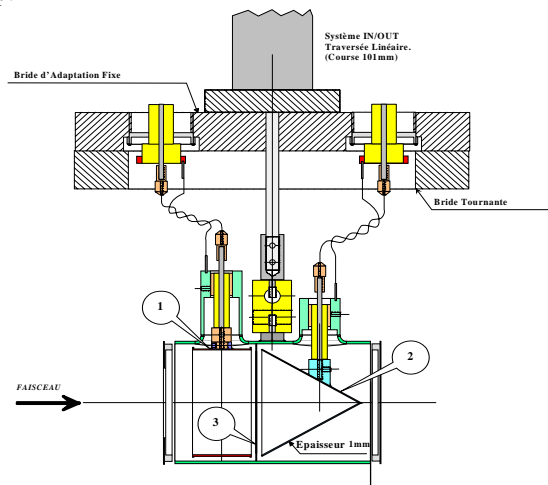


Figure 1: A simple Faraday Cup

Secondary electrons leaving the sensor would of course result in wrong intensity measurements. Since secondary electrons have very low energies of less than 20 eV a polarisation voltage of some 100V is sufficient. Figure 2 shows the current on the sensor with increasing polarisation voltage. At ~30V increasing the voltage further has no more effect on the measured current.

A typical application of Faraday Cups is the measurement of charge state distributions after the ion source. A whole range of different ion charge states is created of which only a single one can be accelerated through the following accelerator chain.

A spectrometer in conjunction with a slit is used to filter out this state. Before doing this however the full charge state spectrum is measured by ramping the spectrometer magnet and measuring the beam current passing through the slit into a Faraday Cup.

## COMMISSIONING OF SNS BEAM INSTRUMENTATION

T.J. Shea, ORNL, Oak Ridge, Tennessee

### *Abstract*

The Spallation Neutron Source (SNS) is an accelerator-based neutron facility under construction in Oak Ridge, Tennessee. The project is a collaboration of 6 partner laboratories: Lawrence Berkeley (LBNL), Los Alamos (LANL), Argonne (ANL), Brookhaven (BNL), Jefferson (Jlab), and Oak Ridge (ORNL). To achieve the performance goals, the SNS accelerator facility must deliver over one megawatt of beam power to a mercury target. This talk will describe the beam diagnostic instrumentation required to commission and operate such a facility at high beam power. Status of the SNS construction and recent beam commissioning results will also be presented.

**NO SUBMISSION RECEIVED**

# BEAM HALO OBSERVATION BY CORONAGRAPH

T. Mitsuhashi, KEK, TSUKUBA, Japan

## Abstract

We have developed a coronagraph for the observation of the beam halo surrounding a beam. An opaque disk is set in the beam image plane to block the glare of the beam image. We succeeded in obtaining a signal to background ratio of  $6 \times 10^{-7}$ . As a test, we tried to observe the beam halo at the Photon Factory storage ring. We succeeded in observing the tail of the beam, which has an intensity range of  $10^{-4}$  to  $10^{-6}$  of the peak intensity.

## INTRODUCTION

The beam tail or halo is one of the significant problems in proton machines and future Linac-based machines such as LC and ERL. To develop an apparatus to observe the beam tail or halo, we used the concept of the coronagraph. The coronagraph is a spatial telescope observing the sun-corona via artificial eclipse [1]. The concept of this apparatus is to create an artificial eclipse by blocking the glare of the sun's image and thereby observe the weak image of the sun's corona. We applied this concept to the observation of the halo surrounding a beam. In the coronagraph, the diffraction fringe surrounding the sun image is eliminated by a re-diffraction system with a mask (Lyot stop). Since the background mainly comes from scattered light from defects in the objective lens, such as scratches and digs on the surface, the key point to realize good performance of the coronagraph is to reduce scattering light from the objective lens. We used a very well-polished lens for the objective lens, and succeeded in obtaining a signal to background ratio of better than  $10^{-6}$ . We observed the beam halo by coronagraph at the Photon Factory storage ring. We succeeded in observing the halo of the beam which has an intensity range from  $1/10^4$  to  $1/10^6$  of the peak intensity. The use of the words beam halo or beam tail can introduce some confusion: I use the word "halo" to mean both beam halo and beam tail in this paper.

## BEAM HALO OBSERVATION WITH NORMAL TELESCOPE

Let us consider the observation of the sun's corona with a normal telescope. To create an artificial eclipse, we can set an opaque disk on the focal plane of the objective lens to block the glare of the sun image as shown in Fig. 1. In the normal telescope setup, the objective lens aperture makes a bright diffraction fringe surrounding from the sun image. The ratio of intensities between the diffraction fringes to the peak of the Airy disc is approximately  $10^{-2}$  at the first peak of the fringe. These intense diffraction fringes inhibit the observation of the weak image of the sun corona which has an intensity range of  $10^{-5}$ .

In the case of beam halo observation with typical beam profile monitor using the visible synchrotron radiation in the particle accelerator, we have the same difficulty as in the sun corona observation. Let us consider the observation of beam halo at the Photon Factory. As shown in Fig.2, the second diffraction fringe has the same intensity as the geometrical image of the beam. The beam halo near the third diffraction fringe has a weaker intensity than the diffraction fringe, and we cannot observe it by a normal imaging method as in the SR profile monitor.

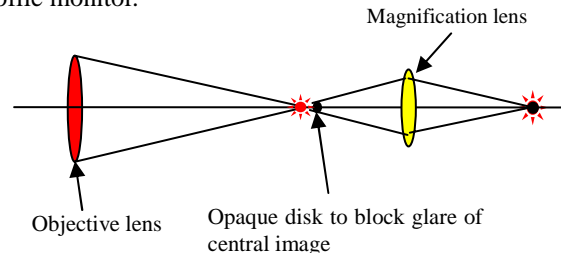


Figure 1: Set up of normal telescope with opaque disk.

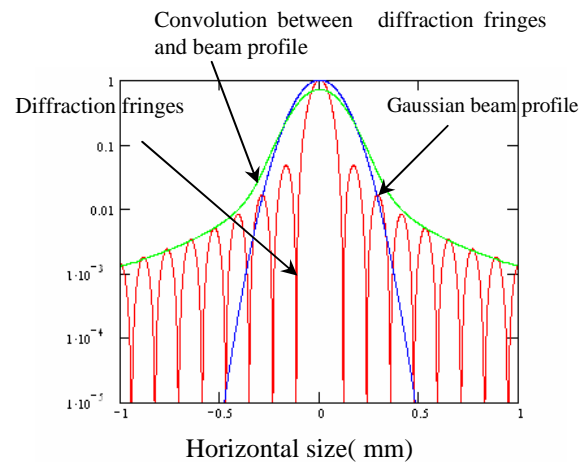


Figure 2: Comparison of the beam profile and point spread function (PSF). The solid red line denotes the PSF, and the blue line denotes the Gaussian horizontal beam profile at the Photon Factory.

## CONCEPT OF THE CORONAGRAPH

The optical layout of the coronagraph is illustrated in Fig.3. The first lens (objective lens) makes a real image of the object (beam image) on to a blocking opaque disk which creates an artificial eclipse. A second lens (field lens) is set just after the blocking disk. The focusing length of the field lens is chosen to make a real image of the objective lens aperture onto a mask (Lyot Stop). The diffraction fringe in the focal plane of the objective lens is not blocked by the opaque disk, and is re-diffracted by the field lens aperture. Then the re-diffracted light makes another diffraction fringe around the geometrical image of

# LARGE DYNAMIC RANGE BEAM PROFILE MEASUREMENTS \*

A. P. Freyberger,

Thomas Jefferson National Accelerator Facility, Newport News, VA 23606, USA

## Abstract

Large dynamic range ( $Peak/Noise > 10^5$ ) beam profile measurements are routinely performed in the Hall-B beamline at Jefferson Lab. These measurements are made with a 1 to 10nA electron beam current with energies between 1 to 6 GeV. The electron beam scatters off of a thin W or Fe wire and the scattered particle/shower is detected via scintillation or Cerenkov light several meters downstream of the wire. This report describes results on increasing the dynamic range by using multiple wires of varying diameters. Profile measurements with this large dynamic range are of use for accelerators with large amount of stored energy (e.g. energy recovering linacs [ERL]) where small beam loss represents a significant amount of beam power. Results on measuring the transverse profile with large dynamic range during the CEBAF energy recovery experiment is also presented.

## INTRODUCTION

Transverse beam profile measurements are typically performed to extract the transverse width of the beam. Such measurements place a modest demand on the signal to noise of the technique. Typically a signal to noise ratio of 100 is more than sufficient for such measurements. This paper describes the large (greater than  $10^5$ ) dynamic range beam profile technique used at JLAB. The technique has been used for two experiments, beam acceptance for the CLAS detector in end-station B and for measuring the width of the energy recovered beam during the JLAB energy recovery [ER] experiment. Transverse beam profiles with five to six orders of magnitude dynamic range represent a challenge for the diagnostics. The technique described in this paper is similar/identical to several other efforts summarized in the recent HALO2003 conference[1].

## CLAS Experiment

Experiments with the CLAS detector [2] in end-station B at Jefferson Lab (JLAB) place strict requirements on the beam halo due to the small diameter target window (2 to 4mm). The target frame represents a large amount of material when compared to that of the target. Beam particles outside of target window interacting in the target frame can result in an event rate comparable to that of interactions in the target proper. The transverse beam profile measured with sufficient dynamic range provides a mechanism for

determining the acceptability of the delivered beam and minimizing or eliminating completely the background from non-target interactions.

## Energy Recovery Experiment

Presently there is interest in constructing energy recovery linacs [3, 4] for different applications. A feature of ERLs is the amount of stored energy in the beam. Small loss of beam will result in energy deposition in the beam pipe and possible loss of vacuum. Continuous operation of an ERL requires that the beam loss from injection to energy recovered beam dump be typically less than 1ppm. The JLAB Energy Recovery [ER] experiment is a test of the energy recovery concept using a large number of RF cavities[5]. The electron beam is injected with 55MeV(20MeV) of energy, accelerated to 1GeV and the phase shifted  $180^\circ$  and energy recovered through the RF section back down to the injected energy. One of the issues of interest is the beam shape of the energy recovered beam. The dynamic range that the transverse beam profile after energy recovery retains a Gaussian shape provides information on how much of the beam is retained [ie not lost] in the Gaussian core.

## TRANSVERSE PROFILES FOR THE CLAS EXPERIMENT

The beam profile is measured by correlating a wire scanner position with count rates in photomultiplier tubes [PMT] located downstream of the wire scanner. The wire scanner assembly consists of a linear actuator which moves the horizontal and vertical wires through the beam. The actuator is driven by a stepper motor, which drives the wire support structure into the beam axis. The wire support is driven at a  $45^\circ$  with respect to the horizontal axis, which enables both the X and Y profiles to be measured with one axis of motion.

The PMTs [6] which detect the resulting scattered electron or shower are located downstream of the wire scanner. The distance between the wire scanner and PMTs is optimized for symmetric Møller scattering at beam energy of 5 GeV. Four 2" diameter PMTs are installed outside of a 3" diameter beam pipe, located in the following configuration: top, bottom, beam left, and beam right. The top-bottom PMT pair uses Cerenkov light in the quartz window to detect the scattered/showering particle(s). The left-bottom PMT pair has 0.5" scintillator in addition to the quartz window for detection of the scattered/showering particle(s). Due to the low operating beam current in Hall-B, typically 1 to 10nA, the PMTs can be operated in "count

\* This work is supported by the Southeastern Universities Research Association (SURA) which operates the Thomas Jefferson National Accelerator Facility (JLAB) for the United States Department of Energy under contract DE-AC05-84ER40150.

## DESIGN AND TESTING OF THE MIT-BATES STERN-GERLACH POLARIMETER CAVITY

P. Cameron, N. D'Imperio, A.U. Luccio, W.W. MacKay, BNL, Upton, Long Island, New York  
M. Conte, INFN Genova, Genova  
W.A. Franklin, E. Ihloff, T. Zwart, MIT, Middleton, Massachusetts  
D.A. Goldberg, LBNL, Berkeley, California

### *Abstract*

Historically, beam polarization measurement has been accomplished by scattering experiments, with the attendant complexity of target and detector installation and operation, and smallness and uncertainty of analyzing powers. The purpose of the present effort is to accomplish fast and accurate polarization measurement not as a scattering experiment, but rather as conventional beam instrumentation, with a resonant cavity pickup. This requires that the coupling of the beam magnetic moment to the pickup be enhanced to bring the signal above the noise floor, and that coupling of the beam charge to the pickup be diminished to reduce the dynamic range problem. We discuss details of cavity design that have been implemented to accomplish these ends. Presently, it is planned to install the cavity in the Bates Ring in early May of this year. Beyond polarimetry, successful polarization measurement will verify the underlying principles, and by pickup/kicker reciprocity will open the serious consideration of the possibility of polarizing the full-energy LHC proton beams in-situ.

**NO SUBMISSION RECEIVED**

## MICRO-STRIP METAL FOIL DETECTORS FOR THE BEAM PROFILE MONITORING.\*

V. Pugatch, V. Aushev, O. Fedorovitch, A. Mikhailenko,  
S. Prystupa, Yu. Pylypchenko, KINR, Kiev, Ukraine  
V. Karengin, V. Perevertailo, IMD, Kiev, Ukraine  
M. Braeuer, H. Franz, K. Wittenburg, DESY, Hamburg, Germany  
Ch. Bauer, M. Schmelling, MPIfK, Heidelberg, Germany

### Abstract

The Micro-strip Metal Foil Detectors (MMFD) designed and used for the Beam Profile Monitoring (BPM) are discussed. The results obtained for the MMFDs produced by different technologies are presented. The MMFD deposited onto the 20  $\mu\text{m}$  thick Si-wafer has been used for the BPM of the 32 MeV alpha-particle beam at the MPIfK (Heidelberg) Tandem generator. Another MMFD with totally removed Si-wafer at the working area has been applied for the on-line X-ray BPM at the HASYLAB (DESY).

### INTRODUCTION

Current developments in fundamental and applied research require non-destructive 'on-line' profile monitoring of micro-beams. For low intensity beams a proper approach could be realized by using silicon micro-strip detectors successfully progressing last two decades. Manufacturing technology allows for a position resolution at sub-micron level. Yet, radiation hardness aspect makes this approach rather limited. The experience was reported [1] for the high intensity micro-beam profiling by means of fine strips supported by thin membranes. In this paper we present the first results of the beam profiling by the MMFD manufactured by different lithography and etching technologies. The MMFD deposited onto the 20  $\mu\text{m}$  thick Si-wafer has been used for the BPM of the 32 MeV alpha-particle beam at the MPIfK (Heidelberg) Tandem generator. Another MMFD with totally removed Si-wafer at the working area of (8 x 10)  $\text{mm}^2$  has been applied for the on-line X-ray beam profile monitoring at the HASYLAB (DESY).

### MMFD PHYSICS AND TECHNICAL DETAILS

The general physics and registration principles of the Metal Foil Detector (MFD) are discussed in details somewhere [2]. Charged particles (or photons) hitting a metal sensor-foil initiate Secondary Electron Emission (SEE) at 10-50 nm surface layers, mainly [3, 4]. The electron yield is measured by a sensitive Charge Integrator connected to a sensor. To stabilize the electron yield two accelerating and two grounding foils are surrounding the sensor from both

sides, creating complete MFD setup as a 5-layer structure. The first SEE monitor has been built in 1955 [5] and in its later modifications a typical position resolution was in the range of a millimeter. We have applied the technology developed for the silicon micro-strip detector manufacturing to produce metal micro-strip detectors for the purposes of the precise beam profile monitoring. 16 or 32 narrow metal strips (10-50  $\mu\text{m}$  width, 20 - 100  $\mu\text{m}$  pitch) are individually connected through the UHV feedthroughs to Charge Integrators (ChI). ChI designed and built for that purpose by the joint effort of the KINR (Kiev) [6] and Max-Planck Institut für Kernphysik (Heidelberg) have reached a  $fA$  level of a sensitivity, also due to the direct conversion of the measured current into the output frequency. Some of the advantages of the Micro-strip MFD BPM are as follows:

- Extremely low mass of the detecting material.
- Simple structure (thin, up to few tens nano-meter, metal strips self-supported in the operating area at Si-wafer).
- Low operating voltage ( $\approx 20$  V), which provides nearly total charge collection.
- Simple read-out electronics (charge integrators and scalers).
- Very high radiation tolerance (at Gigrads level).
- Position resolution of 1  $\mu\text{m}$  is in the reach for the current manufacturing technology.
- Profile monitoring of a bunch train (below thermal electron emission threshold).
- Bunch by bunch profile monitoring possible.

The last two items are prospective for the MMFD connected to the readout microchip [7]. We have built and tested few prototypes of the Micro-strip MFD for the Beam Profile Monitoring (BPM).

### MMFD SETUP FOR THE MONITORING OF THE 32 MEV HE-3 BEAM.

The first MMFD monitor has been used for the on-line control, positioning and focusing charged particles beam (32 MeV alpha-particles at the MPIfK (Heidelberg) Tandem generator for SEU (Single Events Upset) studies of the BEETLE chip [7].

\* Work supported by the DESY Agreement/Contract

# DETAILED EXPERIENCE OF SYNCHROTRON LIGHT EXTRACTION SYSTEM WITH SLOTTED MIRROR AT THE ESRF

B.K. Scheidt, ESRF, Grenoble, France

## Abstract

A slotted, non-cooled, mirror was implemented for the extraction of synchrotron light to feed an Infra-Red spectrometer and microscope in a new laboratory. The slot lets the energetic part of the synchrotron light go through and is kept vertically centred on the heart of the X-ray beam in a slow feed-back loop. This paper reports the experience obtained on : 1) The quality and stability of an imaged light spot that demonstrates the entire system being free of wave-front distortion and vibrations. 2) Elastic deformation study on the Aluminium mirror. 3) Mapping of edge radiation, produced by the interference of light emitted by the edges of up- and down-stream dipoles. 4) UV induced mirror blackening with dependence on the choice of the mirror material.

of the mirror surface and inflicting permanent deformation. This is achieved by thermoprobes (each made up of 3 individual thermocouples) above and below the heart of the beam. At a 1.25mm distance from the beam (at 200mA ESRF current) each probe absorbs at total of ~0.8W which results in a steady-state temperature of 70C. A slight off-centre results in a differential temperature between the upper and lower side, which is then corrected for in a software control loop that keeps the 2 readings equal within a hysteresis value of a few degrees.

Although the control loop is slow it is to be noted that the ESRF electron beam is surveyed by 2 different types of vertical beam machine interlocks. In case of either a sudden large vertical step (>0.7mm), or a fast vertically oscillating beam (amplitude >0.4mm) around a normal average position, these interlocks would cut the stored beam quickly. Therefore the control loop for the mirror does not have to provide itself for a total protection against all sorts of abnormal electron beam behaviour. Nevertheless, for an ultimate protection, a hardwired interlock is triggered directly and independently by the device if any temperature reading exceeds 100C.

The mirror assembly is also equipped with a thermoprobe at the extreme lower end so that it can be operated in a so-called ‘half-mirror mode’. Furthermore the mirror can be also be totally extracted, or fully inserted so the deflect all the impinging dipole light (see fig.2). In the latter case, used only for specific studies reported here below, the thermal deformation is avoided by operation under low (<1mA) electron beam current.

## PRINCIPLE & OPERATION MODES

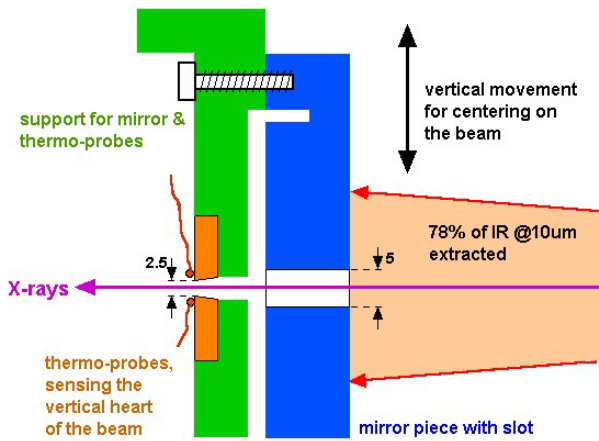


Figure 1: Slotted mirror vertically centred on photon-beam.

The concept of a slotted mirror was adopted for the extraction of InfraRed light from the cell-23 down-stream dipole for reasons of maximum flux extraction and minimum wavefront distortion to preserve the high brightness quality of the source. Although 22% of the lightflux ( $\lambda=10\mu\text{m}$ ) is lost through the 5mm high slot of the mirror, at 3.2m from dipole entrance, the extracted light is free of any distortion if the upper and lower parts of the mirror surface can be manufactured to good flatness (1 $\mu\text{m}$  peak-valley) upto a negligible distance (0.1mm) from the slot-edge. The diamond milling technique employed allowed meeting these requirements on the 10mm thick single block aluminium mirror [1].

The 2<sup>nd</sup> requirement is to keep this slot centred on the photon beam heart under all circumstances and in a highly reliable way so to avoid the occurrence of the high energetic (155W/mrad hor.) X-ray beam hitting any part

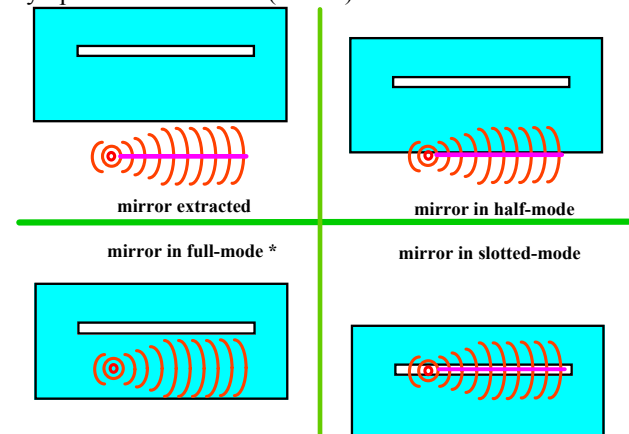


Figure 2: Mirror in 4 vertical positions & operation modes.

Note the absence of cooling to the mirror assembly so to avoid the introduction of any vibrations by a (water) cooling circuit, while allowing keeping the system light, compact and simple. The X-rays going through the slot are absorbed 2.5m downstream by a standard beamport

# DIPOLE LIGHT MONITOR SYSTEM FOR THE ESRF INJECTOR

B.K. Scheidt, ESRF, Grenoble, France

## Abstract

The visible part of the synchrotron radiation produced in a total of 9 dipoles of the ESRF injector is now extracted to obtain simultaneously images of the electron beam profile at these locations. This at each injection and in a non-destructive way to the electron beam. The first transferline (180MeV) contains three monitors on the 2 dipoles (0.38T) and the injection septum magnet. The Booster accelerator has one monitor that allows the profile measurement at any moment in its 50ms acceleration cycle by timing the internal camera shutter. In order to equip each of the 5 dipoles (0.9T) in the 2nd transferline (6GeV) with such a monitor, a compact and low-cost light extraction system was added at the end of the (non-modified) dipole vacuum chamber. All systems use low-cost commercial CCD cameras, sufficient light is produced at beam-currents a factor  $\sim 100$  below nominal values. The video images are displayed to the control room operator at each injection, giving a quick & complete view of injection conditions all along the injector path. This paper describes the mechanics and optics of light extraction and collection, and the results obtained since mid-2004.

## OVERVIEW AND TL-1 MONITORS

The position of the total of 9 Dipole light monitors in the injector complex (TL-1, SY, TL-2) is shown in fig.1.

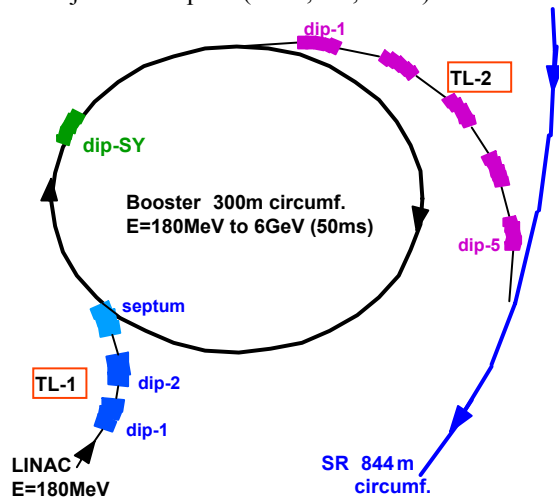


Figure 1: The location of the 9 dipole light monitors.

The 2 dipoles in the TL-1 transferline are of 40cm length with a deflection radius of 1.5m ( $E \sim 180\text{MeV}$ ,  $B=0.38\text{T}$ ). This relative short length and the strong deflection angle (15deg.) permits to equip the simple vacuum chamber with 2 separate vacuum flanges : one for the electron beam exit and another one for the extraction of synchrotron light. The latter, straight aligned on the dipole entrance, uses a sapphire UHV vacuum window (W) to let the visible light through. An aperture directly

after the window selects the light from a source point inside the nominal dipole field. A commercial achromat lens of 200mm focal length projects an image on the  $\frac{1}{2}$ " CCD with a de-magnification factor of 3.1 (fig.2 left).

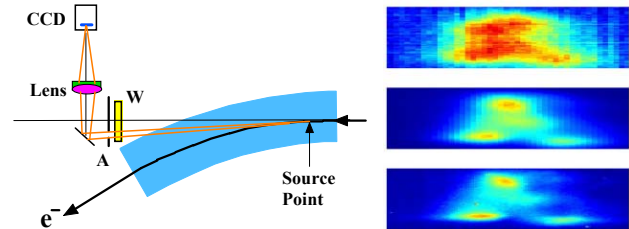


Figure 2: TL-1 dipole light extraction principle and results obtained with it, compared to that of screen monitors.

An existing screen monitor just in front of the 1st dipole allowed to compare the obtained images from three different devices (fig.2 right): a former screen monitor with an alumina (AF-995-R) screen in air (upper image), a new screen monitor in vacuum (middle), and the dipole light monitor (lower image). [1] The images show several spots that are caused by the emission characteristics of the Linac Gun. The spatial resolution of the dipole light monitor is of superior quality and estimated at  $< 100\mu\text{m}$ , mainly determined by diffraction for 500nm wavelength and 6mrad hor. aperture. The vertical emission angle is  $\sim 8\text{mrad}$ . The collected light flux is enough to attain sufficient image quality down to 0.1mA (compared to 5mA nominal TL-1 current).

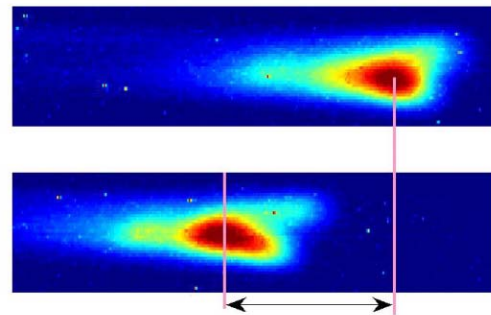


Figure 3: Results from 2<sup>nd</sup> Dipole Light Monitor in TL-1

The 2<sup>nd</sup> TL-1 dipole monitor is of similar design, with a 150mm lens offering a larger view area (24x18mm, HxV) so to cover the full excursion of the beamspot. Being at a location of high dispersion it serves the measurement of energy variation & fluctuations from the Linac as shown in the 2 (zoomed) images in fig.3 with a 4mm shift.

For the imaging of the injected beam inside the Septum magnet (injection TL-1 to SY), a 75cm long vacuum chamber had to be added directly after the Septum Tank with an in-vacuum aluminium mirror. Its edge is at 15mm horizontal distance to let the circulation SY beam unobstructed under all circumstances. The so extracted light

# ADVANCES TOWARDS THE MEASUREMENT AND CONTROL OF LHC TUNE AND CHROMATICITY\*

Peter Cameron, John Cupolo, Christopher Degen, Al Dellapenna, Lawrence T. Hoff, Joe Mead, Robert Sikora, BNL, Upton, NY 11973, USA

Marek Gasior, Rhodri Jones, Hermann Schmickler, CERN, Geneva, Switzerland  
 Cheng-Yang Tan, FNAL, Batavia, IL 60439, USA

## Abstract

Requirements for tune and chromaticity control in most superconducting hadron machines, and in particular the LHC, are stringent. In order to reach nominal operation, the LHC will almost certainly require feedback on both tune and chromaticity. Experience at RHIC has also shown that coupling control is crucial to successful tune feedback [1]. A prototype baseband phase-locked loop (PLL) tune measurement system has recently been brought into operation at RHIC as part of the US LHC Accelerator Research Program (LARP) [2]. We report on the performance of that system and compare it with the extensive accumulation of data from the RHIC 245MHz PLL [3].

## INTRODUCTION

Tune Feedback was formally accepted as a LARP task in 2003. For two years prior to that time there existed a bilateral collaboration between CERN and BNL for the purpose of research into the development and refinement of reliable tune feedback, as well as the associated development of means for improved control of chromaticity and coupling. Significant progress has been made as a result of these collaborative efforts.

The LHC Specifications for Tune, Chromaticity, and Coupling Measurement are clearly defined [4]. To meet these specifications requires improvement upon the performance of the present RHIC 245MHz PLL tune measurement system. Limitations of the present system arise from the dynamic range requirements imposed by transition crossing in RHIC, and from the effect of coupling on the tune feedback loop. Recent advances [1,5] are addressing these limitations, and prospects appear favourable for reliable operational tune feedback, both at RHIC and in the LHC.

## TUNE MEASUREMENT AND FEEDBACK

We present results from the present RHIC 245MHz PLL and a prototype baseband PLL, as well as plans for the proposed LHC baseband system.

### 245MHz PLL

The RHIC 245MHz PLL system is mature. It has proven useful for tune and chromaticity measurements, particularly during ramping, as well as for a variety of

accelerator physics experiments. Figure 1 shows typical tune data for a RHIC ramp during the 2004 Gold run.

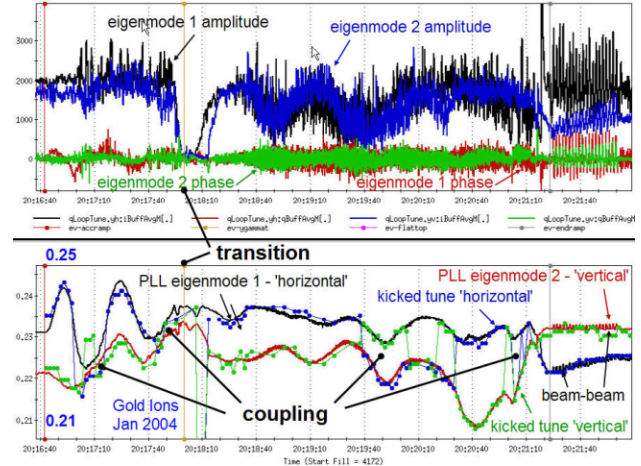


Figure 1: PLL tune tracking during a RHIC ramp.

The lower portion of the figure shows tunes as measured by both the PLL and the conventional kicked tune measurement system during the 5 minute ramp. It can be seen that, as a result of coupling, the kicked tune measurement hops back and forth between the eigenmodes tracked by the PLL. The upper portion of the figure shows the PLL amplitudes and phases. Despite feedback within the PLL on both kicker excitation and signal path gain, the amplitudes are driven to zero around transition. This results from bunch lengths becoming short near transition, which extends the coherent spectrum of the bunches in the 28MHz acceleration buckets up into the passband of the 245MHz resonant pickups. In addition, there are fast orbit changes around transition. These circumstances create a dynamic range problem that frequently results in the failure of PLL tune tracking. This problem is being addressed by the Direct Diode Detection analog front end [5].

Figure 2 shows data from a RHIC ramp with tune feedback on during the 2004 polarized proton run. This was the last of ~25 ramps that were attempted with tune feedback over the course of 3 years. The success rate for ramps with tune feedback was ~50%. Given the great potential benefit of reliable tune feedback during normal operations, this success rate was sufficient to justify continued attempts until the obstacles were fully understood. The first obstacle was the dynamic range problem at transition, as mentioned in the previous paragraph. This problem was understood early on for ion

\*Work supported by US LARP and US DOE

# A FIRST LOOK AT BEAM DIAGNOSTICS FOR THE RHIC ELECTRON COOLING PROJECT\*

Peter Cameron, Ilan Ben-Zvi, Jorg Kewisch, Vladimir N. Litvinenko

BNL, Upton, NY 11973, USA

## Abstract

High energy electron cooling [1] is essential to meet the luminosity specification for RHIC II [2]. In preparation for electron cooling, an Energy Recovery Linac (ERL) test facility [3] is under construction at BNL. A preliminary description of Diagnostics for the ERL was presented at an earlier workshop [4]. A significant portion of the eCooling Diagnostics will be a simple extension of those developed for the ERL test facility. In this paper we present a preliminary report on eCooling Diagnostics. We summarize the planned conventional Diagnostics, and follow with more detailed descriptions of Diagnostics specialized to the requirements of high-energy magnetized cooling.

## INTRODUCTION

The RHIC electron cooler is designed to cool 100GeV/nucleon ions using 54MeV electrons. The electron source will be a superconducting RF photocathode gun. The accelerator will be a superconducting energy recovery linac. The frequency of the accelerator is set at 703.75MHz. The maximum electron bunch frequency is 9.38MHz, with bunch charge of 20nC.

Electron cooling at high energy imposes a variety of unique requirements. Of these many requirements, we mention here those that are relevant to the diagnostics discussed in this paper.

While other coolers use DC electron beams, the only way to make a high quality 54MeV beam is with a super-conducting Energy Recovery Linac. High resolution differential current measurement is needed to monitor the efficiency of current recovery.

In typical ERL applications, considerable effort is devoted to generating the shortest possible bunches. In the present application, the need is to match the electron bunch length to that of the ions, as well as to lower the bunch density to insure that Debye shielding doesn't degrade the cooling efficiency. This requires a bunch stretcher, and diagnostics to confirm that the contribution of longitudinal space charge to transverse emittance during bunch stretching is minimized.

Suppression of the transverse temperature of the electron beam in the cooling region requires the generation and transport of magnetized beams, as well as solenoids in the cooling region. Diagnostics are required to measure the *non-magnetized* transverse emittance of the electron beam at the end of the linac matching section, as well as within the solenoid.

Field errors in the cooling solenoids contribute to the transverse temperature of the electron beam [5]. For efficient cooling, local field errors must be at the level of  $10^{-5}$  or less. This requirement is beyond construction tolerances, and will require beam-based diagnostics to permit local correction of field errors.

A layout of the cooler is shown in Figure 1. The magnetized electron beam from the source is accelerated to 54MeV through four superconducting RF cavities, then passes through the stretcher and a bunch rotation cavity (not shown). A dipole in the bend after the cavity has the option to be operated at high field, functioning as a spectrometer to permit energy spread measurement for cavity phasing. The electron and ion beams enter the solenoid from the right. After the solenoids the electron beam enters a second bunch rotation cavity (again not shown). Between the cavity and the compressor there is the option to divert the electron beam to a diagnostic line, where a matching section similar to that at the end of the linac permits measurement of the unmagnetized emittance. A streak camera situated after the compressor permits measurements before the beam re-enters the linac for energy recovery.

## CONVENTIONAL DIAGNOSTICS

Preliminary estimates of types and quantities of conventional diagnostics are shown in Table 1.

Table 1: Conventional Diagnostics

Device	Qty	Comments
<b>Position/Phase</b>		
BPM (button)	~70	Dual plane
BBU/Energy Feedback	1	Sample scope
Beam Transfer Function	1	Include BTF kicker
Energy Spread	~8	Dispersive BPMs
Phase	~16	BPMs w/ I/Q
<b>Loss</b>		
BLM (PMT/ photodiodes)	~40	20μsec and 1sec
BLM (cable ion chamber)	~10	20μsec and 1sec
<b>Current</b>		
Current	1	DCCT
Differential	1	DCCTs w/ null
<b>Profile</b>		
Flags	4?	Phosphor
Wire Scanner - profile	3?	SEM mode
Wire Scanner - halo	3?	BLM mode
Scraper	2?	SEM + BLM
Synch Light	3?	
Streak Camera	1?	Dual sweep

# THE EFFECTS AND POSSIBLE ORIGINS OF MAINS RIPPLE IN THE VICINITY OF THE BETATRON SPECTRUM \*

Peter Cameron, BNL, Upton, NY 11973, USA  
 Marek Gasior, Rhodri Jones, CERN, Geneva, Switzerland  
 Cheng-Yang Tan, FNAL, Batavia, IL 60439, USA

## Abstract

With the advent of significant improvement in the sensitivity of observation of the betatron spectrum[1], the appearance of spectral lines at harmonics of the mains power frequency has been observed in the PS and SPS at CERN, the Tevatron at FNAL, and RHIC at BNL. **These lines are potentially problematic for accurate tune tracking and the implementation of tune feedback.** We discuss the possible origins of these lines, and present data to support our discussion.

## INTRODUCTION

Identification of the source of mains ripple in beam spectra is often problematic. The difficulty is to clearly demonstrate that the observed ripple originates in the beam, rather than entering the signal path spuriously. Recent data collected at the CERN PS and SPS, the Tevatron at FNAL and RHIC at BNL using a newly developed, highly sensitive, baseband tune (BBQ) measurement system [1] suggests that the beam is being excited at the betatron resonance by high harmonics ( $h > 100$ ) of the mains frequency.

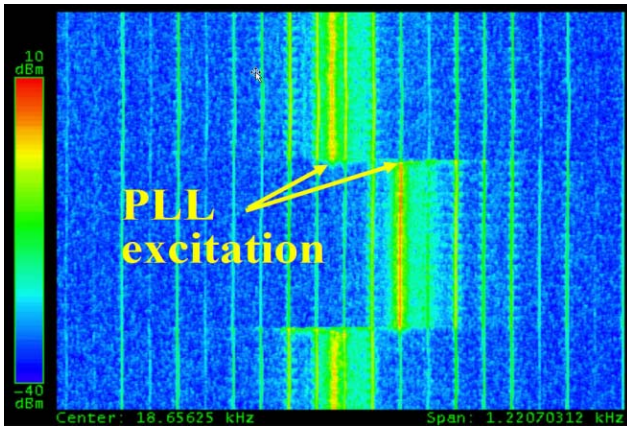


Figure 1: Spectrum with PLL excitation and 60Hz lines

Figure 1 shows the spectrum obtained from a 1m stripline pick-up looking at Copper ions in RHIC, using the Direct Diode Detection (3D) analog front end (AFE) of the BBQ system. The horizontal axis spans  $\sim 1.2$  KHz, centered on the betatron resonance at  $\sim 18.65$  KHz. The vertical axis spans  $\sim 30$ s, with the most recent time at the bottom. The baseband PLL tune tracker [2] is locked on the betatron resonance, which can be seen to shift by  $\sim .002$  when the quadrupole currents are changed and then returned to their original values. The 60Hz lines don't move. This illustrates the conundrum - what mechanism

might cause high harmonics of the mains frequency to appear in the vicinity of the betatron resonance, yet not be sidebands of the betatron line? The obvious conclusion is that the beam is being directly excited at these frequencies. This interpretation was met with considerable scepticism from accelerator physicists and power supply specialists, the question being what mechanism might generate field ripple at such relatively high frequencies. Some of the means employed to rule out spurious sources included:

- Batteries - AFE electronics were powered from batteries, with no change in the observed spectrum.
- Electronics location - AFE was situated immediately adjacent to the pickup in the tunnel, and then  $\sim 70$ m away in the instrumentation room, with no change in the observed spectrum.
- Isolation transformers - AFE was operated with and without isolation transformers in the signal path, with no change in the observed spectrum.
- High pass filtering - 70MHz high pass filtering was inserted between pickup and AFE, with no change in the observed spectrum.
- Pickup movement - no spectral variation was seen with large ( $\sim 1$ cm) changes in the position of a moveable pickup.
- Intensity variation - no spectral variation was seen with large changes in bunch charge.
- Different pickups - mains harmonics were observed from a homodyne detection AFE, a 245MHz resonant pickup, and a million-turn BPM.

All testing indicated that the apparent mains excitation was not spurious and that the beam was truly being excited at the betatron frequency by high harmonics of the mains frequency. The clue leading to the final crucial observation came from the Tevatron, where a change in the relative amplitudes of the observed mains harmonics in the horizontal and vertical planes was seen when the beam separation helix was turned on. The helix is known to introduce coupling. This prompted a brief experiment at RHIC, in which the relative amplitudes of the mains harmonics in the two planes were monitored while coupling was varied. The spectral power of the mains harmonics in the vertical plane was seen to be a linear function of the coupling strength, and was almost entirely absent when the machine was well decoupled. There was no dependence on coupling in the horizontal. From this it was definitively concluded that the observed mains harmonics are indeed on the beam, and that the excitation, at RHIC at least, is in the horizontal plane.

\*Work supported by US LHC Accelerator Research Program

# ABSOLUTE CURRENT CALIBRATION OF 1 $\mu$ A CW ELECTRON BEAM \*

M. Bevins, A. Day, P. Degtiarenko, A.P. Freyberger, A. Saha, S. Slachtouski  
 Jefferson Lab, Newport News, Virginia  
 Ronald Gilman  
 Rutgers University, Piscataway, New Jersey

## Abstract

The future experimental program at Jefferson Lab requires an absolute current calibration of a 1  $\mu$ A CW electron beam to better than 1% accuracy. This paper presents the mechanical and electrical design of a Tungsten calorimeter that is being constructed to provide an accurate measurement of the deposited energy. The energy is determined by measuring the change in temperature after beam exposure. Knowledge of the beam energy then yields number of electrons stopped by the calorimeter during the exposure. Simulations show that the energy lost due to electromagnetic and hadronic particle losses are the dominant uncertainty. Details of the precision thermometry and calibration, mechanical design, thermal simulations and simulations will be presented.

## INTRODUCTION

An experiment scheduled for the Hall A end station of the Thomas Jefferson National Accelerator Facility (JLab) CEBAF accelerator requires absolute beam current measurements with 0.5% to 1.0% accuracy for beam currents around 1 $\mu$ A [1]. The beam current monitor is based on a pair of resonant RF cavities which need to be cross calibrated against an absolute current reference. The present absolute current calibration system is designed for currents greater than 50 $\mu$ A and extrapolation is required for lower beam currents [2]. In order to perform a cross calibration of the cavity response at 1 $\mu$ A of beam current, a new calibration device based on calorimetry is being fabricated.

The calorimeter is a slug of material that is inserted on the beam axis for a well defined period of time. The energy deposited in the calorimeter is:  $E_{cal}(Joules) = E_{beam}(MeV)I_{beam}(\mu A)\Delta t(sec) - E_{loss}$  where  $E_{cal}$  is the energy absorbed by the calorimeter,  $E_{beam}$  is the energy of the beam,  $I_{beam}$  is the average beam current,  $\Delta t$  is the duration of the exposure and  $E_{loss}$  is the energy that escapes the slug via particle loss or thermal loss [radiation and conduction]. It is important that  $E_{loss}$  be small so that the average beam current can be extracted without additional uncertainties. The calorimeter is designed to operate with  $0.8GeV < E_{beam} < 11GeV$  and  $0.1\mu A < I_{beam} < 5\mu A$ .

The change in temperature of the calorimeter after a

beam exposure is proportional to the energy deposited,  $\Delta T = E_{cal}/C_m$  where  $C_m$  is the specific heat of the slug. Typically heat capacities of materials are not known with the precision required for this application so  $C_m$  must be measured. A resistive heater inserted in the calorimeter, will be used to determine a precise value for  $C_m$ . With nominal values of  $C_m$  and a 48sec exposure to a 5kW beam, the expected temperature rise is 30K.

Large copper and silver calorimeters built in the late 1960's achieved precisions of about 1% [3] and influenced the design of this calorimeter. The following sections describe the design of the calorimeter and estimates of  $E_{loss}$  and the instrumental error budget.

## PARTICLE CONTAINMENT

The incident electron beam interaction in the calorimeter will result in the creation of secondary electromagnetic and hadronic particles. Electromagnetic particle/shower formation and energy leakage was studied using GEANT and EGS4 simulations. Hadronic particle formation and leakage was studied using GEANT/DINREG [5]. The optimal size, shape and material of the calorimeter from these studies is a Tungsten cylinder 16cm in diameter and 16cm long. Most of the losses are backscattered particles, and to minimize these losses the beam strikes the calorimeter within 1cm diameter by 2.5cm deep cylindrical bore. The electromagnetic loss estimate from the simulations is  $0.1 \pm 0.1\%$  and the hadronic loss estimate from the simulation is  $0.3 \pm 0.2\%$ .

## MECHANICAL DESIGN AND THERMAL CONTAINMENT

Pure tungsten shapes are typically produced by pressing and sintering tungsten powder followed by an extrusion or swaging operation to reduce porosity. Subsequent operations to reduce porosity are not practical for a part this large. An extensive search for a high thermal conductivity, high density, tungsten composite material identified a tungsten-copper (95:5) produced by OSRAM/Sylvania. This material is produced using a unique process that does not require an infiltration of copper into a sintered tungsten framework. The blended tungsten and copper powders are pressed then sintered producing a very dense (99%), homogeneous, machinable part. Copper infiltration would not be an option for a part this large.

Since the calorimeter must be installed upstream of the

\* This work is supported by the Southeastern Universities Research Association (SURA) which operates the Thomas Jefferson National Accelerator Facility (JLAB) for the United States Department of Energy under contract DE-AC05-84ER40150.

# PRELIMINARY TESTS OF A NEW KIND OF BPM SYSTEM FOR SOLEIL

J-C. Denard, L. Cassinari, F. Dohou, N. Hubert, N. Leclercq, D. Pedeau;  
 Synchrotron SOLEIL; FRANCE

## Abstract

SOLEIL is a third generation light source in construction near Paris. Its small emittance requires improving the resolution of existing BPM systems to submicron level up to 100 Hz and stability to the micron level. The same BPM system has also to perform turn-by-turn acquisitions at high rate (846 kHz) with a resolution of a few microns for machine physics studies. SOLEIL entrusted the design of a new digital BPM system to a young Slovenian company, Instrumentation Technologies. SOLEIL defined technical specifications that seemed attainable and proposed a way of improving beam position measurement stability when the current or the bunch pattern of the beam changes. This paper presents the preliminary tests performed in the laboratory with signal generators simulating the electron beam as well as those done with real beam at ESRF in order to evaluate the SOLEIL BPM Electronics.

## INTRODUCTION

SOLEIL, a third generation light source being built near Paris (France), will provide users with 24 beam lines [1]. Its small emittance leads to small beam sizes, especially in the vertical direction with 8  $\mu\text{m}$  (at 1% coupling) at the insertion device source points.

The Beam Position Monitor (BPM) system comprises 120 monitors located around the storage ring next to quadrupoles. The system fulfils several important tasks:

- Slow acquisition: the closed orbit is measured at about 10 Hz acquisition rate for stabilizing it with a slow global orbit feedback via the control system and the dipole corrector coils located in the sextupole magnets. The important performances are current and bunch pattern dependences in order to always deliver photon beams at the same spot to the users for all beam currents and bunch patterns they work with.
- Fast acquisition: the closed orbit is measured at a high acquisition rate ( $> 4$  kHz). In addition to the performances previously mentioned a good resolution (rms position fluctuation) is necessary. This mode is used for the fast orbit feedback [3].
- Turn-by-turn: for machine physics applications (machine model, non linear beam dynamic studies) and for tune measurements. High resolution ( $\leq 3$   $\mu\text{m}$ ) beam positions are measured at the revolution frequency (846 KHz).
- First turns: this is mainly for the commissioning. The system must accommodate low currents on a single beam passage.

- Interlock: when the beam goes outside a predefined position range at any selected BPM, the BPM electronics gives an interlock signal which is used to prevent possible damage to the machine.
- Post mortem: records the last few thousand turns of beam position data in case of a sudden beam loss.

## BPM ELECTRONICS

Each BPM has four button electrodes delivering narrow pulses to an electronic processing unit located outside the machine tunnel, via four coaxial cables. The spectrum line at the RF frequency (352 MHz) is the useful part of the signal processed by the electronics. The BPM electronics requirements for the Storage Ring are shown in table 1.

Table 1: Storage Ring BPM electronics requirements

	Slow acquisit.	Fast acquisit.	First turns	Turn-by- turn
Absolute accuracy	$\leq 20$ $\mu\text{m}$	$\leq 20$ $\mu\text{m}$	$\leq 500$ $\mu\text{m}$	$\leq 200$ $\mu\text{m}$
Resolution rms	$\leq 0.2$ $\mu\text{m}$	$\leq 0.2$ $\mu\text{m}$	$\leq 500$ $\mu\text{m}$	$\leq 3$ $\mu\text{m}$
Measurement rate	10 Hz	$\geq 4000$ Hz	847 kHz	847 kHz
Dynamic range	20 – 600 mA	20 – 600 mA	0.4 – 4 mA	4 – 600 mA
Current dependence	$\leq 1$ $\mu\text{m}$	$\leq 1$ $\mu\text{m}$	$\leq 500$ $\mu\text{m}$	×
Bunch pattern depend.	$\leq 1$ $\mu\text{m}$	$\leq 1$ $\mu\text{m}$	$\leq 500$ $\mu\text{m}$	$\leq 500$ $\mu\text{m}$
8-h drift	$\leq 1$ $\mu\text{m}$	$\leq 1$ $\mu\text{m}$	$\leq 500$ $\mu\text{m}$	×
1-month drift	$\leq 3$ $\mu\text{m}$	$\leq 3$ $\mu\text{m}$	$\leq 500$ $\mu\text{m}$	×

The same electronics equips the Booster and the measurement rate reaches 1.9 MHz. Booster resolution and stability requirements are relaxed. A Booster specific mode provides beam positions over the acceleration cycle with a choice of data averaging; it is called Booster Normal mode.

Instrumentation Technologies, a Slovenian company, has been chosen to design and build the electronics. There is one 1U-19" chassis (figure 1) per monitor. It takes its power from the 220 V 50 Hz mains and provides the X and Z positions directly to the control system via an Ethernet port. It also provides the four electrode signals, their sum, and a signal for checking the BPM.

## APPLICATION OF THE BEAM PROFILE MONITOR FOR VEPP-4M TUNING

#O. I. Meshkov, A. V. Bogomyagkov, F. Gurko, A. N. Zhuravlev, P. V. Zubarev, V. A. Kiselev, N. Yu. Muchnoi, A. N. Selivanov, A. D. Khilchenko.

### Abstract

A transverse beam profile monitor based on the Hamamatsu multi-anode photomultiplier with 16 anode strips is used at VEPP-4M collider. The monitor is used to study turn-to-turn dynamics of the transverse beam profile during  $2^{17}$  turns. In addition, it provides a permanent measurement of synchrotron and betatron frequencies. The operation of the device for tuning the collider and studying of collective effects is described.

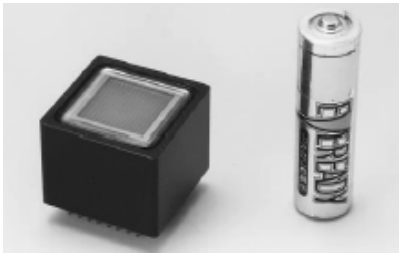


Figure 1. MAPMT R5900U-00-L16 HAMAMATSU

### INTRODUCTION

The interest in the study of beam distribution within fast instabilities like beam-beam effects has always existed in accelerator physics. The corresponding diagnostics should provide a one-turn distribution for a few ten thousand turns of the beam. For this purpose we have designed a device based on the Multi-Anode Photomultiplier Tube (MAPMT, Fig. 1). The Fast Profile Meter (FPM) is a part of the VEPP-4M optical diagnostic system [1,2]. It is applied also for determination of synchro-betatron resonances, phase oscillation monitoring and studying of collective effects.

### DESIGN OF THE FPM.

The device includes a MAPMT, a 12-byte ADC, a controller module, an internal memory of 4Mb and 100 Mb ethernet interface. It can record  $2^{17}$  profiles of a beam at 16 points. Discontinuity of the records can vary within  $1 \div 2^8$  turns of a beam. Revolution time of a beam in the VEPP-4M collider is 1220 ns and the recording time can last between 0.16 s to 20 s. As a result, the device can analyze the frequency oscillation of a beam in

#O.I.Meshkov@inp.nsk.su

range of 10 Hz — 1MHz. The main parameters of the device are listed in Tab. 1

Table 1. The technical data of the Fast Profile Meter.

Size	250 x 100 x 100 mm
Interface	100Mb ethernet
Internal memory	~4 M ( $2^{17}$ beam profile at 16 points)
Discontinuity of record	1 to $2^8$ turns
Analyzable frequency range	10 Hz to 1 MHz
Single anode size	$0.8 \times 16$ mm

The optical arrangement (Fig. 2) allows to change the beam image magnification on the cathode of MAPMT from  $6\times$  to  $20\times$ , which is determined by the experimental demands.

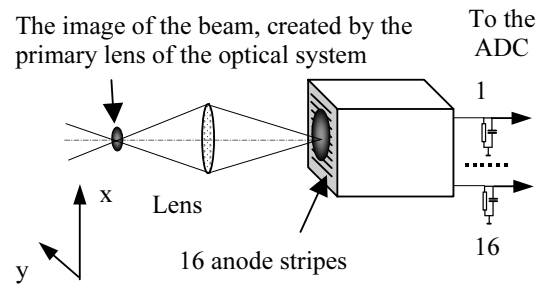


Figure 2. Optical layout of the diagnostics. The lens sets up a beam image on the photocathode of the MAPMT. The radial profile measurement is shown.

The operating cycle of the device is as follows. MAPMT signals are recorded to the ADC after start pulse. The starting moment is either chosen by user or coincides with the beams convergence in the interaction point, “kick”, beam pass by, etc. The ADC triggering is synchronized with the beam revolution frequency. The recorded signals are stored in the internal memory and read out to the PC.

# ROSALI: AN APPLICATION ALLOWING ONLINE/OFFLINE ALGORITHM IMPLEMENTATION TO ASSESS BEAM INSTRUMENTATION PERFORMANCE

M. Moles  
CERN, Geneva, Switzerland

## Abstract

A software tool called “Rapid Online Software ALgorithm Implementation (ROSALI)” has been developed at CERN. This application is intended to provide instrumentation experts and accelerator physicists with a tool, which allows monitoring and storage of beam measurements and rapid algorithm implementation via specialized actions on the embedded Mathematica kernel. The users are able to build or modify online a sequence of actions implementing their algorithms. Those sequences can subscribe to ongoing measurements from several beam instruments or retrieve data from previous recordings, merge these measurements to obtain correlation diagrams or perform dedicated calculations. This document presents the current state and the foreseen extensions of this application. The application has been tested last year on the SPS and it will be used this year on the new LEIR machine at CERN.

## INTRODUCTION

The AB/BDI software section at CERN is responsible for providing all the software necessary to develop, test, diagnose and maintain the different instruments produced by the group. This control software for front-end computers is implemented using the FESA framework [1].

The *Rapid Online Software ALgorithm Implementation* application; known as ROSALI [2] is an application for the instrumentation experts and accelerator physicists to monitor, store and analyse the beam measurements made by our instruments. As Figure 1 shows, ROSALI can retrieve these measurements directly from the acquisition front-ends or from previously stored data files. The storage of these measurements can be made through a C library following the ROSALI file format (explained later on) directly in the front end software or using the ROSALI application itself. This file format ensures that all data saved from the front-ends or ROSALI will be consistent and readable from the ROSALI application.

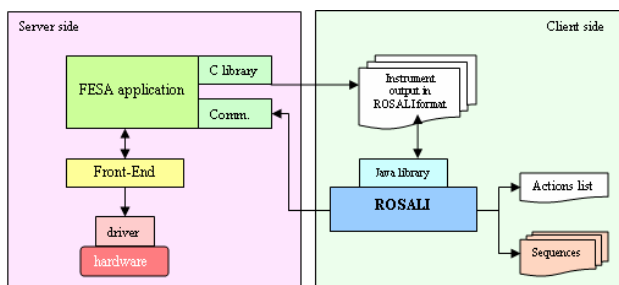


Figure 1: System architecture

ROSALI also provides a rapid and easy way to build and play sequences of actions for testing and assessing the instruments. These actions can subscribe to, store or display ongoing measurements from several beam instruments, retrieve offline data and perform dedicated calculations in the Mathematica kernel [3]...

Another characteristic of ROSALI is to provide harmless access to the instruments. This is achieved by giving full access to the acquisitions and status but restricting the access to the settings to authorized users.

## ROSALI FILE FORMAT

To store and share between actions all data coming from the instruments a new file format has been designed based on the following requirements:

- The data files should be human readable.
- This format should be able to handle the main types of data coming from beam instrumentation, i.e lines, XY scatters and surfaces.
- This format should allow the storage in a single file of heterogeneous types of data related to the same acquisition such as 2 profiles, 1 image and the corresponding setting's values.
- This format should be easy to handle in Excel, Mathematica and in-house C/C++/Java programs.

It is composed of tab-separated variables implemented in an XML light format allowing direct use in Excel. Dedicated Mathematica, C and Java libraries [2] have been provided to cover other usages.

## ROSALI APPLICATION

As shown in Figure 2, the graphical interface of the application is divided into three main areas together with the toolbar.

- The *Sequence* area contains the list of actions to execute.
- The *Parameters* area contains the parameters of the selected action. These parameters can be used as input (equipment name, target storage directory...) and/or output (result file name, ) by the action. The value of an input parameter can also be set as a reference to the value of an output parameter of another action.
- The *Viewer* area shows the result after the execution of the selected action. Each action can have its own viewer (simple table, standard data viewer or custom panel dedicated to beam profile measurements for instance)

# MEASUREMENTS WITH A NOVEL NON-INTERCEPTING BUNCH SHAPE MONITOR AT THE HIGH CURRENT GSI-LINAC\*

P. Forck, C. Dorn, Ges. für Schwerionenforschung GSI, Darmstadt, Germany, p.forck@gsi.de

## Abstract

For bunch length determination in the range of 0.3 to 5 ns at the GSI heavy ion LINAC a novel, non-intercepting device has been realized. It uses the time spectrum of secondary electrons created by atomic collisions between beam ions and residual gas molecules. These electrons are accelerated by an electric field of 420 V/mm toward an electro-static energy analyzer, which is used to restrict the effective source region. Then the electrons are deflected by an rf-resonator running in phase with the acceleration frequency (36 or 108 MHz) to transform the time spectrum into spatial separation. The detection is done with a  $\varnothing$  70 mm multi-channel plate. The achieved time resolution is about 50 ps, corresponding to 2 degree of 108 MHz phase.

## MONITOR OVERVIEW

The determination of the longitudinal density distribution of a bunched beam is an important issue because it is required for an optimal matching between different LINAC-modules as well as for the comparison with numerical calculations. At proton and ion LINACs the bunch structure cannot be determined by capacitive pick-ups due to the non-relativistic beam velocities ( $\beta < 20\%$  at the GSI-LINAC) causing a faster propagation of the electric field of the bunches. At most LINACs the bunch structure is determined by secondary electrons emitted from a wire crossing the beam [1, 2]. The wire is biased with about  $-10$  kV to pull the secondary electrons toward a slit outside the beam path. An rf-deflector follows, where the electrons are modulated in transverse direction by an electric rf-field. The deflection angle depends on their relative phases, i.e. the device transforms the time information into a spatial distribution.

For the high current beam operation at GSI with heavy ions and currents up to 20 mA [3], the beam power is sufficient to melt intersecting materials. The described principle is adapted to a non-intersecting device by performing the time spectroscopy of secondary electrons created by atomic collisions between beam ions and residual gas molecules. The electrons are accelerated by a homogeneous electrical field formed by electrodes outside of the beam pass, as usually used for Ionization Profile Monitors. To restrict the source region for the secondary electrons, an aperture system and an electro-static energy analyzer is used. The time-to-spatial transformation is performed with an rf-deflector developed at INR (Moscow) [2].

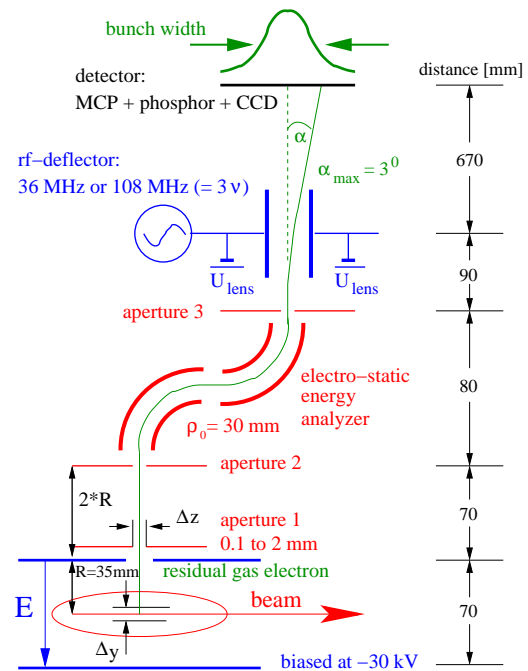


Figure 1: Schematic sketch of the bunch shape monitor.

## MONITOR HARDWARE

The schematic layout of the monitor is displayed in Fig. 1: At the detector location, the beam passes a static electric field region generated by a  $160 \times 60 \text{ mm}^2$  electrode biased up to  $-30$  kV. With the help of field forming strips, a homogeneous field of 420 V/mm perpendicular to the beam direction guides the secondary electrons toward a grounded plate with a horizontal slit of 1.5 mm in beam direction, see Fig. 2. To shorten the source length  $\Delta z$  in beam direction and the corresponding divergence of the secondary electron beam, two apertures with a distance of 70 mm are used. Their opening can be varied remotely between 0.1 and 2 mm by dc-motors. The second aperture serves as entrance slit of a  $90^\circ$  cylindrical electro-static energy analyzer with a bending radius of  $\rho_0 = 30$  mm. The nominal voltages are  $\pm 5.5$  kV for the opposite cylinder segments. Two similar devices are installed to place the electron detector perpendicular to the beam pipe. A third aperture is located 10 mm downstream from the second cylinder edge to enable a point-to-point focusing from the entrance- to the exit-slit [5]. Using  $\pm 0.25$  mm opening for aperture 1 and 2 as well as  $\pm 0.5$  mm for aperture 3, the vertical source prolongation is restricted to about  $\Delta y = \pm 0.2$  mm [4], which is comparable to the wire thickness in the standard method [1].

After a drift of 90 mm the time information is transferred into spatial distribution by the rf-deflector synchronized

\*Partly funded by EU-FP6-CARE-HIPPI

# DESIGN OF THE FARADAY CUPS IN DIAMOND.

A.F.D. Morgan, Diamond Light Source, UK

## Abstract

This paper details the work done on the design of the faraday cups for the DIAMOND light source. Diamond has faraday cups in positions covering the complete energy range of the machine from the 90keV gun to the 3GeV storage ring.

The Linac cups were modified from an existing design, while the higher energy designs were done using Monte Carlo code. The Monte carlo led designs achieved an electron capture rate of around 99%, allowing them to be used with reasonable certainty as calibration references.

Due to the modest 5Hz repetition rate of the electron gun, power loading of the structures is minimal and active cooling is not required for any of the cups.

Ablation is also not thought to be a significant problem for these designs.

## OVERVIEW

Diamond light source is a 3GeV 3<sup>rd</sup> generation synchrotron. The electrons are initially ejected from a 90keV gun. A linear accelerator increases the energy of the electrons to 100MeV. A booster ring further increases the energy to 3GeV. Finally the beam is injected into the storage ring to generate the synchrotron radiation [1].

Faraday cups are a basic charge capture device which can be used as reference points for current measurement calibration. Diamond has faraday cups after the 90keV gun and the 4MeV bunching section, in the linac to booster transfer line at 100MeV and at 3GeV in the booster to storage ring transfer line.

An initial design decision was made to make the designs passive to increase reliability and reduce complexity.

Due to the modest 5Hz repetition rate of the electron gun, power loading of the structures is minimal and active cooling is not required for any of the cups.

The 90keV and 4MeV cups were modified from an existing design using analytical formulæ and MathCAD. Monte carlo modeling was used to confirm the new design. The high energy 100MeV and 3GeV designs were done using the EGSnrc Monte Carlo code<sup>1</sup> from the national research council Canada, with MatLAB being used for interfaces and post analysis.

This paper will cover the basic methodologies used to obtain each design as well as the final design details and expected performance.

<sup>1</sup><http://www.irs.inms.nrc.ca/inms/irs/EGSnrc/EGSnrc.html>

## THE LINAC FARADAY CUPS

The 90keV/4MeV cup is an in vacuum design, based on the SLS 90keV design [2]. The design maintains the coaxial structure as much as possible in order to obtain a high bandwidth (figure 1).



Figure 1: The linac faraday cup assembly

The design changes were calculated using analytical formulæ taking into account collisional losses, radiative losses due to bremsstrahlung, the photoelectric effect, compton scattering and pair production. The final design was verified using the EGSnrc code (figure 2).

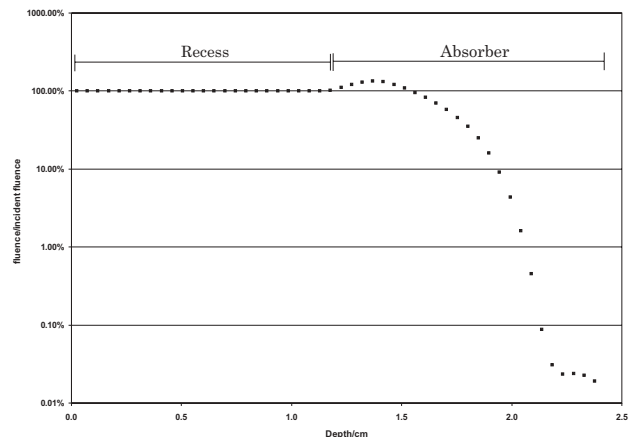


Figure 2: Data from the EGSnrc code

The cup is mounted on an actuator to enable it to be inserted into the beam path of the linac. The main absorber is made from a 24mm aluminium block with a 12mm deep recess cut into it. This enables the design to work at both 90keV and 4MeV.

At this energy the backscatter from the absorber block is the dominant effect. The recess diameter was chosen to be 13mm to accommodate some beam movement while still keeping backscatter low. A carbon cup with 1mm wall thickness was inserted into the recess to act as a soft stop to reduce the backscatter from 12% to 3.5% in the 90keV

# DESIGN ALTERNATIVES FOR BEAM HALO MONITORS IN HIGH INTENSITY ACCELERATORS

C.P. Welsch<sup>1</sup>, H. Braun, E. Bravin, R. Corsini, T. Lefèvre, D. Schulte, F. Tecker  
CERN, Geneva, Switzerland

## Abstract

In future high intensity, high energy accelerators it must be ensured that particle losses are minimized as activation of the vacuum chambers or other components makes maintenance and upgrade work time consuming and costly. It is imperative to have a clear understanding of the mechanisms that can lead to halo formation and to have the possibility to test available theoretical models with an adequate experimental setup.

Optical transition radiation (OTR) provides an interesting opportunity for linear real-time measurements of the transverse beam profile with a resolution which has been so far at best in the some  $\mu\text{m}$  range. However, the dynamic range of standard OTR systems is typically limited and needs to be improved for its application for halo measurements.

In this contribution, the existing OTR system as it is installed in the CLIC test facility (CTF3) is analyzed and the contribution of each component to the final image quality discussed. Finally, possible halo measurement techniques based on OTR are presented. Later beam tests are foreseen to be carried out in CTF3.

## INTRODUCTION

Optical transition radiation is produced when charged particles pass through media with different dielectric constants. It took about 10 years from the first demonstration of its practical application for measuring a wide range of important beam parameters [1] until it was used in a number of accelerators as one of the main diagnostic tools [see for example 2, 3].

Since then, OTR has proven to be a flexible and effective diagnostic method for measuring a wide range of beam parameters like the beam profile, its divergence and the beam emittance. Its fast time response in combination with e.g. a streak camera makes it the ideal tool even for the analysis of the longitudinal beam shape in single shot measurements.

In order to be applicable for investigations of the beam halo, i.e. measurements with large differences in intensity between the beam core and the tail region, a highly optimized diagnostic system is needed, where the influence of all components on the final data is known in detail.

In CTF3, different constraints have to be respected, which directly influence possible measurement techniques: The high radiation level in the machine

requires special shielding of the CCD cameras used and the power deposited in the screen limits the type of material of the screens. Either Aluminum or carbon screens are used depending on whether the focus lies on high reflectivity or good thermal resistance.

To get a better understanding of the characteristics and present limitations of the optical systems used in CTF3 at the moment and to find possible improvements systematic measurements and associated simulations were started.

## ANALYSIS OF THE LENS SYSTEM

If a charge  $q$  hits a boundary surface with an oblique incidence, the emitted electric field has two components: One in the plane of observation and the other one perpendicular to it. The total emitted intensity  $W$  of a beam with a given relativistic  $\gamma$  therefore has to be calculated as the sum of these two components [1]

$$\begin{aligned} \frac{d^2W}{d\Omega d\omega} &= \frac{d^2W_{\parallel}}{d\Omega d\omega} + \frac{d^2W_{\perp}}{d\Omega d\omega} \\ &\approx \frac{q^2}{\pi^2 c} \frac{\theta^2}{(\gamma^{-2} + \theta^2)^2} \end{aligned} \quad (1)$$

By direct differentiation of equation (1), the maxima of the resulting intensity distribution can be found at angles  $\theta_{max}=1/\gamma$ . In calculations with the ZEMAX code [4], this opening angle was used as one initial parameter to qualify the lens systems installed at CTF at different energies.

A typical installation consists of a set of achromats as shown in the following Fig. 1.

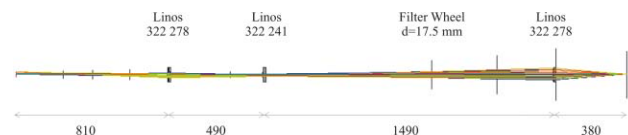


Figure 1: Overview of an optical line as it is presently used in CTF3

With ZEMAX, a detailed analysis of the present installation was performed to find out the main limiting factors.

It was found that, in contrast to the existing systems, the two first lenses should be installed in a so-called confocal arrangement, i.e. where the lens spacing equals

<sup>1</sup>Carsten.Welsch@cern.ch

# SCINTILLATING SCREENS STUDY FOR LEIR/LHC HEAVY ION BEAMS

C. Bal, E. Bravin, T. Lefèvre\*, R. Scrivens and M. Taborelli, CERN, Geneva, Switzerland

## Abstract

It has been observed on different machines that scintillating ceramic screens (like chromium doped alumina) are quickly damaged by low energy ion beams. These particles are completely stopped on the surface of the screens, inducing both a high local temperature increase and the electrical charging of the material. A study has been initiated to understand the limiting factors and the damage mechanisms. Several materials,  $ZrO_2$ , BN and  $Al_2O_3$ , have been tested at CERN on LINAC3 with 4.2MeV/u lead ions. Alumina ( $Al_2O_3$ ) is used as the reference material as it is extensively used in beam imaging systems. Boron nitride (BN) has better thermal properties than Alumina and Zirconium oxide ( $ZrO_2$ ). BN has in fact the advantage of increasing its electrical conductivity when heated. This contribution presents the results of the beam tests, including the post-mortem analysis of the screens and the outlook for further measurements. The strategy for the choice of the screens for the Low Energy Ion Ring (LEIR), currently under construction at CERN, is also explained.

## INTRODUCTION

Luminescent screens, ceramics or crystals, have been used widely for the past 25 years for beam observation [1]. Radiation hardness was a major concern and experimental studies led to the development of special  $Al_2O_3$  with  $Cr_2O_3$  as a doping material, known as Chromox 6 [2]. Thermal quenching of fluorescence and the dependence of lifetime on temperature have been studied using a 30keV electron beams [3]. These effects are due to competing radiative and non-radiative decay processes, the latter increasing in probability with temperature. At CERN screens have withstood integrated proton fluxes of up to  $10^{20}$  p/cm<sup>2</sup> at flux levels up to  $7 \cdot 10^{14}$  p/cm<sup>2</sup>/pulse (~500ns). In the SLC linac [4], a phosphorescent deposition ( $Gd_2O_2S:Tb$  known as P43) on a thin aluminium foil was used as a screen without any sign of damage after bombardment with  $4 \cdot 10^{18}$  e/cm<sup>2</sup>. Chromium doped alumina has been also successfully used on 10 and 100GeV/u low intensity oxygen ion beams in injection and extraction lines of the SPS machine at CERN [5]. Some investigations were done in the following years in order to find a luminescent material with a better sensitivity [6]. Thallium doped caesium iodide was found to have a 30 times better sensitivity than chromium doped alumina. In low energy ions accelerator, profile monitoring is most of the time done using SEM grids or wire scanners. Some tests were done on low energy lead ions using Chromox [6] screens but their performances were very poor with a strong reduction of the light intensity limiting the life time of the screen to very short time periods [7]. The range of low energy ions

in matter is very small, (few tens of  $\mu m$ ), so that the ions are stopped in the screen inducing a local charging of the material and the high thermal load.

The Low Energy Ion Ring (LEIR) [8] will start operation at CERN by the end of 2005. Its main task is to prepare the ion beams to reach the required brilliance for LHC. In LEIR 4.2MeV/u ions from the LINAC3 [9] are accumulated, cooled and pre-accelerated up to 72MeV/u. They are then injected into the consecutives accelerator rings PS, SPS and finally LHC.

In 2004 a new study has been initiated with the aim of understanding the degradation mechanism of the screen and finding an alternative for the imaging system needed for the LEIR instrumentation. In this paper we present the test of different luminescent materials irradiated by 4.2MeV/u lead ions.

## SETUP AT LINAC3

A sketch of the experimental set-up in LINAC3 at CERN is given in Figure 1.

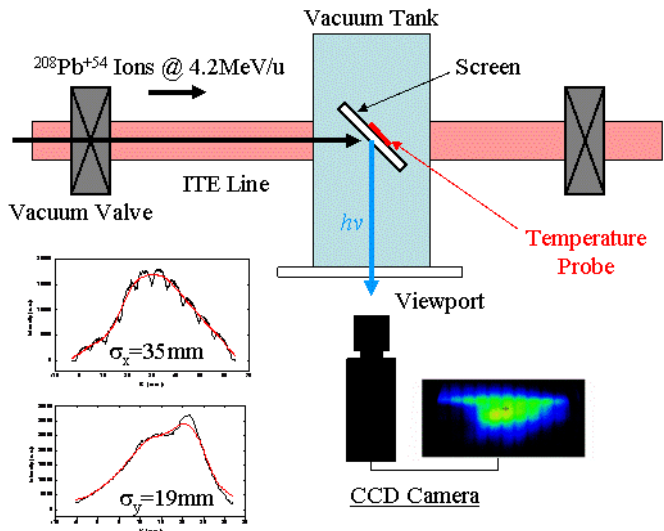


Figure 1: Set-up for the screen test in the LINAC3

The irradiation tests have been carried out in the ITE bypass line with a  $100\mu A$ ,  $600\mu s$  lead ions beam every 1.2s. This line, normally used for emittance measurements is already equipped with a TV observation tank. The system was slightly modified in order to install 1mm thick and 50mm diameter screens. Mounted on an aluminium support the screen was tilted by 45 degrees with respect to the beam trajectory. The screen was then imaged onto a normal CCD camera using a 50mm focal length camera lens. A temperature probe was installed on the back of the screen through a hole in the support in order to monitor the temperature variations due to the beam impact.



# SINGLE PHOTON DETECTOR TESTS FOR THE LHC SYNCHROTRON LIGHT DIAGNOSTICS

S. Hutchins, CERN, Geneva, Switzerland

S. Cova, I. Rech, I. Labanca, M. Ghioni, Politecnico di Milano, IT

G. Buller, S. Pellegrini, K.J. Gordon, Herriot Watt Univ. Edinburgh, UK

## *Abstract*

A synchrotron light detector using a Single-Photon Avalanche Detector (SPAD) is planned for the LHC longitudinal diagnostics monitor, an application which requires high count rate, low noise and good time resolution. SPAD detectors have been developed at Milan Polytechnic with active quenching circuits. Initial tests of these detectors and currently available commercial time-to-digital data acquisition equipment were made at the ESRF. We present the results of those tests, an estimation of the performance that can be expected for the LHC case and an analysis of the difficulties, constraints and potential of this type of detector.

## THE SPAD MODULE

The advantages of using SPADs[1,2] as opposed to other detectors such as photomultiplier tubes, is that they exhibit high count rates, low timing jitter <50ps, and low dark noise <100 counts per second[3,4].

A thorough experimental characterisation of SPAD devices with active area diameters of 8, 20 and 50  $\mu\text{m}$  was carried out, in order to carefully ascertain the performance of the detectors. All the main parameters, i.e. photon detection efficiency (PDE), dark counting rate (DCR) and timing resolution were measured as a function of excess bias voltage and operating temperature.

The best compromise between PDE and DCR was found by operating the SPAD at an excess bias voltage of 5 V. At room temperature, devices with 8 and 20  $\mu\text{m}$  diameter size met the specifications, while devices with 50  $\mu\text{m}$  size showed too high a DCR (about 2 kc/s for the best devices). On the other hand, a larger active area is a definite advantage in the foreseen experiments, since it makes it possible to relax the optical alignment requirements without sacrificing the photon collection efficiency. Furthermore, fibre pigtailing may be routinely made on these devices. We therefore decided to exploit a 50  $\mu\text{m}$  SPAD device, even though moderate cooling is required to meet specifications. When operated at 5V excess bias voltage the selected device shows: peak detection efficiency 48% at a wavelength of 530 nm (> 30% all over the visible range); 44 ps FWHM time resolution; dark counting rate of 80 c/s with device cooled at  $-15^\circ\text{C}$ .

## *Integrated Active Quenching and Reset Circuit (i-AQC)*

The SPTM employs a fully integrated active quenching and active reset circuit (i-AQC), which is the first monolithic circuit of this kind [5]. This circuit had been

previously developed at Politecnico di Milano and is covered by US and European patents[6]. After the detection of a photon, the dead time is given by the sum of the quenching delay plus an adjustable hold-off time plus the reset time. The dead time was set to 125ns, corresponding to a saturated photon counting rate of 8 Mc/s. The i-AQC power dissipation is quite low (30 mW at 2Mc/s, 170 mW at 8 Mc/s).

In order to achieve the required time resolution, a patented timing board including a linear network that feeds a fast comparator must be connected to the high voltage terminal of the SPAD [7,8,9]. The purpose of the timing board is to extract the avalanche current pulse at a very low threshold level, corresponding to an avalanche current of a few hundreds  $\mu\text{A}$ . The time resolution improves by reducing the threshold voltage of the comparator. By lowering the threshold to 10 mV, the SPTM can achieve a time resolution of about 40 ps FWHM. The TCSPC card used in these measurements was a Becker and Hickl SPC600 photon counting card [10].

In various applications, it is necessary or at least advantageous to operate the SPAD under the control of a gate command [1]. In this case, the SPAD is turned on only in a time window centred on the optical pulses of interest. A standard TTL gate signal can be provided to the SPTM. The minimum duration of the gate-on TTL signal is 20 ns, corresponding to an effective minimum gate-on duration of 10 ns.

## *Performance evaluation*

Preliminary tests of the performance of the SPTM with the selected SPAD sample were carried out on the bench at Politecnico di Milano. The operating temperature of the SPAD was set at  $-15^\circ\text{C}$  and the dark counting rate was checked to be 80 c/s at +5V excess bias voltage.

Photon detection efficiency (PDE) of the SPTM has a peak of 48% around 530 nm and it stays well above 30% in all the visible range.

Time resolution measurements were performed in a conventional time-correlated single photon counting (TCSPC) setup by using an ultra fast laser diode (Antel MPL-820 laser module) emitting 10 ps FWHM optical pulses at 820 nm wavelength. The unit has a prompt peak with a full-width at half maximum of 44 ps and a clean exponential diffusion tail with 300 ps lifetime. The overall duration of the diffusion tail is less than 2.5 ns. A signal-to-background ratio (SBR) higher than  $10^4$  is clearly demonstrated.

# MEASUREMENT OF THE LONGITUDINAL PHASE SPACE AT THE PHOTO INJECTOR TEST FACILITY AT DESY IN ZEUTHEN (PITZ)\*

J. Rönsch<sup>†</sup>, Hamburg University, 22761 Hamburg, Germany

K. Abrahamyan, G. Asova, J. Bähr, G. Dimitrov, H.-J. Grabosch, J.H. Han,  
S. Khodyachykh, M. Krasilnikov, S. Liu, H. Lüdecke, V. Miltchev, A. Oppelt,  
B. Petrosyan, S. Riemann, L. Staykov, F. Stephan, DESY, 15738 Zeuthen, Germany  
M.v. Hartrott, D. Lipka, D. Richter, BESSY, 12489 Berlin, Germany

## Abstract

PITZ generates electrons with an energy of about 5 MeV. To optimize the RF-gun parameters and to fulfill the requirements of the bunch compressor the longitudinal phase space behind the gun has to be studied. A measurement of the longitudinal phase space comprises a correlated measurement of momentum and temporal distribution. The momentum distribution is measured by deflecting the electron bunch using a spectrometer magnet. A subsequent Cherenkov radiator transforms the electron bunch into a light pulse with equal temporal and spatial distribution, which is imaged onto a streak camera by an optical transmission line to measure the longitudinal distribution. The longitudinal phase space was measured for different temporal photo cathode laser distributions, bunch charges and phases between RF field and laser. Physical effects in the dipole magnet, optical transmission line and streak camera, which influence the longitudinal phase space measurements, are taken into account. The measurement results were compared with simulations and with directly measured momenta and temporal distributions.

## INTRODUCTION

The main goal of PITZ is the test and optimization of photo injectors for Free-Electron Lasers (FELs). The demands on such a photo injector are a small emittance, short bunches and a charge of about 1 nC. The linac of a FEL incorporates a RF gun, capable of producing a high bunch charge, followed by an acceleration section and a magnetic bunch compressor. For an effective bunch compression detailed studies of the longitudinal phase space have to be performed. Besides the projections of the longitudinal phase space, i.e. temporal and momentum distribution of the electron bunch, the correlation between the positions of the particles in the bunch and their longitudinal momenta has to be understood. The non-linearities of the longitudinal phase space have to be analysed. Typical high energy diagnostics for longitudinal phase space tomography can not be used, therefore a special apparatus for an energy around 5 MeV was developed.

\*This work has partly been supported by the European Community, contract numbers RII3-CT-2004-506008 and 011935, and by the 'Impuls- und Vernetzungsfonds' of the Helmholtz Association, contract number VH-FZ-005.

<sup>†</sup>jroensch@ifh.de

## SETUP

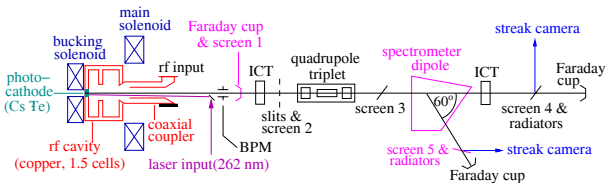


Figure 1: Schematic of PITZ1 setup.

Fig. 1 shows a schematic of the PITZ1 setup. To measure the longitudinal distribution of the electron bunch a Cherenkov radiator (silica aerogel) [1] is used to transform the bunch into a light distribution at screen station 4 in the straight section (SS). This light distribution is imaged by an optical transmission line onto the entrance slit of a streak camera. The momentum distribution is measured with a YAG-screen at screen station 5 in the dispersive arm (DA). To measure the longitudinal phase space both methods are combined. The YAG-screen in the DA can be replaced by silica aerogel using a movable actuator. The light pulse which presents the longitudinal phase space is transported to the streak camera. The momentum axis of the longitudinal phase space measured by the streak camera is scaled using the momentum distribution directly measured at the YAG-screen.

Several physical effects of the main components of the apparatus (as dipole magnet, streak camera and optical transmission line) impact the results of the measurements of the longitudinal phase space. These effects will be described in the following subsections. They have to be corrected successively, but reversely, i.e. starting from the streak camera.

### Spectrometer Dipole

The dipole magnet at PITZ1 deflects the electron bunches by  $60^\circ$  in vertical direction to transform the momentum distribution into a spatial one. The vertical position  $y$  of an electron behind a hard edge sector dipole is given by the first order transport matrix of a dipole [2]:

$$y = \cos \alpha \cdot y_0 + \rho_{\text{eff}} \cdot \sin \alpha \cdot y'_0 + \rho_{\text{eff}} \cdot (1 - \cos \alpha) \cdot \frac{\delta p_0}{\langle p_0 \rangle}, \quad (1)$$

# REAL-TIME, SINGLE-SHOT TEMPORAL MEASUREMENTS OF SHORT ELECTRON BUNCHES, TERAHERTZ CSR AND FEL RADIATION

G. Berden\*, B. Redlich, A.F.G. van der Meer,  
FOM Institute Rijnhuizen / FELIX, Nieuwegein, The Netherlands

S.P. Jamison†, A.M. MacLeod,  
School of Computing and Creative Technologies, University of Abertay Dundee, Dundee, UK

W.A. Gillespie,  
Division of Electronic Engineering and Physics, University of Dundee, Dundee, UK

## Abstract

Electro-optic detection of the Coulomb field of electron bunches is a promising technique for single-shot measurements of the bunch length and shape in the sub-picosecond time domain. This technique has been applied to the measurement of 50 MeV electron bunches in the FELIX free electron laser, showing the longitudinal profile of single bunches of around 650 fs FWHM [1]. The method is non-destructive and real-time, and therefore ideal for on-line monitoring of the longitudinal shape of single electron bunches. At FELIX we have used it for real-time optimization of sub-picosecond electron bunches. Electro-optic detection has also been used to measure the electric field profiles of far-infrared (or terahertz) radiation generated by the relativistic electrons. We have characterized the far-infrared output of the free electron laser, and more recently, we have measured the temporal profile of terahertz coherent synchrotron radiation (CSR) generated at one of the bending magnets.

## ELECTRON BUNCH MEASUREMENTS

At the Free Electron Laser for Infrared eXperiments (FELIX) the longitudinal shape of an electron bunch has been measured via electro-optic (EO) detection of its radial electric field. In this scheme, the electric field induces birefringence in an EO crystal placed in the vicinity of the electron beam. The amount of birefringence depends on the electric field strength and is probed at a single radial position by monitoring the change of polarization of a short optical pulse that is focused to the desired 'observation point'.

In the present FELIX setup, the EO bunch diagnostic is situated at the exit of the undulator of the FEL. A 0.5 mm thick ZnTe crystal is used as an electro-optic sensor and is placed with its front face perpendicular to the propagation direction of the electron beam. The probe laser beam passes through the ZnTe crystal parallel to the electron beam. Figure 1 shows a photograph of vacuum flange containing the EO sensor. The electron beam (50 MeV,

250 pC) passes through the rectangular shaped beam pipe (shape is determined by the undulator). The probe laser beam enters and leaves the vacuum pipe through a side window. On the opposite side of the electron beamline, the EO crystal and two small mirrors are mounted on a translation stage.

Several ways have been demonstrated to measure the electric field induced birefringence in the EO crystal using short optical laser pulses (for an overview see e.g. Ref. [2]). At FELIX, high temporal resolution, single-shot bunch profile measurements have been performed using 'temporal decoding' [1, 3]. The probe laser, which is actively synchronized to the accelerator RF clock, delivers short optical pulses with a duration of 30 fs at a wavelength of 800 nm. Each pulse is split into a probe and a reference pulse. The linearly polarized probe pulse is stretched to a length that is longer than the electron bunch, and is passed through the EO crystal. On exiting the beamline, the electric field induced birefringence is translated into an intensity modulation by passing the probe laser through a



Figure 1: Photograph of the vacuum flange containing the EO sensor. The EO crystal together with two small metal mirrors are mounted on a translation stage (visible on the right). The entrance/exit window for the probe laser beam is visible on the left.

\* g.berden@rijnh.nl

† also at: University of Strathclyde, Glasgow, UK

# OTR BASED MONITOR OF INJECTION BEAM FOR TOP-UP OPERATION OF THE SPRING-8

S. Takano\*, M. Masaki, T. Masuda and A. Yamashita

Japan Synchrotron Radiation Research Institute, SPring-8, Hyogo 679-5198, Japan

## Abstract

We have developed an optical transition radiation (OTR) based monitor of injection beam at the SPring-8. The monitor has been installed near the injection point of the storage ring downstream of the beam transport line from the booster synchrotron. A screen made of an aluminum coated polyimide film is used as a non-destructive OTR radiator. A CCD camera with an electric shutter is used to observe the OTR image of the injection beam. The electric shutter is synchronized with the external injection trigger signals. At every injection, the image signal from the CCD camera is captured and analyzed by a personal computer, and the position, size and intensity of the injection beam are recorded by the real-time database of the SPring-8 control system. The OTR screen monitor provides real-time and non-destructive diagnostic tool useful for the top-up operation of the SPring-8.

## INTRODUCTION

The 8 GeV electron storage ring of the SPring-8 is a third generation synchrotron light source operating since 1997. In May 2004, the so-called top-up operation started to realize practically infinite life time of the storage ring beam [1]. In the top-up operation, continuous beam injections at short time intervals keep the beam current approximately constant. In order to monitor the injection beam to the storage ring non-destructively and continuously in the top-up operation of the SPring-8, we have developed an OTR based screen monitor.

## OTR SCREEN MONITOR

The injection section of the SPring-8 storage ring is shown schematically in Fig.1. The electron beam from the booster synchrotron is injected at the full energy of 8 GeV. We have installed the OTR based screen monitor in a vacuum chamber of the beam transport line near the injection septum magnet #5. In the end part of the beam transport line, downstream of the septum magnet #7, the injection beam goes through a vessel filled with helium at atmospheric pressure. We have two fluorescent screen monitors instead of OTR ones there, because intense Cherenkov radiation could disturb observations by contaminating transition radiation. The fluorescent

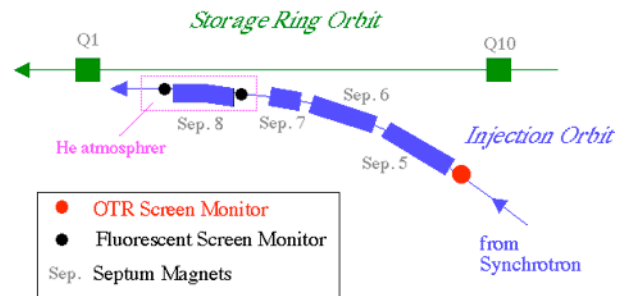


Figure 1: Injection section of the SPring-8 storage ring.

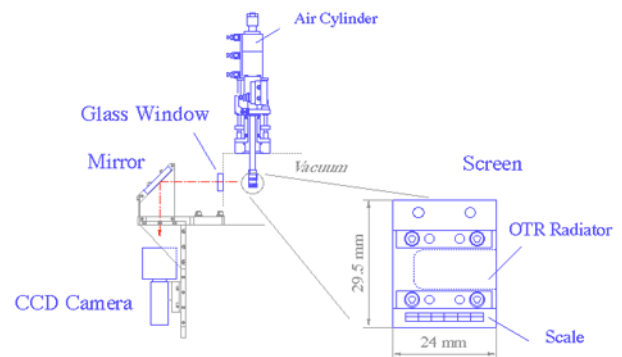


Figure 2: Set up of the OTR screen monitor.

screens are destructive to the injection beam, and they are retracted from the beam orbit during periods of top-up injections.

The setup of the OTR screen monitor is shown in Fig. 2. The OTR screen consists of a frame made of brass and a radiator made of an aluminum coated polyimide film. The thickness of aluminum and polyimide are about 0.5  $\mu\text{m}$  and 50  $\mu\text{m}$ , respectively. Scales for calibration are marked on the lower part of the screen holder. The screen is actuated by an air cylinder, which has three operating positions for 1) beam observation, 2) scale calibration, and 3) retraction. The screen is set at an angle of 45° with respect to beam direction. Backward OTR directed horizontally is transmitted in the atmosphere through a glass window and is deflected by a mirror downward, towards a CCD camera. To protect the camera from radiation damages, it is shielded by a cover made of lead. The OTR image of the injection beam is observed by the camera through a lens ( $F=1.3$ ,  $f=75\text{mm}$ ). The CCD camera has an electric shutter, which is synchronized

\* Email: takano@spring8.or.jp

# OPTIMIZATION OF BEAM INJECTION INTO THE FIRST ACCELERATING MODULE AT TTF WITH CAVITY DIPOLE MODE SIGNALS

N. Baboi\*, H. Schlarb, M. Wendt†, G. Kreps (DESY, Hamburg),  
O. Napoly, R.G. Paparella (CEA/DSM/DAPNIA, Gif-sur-Yvette),  
J. Frisch, M. Ross, T. Smith, D. McCormick (SLAC‡, Menlo Park, CA)

## Abstract

The TESLA Test Facility (TTF) is a user facility for intense VUV-FEL light. The facility is densely equipped with diagnostics, essential in obtaining the necessary beam parameters, in particular the low emittance. However there is no dedicated component for alignment of the beam in the accelerating modules, each containing eight superconducting cavities. Large beam offsets can lead to an increase of the beam emittance. The centering of the beam in these modules is therefore important, mostly at the low energy end. A misalignment of the first TTF module with respect to the gun axis has already been observed using cavity dipole modes. This paper presents the experimental results of the optimization of the beam injection into the first module, based on the monitoring of dipole modes through the couplers installed for wakefield damping. For this we use a spectrum analyzer together with a multiplexer. By scanning the beam position and tilt with two pairs of steerers, we can find the trajectory which minimizes the dipole modes amplitude. The impact of the beam steering in the module on the beam is discussed. A time domain setup is also being presented.

## INTRODUCTION

The TESLA Test Facility linac (TTF) at DESY serves as a user facility for intense VUV-FEL light [1]. Each of the five TESLA cryo-modules contains eight 9-cell superconducting cavities, which accelerate the electron beam generated by a photo-cathode to about 450 MeV. Transverse higher-order modes (HOM), resonant fields excited in the cavities by off-axis charged particles, can give kicks on the subsequent beam, leading to emittance growth of the pulse train. In particular, at low energies the effect can be significant. Dipole modes are of main concern. The modes of individual cells are degenerated into 9 modes grouped into passbands.

Although there are various monitors for beam diagnostics in the facility, there is no dedicated device for beam alignment in the modules. Signals suitable for beam alignment are however available, from the HOM couplers with which each cavity is equipped [2]. These couplers extract energy from the HOM, particularly the first two dipole passbands, where most modes with highest impedance can

be found. The amplitude of the resonant fields is proportional to the beam offset with respect to the cavity axis and to the bunch charge. Each dipole mode is split into two modes, with different polarizations. The axes of the two polarizations are orthogonal to each other for a circularly symmetrical structure.

From the coupler, the modal energy is normally brought through long coaxial cables to loads. We have disconnected the loads and monitored the amplitude of each mode with a spectrum analyzer. With a multiplexer we are able to choose one coupler out of 16 present in each module, as shown in Fig. 1. Therefore we can monitor the beam position in each cavity individually.

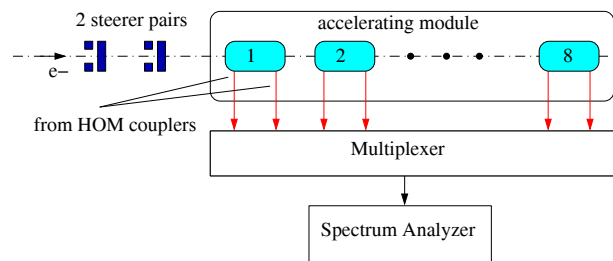


Figure 1: HOM setup for frequency domain measurements

In the next section we describe the procedure used for the alignment on the axis of the first cavity of the first TTF accelerating module. The results are compared to results from studies on beam properties. In the following section a time-domain recorder system is presented, which has recently been installed at TTF. Measurements made with this system are mentioned. There are four modes with high loss factors in the first two dipole bands, which makes them most suited for monitoring<sup>1</sup>. In this paper we have used modes 6 and 7 from the first band, at about 1710 MHz and 1730 MHz.

## BEAM ALIGNMENT IN ACC1

The purpose of the measurements was to align the beam on the axis of cavity 1 of the first accelerating module, denoted by ACC1. The beam alignment is most critical here since kicks on the beam are highest due to the low energy of 4.6 MeV given by the gun. We chose mode number 6 from the first dipole passband, with  $R/Q = 11 \text{ M}\Omega/\text{m}^2$ . The

<sup>1</sup>A strong mode in the third passband is not suited, since it is very close to other modes.

\* nicoleta.baboi@desy.de

† currently at FNAL, Batavia, IL

‡ work supported in part by US DOE: DE-AC02-76SF00515

## NEW TUNE MEASUREMENT SYSTEM FOR THE ESRF BOOSTER

J.M. Koch, J. Meyer, E. Plouviez  
European Synchrotron Radiation Facility (ESRF), Grenoble, France

### Abstract

The injection of electrons in the ESRF storage ring is performed at full energy, i.e. 6GeV. A linear accelerator provides the booster with a beam at an energy of 200MeV. During the accelerating cycle of the booster, from 200MeV to 6GeV, the tune of the electron beam varies according to the non-proportionality of the magnetic field in the quadrupole magnets as compared to the dipole field. This is mainly due to the harmonic content of the current in the magnets which differs with the load of these systems resonating at 10Hz and their saturation level. In order to measure the fractional part of the tunes all along the accelerating cycle, (50ms) it is necessary to acquire the beam position at a rate of at least one sample per turn, each  $\mu$ s. A set of 48 tune values can be extracted from this record with an accuracy of better than  $10^{-3}$ .

### INTRODUCTION

The measurement of the tune of the booster has been made automatic in the last few years, but due to the fact that the beam is excited with short kicks, it is only possible to obtain one measurement per accelerating cycle. To build the curve of the tune, we have to reconstruct it point by point by delaying the excitation from the injection time. With an injection rate of one second and an average of a few data per point, it takes a few minutes before the curve for the full cycle can be established and the different points do not belong to the same cycle. Therefore, it was decided to use a white noise excitation present all along the cycle, and an acquisition system that can compute the tunes for the whole accelerating cycle in one go. Although this system is not already in operation, the first tests have shown that it works as expected. In addition to the increase in the tune measurement rate, it will be possible to add new features like the automation of the chromaticity measurement.

### SYSTEM LAYOUT

#### Excitation of the Beam Oscillation

We excite the beam oscillation using magnetic kickers; these kickers are made of 6 coils enclosed in a ferrite box, with a ceramic vacuum chamber surrounding them. The kickers have a 0 to 600 KHz bandwidth when terminated on a 50 $\Omega$  load and an efficiency of 3 G.m/A. The kickers are driven by a 50W amplifier. The input signal is a white noise in a bandwidth from 0 to 500 KHz.

#### Analog Front End

The beam position is measured using 2 sets of 4 capacitive pick-ups. The sensitivity of the electrode is improved by using resonant RF transformers to match the pick up capacitance to the 50 $\Omega$  line impedance. The electrode signals are combined in  $\Delta\Sigma$  RF combiners to produce signals proportional to the horizontal and vertical beam offset and beam intensity.

The pick up signals are detected using a 2 stage synchronous detection electronic scheme: The first stage is a 352.2 to 10.7MHz down converter. The second stage is a synchronous vector detection circuit of the  $\Delta$  signal; the reference signal is the output of a limiting amplifier fed by the  $\Sigma$  signal. This scheme aims at getting the best signal to noise ratio rather than good position accuracy, which is pointless in a tune measurement.

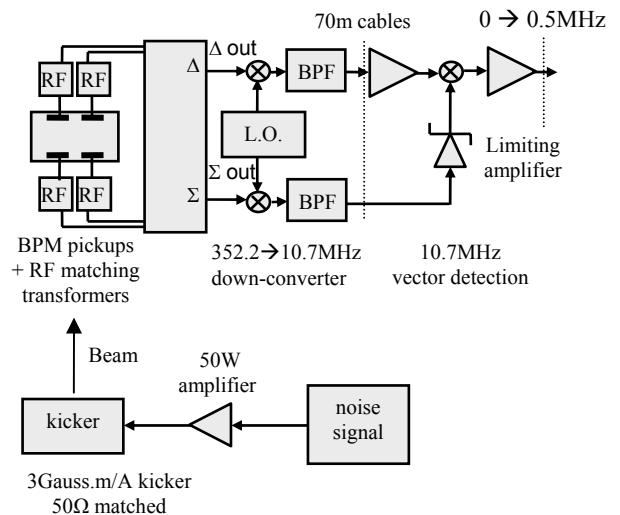


Figure 1: Analog front-end

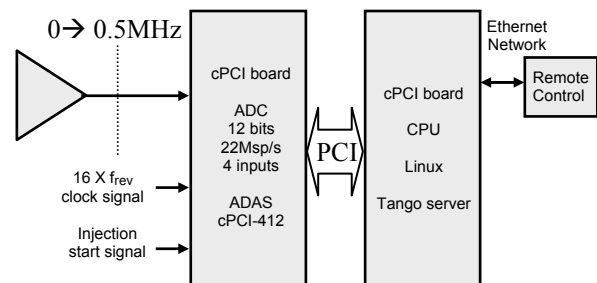


Figure 2: Digital acquisition & processing hardware

# MEASUREMENTS OF TRANSVERSE EMITTANCE AT THE TTF VUV-FEL

K. Honkavaara\*, F. Löhl, Hamburg University, 22761 Hamburg, Germany  
Y. Kim, DESY, 22603 Hamburg, Germany

## Abstract

The TESLA Test Facility (TTF) linac at DESY has been extended to drive a new free electron laser facility, the VUV-FEL. The 250 m long electron linac has been commissioned in 2004 and in the beginning of 2005. Characterization of the electron beam is an essential part of the commissioning. The transverse projected emittance has been measured at a beam energy of 127 MeV with the four-monitor method using optical transition radiation (OTR). We describe the experimental set-up and discuss the data-analysis methods. Experimental results as well as simulations are presented.

## INTRODUCTION

The TESLA Test Facility (TTF) linac has been extended to drive a new free electron laser, the VUV-FEL [1], in the wavelength range from vacuum-ultraviolet to soft X-rays. The commissioning of the new facility started in the beginning of 2004, and the first lasing was achieved in January 2005.

Figure 1 shows the present layout of the TTF VUV-FEL linac. Electron bunch trains with a nominal bunch charge of 1 nC are generated by a laser-driven RF gun. Five accelerating modules with eight 9-cell superconducting TESLA cavities are installed to provide electron beam energy up to 750 MeV. The electron bunch is compressed using two magnetic chicane bunch compressors. At the location of the first bunch compressor the beam energy is 127 MeV and at the second one 380 MeV. During the commissioning the main emphasis has been on lasing with the wavelength of 30 nm, corresponding to an electron beam energy of 445 MeV. The lasing process requires a high quality electron beam in terms of transverse emittance, peak current and energy spread. The design normalized emittance of the VUV-FEL is 2 mm mrad. A more detailed description of the machine and first experimental results can be found in [2, 3].

At the VUV-FEL, measurements of the transverse projected emittance are performed using a four-monitor method. In this method the transverse beam distribution is measured at four locations along the linac with a fixed beam optics. The emittance is calculated by two different techniques. The first one is based on fitting of the Twiss parameters and the emittance to the measured beam sizes. The second one uses a tomographic reconstruction of the phase space distribution. A detailed description of the emittance

measurements and analysis techniques presented in this paper can be found in [4].

## EXPERIMENTAL SET-UP

The VUV-FEL has two diagnostic sections dedicated to emittance measurements (see Fig. 1). The first one is located downstreams of the first bunch compressor at the electron beam energy of 127 MeV. This section consists of four OTR monitors combined with wire scanners embedded in a FODO lattice of six quadrupoles with a periodic beta function. A second FODO lattice with four OTR monitors is located upstreams of the undulator. In this paper we concentrate on emittance measurements in the first section using OTR monitors only.

The OTR system is designed and constructed by INFN-LNF and INFN-Roma2 in collaboration with DESY. The system can be controlled remotely, and it provides three different image magnifications (1.0, 0.39, and 0.25). The read-out system is based on digital CCD cameras with IEEE1394 (firewire) interface. The measured resolution of the system is 11  $\mu\text{m}$  rms for the highest magnification. More details of the OTR monitor system are in [5, 6, 7].

## EMITTANCE CALCULATIONS

The four (multi) monitor method is based on measurements of the transverse beam distribution (shape and size) at four (or more) locations with a fixed beam optics. The transverse emittance is determined from the measured beam distributions and the known transport matrices between the monitors using two different methods. The first one uses a least square (chi-square) fitting of the Twiss parameters and the emittance to the measured beam sizes. A general description of the least square fitting technique can be found, for example, in [8], and an application for emittance measurements in [9]. The second method is based on a tomographic reconstruction of the phase space distribution using the maximum entropy algorithm [10].

In the error estimation for the fitting method, we take into account both statistical and systematic errors. Statistical errors are caused by fluctuations on the measured beam sizes, and they are calculated as in [9]. Systematic errors are estimated using a Monte Carlo simulation assuming 5% error in the beam energy, 6% error in the gradient of the FODO lattice quadrupoles, and 3% error in the calibration of the optical system. Statistical errors are typically 2-4% and systematic ones 5-6%. For the tomographic reconstruction, no error analysis is performed yet.

\*katja.honkavaara@desy.de

## UPGRADE OF THE GLOBAL FEEDBACK OF THE ESRF STORAGE RING

E. Plouviez, F. Uberto, J.L. Pons, J.M. Koch  
 European Synchrotron Radiation Facility (ESRF), Grenoble, France  
 e-mail: plouviez@esrf.fr

### Abstract

We have recently upgraded the fast orbit correction system of the ESRF storage ring. We are now operating a global feedback system using 32 BPMs and 24 correctors in the horizontal and vertical planes to compute and apply corrections at a rate of 4.4 KHz from .1 to 150Hz. This new system has greatly improved the damping of the orbit distortion up to 100Hz. It also provides new diagnostics tools thanks to its new data logging capabilities. We report the performance of this new system and some of its applications as a diagnostic.

### INTRODUCTION

Until the end of 2004, the damping of the fast beam orbit distortions of the ESRF was done in the vertical plane by a global feedback system using 16 BPM and 16 correctors; in the horizontal plane we were using a set of 4 local feedback systems to stabilize the beam in the 4 most sensitive ID straight sections [1]. This fast orbit correction is working in parallel with a slower correction system using 224 BPM and 96 correctors to perform 2 corrections per minutes with a very good accuracy and long term reproducibility. The goal at ESRF is to keep the amplitude of the fast beam movement time  $\beta^{1/2}$  below  $2\mu\text{m}$  inside the insertion devices straight sections (integrated over the frequency span going from .1 to 200Hz). Since the implementation of vibration damping pads on the girders supporting the storage ring magnets in 2001 [2], the beneficial effect of the vertical feedback had become a bit marginal; in the horizontal plane, there was no way to increase the number of local systems, due to the imperfect closure of the local correction bumps at high frequency: with more than 4 systems in operation, the cross talks between the local feedbacks resulted in instabilities. In order to overcome these limitations, we decided in 2001 to upgrade our fast correction scheme and to implement a fast global correction system active in both horizontal and vertical planes. One of the constraint for this upgrade, was to use as much as possible of the components of the old system: BPM, correctors, front end electronics and data links, in order to reduce the cost of the project and to avoid leaving the ring without fast orbit correction during the implementation of the new system. We kept the same approach of separating the slow and fast orbit correction in 2 systems so this new system do not perform any orbit correction below .1Hz.

### UPGRADE LAYOUT

The constraint was to achieve an efficient correction in both planes, given the value of the tunes of our storage ring ( $\nu_H=36.44$  and  $\nu_V=14.39$ ), the number of BPM and correctors that could be easily integrated in our upgraded system and the frequency range needed for an efficient damping of the orbit distortion.

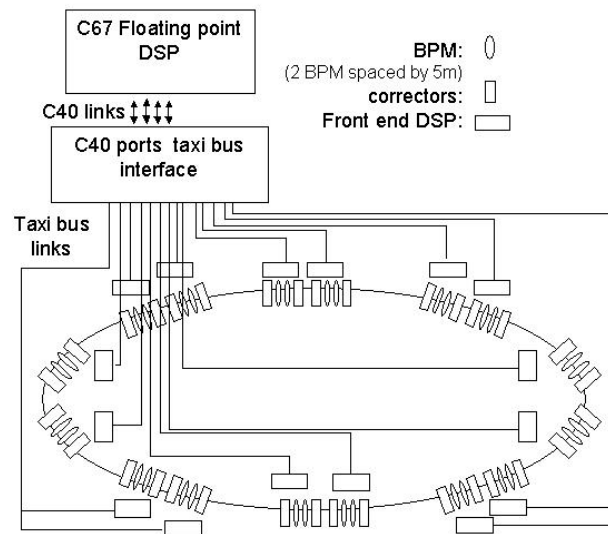


Figure 1: Layout of the global feedback system.

#### Static correction: BPM and correctors number

The layout of the upgraded global feedback is shown in figure 1. The upgrade had to be compatible with some limitation put by the existing hardware. A front end DSP has 8 ADC inputs and 3 DAC outputs so it can handle the data of the 8 electrodes of 2 BPM blocks and drive 3 correctors amplifiers inputs. At the other end of the data link the most convenient interface available for data transmission between a commercially available central DSP board and our data links was the TI C40 port. The central DSP board that we chose can handle four C40 ports and we can concentrate on one C40 port the data stream of four front end DSP; so the size of our system is limited to 32 BPM for both planes and 48 correctors. Presently the correctors output are shared equally by the 2 planes: 24 vertical and 24 horizontal correctors (but this may not be the most efficient repartition). A rule of thumb is that it takes a number of BPM and correctors roughly equal to the tune value to obtain a significant fast

# RECENT DIAGNOSTIC IMPROVEMENTS FOR THE PSI ACCELERATOR

P. A. Duperrex, U. Frei, G. Gamma, U. Müller, L. Rezzonico, PSI, Villigen, Switzerland

## INTRODUCTION

Two recent developments for the PSI proton accelerator are presented: a) a new remote control system that is being implemented for the numerous wire scanner based profile monitors of the proton accelerator, b) a new current monitor as replacement of an older system.

## CONTROL SYSTEM FOR PROFILE MONITORS

A new remote control system [1] for the profile monitors has been developed and is being currently implemented on various beam lines of the proton accelerator. The development of this new system was motivated by maintenance difficulties due to an aging system, by some shortcomings related to the old technology and by the better performances offered with the electronics of today.

### *Shortcomings of the old system*

The profile monitor controlling system has been in operation for 20 years. It is made of 3 multiplexed systems controlling all together more than 200 profile monitors.

Several shortcomings motivated the development of a new remote control system. First, the maintenance of this aging system is problematic because some critical electronic components are no more available. Furthermore, the multiplexed nature of the system has a negative impact on the system availability. The wire current measurement of the old system relies on a linear circuit. The correct amplifier gain setting is most of the time requiring several profile measurements. These repeated scans have a negative influence on the longevity of the wire. In addition, the analysis of the raw data is difficult because of the particular ADC used. Indeed, with the old system, the data are sampled at regular position intervals and not at regular time intervals. FFT or time based filtering of the data is then not possible.

### *Improvements*

Improvements addressing these shortcomings are: i) a distributed system structure based on an internally developed CAMAC board controlling up to 8 profile monitors ii) a fixed gain logarithmic measurement of the wire current covering the whole operation range iii) the new control of the DC motor can adjust the motor speed to beam conditions, iv) position and current measurement with a dedicated 14 bit ADC for improved resolution and further off-line processing.

### *Overview of the new system*

Fig.1 gives a conceptual overview of the system. It is made up of 3 subsystems: i) a CAMAC based WIPAM

(Wire Profilemonitor Acquisition Module) including the DASH (Data Acquisition module with Hitachi SH2 microcontroller) back-end, ii) up to 4 Motor Drive Modules (MDM), iii) up to 8 profile monitors.

Control signals are generated from the CAMAC based electronics (WIPAM). They are then decoded and conditioned for driving the motor in the power stage electronics (MDM). Measurement signals from the profile monitor are first conditioned at the MDM then further processed in the WIPAM. The following sections provide a more detailed explanation of the subsystems.

## WIPAM

The DASH back-end has been developed as a standardised universal controller, which can support various front ends. The firmware is responsible for controlling the motors, processing and storing the raw data, calculating the current profile and checking interlock conditions.

The microcontroller 10 bit ADC is used for sampling the DC motor voltage and current. A control program uses these data to drive the DC motor at the required speed. In addition, the scanning wire position is also used to initiate the braking sequence early enough to avoid overshoots. The actual motor speed ranges from 1000 to 5000 rpm. With a 20 gear ratio factor and taking into account the acceleration and deceleration phases, typical time for a run ranges from 0.3 sec to 2 seconds.

The status of the different rest position switches are continuously monitored to make sure that all profile monitors are in their rest position when not in use. The program will otherwise attempt to bring a faulty monitor back into its rest position. If unsuccessful, the program will generate an interlock to avoid any possible damage.

The analogue front-end (AFE) provides correctly conditioned signals for the MDM. In addition, scanning wire current and position signals are filtered and sampled at 10 kHz using a MAXIM 14 bit ADC.

Parameter limits such as beam width or position can be defined so that interlocks may be generated in case the measured parameters go over these limits.

## MDM

The MDMs decode the information from the WIPAM, in particular the profile monitor to be activated and the rotation direction of the motor. They provide the necessary power for driving the DC motors, as well as the 10 V reference signal for the position potentiometer measurements. The logarithmic conversion of the current from the scanning wire is also performed in the MDM: 800 mV correspond to a decade with a 0 V output voltage corresponding to 1  $\mu$ A. Almost 8 decades can be measured this way.

## THE BEAM DIAGNOSTICS FOR SESAME

Seadat Varnasseri<sup>\*</sup>, SESAME -c/o UNESCO Office, P.O.Box 2270, Amman

### Abstract

SESAME<sup>†</sup> (Synchrotron-light for Experimental Science and Applications in the Middle East) is an Independent Intergovernmental Organization developed and officially established under the auspices of UNESCO. SESAME will become a major international research center in the Middle East, located in Allan, Jordan. The machine design is based on a 2.5 GeV 3rd generation Light Source with an emittance of 26 nm.rad and 12 straights for insertion devices. The conceptual design of the accelerator complex has been frozen and the engineering design is started [1]. The completion of the accelerators complex construction is scheduled for the end of 2009. In the following an overview of the electron beam diagnostic system is presented, with special emphasis on the beam position monitoring system and the synchrotron light monitor for the main storage ring.

### INTRODUCTION

In SESAME the electrons are injected from a 20 MeV microtron into a 800 MeV booster synchrotron, with a repetition rate of 1 Hz. The 800 MeV beam is transported through the transfer line to the main storage ring and after accumulation, accelerated at 2.5 GeV. Through the path from microtron to and within storage ring both destructive and non-destructive monitoring of beam are performed, consisting of Faraday cup, florescent screen, current transformer, strip line, scraper, beam loss monitor, synchrotron light monitor and beam position monitor pick ups [2].

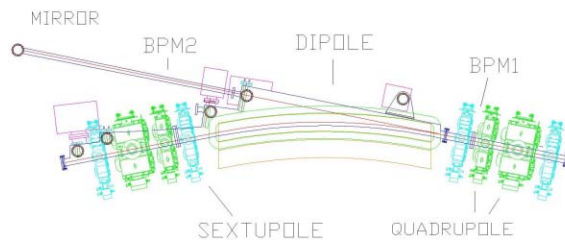


Figure 1 : Arrangements of BPM and light monitor within half cell of the storage ring SESAME.

The aim is to use the destructive monitor instruments mainly for commissioning and first day operation and non-destructive devices for the normal operation of the machine.

Fig.1 shows the half cell of the machine with the proposed diagnostic elements.

<sup>\*</sup> s.varnasseri@unesco.org.jo

<sup>†</sup> It involves at present the following Member States: Bahrain, Egypt, Iran, Israel, Jordan, Pakistan, Palestinian Authority, Turkey and United Arab Emirates.

Table 1: SESAME storage ring parameters relevant to beam diagnostics and their normal values.

Energy (GeV)	2.5
RF frequency (MHz)	499.564
Natural emittance $\epsilon_x/\epsilon_y$ (nm.rad)	25.24/0.2524
Injection energy (MeV)	800
Max. Average current(mA)	400
Harmonic number	222
Revolution period(ns)	444
Bunch length (cm)	1.16
Horizontal beam size ( $\mu\text{m}$ ) LS/SS/Dipole	794.8/789.7/232
Vertical beam size ( $\mu\text{m}$ ) LS/SS/Dipole	28.1/16.6/71.5
Horizontal divergence( $\mu\text{m}$ ) LS/SS/Dipole	45.3/45.9/260.9
Vertical divergence( $\mu\text{m}$ ) LS/SS/Dipole	9/15.2/12.1

The tunnel air temperature for SESAME storage ring will be stabilized at  $(25 \pm 1)^\circ\text{C}$ . The vacuum chamber temperature gradient per the horizontal distance between the button PUs will not exceed  $0.5^\circ\text{C}$ . This gives a maximum of  $8\mu\text{m}$  repositioning of button pick ups due to the temperature differential on the stainless steel vacuum chamber.

### BEAM POSITION MONITORS [3,4,5]

Overall there are 32 BPM sets, four BPMs in each cell of the storage ring. They will be placed at the exit and entrance of each bending magnet and between sextupoles and quadrupoles, to measure the closed orbit distortion all around the ring. Fig.2 shows the SESAME optical function and 4-buttons BPM arrangements.

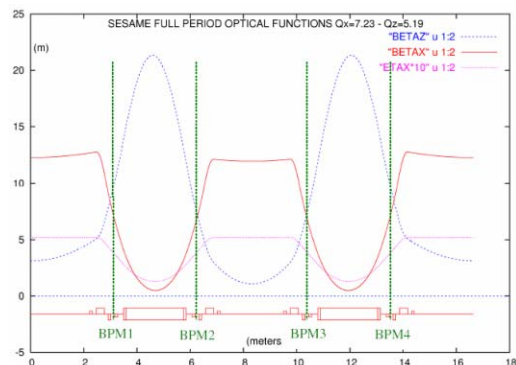


Figure 2: Optical function of SESAME and the BPM arrangements.

# AN X-RAY PINHOLE CAMERA SYSTEM FOR DIAMOND

C.A. Thomas, G. Rehm, DIAMOND, RAL, Great Britain

## Abstract

In this paper we present the X-ray pinhole camera designed for the measurement of the size, the emittance and energy spread of the electron beam at Diamond. The system has been kept as simple as possible. The pinhole and the imaging system are in air, and the X-ray beam from the bending magnet is filtered out through an Al window. The beam is imaged using a fluorescent screen and an IEEE 1394 camera. We describe the system from the problems encountered for the extraction of the X-ray beam, to the optimisation of the imaging system. Taking into account the results of preliminary tests, we estimate the expected performance of the system.

## INTRODUCTION

The DIAMOND synchrotron light source is the third generation light source under construction in the UK [1]. The expected performance of the source, in terms of brightness, imposes the electron to occupy a very small phase space volume. To measure the energy spread ( $\approx 10^{-3}$ ) and the emittance ( $\approx 2.7$  nm rad) of the DIAMOND electron beam, an X-ray pinhole camera [2] is probably the most simple and accurate device. The pinhole camera is a known device and the instrumentation very straightforward. However, the adaptation and the optimisation of the camera to the case of Diamond requires to investigate in details the extraction and the imaging of the of the X-Ray beam. For the extraction of the beam, the number of X-Ray photons is an issue, but at the same time, the heat-load of the extraction window has to be considered. To image the electron beam profile, two steps are considered. The first one is to find the best screen that would absorb the X-ray photons and convert them into visible photons. The second step is to investigate the best way to image the fluorescent screen.

In this paper we present the design of the pinhole camera, showing the heat-load taken by the Al window, and then the optimisation of the imaging system.

## X-RAY PINHOLE CAMERA

The X-ray pinhole camera, like any pinhole camera, is composed of a source, a pinhole and a screen to image the source. At Diamond, two X-ray pinhole cameras will be installed to measure the beam size in high and low bending magnet dispersive sections. The two systems are identical, as described in figure 1. The X-ray beam from the bending magnet goes through the beam port absorber. The absorber is a copper block, designed to absorb the totality of the X-ray beam, and in our case a modification allows the

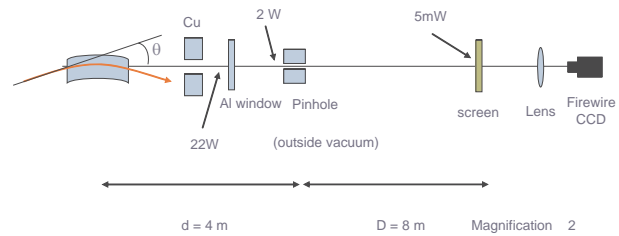


Figure 1: Scheme of the pinhole camera system for measuring the electron beam transverse profile. Electron beam size, emittance and energy spread can be calculating from the image of the beam profile.

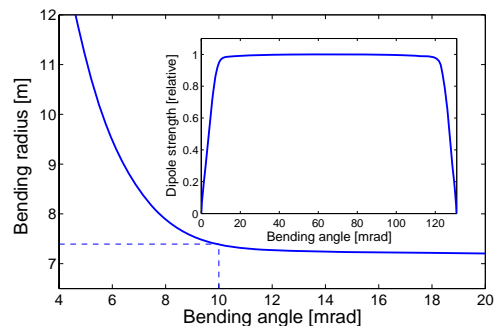


Figure 2: DIAMOND bending magnet radius vs. angle.

transmission of the beam through an aluminium window. The window transmits only the high energy photons from vacuum to air. The position of the window as to be carefully chosen. We show in figure 2 the bending radius as a function of the angle,  $\theta$ , between the electrons' entering straight direction and the photon beam line. In our particular case, the radiation flux become significant only after 10 mrad (see fig 3). The  $25$  by  $25 \mu\text{m}^2$  pinhole is placed behind the window, as close as possible from the source, 4 m in our case. To image the source (2D gaussian, r.m.s  $25$  by  $50 \mu\text{m}^2$ ) we use a fluorescent screen that absorbs X-rays and fluoresces in the visible. The screen is placed at twice the distance source-pinhole, so that the image is magnified by a factor  $\approx 2$ . Three different screen have been tested at ESRF,  $\text{CdWO}_4$  (0.5 mm thick), P43 ( $5 \mu\text{m}$  thick) and YAG:Ce (0.1 mm thick). To acquire and measure the size of the source we image the screen with a macro-lens (Componon 2.8/50 from Schneider-Kreuznach) focussing on a compact IEEE 1394 CCD camera (Flea from Point Grey). A Matlab application has been developed to control the camera.

# OPERATIONAL EXPERIENCE WITH BEAM ALIGNMENT AND MONITORING USING NON-DESTRUCTIVE BEAM POSITION MONITORS IN THE CYCLOTRON BEAMLINES AT ITHEMBA LABS \*

J. Dietrich, I. Mohos, Forschungszentrum Jülich, Postfach 1913, D-52425 Jülich, Germany  
 J.L. Conradie, Z. Kormany, P.F. Rohwer, P.T. Mansfield, D.T. Fourie, J.L.G. Delsink, M. Sakildien,  
 A.H. Botha, iThemba LABS, P. O. Box 722, Somerset West 7130, South Africa

## Abstract

At iThemba LABS proton beams, accelerated in a K=200 separated-sector cyclotron with a K=8 solid-pole injector cyclotron, are utilized for the production of radioisotopes and particle radiotherapy. Low-intensity beams of light and heavy ions as well as polarized protons, pre-accelerated in a second injector cyclotron with a K-value of eleven, are available for nuclear physics research. Beam position monitors and associated computer-controlled electronic equipment have been developed for non-destructive alignment and continuous display of the beam position in the beam lines for the more intense beams used for therapy and the production of radioisotopes in cooperation\* with Forschungszentrum Jülich. The monitors consist of four-section strip lines. Narrow-band super-heterodyne RF electronic equipment with automatic frequency and gain control measures the signals at the selected harmonic. A control module sequentially processes the signals and delivers calculated horizontal and vertical beam position data via a serial network to the computer control system. Eleven monitors have been installed in the beam lines. Operational experience with alignment and monitoring of the beam position is discussed.

## BACKGROUND

The design and implementation of a prototype non-destructive beam position monitor and associated electronic module for signal processing in beam lines at iThemba LABS [1] have been reported before [2]. Since then eleven monitors and electronic modules have been manufactured. Four of these monitors, which have been planned for beam intensities of one  $\mu\text{A}$  and more, have been installed in the transfer beam line between the light-ion injector and the separated-sector cyclotron and the remaining ones in the high-energy beamlines leading to the neutron therapy and isotope production vaults. The main design considerations and limitation for the monitors, which should measure the beam position in both the horizontal and vertical directions, are that they have to be installed through the beam ports of the diagnostic vacuum chambers in the beam lines and fit into the available space together with the existing other diagnostic components. Since the cyclotrons are in operation for 24 hours per day and seven days a week the diagnostic chambers could not be removed for machining

of additional flanges. The electronic modules were designed and built at the Forschungszentrum Jülich-IKP, as part of the work done under a scientific and technological agreement between Germany and South Africa.

## THE POSITION MONITOR

The four electrodes of the monitors are mounted coaxially inside a cylindrical copper housing as shown in Fig. 1. Although the prototype monitor, described before [2], could fit in the diagnostic vacuum chambers installation of the semi-rigid cables inside some of the chambers was difficult. In the final design the overall length of the monitors is therefore 15.5 mm shorter than before and have the dimensions shown in Fig. 1. The length of the electrodes, which are connected through 50 ohm resistors to ground inside the vacuum chambers, remained the same as before.

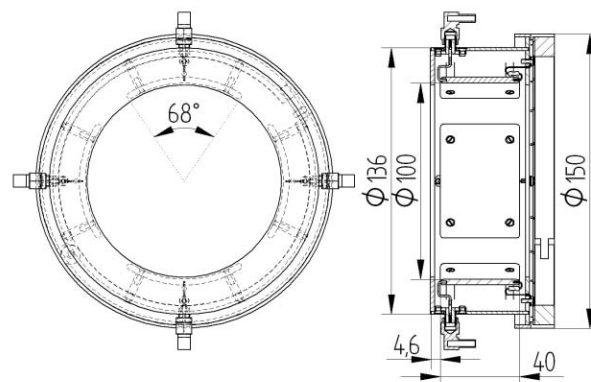


Figure 1: Front view and cross-section drawings of the beam position monitor with 50 ohm terminations on the electrodes.

## ELECTRONIC SIGNAL PROCESSING

A block diagram of the electronic equipment used for signal processing of each of the eleven monitors is shown in Fig. 2. A GaAs RF multiplexer switches the monitor signals to the input of the common signal chain. In each acquisition cycle the four signals are sequentially measured before the position data are computed. The RF part, consisting of narrowband super-heterodyne RF electronics, processes the monitor signal components at the selected higher harmonic of the cyclotron RF frequency. The center frequency is programmable between 49 and 82 MHz. Automatic frequency and gain

\*Supported by BMBF and NRF, project-code 39.1.B0A.2.B.

# PERFORMANCE VERIFICATION OF THE DIAMOND EBPM ELECTRONICS

G. Rehm, M. Abbott

Diamond Light Source Ltd., Rutherford Appleton Laboratory, UK

## Abstract

The Electron Beam Position Monitor electronics for Diamond are a newly developed product. As such, extensive testing was carried out as part of the acceptance tests. These tests included measurement of the resolution, beam current dependence, fill pattern dependence, temperature dependence and long term reproducibility in the lab. A setup of signal generators was chosen to simulate the signals from button pickups as realistically as possible. Additionally, tests have been carried out with “real beam” signals at the SRS in Daresbury. Solutions for problems identified during these tests have been developed and their suitability is demonstrated.

## INTRODUCTION

Diamond will incorporate 202 *Libera* beam position processors from Instrumentation Technologies for use in the transfer lines, booster and storage ring. The specifications required the resolution to be measured for a range of beam currents and for different acquisition bandwidths and data rates to cater for fast feedback (FFB) and turn-by-turn (TBT) applications (see table 1). Additionally, any systematic offset of the beam position reading correlated with the beam current had to be recorded and within the given limits.

The resolution and beam current dependency test are carried out as part of the factory acceptance test. They were repeated for a sample of the delivered units and additional long term tests were conducted.

## LAB TEST SETUP

To facilitate parallel tests of 6 sets of BPM electronics in the lab they were put in one rack and connected to an RF signal generator (Rohde & Schwarz SML01,  $f_{RF} = 499.654$  MHz) through a network of power splitters. Additionally, an arbitrary waveform generator (Agilent 33250A) simulated the 2/3 fill of the storage ring by producing a  $f_{rev} = 533818$  Hz with 66% duty cycle and delivering this to the fast gate input of the RF generator. This signal was also sent to a custom built trigger fan-out unit, which provided it as machine clock to the BPM units. To phase lock RF and machine clock as well as to ensure frequency stability during long term tests, both generators had their 10 MHz reference inputs connected to a Stanford FS725 rubidium standard. BPMs and the RF generator were connected to Ethernet so that all tests could run completely remote controlled.

Table 1: Specified r.m.s noise and beam current dependence on position readings for different sample rates and beam current ranges

beam current	resolution@bandwidth		beam current dependence
	2 kHz	266 kHz	
60-300 mA	0.3 $\mu\text{m}$	3 $\mu\text{m}$	1 $\mu\text{m}$
10-60 mA	0.6 $\mu\text{m}$	6 $\mu\text{m}$	50 $\mu\text{m}$
1-10 mA	1.5 $\mu\text{m}$	15 $\mu\text{m}$	100 $\mu\text{m}$

## DEGRADED RESOLUTION DUE TO HARMONIC FOLD BACK

During the initial resolution tests a strange phenomenon was noted. As long as the sampling frequency of the ADCs is free running, the results are as expected. However, as soon as the machine clock is supplied and the frequency locked loop (FLL) sets the sampling frequency  $f_S = 220f_{rev} = 220/936 \cdot f_{RF}$ , the noise on the position readings increases by a factor of 3-5.

An understanding of this phenomenon requires a look at the processing chain (see figure 1). The source for this behaviour is some nonlinearity in the ADCs. This nonlinearity creates the third harmonic of the input signal. In the digital domain, the signal is at  $56f_S$ , so the third harmonic will be folded back to  $(220 - 56 \cdot 3) \cdot f_S = 52f_S$ . Here, the third harmonic would still be filtered out by the decimation filters in the digital down converter (DDC). However, with the fill pattern square wave modulation at  $f_{rev}$ , the signal as well as its third harmonic, carried sidelines at  $\pm n \cdot f_{rev}$ . The fourth sideline of the third harmonic will then come to lie at  $56f_S$ , which is the signal frequency. As the FLL locks the VCXO within about 1 Hz, the third harmonic signal will move around and depending on the individual nonlinearities of the four ADCs, create a position fluctuation.

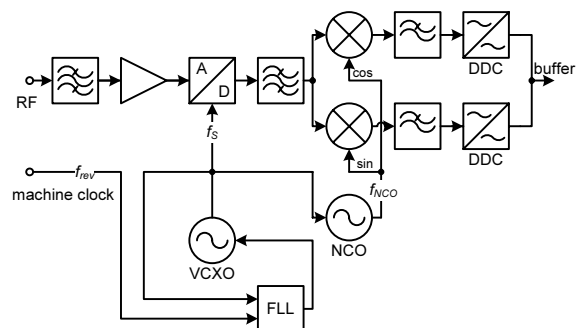


Figure 1: Simplified processing chain for one channel

# HIGH DYNAMIC MAGNETIC BEAM CURRENT MEASUREMENTS BY MEANS OF OPTIMISED MAGNETO-RESISTANCE (MR) SENSOR ENGINEERING

Markus Häpe, Wolf-Jürgen Becker, Werner Ricken, University of Kassel (UNIK), Germany  
 Andreas Peters, Hansjörg Reeg, Piotr Kowina, GSI Darmstadt, Germany

## Abstract

A new sensor for the beam current measurement is under design at the department of Measurement Engineering at University of Kassel and GSI Darmstadt. An overview of the commercial available magnetic sensors like AMR- (anisotropic magneto-resistance) and GMR- (giant magneto-resistance) sensors and also the new magnetic GMI-effect (giant magneto-impedance) is given. These sensors have been investigated for their suitability for the clip-on ampere-meter. The results will be discussed and an outlook for further development will be presented.

## BASIC IDEA

The GSI-FAIR project (facility for antiprotons and ion research) will comprehend DC currents up to around 1.2 A in the SIS 100 synchrotron and after bunch compression down to 30 ns pulse length the peak currents will reach up to 200 A.

The current measurement device itself will be designed in form of a clip-on ampere-meter, see Figure 1.

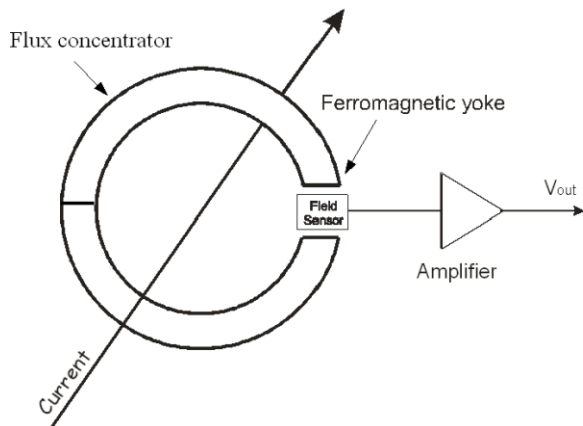


Figure 1: The open loop sensor

This configuration would have big advantages in contrast to a normal DCCT, because it can be dismantled without opening the vacuum due to its separable core. An alternative to a DCCT was looked for because of their problems with the high peak current in the bunch structure of 1 MHz up to 5 MHz. This difficulty was discussed at the 2<sup>nd</sup> CARE-HHH-ABI-meeting in Lyon end of last year, see Ref. [9] for more details.

To meet the challenging demands of beam current measurements – high dynamics, large current peaks – at the SIS100 new sensor techniques are foreseen, which will be reviewed in this paper.

## SIMULATION OF THE MAGNETIC FLUX CONCENTRATOR

The flux concentrator consists of soft-magnetic VITROVAC 6025F. The air gap of the flux concentrator is assumed to be around 5 mm, the inner diameter to be 200 mm (cf. Figure 1). The contour plot of the absolute values of the magnetic flux for an excitation current of 10 A is shown in Figure 2. The simulation has been carried out at GSI.

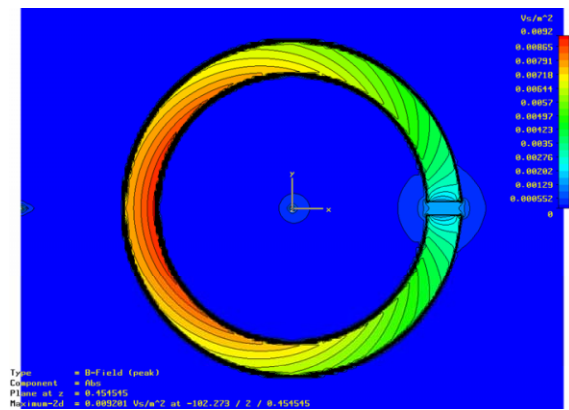


Figure 2: Contour plot of the magnetic flux

The estimated maximal field in the gap is derived to be around 27.4 mT for a beam current of 200 A peak, whereas the magnetic field in the core still keeps away from saturation. The resolution of this device is aimed to be 1 mA (corresponding to only 137 nT in the gap) in beam current, corresponding to a system dynamic of around 106 dB ( $2 \cdot 10^5$ ). The results of the magnetic flux simulation deliver the input data for the sensor parameters – the range of the detectable fields can only be influenced by the material choice and geometry optimisation.

## PRINCIPLE INVESTIGATIONS ON MR-SENSORS

The characteristics like hysteresis, linearity and sensitivity of commercial AMR- and GMR-sensors as well as a GMI prototype sensor have been measured within the magnetic field of Helmholtz coils in a range of  $\pm 4$  mT at UNIK (see Figure 9).

The lowest detectable value (S/N) must be determined. Therefore the  $1/f$ -noise, the Barkhausen noise and the thermal noise from the different sensors and the flux concentrator need to be investigated.

## SCRAPING FOR LHC AND COLLIMATION TESTS IN THE CERN SPS

M. Facchini, C. Fischer, J.J. Gras, S. Hutchins, R. Jung  
 CERN, Geneva, Switzerland

### Abstract

Scraping of the SPS beam prior to extraction towards the LHC will be important in order to remove the beam tails and ensure clean injection conditions. Scrapers recuperated from the ISR were installed in the SPS for this purpose. The scrapers are associated with a two stage collimation system using collimators previously installed in LEP to reduce the irradiated area in the SPS.

Tests have been performed to demonstrate that with the help of these collimators, it is possible to scrape with very little contamination outside the scraping area. Another issue was whether enough time is left for ejection towards the LHC after scraping, before repopulation of the removed tails. This was investigated with the SPS rest gas profile monitor and synchrotron radiation telescope.

The system is described and the results of these tests are presented and discussed.

### INTRODUCTION

Scraping of the beam tails will be required in the SPS prior to extraction in order to maintain clean injection conditions into the LHC, hence avoiding the risk of quench in the cryo-magnets. One horizontal and one vertical scraper, recuperated from the ISR, are installed in the SPS and have been used for various tests. The questions addressed were whether enough time is available after scraping to extract before the tails repopulate and what is the achievable sensitivity of the process. The scrapers are associated with one horizontal and one vertical primary collimator installed at a phase advance of 90 degrees and complemented by two secondary collimators located again at 90 degrees from them. Each collimator consists of two moveable blocks. Photomultipliers and ionisation chambers are positioned close to the scrapers and collimators to watch the losses in comparison to the rest of the machine. Tests were also performed to try to confine the radiation induced from the scraping at these locations.

### HARDWARE

#### Scrapers

A scraper consists in a moveable 30 mm copper jaw (Fig.1) activated linearly by a stepping motor and adjusted with a resolution of about 10  $\mu\text{m}$  at a position which determines the amount of current scraped. It is then moved through the beam at a speed of 0.2 m/s by another stepping motor.

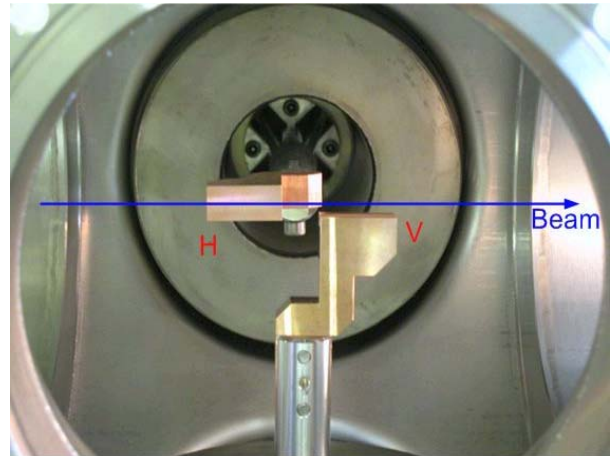


Figure 1: Side picture of the H and V scraper Cu jaws.

#### Collimators

Each primary collimator block is made of a 100 mm long tungsten core inserted within two transition end pieces made of copper, for RF loss minimization and heat extraction. A block has an overall length of 450 mm and can be positioned with a resolution of 5  $\mu\text{m}$  [1]. The collimator blocks are aligned with respect to the beam axis with an rms precision of 0.1mm. Figure 2 shows a picture of the horizontal and vertical primary collimator assembly.

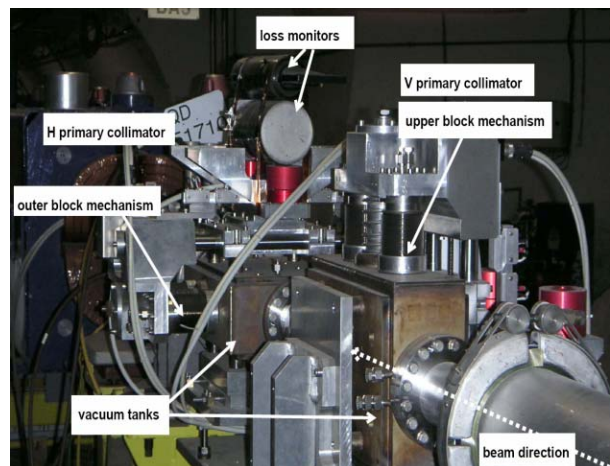


Figure 2: Horizontal and vertical primary collimator tanks and mechanisms with associated loss monitors.

The secondary collimator blocks have shorter copper transition pieces; their overall length is therefore reduced to 250 mm.

# SINGLE BUNCH TRANSIENT DETECTION FOR THE BEAM PHASE MEASUREMENT IN SUPERCONDUCTING ACCELERATORS\*

P. Pawlik, M. Grecki, DMCS, Technical University, Lodz, Poland  
S. Simrock Deutsches Elektronen-Synchrotron, Hamburg, Germany

## Abstract

During commissioning and operation of linear accelerators the beam phase must be determined with respect to the accelerating rf fields. It is desirable to perform these measurements at low beam current and with a short beam pulse duration to avoid unnecessary beam loss during start-up when the correct beam phase is not guaranteed. In the case of the European X-FEL and the International Linear Collider the requirements are to measure single bunch transients at a bunch charge of 1nC to 8nC with an accuracy of a few degrees in phase and a few percent in amplitude in presence of accelerating fields up to 35 MV/m. This implies that transients of the order of 1e-3 must be measured with a few percent resolution resulting in a relative resolution of the order of 1e-5. The concept of the transient detector for the X-FEL is based on nulling method, where the cavity probe signal is split into two branches, one delayed by a up to 100 ns and phase shifted by 180 degrees before adding the two signals. The nulled signal is amplified by 60-80 dB with an rf amplifier and the transient induced by a single bunch is detected by a schottky diode based rf vector detector to achieve the required low noise performance. The principle of rf transient detection, the electronics design and measurements at the VUV-FEL at DESY will be presented.

## INTRODUCTION

The measurement and adjustment of the phase of the accelerating field with respect to the beam phase is essential for the operation of any accelerator. In the case of vector-sum control of many cavities driven by one klystron it is even more important to guarantee the stability of the vector-sum [1]. For this purpose each individually measured cavity field vector is multiplied by a rotation matrix before adding the vectors to the calibrated vector-sum.

The measurement of the relative phase between accelerating field and beam can be based on the beam induced voltage. The measurement can be realized as a transient measurement or as a steady state measurement. In both cases the beam must be turned on and off to detect the change.

\*We acknowledge the support of the European Community-Research Infrastructure Activity under the FP6 „Structuring the European Research Area” program (CARE, contract number RII3-CT-2003-506395), and Polish National Science Council Grant “138/E-370/SPB/6.PR UE/DIE 354/2004-2007”

## PRINCIPLE OF TRANSIENT DETECTION

Single bunch running through the cavity induces RF field vector change called transient (Fig. 1) [2]. This transient is very small and for X-FEL and 3nC bunch at gradient 25MV/m is about 3 orders of magnitude smaller than the RF field. The vector model of the RF field without and with beam presence is shown in Fig. 1. The RF field change induced by the beam is subtracted from the vector of accelerating RF field. For maximum acceleration (on crest acceleration) the beam phase is 0° and the transient vector has opposite direction to the accelerating RF field resulting in a maximum decay in the RF field. For other beam phase the transient adds to the accelerating RF field geometrically. Knowing the phase of accelerating RF field and beam induced transient one can calculate the beam phase.

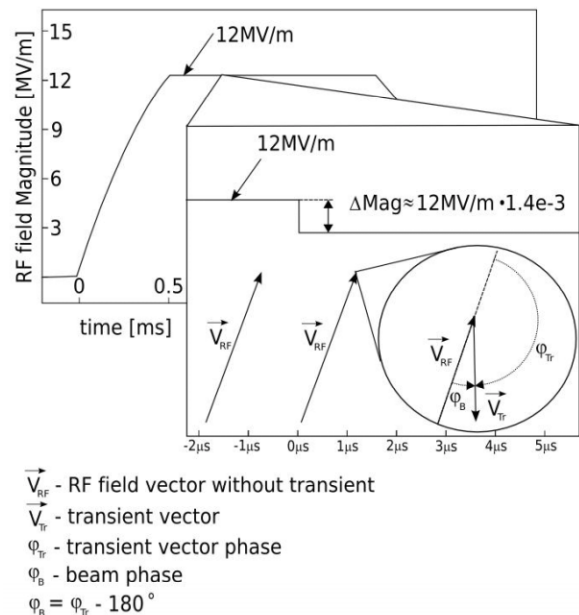


Fig. 1 Single 3nC bunch induced transients

To measure phase of these very small transients it is necessary to reduce carrier 1.3GHz frequency while leaving transients not attenuated. Method that is suitable for this purpose is based on subtracting actual signal from cavity probe from delayed one (Fig. 2) [3]. Short pulse with a width of a time delay is a subtraction result. This pulse carries information about transient.

# RADIATION-HARD BEAM POSITION DETECTOR FOR USE IN THE ACCELERATOR DUMP LINES \*

P. Degtiarenko, D. Dotson, A. Freyberger, V. Popov, Jefferson Lab, Newport News, VA 23606, USA

## Abstract

A new method of beam position measurement suitable for monitoring high energy and high power charged particle beams in the vicinity of high power beam dumps is presented. We have found that a plate made of Chemical Vapor Deposition (CVD) Silicon Carbide (SiC) [1] has physical properties that make it suitable for such an application. CVD SiC material is a chemically inert, extremely radiation-hard, thermo-resistive semiconductor capable of withstanding working temperatures over 1500 °C. It has good thermal conductivity comparable to that of Aluminum, which makes it possible to use it in high-current particle beams. High electrical resistivity of the material, and its semiconductor properties allow characterization of the position of a particle beam crossing such a plate by measuring the balance of electrical currents at the plate ends. The design of a test device, and first results are presented in the report.

## INTRODUCTION

Some of the new fixed target experiments approved for runtime at the Continuous Electron Beam Accelerator Facility (CEBAF) at Jefferson Lab (JLab) require complicated beam steering efforts to keep the electron beam at its nominal position at the face of the beam dumps after it passes through the experimental targets. The new experiments employ magnetic fields in the areas near the target, which are capable of moving the beam away from the dump face and damaging the dumpline equipment with the few hundred-kW beams. Therefore, the problem of reliable beam position measurement in the dumpline areas has become more critical.

Precise and reliable position monitoring of high energy and high power accelerated particle beams in the vicinity of high power beam dumps has always presented a technical challenge. The beam quality in those areas is often very poor, and any equipment positioned there must be extremely resistant to radiation damage. Methods involving Radio Frequency (RF) beam time structure measurements often do not work in these areas due to the RF disturbances, and the disturbances in the transverse beam profiles, caused by beam scattering in the irradiated targets. The methods involving moving parts to perform beam profile scans, and optical beam viewers all require high reliability of the control and measurement equipment working in the high radiation environment.

Until recently, the only means to see the beam position at the entrance of the beam dump tunnel at JLab was a phos-

phorescent viewscreen (Refs. [2], [3]) with a video camera readout system. A special optical design was required to bring the image of the viewscreen to a shielded enclosure, in which a camera could survive the radiation. Despite this effort to protect the optical components, cameras typically have a short lifespan in these conditions, and the viewscreens fail after prolonged irradiation. The need for an independent beam position measurement system for the dumpline has brought us to the subject of this work.

## NEW BEAM POSITION DETECTOR

The schematic drawing of the device is shown in Fig. 1.

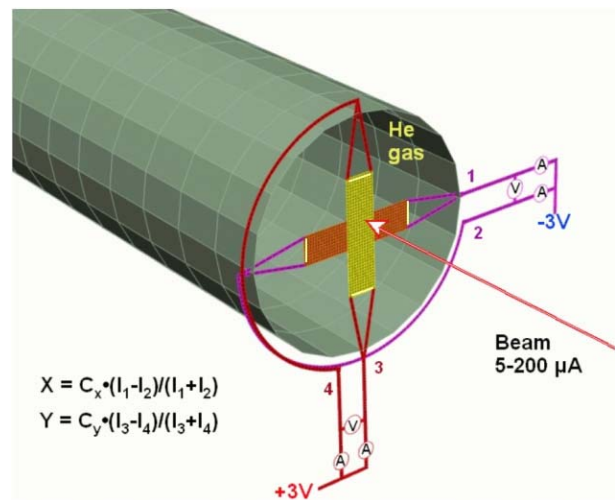


Figure 1: Schematic layout of the BPD.

## General Layout and Detector Design

The Beam Position Detector (BPD) consists of the two thin plates (200x50x0.25 mm) made of CVD SiC material of standard (high) resistivity; typical electric resistance between plate ends is 200-600 kΩ. One of the plates is suspended horizontally, and the other one vertically in the middle of He gas - filled pipe leading to the CEBAF high power beam dump. The plate width was determined by the need to measure the transverse beam position within the 5 cm by 5 cm area, determined by the dimensions of the dump entrance window. The plate thickness was chosen to be as thin as technologically feasible, and the plate length was sized sufficiently large to bring the plate endpoints farther away from the center to avoid the beam damage to the end contacts. The vertical and horizontal plates are separated by 5 mm and are orthogonal to the beam direction.

\* Work supported by the U.S. Department of Energy under contract DE-AC05-84ER40150; U.S. patent pending

# OPTIMISATION OF "SHOE-BOX TYPE" BEAM POSITION MONITORS USING THE FINITE ELEMENT METHODS

P. Kowina \*, W. Kaufmann, J. Schölles and M. Schwickert, GSI, Darmstadt, Germany

## Abstract

The enhancements of the sensitivity and linearity of the position determination are the main goals in the optimisation of the Beam Position Monitors (BPMs) for ion synchrotrons. High position sensitivity can be achieved by the reduction of the coupling capacities and the plate-to-plate cross talks. For instance, the insertion of an additional guard ring into the gap between the active plates increases the sensitivity even by a factor two due to reduction of the cross talk. High linearity is typical for the shoe-box type BPM, however, it might be strongly influenced by discontinuities or/and imperfections of the components which are spoiling the fields homogeneity in the BPM volume. This requires a very careful design, especially in the regions close to the edges of the active plates. The BPM response has been investigated in the frequency range from 0 – 200 MHz. It is shown that the transversal transfer impedance is frequency dependent; however, in the range up to 50 MHz (typical for the BPM applications) it varies only in the order of a few percent. The displayed simulations are performed using CST Microwave Studio.

## INTRODUCTION

Motivation for the investigation described in the present work were the optimisations of the BPM's construction for the HICAT synchrotron dedicated for the cancer therapy [1]. The synchrotron will be operated with the maximal bunch frequency of 6.74 MHz (at the maximal extraction energy). The  $^{12}\text{C}$  and  $^{16}\text{O}$  ions will be accelerated up to 50 – 400 MeV/u.

The investigations presented in this contribution are based on existing constructions of the shoe-box type pick-ups used at Heavy Ion Synchrotron (SIS) and Experimental Storage Ring (ESR) at GSI. The schematic views of the SIS- and ESR-BPMs are shown in Fig. 1.

The typical bunch frequency of SIS and ESR is in the range from 800 kHz up to 5 MHz at the maximal energy of about 1 GeV/u depending on the charge state of the ions.

The ESR BPM construction differs from the SIS one, since only in the ESR pick-ups the additional ground ring in the diagonal cut has been used, see Fig. 1. This separating ring is supposed to reduce the cross talks between the two close laying signal plates. Both setups are equipped with guard rings, however, the width of the guard rings and the width of the cuts between plates and guard rings for SIS- and ESR-like construction are different.

The main objective of the studies was to investigate how the presence of the certain pick-up's components (like

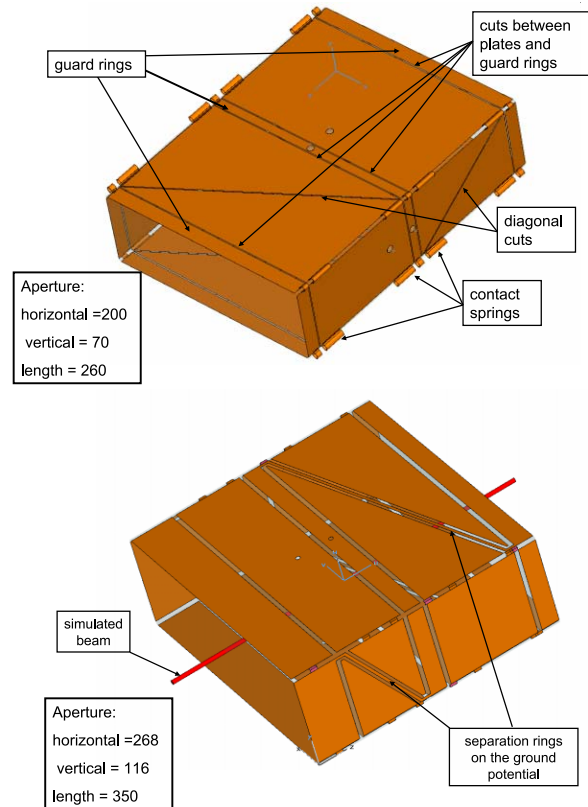


Figure 1: Schematic view of the SIS (top) and ESR (bottom) BPMs— here shown without chassis.

guard rings, separating ring etc.) and their geometrical dimensions influence on the pick-up sensitivity and linearity of the beam position determination.

As the simulation tool "CST Microwave Studio" (CST-MW) version 5 has been used. All simulations were performed using the transient solver.

The bandwidth of 0–100 MHz, typical BPM preamplifiers [2], allows to observe up to the 20 harmonics of the bunch frequency. Since it is interesting, how a BPM behaves in frequency range slightly exceeding this limit the frequency regarded in the simulations was chosen to be in the range of 0-200 MHz.

In the present contribution by "horizontal plates" or "horizontal contact" etc. we understand those pick-up components, which are used for the measurements in the horizontal direction. Analogous nomenclature is used for the "vertical" components.

\* p.kowina@gsi.de

# BEAM LOSS MONITOR SYSTEM FOR MACHINE PROTECTION

B. Dehning, CERN, Geneva, Switzerland

## Abstract

Most beam loss monitoring systems are based on the detection of secondary shower particles which deposit their energy in the accelerator equipment and finally also in the monitoring detector. To allow an efficient protection of the equipment, the likely loss locations have to be identified by tracking simulations or by using low intensity beams. If superconducting magnets are used for the beam guiding system, not only a damage protection is required but also quench preventions. The quench levels for high field magnets are several orders of magnitude below the damage levels. To keep the operational efficiency high under such circumstances, the calibration factor between the energy deposition in the coils and the energy deposition in the detectors has to be accurately known. To allow a reliable damage protection and quench prevention, the mean time between failures should be high. If in such failsafe system the number of monitors is numerous, the false dump probability has to be kept low to keep a high operation efficiency. A balance has to be found between reliable protection and operational efficiency.

## BEAM LOSS MEASUREMENT DESIGN APPROACH

For the design of a safety system, in addition to the standard specifications, like dynamic range, resolution, response time, also a value for the “Mean Time Between Failures” (MTBF) is needed to quantify the level of the protection. The estimate of the MTBF value was based in the case of CERN’s LHC on the SIL (Safety Integrity Level) approach [1]. Other approaches like “As Low As Reasonably Practicable” (ALARP) are also often used. For both approaches the MTBF value is estimated by the calculation of the risk of damage and the resulting down time of the equipment [3]. In the case of a failure in the safety system itself, it will fall in a failsafe state with the consequence of making the protected system unavailable.

The design considerations of a beam loss monitor system for machine protection are schematically shown in Figure 1. In the first row the above discussed key words are listed. A risk requires a safety system which provides protection but it also reduces the availability of the protected system. In the risk column the consequences (damage and quench) of a non nominal operation (beam loss) are listed. A further consequence for both is the increase of the downtime of the accelerator. The risk is scaling with the consequences of the proton loss event and its frequency. From the risk the MTBF value is deduced. This main design criterion for the safety system is listed in the safety column as well as the means (failsafe, redundancy, survey, check) to reach the

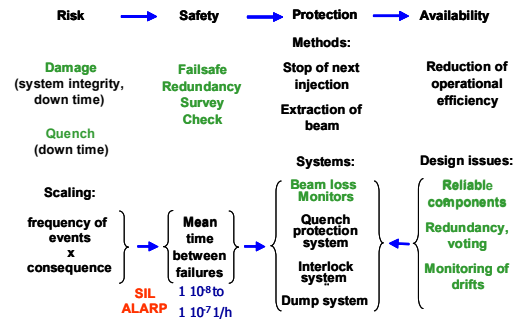


Figure 1: Schematic of the LHC beam loss system design approach (items in green are discussed in this paper).

envisaged MTBF value. In the protection column the methods of protection are listed (stop of next injection and extraction of beam) for a one path particle guiding system (linac, transfer line) and for a multi path system (storage ring). The safety system is consisting of a beam loss measurement system, an interlock system and a beam dump system. In the case of the usage of superconducting magnets, some protection could also be provided by the quench protection system. The availability column lists the means used in the design of the safety system to decrease the number of transitions of the system into the failsafe state. The effect of the components added to the system to increase the MTBF value results in a reduction of the availability of the system. This negative consequence of the safety increasing elements are partially compensated by the choice of reliable components, by redundancy voting and the monitoring of drifts of the safety system parameters (see Figure 1, fourth column). The key words listed in green will be discussed below.

## Damage and Downtime

The damage potential at CERN’s LHC is over two orders of magnitude higher than at all other existing accelerators (see Figure 2), since the stored beam energy given by the product of the single particle energy and intensity is largest at LHC. The consequence of a dangerous proton loss event was “illustrated” by an accidental loss at Fermi labs Tevatron (200 times lower stored beam energy as at LHC) where the proton beam was lost in a duration of a few revolutions melting some components. The loss was initiated by a moveable measurement instrument. The number of such moveable objects at LHC is also an order of magnitude higher than at Tevatron. This example may indicate the risk associated with the operation of LHC like beams leading to downtimes of months or even years.

# DIAGNOSTICS OF ACCELERATOR PERFORMANCE UNDER THE IMPACT OF ELECTRON CLOUD EFFECTS

H. Fukuma<sup>#</sup>, KEK, Tsukuba, Japan

## Abstract

A large number of electrons called electron clouds are observed in many accelerators. The electron clouds produce various effects such as pressure rise, beam induced multipacting, tune shifts, coupled bunch instability, beam size blow-up and so on which often limit performance of the accelerators. Characteristics of the electron clouds are studied not only by direct measurements of the electrons but also by measurements of beam behavior affected by the electron clouds. This paper reviews various diagnostic methods to study the electron clouds with a short summary of the electron cloud effects on the accelerators.

## INTRODUCTION

Many electrons are generated and accumulated in accelerators. Primary electrons can be produced by synchrotron radiation or lost particles hitting a chamber wall, or by ionization of the residual gas. If charge of a beam is positive, the primary electrons receive kicks from the beam toward the center of the beam chamber and hit the opposite wall, then secondary electrons are produced. Under some operational conditions of the accelerators rapid growth of the electrons known as beam induced multipacting can occur. The primary and secondary electrons form a group of the electrons called the electron cloud.

Spatial distribution of the electron cloud is strongly affected by magnetic fields as shown in Figure 1 of Reference[1] as an example. In drift space the electrons concentrate at the center of the chamber. In a dipole magnet several strips of the electrons sometimes appear. In a quadrupole magnet eight spots which have large density of the electrons are seen on the chamber wall. In a solenoid magnet most electrons are confined near the chamber wall.

Energy of the electrons is low, typically less than 100eV [2,3,4]. Owing to a low energy nature of the electrons it is possible to measure the energy distribution by applying a manageable voltage to grids as described later.

The electron cloud is built up along a bunch train [5]. In proton rings with a long bunch the electrons produced on the chamber wall are multiplied toward the tail of the bunch and lead to the trailing edge multipacting. Low energy electrons which stay near the center of the chamber before the bunch comes are trapped in the bunch by the beam potential and released at the tail of the bunch [6]. Due to two mechanisms a large number of electrons are observed at the tail of the bunch. The electrons can be

trapped in a quadrupole and a sextupole magnetic fields as shown by a simulation [7]. The survived electrons between train gaps would lead to accumulation of the electrons by the passage of many bunch trains. The measurement of the time evolution of the electron cloud is thus important to study the characteristics of the electron cloud.

It is mentioned that the electron cloud can affect electron beams as well as positron beams [2,5,8].

## ELECTRON CLOUD EFFECTS AND CURES

The electron clouds produce various effects [9] such as 1) nonlinear pressure rise due to gas desorption by the bombardment of the electrons, 2) electrical noise to instrumentations, 3) beam induced multipacting, 4) heat load to a cold chamber wall of superconducting accelerators such as LHC, 5) tune shifts caused by Coulomb force by the electron cloud, 6) transverse coupled bunch instability mediated by the electron cloud and 7) single bunch (strong head-tail) instability due to the short range "wake" by the electron cloud which causes a beam size blowup. A combined phenomenon of the electron cloud and the beam-beam effect is predicted though it is not yet confirmed by experiments [10].

Various cures have been taken to mitigate the electron cloud effects [9]. Ante-chambers are introduced to reduce the number of the primary electrons from synchrotron radiation. In order to reduce the secondary electrons, processed chamber surface by TiN coating and NEG(TiZrV) coating are used and a grooved surface is considered. The reduction of the secondary electron yield by beam scrubbing is observed. In B factories weak solenoids installed almost all drift space around the ring are very effective to moderate the beam size blowup by the electron cloud. Coupled bunch instability by the electron cloud can be cured by bunch-by-bunch feedback system and Landau damping by nonlinear magnetic fields if the growth rate is not large.

## ELECTRON CLOUD DIAGNOSTICS

Many dedicated or standard instrumentations have contributed to understand the electron cloud effects. They also give the data for a benchmark of simulation programs. In this section diagnostics of the electron clouds themselves are reviewed. Diagnostics of the beam behavior under the impact of the electron clouds are discussed in the next section.

### Pressure gauge

Pressure rise which is caused by desorption of the gas by the electrons hitting the chamber wall, gives an

<sup>#</sup>hitoshi.fukuma@kek.jp

# ANALOG FRONT-END ELECTRONICS IN BEAM INSTRUMENTATION

A. Boscolo - DEEI Trieste University - Italy. boscolo@univ.trieste.it.

## Abstract

The work gives an overview of present and near future technological opportunities for the analog first conditioning and subsequent processing of sensor signal. The interactions between beam sensor capability, their signals characteristics and the system requirements are analyzed from different approaches as: full analog continuous, sampled time discrete, full digital time and amplitude discrete. Special attention will be given to the impact of measurement methods and new devices in circuits and instrumentation architecture design, especially from the metrological point of view

## BASIC INSTRUMENTATION STRUCTURE

In order to reach the paper aim it is better to start little bit away, taking in consideration the basic structure of generic monitoring or control system, figure 1. We can identify several sub systems, characterized by specific functionalities, and devoted to collect some aspects of a physical event, modify them in order to allow the comparison with a reference and codify them in order to make easier any reasoning on it. The first reasoning results can be reprocessed with different strategies in order to reach a specific goal, decoded in physical attribute and actuated on the physic domain.

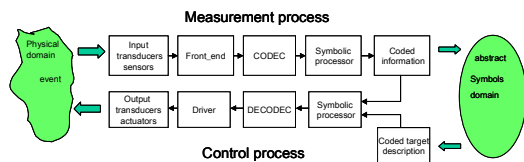


Figure 1. Structure of basic monitoring or control system

From the abstract point of view, in the main loop flow the same information but carried by different physical supports and code figure 2.

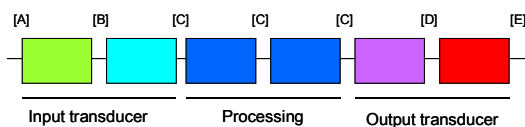


Figure 2. The same information is carried by different physical supports and code.

That is the physical world act as an information source, some of these are captured by a measurement process and converted in to symbols by a coding process, then some actions on the physical world can be performed by reasoning on the coded information and on the activity aim. With this approach we can define a criteria able to identify the transition from the transduction and the processing. We can consider transduction processes where the information carrier change block to block and

processing where the physical carrier is stable. Taking in consideration how the information processing can be performed we can identify two different approaches: first based on a physical platform able to modify the carrier by different and controlled phenomena in order to approximate a required model, the analog solution, and the second based on coding processes and symbols manipulations driven by a defined paradigm, the symbolic or numeric solution. Which is the best? It is not easy to answer this question because the best performances or better the suitable performances depend on a large number of aspects as the system aim, the technology state of art, the number of systems required, the available technologies, the time to market, the available design tools, the cost performance ratio, the compliance with specific regulations, without to neglect the designer know-how and habits, his creativity, and his risk propensity etc. and in the end from the functional and technical specifications as accuracy, resolution bandwidth etc..

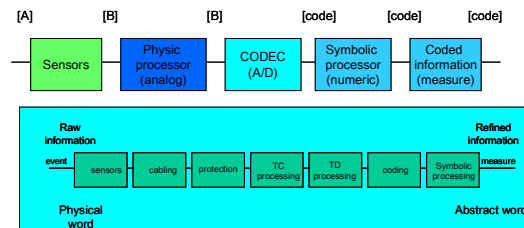


Figure 3. Model of information capture process

The information capture process can be modelled as shown in figure 3 where the coding process can be taken as the border from the physical processing, the analog space, and the symbolic or numeric processing, the digital space, moving this border, basically the A/D converter which perform the measurement process, we can modify dramatically architecture, performance, time delay, cost, knowledge engaged in the design etc. The works aim is to give an overview of some of these aspects and in special manner those related with the analog front end.

## SILICON STATE OF ART

The silicon based integrated circuit (IC) industry has followed a strategy of shrinking device geometries for more than 30 years. With the assumption that the basic MOS transistor will remain the dominant switching device and the silicon will remain the dominant substrate material, it is widely believed that this process will continue for at least another ten years. However, there is great uncertainty about the ability to continue scaling metal-oxide-semiconductor field-effect transistor structures due to the considerable increasingly difficult materials and technology problems to be solved. The strategy of constantly shrinking device geometries and

# FPGA TECHNOLOGY IN INSTRUMENTATION AND RELATED TOOLS

J. Serrano, CERN, Geneva, Switzerland

## Abstract

Field Programmable Gate Arrays (FPGA) have become an alternative to traditional Digital Signal Processors (DSP) in many applications. In some cases, where high throughput is the main concern, an FPGA-based system may in fact be the only solution to fulfil the requirements. In the area of particle accelerators, FPGAs are used in many contexts, ranging from digital feedback loops for power converters and RF cavities to Digital Signal Processing for beam instrumentation. These designs harness the vast amount of logic resources inside FPGA chips to deliver unprecedented performance through parallelism and pipelining. After an introduction to the internal architecture of FPGAs and the design process, including advanced issues such as floorplanning, we look at two important techniques to implement arithmetic in FPGAs: Distributed Arithmetic (DA) and the COordinate Rotation DIgital Computer (CORDIC) algorithm. The goal is not to exhaust the list of Digital Signal Processing techniques for FPGAs, but rather to illustrate ways in which FPGAs are used to maximize performance.

## INTRODUCTION

Programmable logic technology has been a central player in the glue logic and bus interface arena since the 1980's. In the last decade, due to the exponential growth in silicon densities and the maturity of the associated software tools, new segments of the digital design market have found solutions in the FPGA realm. One of the most impressive examples is the growing number of Digital Signal Processing (DSP) systems implemented in FPGAs. Accelerator subsystems, where purely digital applications such as those based on counters and state machines have existed for years, are now benefiting as well from the determinism and the speed of FPGA-based DSP solutions.

While this article presents general ideas applicable to any FPGA manufacturer, the examples and specific terminology, when needed, are those of Xilinx [1] products, with which the author is most familiar.

## FPGA INTERNAL STRUCTURE

The architecture of an FPGA chip is essentially a rectangular array of Configurable Logic Blocks (CLB) interconnected by a programmable routing matrix. Figure 1 shows the internals of a generic chip from the Spartan IIE family, chosen for purposes of illustration due to its simplicity. CLBs can implement basic combinatorial functions and the result of these operations can either be routed directly out of the CLB or be clocked in internal CLB flip-flops before going out to the routing matrix.

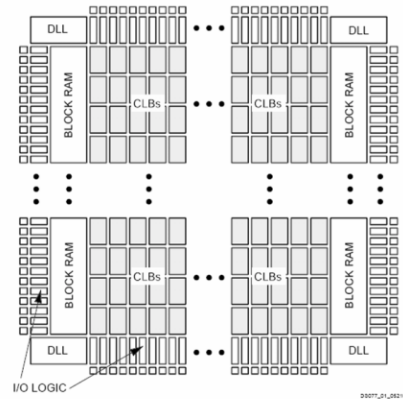


Figure 1. Internal structure of the Spartan IIE family. (Xilinx corp.)

Even in this low-range family, the designer has some extra resources available, namely internal RAM blocks and Delay Locked Loops (DLL) used to manage the phases and frequencies of inter-related internal clocks. Other blocks found in modern FPGA families include, among others, hard-wired Multiply and Accumulate (MAC) units, fast dedicated serial transceivers (useful to cluster several distant FPGA systems in global orbit correction applications) and Digitally Controlled Impedance (DCI) for on-chip high speed signal termination. Figure 2 gives a simplified view of the internals of a CLB.

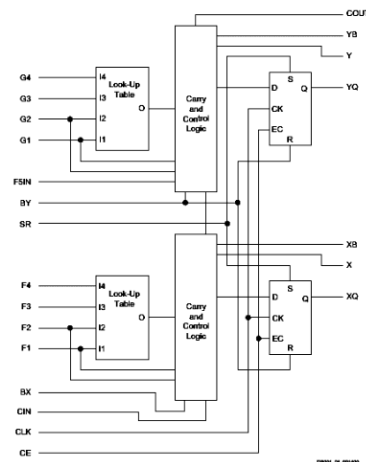


Figure 2. Spartan IIE CLB internal structure. (Xilinx corp.)

The Look Up Tables (LUT) can implement any combinatorial function of four inputs and one output (of the type you would write down using AND and OR operators). An interesting feature is the Carry In (CIN) – Carry Out (COUT) daisy chain, which links each CLB with its two vertical neighbours through dedicated routing

# A NEW TRAJECTORY MEASUREMENT SYSTEM FOR THE CERN PROTON SYNCHROTRON \*

J.M. Belleman, CERN, Geneva, Switzerland

## Abstract

We describe the projected new trajectory measurement system for the CERN PS, currently under design, in which the trajectory of each particle bunch is calculated on the fly from a continuous high-rate stream of digitised PU signal samples. The system will store data for a full acceleration cycle. Multiple clients will then be able to select subsets of the data for further treatment and display.

Using a prototype of the projected hardware, raw PU signals have been accumulated during the 2004 run and processed off-line, validating the algorithms for beam synchronisation and calculation of trajectories for all current and known future beam types (subject to pick-up bandwidth limits) in the PS.

Records of the system behaviour, as implemented by the off-line processing chain and using real pre-recorded pick-up signals, will be shown.

## THE PS

The CERN Proton Synchrotron (PS) is the oldest particle accelerator still operating at CERN. It was commissioned in 1959 as the world's first alternating gradient, strong focusing machine. Still today, it is the kingpin of the CERN complex of accelerators, in which it now serves as the injector machine to the Super Proton Synchrotron (SPS). Today, the PS accelerates mainly protons ( $p^+$ ), but in the near future, it will also produce  $^{208}\text{Pb}^{54+}$  ions for LHC.

## PICK-UPS AND SIGNALS

The particle trajectories are measured with forty electrostatic pick-ups (PUs) distributed around the ring.

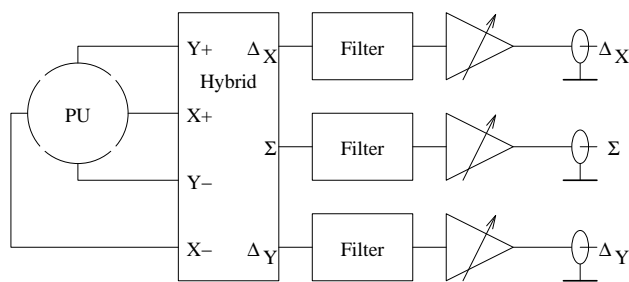


Fig 1 Pick-up analogue signal processing

Passive hybrids combine the electrode signals into a common sum ( $\Sigma$ ) and horizontal and vertical difference signals ( $\Delta_x$ ,  $\Delta_y$ ) (Fig 1). Pre-amplifiers installed near each PU shape and amplify the signals before they are carried over high-quality coaxial cable to the PS central building, where the signals are further treated. A VME-based computer controls the amplifier gains according to the expected beam intensity.

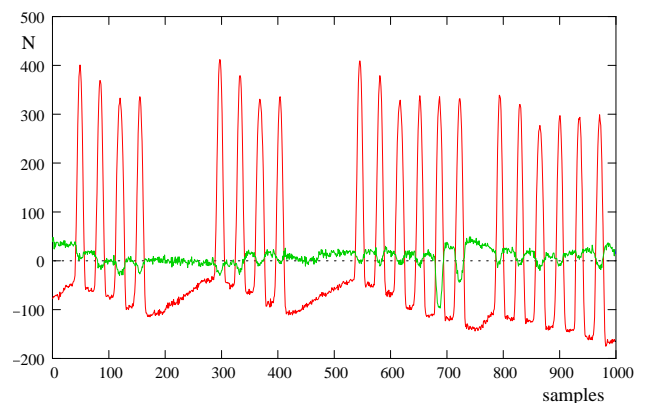


Fig 2 Example of PU signals: LHC beam at 2<sup>nd</sup> injection.  $\Sigma$  and  $\Delta_x$ .

The position of the centre of charge of a particle bunch is derived by integrating the three signals,  $\Sigma$ ,  $\Delta_x$ , and  $\Delta_y$ , over the length of a bunch, and normalising against  $\Sigma$ :

$$x = S_x \frac{\Delta_x}{\Sigma} + E_x \tag{1}$$

Here,  $S_x$  is a proportionality constant expressed in mm, and  $E_x$  is an additive error correction.

## Digital signal processing

The system digitises the analogue PU signals at a constant 125 Ms/s rate. The samples are pre-processed into per-bunch integrals on the fly before being stored in a memory big enough to hold the results for all bunches in the machine for the full duration of an acceleration cycle.

Given that different bunches may follow different trajectories, due, e.g., to being of different intensity, or to being injected at a different time, it is necessary to have a timing reference that can track each bunch from injection all the way through to ejection. The cavity RF is not suitable as a timing reference, because its phase with respect to the beam changes according to whether the beam is coasting or being accelerated, below or above  $\gamma$ -

\* We acknowledge the support of the European Community-Research Infrastructure Action under the FP6 "Structuring the European Research Area" programme (DIRAC secondary-Beams, contract number 515873)



# BEAM DIAGNOSTIC DEVICES AND DATA ACQUISITION FOR THE HICAT FACILITY

A. Peters, T. Hoffmann, M. Schwickert,

Gesellschaft für Schwerionenforschung (GSI), Planckstr. 1, 64291 Darmstadt, Germany

## Abstract

A set of 92 diagnostic devices for beam diagnostics in the **Heavy Ion Cancer Therapy** facility (HICAT) at the university hospital in Heidelberg is currently under development at GSI. All beam diagnostic devices will be fully computer controlled and will allow an automated detection of all relevant beam parameters. The HICAT raster scan method with active variation of intensity, energy and beam size requires the exact knowledge of the time resolved and spatial structure of the ion beam. An overview of the integrated devices is presented, particularly the time-of-flight method for energy measurement using electro-static pick-ups in the Linac is described in detail. The real-time PXI data acquisition system is explained as well as the embedding of the diagnostic devices in the timing and control system of HICAT.

## INTRODUCTION

A first technical proposal for the HICAT facility had been presented in 1998 [1], a more detailed description of the final HICAT layout is given in [2]. The building is under construction since November 2003 and the installation of the accelerator will start in the last quarter of 2005. Fig. 1 shows the final layout of the accelerator facility. The outer dimensions of the accelerator building are 60m x 70m. HICAT consists of a 7 MeV/u-Linac (including the LEBT – low energy beam transport – and the MEBT – middle energy beam transport – lines), a Synchrotron (magnetic rigidity  $B\rho=0.38-6.5$  T·m), two horizontal treatment stations (H-1, H-2), a Gantry-Section for 360°-patient irradiation and additionally a section for Quality Assurance (Q-A).

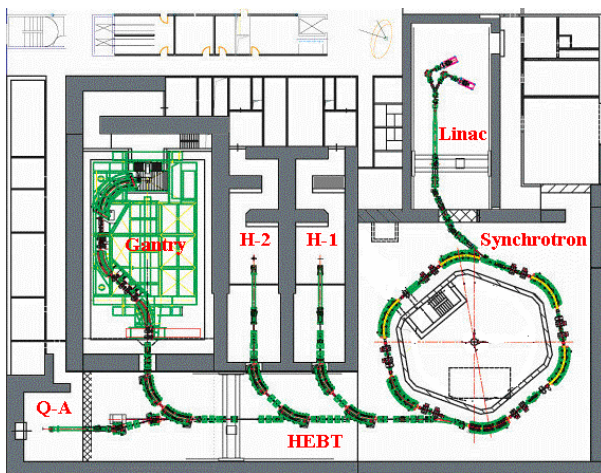


Figure 1: Layout of the first underground floor, housing the accelerator complex [2]

## BEAM DIAGNOSTICS AT HICAT

Because no industrial supplier could be found, the beam diagnostics group at GSI was charged with the delivery of all measuring systems. The mechanical parts, such as detectors, linear vacuum feed-throughs, etc. are produced by GSI with sub-contractors. For the software and the electronic devices, however, commercial solutions with industrial partners were preferred.

Table 1: Overview of beam diagnostic devices for HICAT

Device	Qty.	Position	Device class
Faraday-cup (cooled/uncooled)	7	Linac	DC/AC-beam current
Profile grid	8	Linac	Profile measurement
El.-static pick-up	4	Linac	Phase measurement
DC-transformer	3	Lin/Sync	DC-beam current
AC-transformer	4	Lin/Sync	AC-beam current
Position monitor	6	Sync	Beam position
Beam loss mon.	6	Sync	Particle counting
Ioniz. chamber	13	Sync	Particle counting
Viewing screen	12	Linac/Sync/HEBT	Optical diagnostics (2D-Profile-Meas.)
Scintil. Counter	5	HEBT	Particle counting
MWPC	13	HEBT	Profile measurement
Isocenter-diagnostic screen	4	T1-T4	Optical diagnostics (2D-Profile-Meas.)
Slits	4	Linac	Command device
Foil stripper	1	Linac	Command device
Scraper	2	Sync/HEBT	Command device

The 92 beam diagnostic devices were deliberately assorted to measure all relevant beam parameters (current, energy, beam profile, position and phase information) of the therapy accelerator [3]. Concerning the layout of the electronic hardware the basic idea was to use industrial standards to a maximal degree, in order to achieve a good maintainability of all devices and, as a consequence, to enhance the reliability of the HICAT facility. For example, all data acquisition is uniformly carried out using 11 separate PXI-controllers running LabViewRT [4], as will be described in detail below.

## **BREMSTRAHLUNG DETECTION AND CHAMBER OBSTRUCTION LOCALISATION USING SCANNING RADIATION DETECTORS**

G.A. Naylor, B. Joly, D. Robinson, ESRF, Grenoble

### *Abstract*

Radiation monitors consisting of scintillating plastic coupled to photomultipliers are used for diagnostic purposes. By scanning such a detector or a radiation scatterer, two applications are demonstrated:

- i) Monitoring of vacuum chamber conditioning by monitoring gas Bremsstrahlung from residual gas.
- ii) Localisation of beam interception (beam losses) by longitudinal scanning of a radiation detector.

The measurement of gas pressure inside long, small cross section, vacuum vessels is difficult due to the distance between the centre of the vacuum vessel and vacuum gauges (leading to a low vacuum conductance). The narrow beam of gamma Bremsstrahlung radiation is intercepted by scanning tungsten blades in the beam line front-end allowing a radiation shower to be detected outside the vacuum vessel proportional to the gas pressure in the corresponding storage ring straight section. A second detector mounted on rails can be moved over a length of 6.5m parallel to the ESRF storage ring so as to localise regions of beam loss. The location of a scraper and narrow chamber entry and exit points are clearly resolved.

**NO SUBMISSION RECEIVED**

# THE INSTRUMENTATION OF THE TI8 SPS TO LHC TRANSFER LINE

L. Jensen, CERN, Geneva, Switzerland

## Abstract

The new TI8 transfer-line between the SPS and the future LHC was commissioned during two long machine development sessions in autumn 2004. This paper will present the beam instrumentation linked to the extraction region and along the line from the design and installation up to the tests with beam. After minor modifications copies of these systems will be used for the TI2 transfer-line to be commissioned with beam in 2007.

## INTRODUCTION

The LHC Transfer & Injection (LTI) project started for the BDI group in 2002 with the arrival of the functional specifications [1] and the beginning of the official coordination meetings.

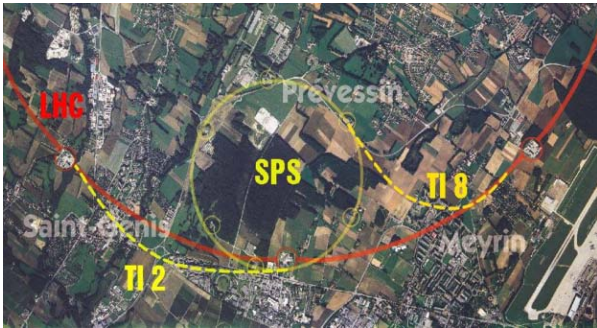


Figure 1: Aerial view of the SPS to LHC transfer-lines

## BDI INSTRUMENTS

From the user requirements, the hardware implementation choices for the different systems were made. Some of the systems below had already been tested with beam in 2003 during tests of the extraction system and the first ~100m of the TI8 transfer line (TT40) [2]. The systems involved are:

- A beam position interlock linked to a pickup in the extraction region (named BPCE) that should allow the extraction of the beam only if the bumped position (nominally close to 30mm) is within pre-programmed limits. To acquire the turn-by-turn position data, the existing SPS orbit system (MOPOS) was used. A dedicated real-time action utilising the pickup linearization algorithm described in [3] was developed and the interface to the interlock system took place through the prototype LHC beam interlock controller (BIC) module [4].

- A beam-loss interlock monitoring the losses during the extraction process. If a problem occurs during the slow (~100 msec) ramping of the orbit corrector bumpers, this system should dump the circulating beam to avoid damaging the downstream extraction elements (septa etc). To cover this requirement, 8 dedicated ionisation chambers were installed in the extraction region, with the fast loss detection system [5] connected to the SPS emergency beam dump.
- A total of 15 beam profile monitors (BTVI) (see figure 2) were requested from the SPS extraction region through to the end of the TI8 transfer-line. They are used to acquire the 3D images of the signal produced when the beam passes through a screen made of either alumina (for luminescence) or titanium (for OTR). New mechanisms to select the filter (for signal attenuation) and the screen position were designed and could be controlled from the newly designed BTVI VME acquisition and control card [6]. To avoid signal cable lengths of more than 3km, VME acquisition systems were positioned at either end of the transfer-line. A dedicated PC system with digital video transmission over Ethernet was



provided to allow the remote real-time observation of a selected screen.

Figure 2: A TI8 beam profile monitor (BTVI)

- Fast beam current transformer devices (see Figure 3) installed at either end of the TI8 transfer-line to measure the transmission of the beam through the line. Fast 40MHz integrators allow the measurement of individual bunches spaced by a multiple of 25ns. More information about the Fast BCT systems can be found in [7].

## IMPROVING THE RELIABILITY OF IPM\*

D. Liakin, V. Skachkov , ITEP, Moscow, Russia, P. Forck, T. Giacomini<sup>#</sup>, GSI, Darmstadt, DE64291, Germany

### Abstract

IPMs measure in a non-destructive way the profile of ion beams independent whether the beam is bunched or not. Our application is the heavy ion synchrotron SIS, which can accelerate ions with a large variety of different masses and charges. The IPM is used to obtain information about the beam matching, the electron cooling and to support for any kind of machine experiments. To ensure reliable function and to increase the data accuracy we executed some important mechanical improvements. The resistive E-field plates were replaced by discrete electrodes. We designed a new MCP-Phosphor-screen assembly of rectangular shape and large active area and in addition a module with a filament mounted in meander shape to monitor the degradation of the MCPs. The whole device was planned with respect of high field uniformity and small mechanical dimensions at a large clearance for the beam.

### INTRODUCTION

Ionization Profile Monitors (IPM) are used in synchrotrons and storage rings to measure the beam profile. The IPM at the GSI heavy ion synchrotron (SIS) measures every 10ms a full beam profile, horizontal and vertical. At the end of the cycle the data are automatically analysed and the users can view the beams evolution of the whole synchrotron cycle. The beam profile and the beam position provide information about the injection matching and the accelerator setting and adaption. The beamwidth shows the effects of electron cooling and of multiple injections, it also gives a hint of beamlosses during the cycle. The benefit of these measurements is connected to the reliability and long term stability of the IPM and the trustiness of the obtained data. The environmental conditions for IPMs are usually vacuum bakeout and long maintenance intervals. Once installed or modified the IPM is not accessible for a long time, often for several years. These conditions make it necessary to restrict the number of functional parts and to control most parameters from outside the vacuum. The device has to be achieved in a way that it withstands all possible burdens during long term operation. The quality and the long term stability of the electrical field (E-field) that accelerates the ionized particles perpendicular to the beam is most important for a true image of the beam. A rectangular (Multi-Channel-Plate) MCP-Phosphor screen assembly fits best the needs of an IPM. These devices are only in concentric form commercially available. We developed a rectangular device with an active area of 100mm by

22mm. The IPM is designed to have the freedom of detecting residual gas ions and electrons. When detecting residual gas electrons the residual gas ions will produce secondary electrons at the bottom of the E-field box. The resulting signal complicates automatic analysis of the data. Therefore a secondary electron suppression is needed. The amplification of MCPs degrades during operation. Partially the areas of the MCP degrade at most where the density of impacts by residual gas particles is biggest. The degradation must be observed careful to obtain a beam profile correction function. A filament can be used both as secondary electron suppression and to generate a test signal for the MCPs.

### ELECTRICAL FIELD BOX

The original E-field design of the IPM was based on resistive side electrodes made of glass coated with germanium [1]. Cracks in the germanium layer occurred probably because of the rough environmental conditions like big temperature changes during multiple vacuum bakeout and the different thermal coefficients of the glass sheet and the coating. The cracks prevented a constant conductivity of the resistive layer. By time the potential difference was equalized by sparks and thus the beamprofiles were strongly deformed. That made it nearly impossible to analyse the IPM data automatically.

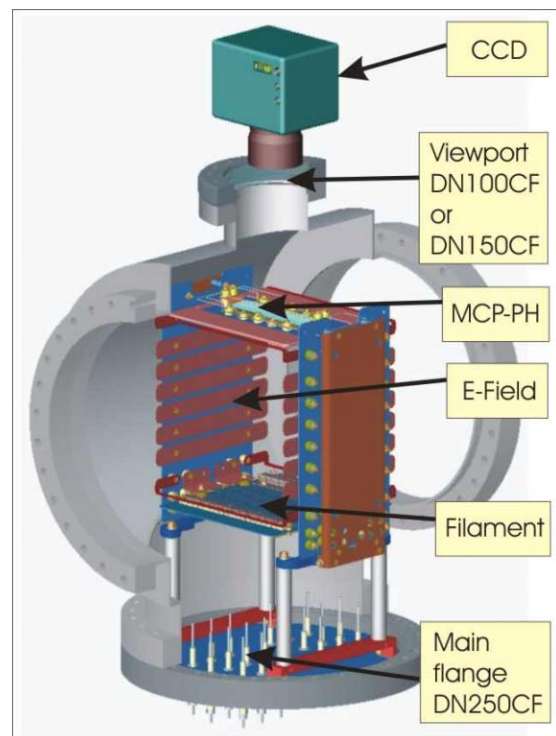


Fig. 1: E-field box vertical side electrodes, double layer filament, corrector electrodes, rectangular MCP-Phosphor assembly.

\* Funded by INTAS, Ref. No.: 03-54-3931

<sup>#</sup> T.Giacomini@gsi.de

# **DETERMINATION OF BEAM CHARGE USING STRIPLINE SIGNALS AT THE RF FREQUENCY BY FAST SIGNAL PROCESSING IN A FPGA**

G.A. Naylor, B. Joly, ESRF, Grenoble

## *Abstract*

Traditional methods of measuring beam charge requires integration of a signal from a fast current transformer. Ultimately the integral of a transformer signal is zero, practical measurements are achieved by taking a finite integration, which leads to some error. In the method proposed here the signal at the carrier frequency (RF frequency) is sampled (from a stripline) and demodulated in an FPGA to determine the total charge. By time multiplexing the stripline signals from different parts of the accelerator complex, cross calibration can be achieved.

**NO SUBMISSION RECEIVED**

# CURRENT STATUS OF THE ADVANCED RESIDUAL GAS MONITOR FOR HEAVY ION SYNCHROTRON APPLICATIONS\*

D.Liakin<sup>#</sup>, V.I.Skachkov, S.Barabin, O.Sergeeva (ITEP, Moscow), P.Forck, T.Giacomini (GSI, Darmstadt), Vic.Skachkov, A.Vetrov (MSU, Moscow), A.Paal (MSL, Stockholm).

## Abstract

The challenge and complexity of the advanced RGM requires very careful design of each structural component and special attention to match the properties of different subsystems. In the present paper the status of the high performance readout electronics is discussed. Single optical decoupled profile measurement channel (one of 100) with 14 bit resolution and 10 MHz bandwidth was tested and step-by-step improved. Special attention had been paid to the noise cancellation and digital data processing algorithms optimization.

Another important point is a proper electromagnetic guiding system design. As it is shown, high field homogeneity, which is required for sub-mm spatial resolution, can be achieved despite the presence of the field distorting hole for the light signal transmitting. The low energy (down to 10MeV per nucleon) beam disturbance compensation methods are also discussed. The ionization process and electron dynamics simulations are used for proving this system design.

## THE STATUS OF THE FAST PROFILE READOUT ELECTRONICS

The advanced RGM structure was described in details in [1] and [2]. It will cover profile measurements with 0.1 microseconds of time and 1mm spatial resolution. A phosphor coated Microchannel Plate (MCP) is proposed as a wide bandwidth high resolution primary detector. A bundle of 100 optically decoupled from the signal source digitizing channels will allow fast measurement option in addition to the slow profile measurements with a CCD camera. Avalanche photodiode (APD) is used as a light receiver to provide required bandwidth, sensitivity and dynamic range. The saturating of the MCP output basically limits the signals level, therefore low noise operation is mandatory [3]. The structure of the data acquisition channel is shown in Fig. 1.

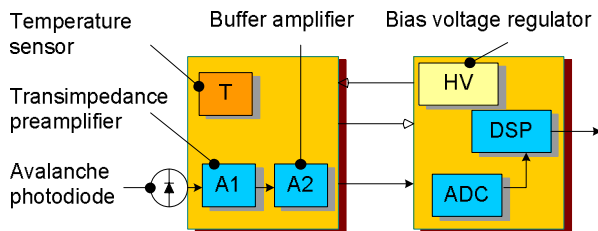


Figure 1: The structure of one photodiode readout channel

A two-module structure was chosen to build a compact, EMI protected head with embedded photodiode and to

connect it to a more sophisticated data processing module. To diminish an induced noise and EMI a two-stage preamplifier (A1 and A2) is placed in the head. The sensor T provides the APD temperature which is then used by a digitally controlled high voltage source (HV) to fix the APD multiplication factor. A 14 bits 65MHz ADC sampling rate exceeds the Nyquist frequency, which reduces the requirements to the analog antialiasing filter.

The test setup consists of the readout channel itself, a wide bandwidth LED emitter fed by a signal generator, Hamamatsu's wide band optical receiver and personal computer for control and data presentation. A serial connection was used to communicate with the PC. A dedicated control software had been designed for the DSP and PC to provide a suitable Windows interface with graphical output. A real-time data filtering and decimation algorithms were implemented in C code for fast on-line data processing in the DSP. Three frequency bands were used to cover full frequency range of further applications.

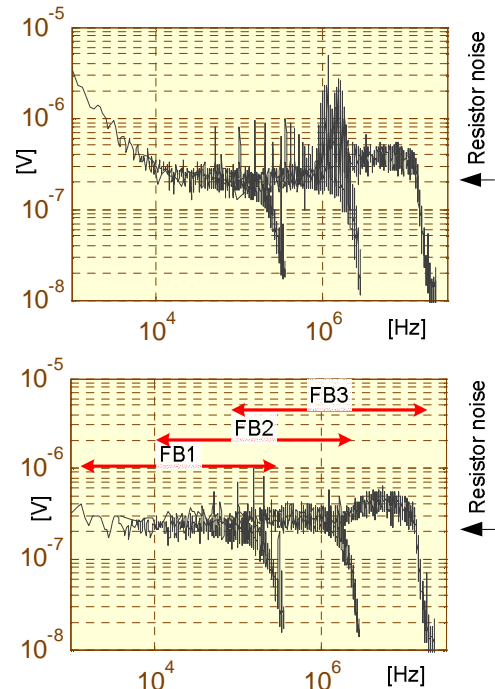


Figure 2: Preamplifier output noise (amplified) before (on the top) and after optimisation

To measure the frequency response of the readout channel the noising properties of the avalanche photodiode were used. The shot noise of a photodiode grows like square root of DC current or incoming light intensity, therefore an illuminated APD can be interpreted as a white noise generator. This APD feature was used to

\*Work supported by INTAS, Reg.No.:03-54-3931

<sup>#</sup>liakin@itep.ru

# OPTICAL DESIGN FOR BIPM IMAGING SYSTEM

D. Kramer, B. Dehning, C. Fischer, S. Hutchins, J. Koopman, CERN, Geneva, Switzerland

## Abstract

The light imaging system for the Beam Ionization Profile Monitor (BIPM) was designed to allow simultaneous operation of a fast Multi Anode Photo Multiplier and two new types of intensified standard resolution CCD cameras.

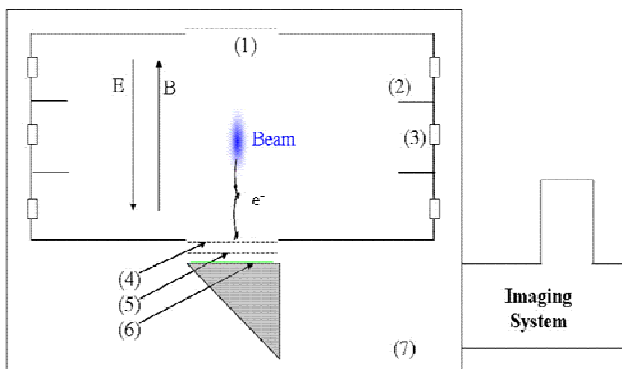
The main reason for designing the optics was the poor resolution of the preliminary setup limiting seriously the detectors performance and the need of a second optical path for the Multi (32) Anode Photo Multiplier (MAPMT). An increase of the optical luminosity was also necessary for low intensity beams. Optimization of the optical system was done in the ZEMAX program.

The imaging error was checked by comparing the ionization profile monitor continuous measurements with wire scanner measurements.

## INTRODUCTION

The BIPM uses the rest gas in the vacuum beam pipe as ionizing medium where electrons are produced during every beam passage. These electrons are accelerated in a uniform vertical or horizontal electric field and are forced to spiral along the magnetic field lines, which are parallel to the electric field. The Electrons are multiplied by means of an MCP and subsequently hit a phosphor plate get converted into photons.

The density profile of the beam is transformed to the spatial distribution of the photons. The image formed on the phosphor plate has to be properly imaged to a CCD and MAPMT placed outside of the vacuum tank. A new Imaging System (Fig. 1) was designed for the detector.



- (1)...HV Cathode grid
- (2)...Field homogenization electrodes
- (3)...Resistors
- (4)...Multi-Channel Plate (MCP<sub>in</sub>) entrance electrode
- (5)...MCP<sub>out</sub> exit electrode
- (6)...Phosphor plate deposited on indium tin oxide and fused silica reflecting optical prism
- (7)...Vacuum tank

Figure 1: BIPM detector schematics.

## DESIGN TARGETS

The main design parameter was the paraxial magnification. It was calculated simply as  $m = \text{image size} / \text{object size}$ . Object size was the length of the phosphor screen and for the image, the shortest side of the larger CCD element was used.

Maximal lens diameter was fixed to 50.2 mm due to the width of the viewing port in the IPM dipole magnet where the light path was leading. The overall system length was limited to approx. 70 cm, including the camera's body. The position of the light splitter was defined by the geometry of the mechanics. It was decided not to place any optics inside the vacuum tank.

Two new CCD type sensors were considered: an EM (Electron Multiplied) CCD and an EB (Electron Bombarded) CCD providing light amplification. It was needed to tilt the EB CCD by 90° (see Fig. 2).

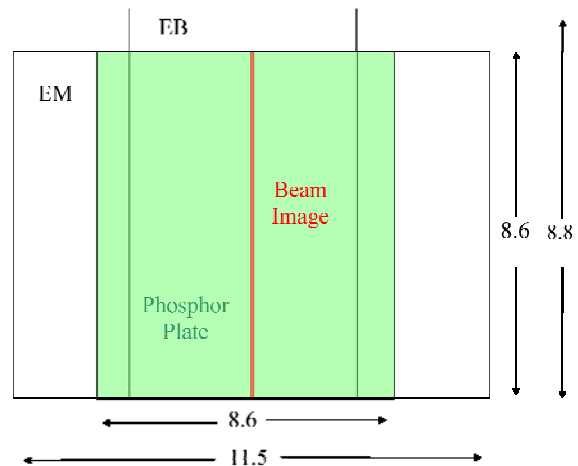


Figure 2: Size and orientation of EM and EB CCDs.

Focusing of the system had to be possible in a reasonable range and the designed optics had to fit inside the C-mount system and have a reasonable cost.

The numerical aperture in the image plane had to be reasonably restricted, because the CCD elements do not accept rays at high angles.

The imaging aberrations should be kept below 1% with respect to the measured transverse beam size.

## DESIGN CONCEPT AND STARTING POINT FOR OPTIMIZATION

Two commercially available doublets are placed between the vacuum window of the detector and the splitting prism with an aperture stop amid. Magnification of this part is matched to the MAPMT and no more lenses are used downstream the splitter. The doublets are optimized for the infinite object position, but as the light

# SIMULATION OF AN ELECTRON SOURCE BASED CALIBRATING SYSTEM FOR AN IONISATION PROFILE MONITOR

H. H. Refsum\*, B. Dehning†, J. Koopman, CERN, Geneva, Switzerland

## Abstract

Measurements have shown that the gain of the imaging system of the Ionisation Profile Monitor (IPM) changes over time, in a non-homogenous way. This ageing effect is caused by changes in the Micro Channel Plate (MCP) channel wall secondary emission coefficient, due to electron scrubbing. The MCP is only capable of emitting a limited number of electrons during its lifetime, and after a large number of electrons have been emitted, the gain is gradually reduced. To measure this ageing effect, and to be able to compensate for it, a remote controlled, built-in calibration system was developed. An Electron Generator Plate (EGP) produced by Burle, Inc. was used as the electron emitter for the calibration system. In this paper, computer simulations of the system is presented. Promising results were obtained from these simulations. Results from experiments conducted at low magnetic fields, coincide with the results of the simulations. Both simulations and experiments indicate that the proposed calibration system should not deteriorate the performance of the IPM during beam profile measurements.

## INTRODUCTION

### The IPM Operation Principle

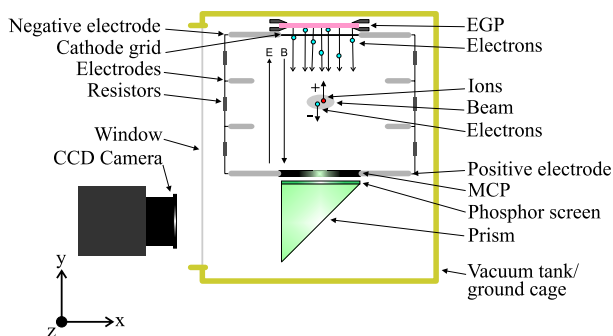


Figure 1: Working principle.

A sketch of the operating principle of the IPM, is shown in Fig. 1. The operating principle of the IPM is based on the ionisation of rest gas atoms and molecules by the passing beam due to the imperfect vacuum. In Fig. 1 the beam is passing in the z-direction, into the paper. Ions and electrons are liberated, and drift up or down respectively, due to the applied electric field. The electric field is created by applying high voltage to the electrodes at the top and bottom

of the cage. The voltages applied are typically -1 to -2 kV for the upper electrode (cathode), and +1 to +2 kV for the lower electrode (anode). Consequently the direction of the electric field is in the +y-direction. The distance between the cathode and anode is 84 mm. The lateral electrodes of the IPM, connected through resistors, are included to increase the homogeneity of the electric field. The function of the cathode grid is to prevent secondary electrons, created when ions hit the grounded chamber, from returning into the HV cage of the IPM.

The electron distribution in space, reflecting the transverse density distribution of the particle beam, is forced down to the anode by the applied electric field. A Micro Channel Plate (MCP) measuring 5.08 cm by 5.08 cm is situated at the anode, and this is used to image the distribution. The function of the MCP is to amplify the electrical current from the incoming electron distribution. The amplified electron distribution then hits a phosphor screen. The phosphor screen converts the electron distribution into a photon distribution, which is viewed by a CCD camera, via a prism. A magnetic field of up to 2000 Gauss is added in addition to the electric field. The direction of the magnetic field is in the -y-direction, as indicated in Fig. 1. The magnetic field, together with the initial velocity, cause the electrons to spiral at a small radius, while the electric field forces them down towards the anode.

### A New Calibration System

One of the difficulties encountered with the current IPMs, is the too rapid and non homogenous ageing of the MCPs. The ageing mainly affects the area of the MCP where the beam is imaged, causing a local decrease in the gain of the MCP. The reduction of the gain is caused by changes in the channel wall secondary emission coefficient due to electron scrubbing. The MCP is only capable of emitting a limited number of electrons during its lifetime, after a large number of electrons have been emitted, the gain is gradually reduced [2].

Because the MCP images the beam more or less in the same position throughout its lifetime, the gain is reduced more in the centre of the MCP than at the edges. With time, this causes distortion to the images created of the beam. In the LHC the IPM is intended as a continuous beam observation device. The ageing of the MCPs is therefore an important issue, as regularly replacement of the MCPs is both difficult and costly, and would have to be done during machine shutdown.

To measure the ageing effect, and to be able to compensate for it, a remote controlled, built-in calibration system is to be developed. The calibration system consists of an elec-

\* helge@refsum.net

† Bernd.Dehning@cern.ch

# SQUID BASED CRYOGENIC CURRENT COMPARATOR FOR MEASUREMENTS OF THE DARK CURRENT OF SUPERCONDUCTING CAVITIES

W. Vodel, S. Nietzsche, R. Neubert, R. Nawrodt, Friedrich Schiller University Jena, Germany  
A. Peters, GSI Darmstadt, Germany  
K. Knaack, M. Wendt, K. Wittenburg, DESY Hamburg, Germany

## Abstract

A newly high performance SQUID based measurement system for detecting dark currents, generated by superconducting cavities for the upcoming X-FEL project at DESY Hamburg, is proposed. It makes use of the Cryogenic Current Comparator principle and senses dark currents in the pA range with a measurement bandwidth of up to 70 kHz.

## INTRODUCTION

The linear accelerator technology, based on superconducting L-band (1.3 GHz) cavities, is currently under study at DESY [1]. The two 10 km long main LINACs (linear accelerator) are equipped with a total of nearly 20,000 cavities. A gradient of 23.4 MV/m is required for a so-called superstructure arrangement of couples of 9-cell cavities. To meet the 2×400 GeV/c energy upgrade specifications, higher gradients of 35 MV/m are mandatory.

The dark current, due to emission of electrons in these high gradient fields, is an unwanted particle source. Two issues are of main concern:

- Thermal load: An emitted electron from the cavity surface follows a path along the electric field lines and will most probable hit somewhere else onto the cavity wall. This leads to an additional thermal load in the cryostat, which has to be covered by the liquid helium refrigerator.
- Propagating dark current: If the energy gain is sufficient, the electrons will generate secondary particles when hitting the cavity wall which then also may generate secondaries. In the following avalanche process some electrons may pass through the iris of the cavity cell and will be further accelerated. In this case the dark current along the LINAC would grow exponentially if on average more than one electron passes the complete FODO (focus/defocus lattice) cell.

Recent studies [2] show that the second issue seems to be the more critical one. It limits the acceptable dark current on the beam pipe "exit" of a TESLA 9-cell cavity to approximately 50 nA. Therefore the mass-production of high-gradient cavities with minimum field emission requires a precise and reliable measurement of the dark current in absolute values.

The presented apparatus senses dark currents down to a few nA. It is based on the cryogenic current comparator (CCC) principle, which includes a highly sensitive LTS SQUID as magnetic field sensor. Further on the setup contains a faraday cup and will be housed in the cryostat of the CHECHIA cavity test stand.

## REQUIREMENTS FOR DARK CURRENT MEASUREMENT APPARATUS

Electrons can leave the niobium cavity material if the force of an applied external electric field is higher than the bounding forces inside the crystal structure. The highest field gradients occur at corners, spikes or other discontinuities, due to imperfections of the cavity shape. Another potential field emitter is due to any kind of imperfection on the crystal matter like grain boundaries, inclusion of "foreign" contaminants (microparticles of e.g. In, Fe, Cr, Si, Cu) and material inhomogeneity. At these imperfections the bounding forces are reduced and electrons are emitted under the applied high electromagnetic fields [3]. With a series of special treatments the inner surface of the TESLA cavities are processed to minimize these effects. A reliable and absolute measurement of the dark current allows the comparison of different processing methods and a quality control in the future mass-production.

TESLA will be operated in a pulse mode with 5 Hz repetition rate. The 1.3 GHz r.f. pulse duration is 950  $\mu$ s. During this time the dark current is present and has to be measured. Therefore a bandwidth of 10 kHz of the dark current instrument is sufficient. As field emission is a statistical process, the electrons leave the cavity on both ends of the beam pipe. Thus, half of the dark current exits at each side, and has to be measured on one side only. With the 1.3 GHz r.f. applied, we expect that the dark current has a strong amplitude modulation at this frequency. This frequency has to be carefully rejected from the instrument electronics to insure its proper operation and to avoid a malfunction of the SQUID. This is realized by the help of careful r.f. shielding, appropriate filtering of all leads feeding to the SQUID input coil, and the low pass characteristic of the transformer used.

The use of a cryogenic current comparator as dark current sensor has some important advantages:

- measurement of the absolute value of the dark current,
- independence of the electron trajectories,
- accurate absolute calibration with an additional wire loop, and
- extremely high resolution.

The required working temperature of 4.2 K (boiling temperature of LHe) for the apparatus is unproblematic to provide because the CHECHIA test stand includes the whole cryogenic infrastructure for cooling the niobium cavities. In order to enable the CCC to measure the magnetic field of the dark current only, an effective shielding against external magnetic fields has to be realized.

## PROFILE MONITORS FOR WIDE MULTIPLICITY RANGE ELECTRON BEAMS

B. Buonomo, G. Mazzitelli, L. Quintieri, Laboratori Nazionali di Frascati LNF - INFN  
 A. Bulgheroni, C. Cappellini, M. Prest, Univ. Insubria e INFN Sez-Milano  
 L. Foggetta, Consorzio Interuniversitario per la Fisica Spaziale, CIFS  
 A.Mozzanica, Univ Milano e INFN Pavia  
 E. Vallazza, INFN Trieste Via Valerio, 2 I - 34127 Trieste- Italia  
 P. Valente, INFN Sez Roma ,P.le Aldo Moro, 2 - 00185 Roma - Italy

### *Abstract*

The DAFNE Beam Test Facility (BTF) provides electron and positron beams in a wide range of intensity, from single particle up to  $10^{10}$  particles per pulse, and energy, from a few tens of MeV up to 800 MeV. The pulse time width can be 1 or 10 ns long, and the maximum repetition rate is 50 Hz.

The large range of operation of the facility requires the implementation of different beam profile and multiplicity monitors. In the single particle operation mode, and up to a few  $10^3$  particles/pulse, the beam spot profile and position are measured by a x-y scintillating fiber system with millimetric resolution and multi-anode PMT readout. From a few tens up to  $10^{6-7}$  particles per pulse, a silicon chamber made of two  $9.5 \times 9.5$  cm<sup>2</sup> wide 400um thick silicon strip detectors organized in a x-y configuration with a pitch of 121um has been developed. Once calibrated, the system can be used also as an intensity monitor. The description of the devices and the results obtained during the data taking periods of several experiments at the facility are presented.

### INTRODUCTION

The DAFNE Beam Test Facility (BTF), operational in Frascati LNF since November 2002, is a beam transfer line optimized for the production of a pre-determined number of electrons or positrons. The main applications of the facility are: high energy detector calibration, low energy calorimetry, low energy electromagnetic interaction studies, detector efficiency and aging measurements, test of beam diagnostic devices, etc.

An attenuating target intercepting the primary Linac beam, together with a system of collimating slits (both along the horizontal and vertical coordinate) and an energy selecting dipole magnet, allows to fine-tune the beam intensity, momentum and spot size, according to the users requirements. The characterization of the beam thus requires several diagnostic devices, optimized in the full range of multiplicity and energy. The facility has been operating both in the single particle production scheme and the high multiplicity operation mode almost continuously since November 2002.

The sensitivity of any standard beam diagnostics (beam current monitors, fluorescence flags, etc.) is not sufficient,

especially in the single particle mode, so that several particle detectors have been used and developed to monitor the BTF beam characteristics during the users running periods. These detectors were mainly intended for the measurement of the number of particles in the beam pulses, in a typical momentum range of 20-800 MeV. However, a very important point for the operation of the facility is the measurement of the beam spot position and size. The typical beam spot at the end of the DAFNE Linac is fairly gaussian, with millimetric size in both the transverse (x-y) coordinates, and is efficiently transported by the BTF transfer line. The exit windows of the BTF beam line have been realized with a thin (500 um) Be alloy, so that the beam size is not spoiled by multiple scattering. The required accuracy for a beam profile detector is then of the order of 1 mm or better.

For this purpose, two different beam profile monitors, a scintillating fiber detector and silicon beam chamber, have been designed, built and tested during the last year. The detectors are described together with some details on the construction and the readout of the systems; and some experimental results with the BTF beam are also reported.

### BEAM PROFILE MONITOR WITH SCINTILLATING FIBER DETECTOR

In order to have a measurement of the beam spot with millimeter accuracy, we have developed and realized a beam hodoscope, consisting of scintillating fibers coupled to multi-anode photomultipliers. This detector has been in fact designed to cope with the wide range of beam conditions, both in energy and multiplicity, and the typical beam spot characteristics[1].

A detector composed of few layers of 1 mm scintillating fibers should be at the same time fully efficient for single electrons and not saturated at intermediate intensities. We built a two views detector of  $48 \times 48$  mm<sup>2</sup> active area. Each one of the two planes of the detector, arranged at 90 degrees with respect to each other, is composed of four layers of fibers staggered by a half-diameter (0.5 mm). Three fibers in width and four in depth are glued together with optical glue and are bundled. Each 12 fibers bundle, corresponding to an active width of 3 mm, is coupled to a pixel of two 16-channels multi-anode photomultipliers (Hamamatsu H6568). The analog signal of each pixel is

# THI SAFETY SYSTEM

Christophe Jamet, Thierry André, Pascal Anger, J.L. Baelde,  
Clément Doutressoulles, Bernard Ducoudret, E. Petit, Eric Swartvagher  
GANIL, BP 55027, 14076 Caen Cedex 5, France

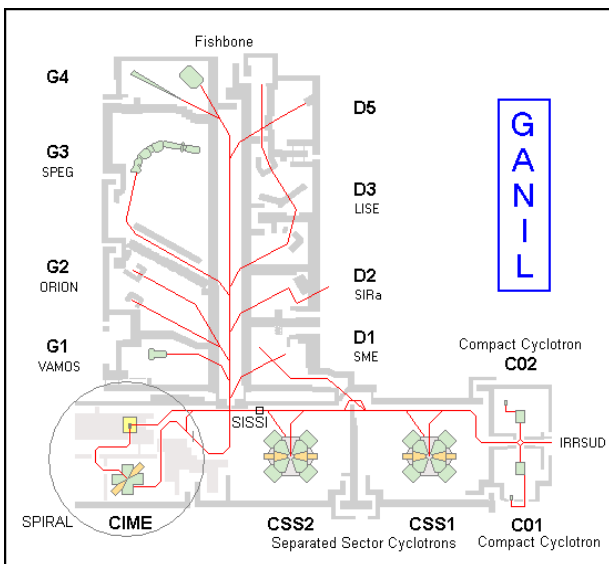
## Abstract

For several years, GANIL has been allowed to reach a maximum beam power of six kilowatts (400W in normal mode) thanks to the THI system (High Intensity Transport System). Three modes of running are necessary to accelerate a THI beam ("Injector" mode, "tuning" mode and "surveillance" mode). The "surveillance" mode requires a safety system to protect equipment against beam losses. Inside cyclotrons, diagnostics measure beam-loss currents at the injection and extraction devices. Along beam lines, diaphragms measure beam-loss currents at the input and output of dipoles. Current transformers are used for beam transmission measurements through beam lines and the cyclotrons. The safety system controls beam losses and quickly cuts the beam with a chopper if losses exceed thresholds. These thresholds can be seen and changed by software.

## INTRODUCTION

The production of exotic ions at GANIL is performed by fragmentation of the projectile in the target of SISSI [5] or/and by the ISOL method with an acceleration of the exotic beams by the cyclotron CIME [3].

### Layout of GANIL



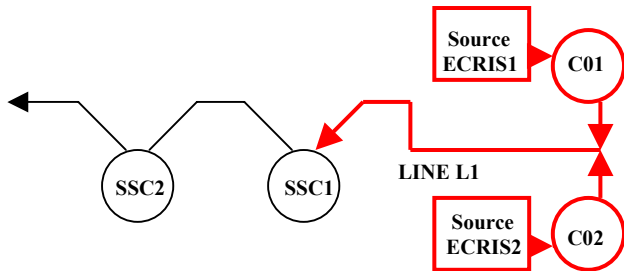
Both devices require high intensity primary beams. Primary beam intensity has been increased up to  $15\mu\text{Ae}$  (3kW) for  $^{13}\text{C}$  at 95MeV/A and  $26\mu\text{Ae}$  (5kW) for  $^{36}\text{Ar}$  at 95MeV/A. Therefore, uncooled or unshielded elements can melt very rapidly and must be protected by a safety system.

## THI MODES

Three modes of running are necessary to tune a THI beam. C01 or C02 can be chosen to post accelerate the THI beam.

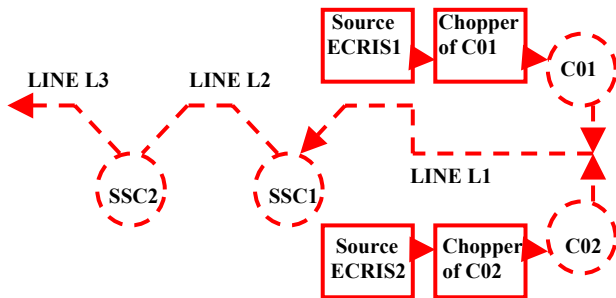
### “Injector mode”

This mode permits us to accelerate the beam at the input of SSC1. ( $P_{\text{beam}} < 400\text{W}$ )



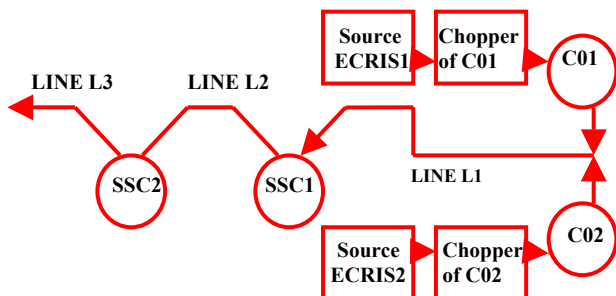
### “Tuning mode”

This mode permits us to tune the beam through the accelerators. Beam chopping rates limit the beam power ( $P_{\text{beam}} < 400\text{W}$ )



### “Surveillance mode”

This mode permits us to tune the beam at a maximum power ( $P_{\text{beam max}} = 6\text{kW}$ ). Beam current average is increased progressively by changing beam-chopping rates. The safety system controls beam losses.



## BEAM DIAGNOSTICS INSTRUMENTATION FOR THE HIGH ENERGY BEAM TRANSFER LINE OF I.P.H.I.\*

P. Ausset, S. Berthelot, J. L. Coacolo, J. Lesrel, J.N. Maymon, A. Olivier, N. Rouvière, M. Solal,  
L. Vatrinet, J.F. Yaniche, I.P.N. 91406 Orsay, France  
G. Belyaev, I. Roudskoy, I.T.E.P. Moscow, Russia.

### *Abstract*

I.P.H.I. is a High Intensity Proton Injector under construction at Saclay (C.N.R.S./I.N.2P.3; C.E.A./D.A.P.N.I.A and C.E.R.N. collaboration). An E.C.R. source produces a 100 keV, 100 mA C.W. proton beam which will be accelerated at 3 MeV by a 4 vanes R.F.Q. operating at 352.2 MHz. Finally, a High Energy Beam Transport Line (H.E.B.T.) will deliver the beam to a beam stopper and will be equipped with appropriate beam diagnostics to carry intensity, centroid beam transverse position, transverse beam profiles, beam energy and energy spread measurements for the commissioning of I.P.H.I. These beam diagnostics will operate under both pulsed and C.W. operation. Transverse beam profile measurements will be acquired under low and high duty factor pulsed beam operation using a slow wire scanner and a C.C.D. camera to image the beam-induced fluorescence. The beam instrumentation of the H.E.B.T. is reviewed and preliminary obtained transverse profile measurements at 100 keV are described.

### INTRODUCTION

IPHI is a high intensity proton injector (C.N.R.S./I.N.2P.3, C.E.A./D.A.P.N.I.A and C.E.R.N. collaboration) and has been designed to be a possible front end for High Power Proton Accelerator (HPPA) devoted to fundamental and applied research: radioactive beams production, neutron sources, neutrino factories and transmutation. IPHI consists of an E.C.R. proton source SILHI (100 mA, 95 keV), under operation at the present time, followed by a Low Energy Beam Transfer Line (LEBT). A Radio Frequency Quadrupole (length: 6m), operating at 352 MHz will then accelerate the proton beam up to 3 MeV. Finally, the High Energy Beam Transfer line (HEBT) will transfer the beam to a beam stopper. Following the necessary commissioning period, a reliability test (several months) operation of the RFQ will be conducted with the support of EUROTRANS (FP6). In the frame of the SPL (Superconducting Proton Linac) study at CERN, a 3 MeV test stand, designed to become the low energy part of the new linear accelerator "Linac4", is being built. The beam acceleration will be performed by the RFQ of IPHI which will be moved from CEA/Saclay to CERN for this purpose. Downstream the RFQ, a chopper line will deliver the beam to the Linac 4 with the appropriate time structure.

IPHI is planned to work under C.W. operation but during tests and commissioning periods, pulsed mode operation has to be considered.

### BEAM DIAGNOSTICS

#### *General considerations*

The general layout of the HEBT is shown in Figure 1. The straight section (dipole "off") will be equipped with beam diagnostics in order to:

- Help to the safe transport of the proton beam to a beam stopper able to withstand the full power of the beam: 300 kW in the C.W. mode operation.
- Provide a sufficient characterization of the beam accelerated by the RFQ during the commissioning period and the daily operation.
- Operate under pulsed mode (pulsed mode operation of the ECR source) for machine commissioning or experimental operation, and under the planned CW operation.
- Test and evaluate non intrusive techniques for measuring transverse beam profiles of high average power beams: Due to the large quantity of beam energy deposited in any possible intrusive sensor leading to its destruction and the resulting high activation induced level in the accelerator structure, non interceptive beam diagnostics have to be put on operation in HPPA.

The deflected section (dipole "on") is primarily devoted to energy spread measurements under pulsed mode beam operation (low average beam power operation). For this purpose, an object slit will be located in the straight section before the dipole and an image slit followed by a Faraday cup at the end of the deflected section.

### BEAM CURRENT MEASUREMENT

This is probably the most important measurement to achieve. RFQ beam transmission efficiency will be drawn from this measurement:

#### *C.W., Low duty factor pulsed mode operation:*

This measurement will be achieved by a DC beam current transformer: a MPCT manufactured by Bergoz Company. It will be housed in a magnetic shielding and placed after the second dipole doublet.

- Resolution reaches 10  $\mu$ A according to at least a one second integrating signal duration and the bandwidth ranges from 0 to 4 kHz.

#### *Pulsed mode operation:*

Under this mode operation, the duration of the beam pulse is expected to be as low as 100  $\mu$ s and the repetition

## A CURRENT MODE INDUCTIVE PICK-UP FOR BEAM POSITION AND CURRENT MEASUREMENT

M. Gasior, CERN, Geneva, Switzerland

### Abstract

An Inductive Pick-Up (IPU) senses the azimuthal distribution of the beam image current. Its construction is similar to a wall current monitor, but the pick-up inner wall is divided into electrodes, each of which forms the primary winding of a toroidal transformer. The beam image current component flowing along each electrode is transformed into a secondary winding, connected to a pick-up output. Such sensors are operated in the CERN CTF3 Drive Beam Linac [1]. This paper describes a similar device developed for the CERN Linac 2 to PSB transfer line. To cope with two orders of magnitude longer beam pulses, the new sensor is operated in current mode. The transformers drive transresistance amplifiers (TRA), converting transformer currents into voltages, which in turn are processed by an active hybrid circuit (AHC), producing one sum ( $\Sigma$ ) signal, proportional to the beam current, and two difference ( $\Delta$ ) signals proportional also to the horizontal and vertical beam positions. The bandwidth of the  $\Sigma$  and  $\Delta$  signals spans 6 and 5 decades, respectively. The transformers have an additional one-turn winding to which a pulse from a precise current source can be applied to calibrate the sensor.

### INTRODUCTION

The Linac 2 can deliver 50 MeV proton beams of up to some 200 mA in 100  $\mu$ s pulses to the PSB. The beam position in the transfer line is currently measured with 20 magnetic pick-ups (MPUs) [2] installed 30 years ago, which now show signs of fatigue. Their mechanics is very complex (e.g. 4 layers of magnetic shielding) and in case of a failure, there are no spare parts. To prepare for a future upgrade of the position measurement system, one of the MPUs was replaced by a recently developed IPU [3]. A successful result with this pick-up would allow the new system to be based on this type of sensor, equipped with an acquisition system very similar to that of CTF3 [4]. This solution would require relatively little manpower. In addition, contrary to the old MPUs, the new IPU can measure the beam current, eliminating the need for many of the separate beam transformers.

The IPU cross-section is shown in Fig. 1. Photographs of its components and the installed sensor are shown in Fig. 2 and 3, respectively. The body A, made from anodized aluminium, houses the ferrite cylinder B, surrounding 8 electrodes C. The separate vacuum assembly D with Helicoflex flanges contains a ceramic insert. The insert is titanium coated on the inside with the optimal coating resistance determined by the method described in [5]. The plate E accommodates 8 current transformers F, through which go M5 copper screws, closing the primary transformer circuits. The transformers

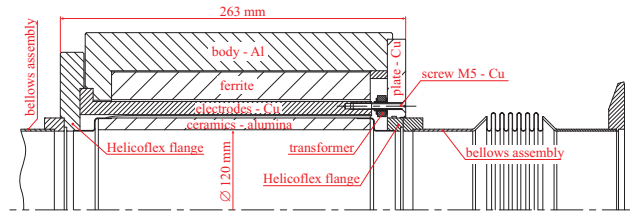


Figure 1: The IPU cross-section.

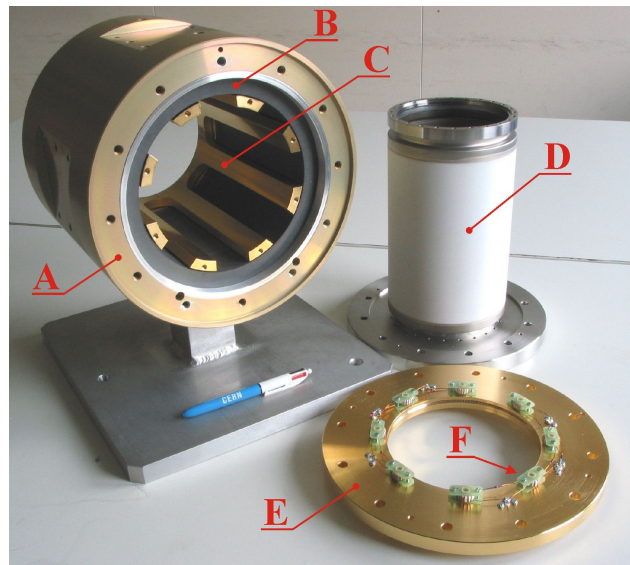


Figure 2: The IPU parts.

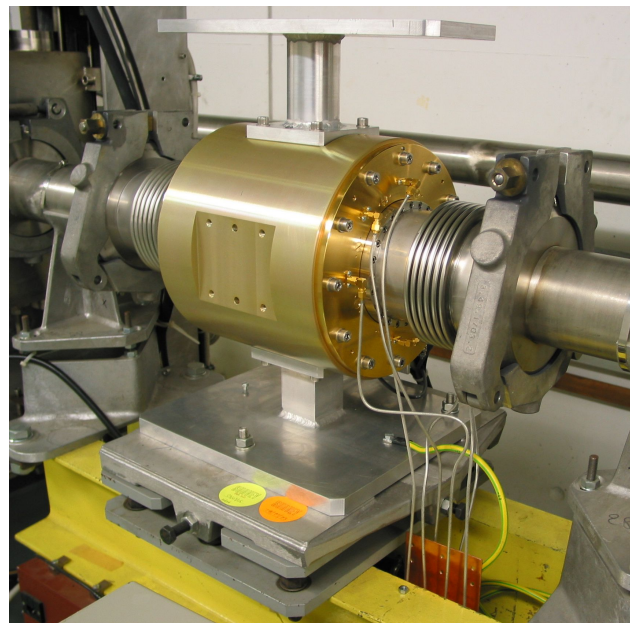


Figure 3: The IPU installed.

## RESULTS FROM THE SPS 1.7 GHz TRAVELLING WAVE SCHOTTKY MONITOR

M.E. Castro, F. Caspers, T. Kroyer, R. Jones, J.P. Koutchouk, G. Tranquille,  
CERN, Geneva, Switzerland

### Abstract

A 1.7 GHz waveguide Schottky detector system was recently built and installed in the SPS accelerator following the design of the detectors of the Fermilab Tevatron and Recycler accelerators. The waveguide detector is designed to measure the transverse and longitudinal Schottky signals of the accelerator at a frequency high enough to avoid coherent effects. This paper describes the first tests carried out with the Schottky detector using LHC type beams. The principal goal of these tests was to check whether such a detector can be used for transverse Schottky diagnostics in LHC.

### INTRODUCTION

Using a suitable detector, one can detect fluctuations in the instantaneous number and position of particles in a circular accelerator. The frequency spectrum of these signals consists of a set of lines at integer multiples of the particle revolution frequency, and a second set which is shifted in frequency from the first one due to the particles' betatron motion. If the beam is bunched, the synchrotron motion splits each line into a set of satellite lines. One can use Schottky signals to obtain a variety of information on a particle beam without perturbing it [1].

Slow wave slotted waveguide pickups were installed in Tevatron and Recycler accelerators at Fermilab and they are used as a means of non-destructive measurement of betatron tunes, chromaticity, momentum spread ( $dp/p$ ), transverse emittances and the synchrotron frequency.

First data obtained from the detector installed in the CERN SPS clearly show Schottky betatron lines and even a faint signal with pilot beam without gating.

### SCHOTTKY PICKUPS

A travelling wave Schottky pickup consists of a rectangular beam pipe with two waveguides on either side (Figure 1). The wall between waveguide and beam pipe is made of slotted thin aluminium foil for coupling signal into the waveguide. This kind of detector is bi-directional and is used in FNAL to provide both proton and antiproton signals [2].

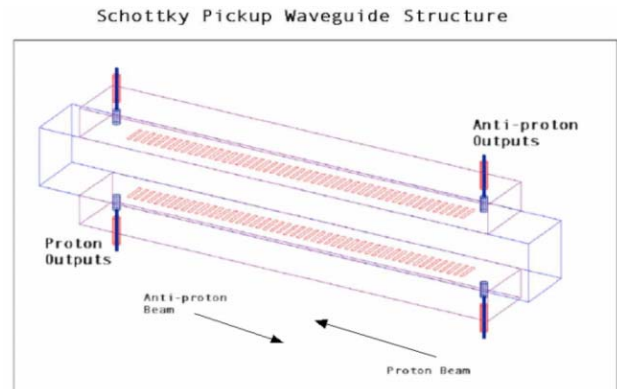


Figure 1: Schottky Pickup design

The designed operating frequency is approximately 1.745 GHz for the DELTA mode and 1.813 GHz for the SUM mode. The Schottky PU at CERN has been used as a vertical detector and tuned for an operating frequency of 1.8 GHz which is a multiple of 40 MHz LHC and 200 MHz fixed target beams harmonics.

### EXPERIMENTAL SET-UP

Measurements were taken using both Delta and Sum signals coming out from the arms of the pickup. The Sum signal is an indicator of the longitudinal sensitivity of the detector whilst the Delta signal was used to get the transverse Schottky spectrum.

In the tunnel, Sum and Delta signals were obtained from the pickup by means of a 180° hybrid. Each of the plates was connected to a set of mechanical attenuators in such a way that attenuation for each channel could be varied in steps of different attenuations between 0 and 7.5dB (Figure 2). The objective of the attenuators was to minimize the longitudinal signal (common-mode lines) in the transverse spectrum by trying to electrically center the beam in the pickup. The control of the attenuators was done from the surface. The Delta signal was fed into a narrowband filter installed in tunnel and centered at 1.803GHz. Taking into account the attenuation of the cables carrying signals to surface (~12dB), the Sum signal provided 100V<sub>peak-peak</sub> and the Delta signal 10V<sub>peak-peak</sub>.

The signal processing was done using a conventional FFT analyzer (SR785 Dynamic Signal Analyzer). The frequency range of the device goes from 195.3mHz to 102kHz and, since signals are expected to appear at frequencies around 1.8GHz, the whole spectrum needed to be shifted to that interval. To do that, a further filtering and two down mixing stages were employed.

# PETRA PROTON BEAM PROFILING BY VIBRATING WIRE SCANNER

S.G. Arutunian, K.G. Bakshetyan, N.M. Dobrovolsky, M.R. Mailian, L.A. Poghosyan,  
I.G. Sinenko, H.E. Soghoian, I.E. Vasiniuk (YerPhI), K. Wittenburg (DESY)

## Abstract

A vibrating wire scanner (VWS) based on the strong dependence of the wire oscillation frequency on temperature was developed and used in the 15 GeV/c proton beam of the proton accelerator PETRA II at DESY. The results show an enormous sensitivity of the scanner and the possibility to use it for weak particle beams and beam halo profiling. Details of the measurements and the results are given. Some investigations of the frequency and the Q-factor of the vibrating wire oscillations dependence on vacuum level are presented.

## INTRODUCTION

Vibrating wire scanners are based on the extremely sensitive dependence of the wire natural oscillations frequency on its temperature [1-6]. On the other hand, the wire temperature depends on the number of interacting particles/photons with the wire.

In this paper experiments with the vibrating wire scanner on a 15 GeV/c proton beam at PETRA are presented. The dependence of Q-factor of the wire on the vacuum pressure is also discussed. This method might give some additional measuring potential to the VWS.

## EXPERIMENT IN PETRA

The experiments in PETRA were done on the proton beam in the bypass, where the electron and proton beams are separated in different beam pipes. Such place was chosen to avoid electromagnetic disturbances induced by electromagnetic wake-fields on the wire, which are much larger for short electron bunches than for long proton bunches.

The vibrating wire resonator consists of a quartz support with a coefficient of thermal expansion of a few  $10^{-7} \text{ K}^{-1}$  and a beryl-bronze vibrating wire with a coefficient of thermal expansion of  $17.5 \times 10^{-6} \text{ K}^{-1}$  [7]. Such a ratio of coefficients provides sensitivity to both surrounding media temperature variations and wire heating by the beam. The beryl-bronze vibrating wire passed preliminarily thermal treatment. More details of the experimental setup can be found in [6].

### Park Position

The wire of the VWS in its parking position had a distance to the beam center of  $6.7 \sigma$ . Beam parameters:  $I = 10 \text{ mA}$ ,  $\sigma_x = 0.6 \text{ cm}$ ,  $\sigma_y = 0.5 \text{ cm}$ . The short term frequency stability was 0.01 Hz at a stable room temperature and at absence of the beam.

Fig. 1 represents the typical picture of the scanner frequency change in park position during 30 hours. The proton and electron beams currents in PETRA are also

presented. Note that during an absence of both beams the frequency changed smoothly connected with the temperature changes of the whole pickup while during operation of electrons and protons the variations are much larger. The temperature change in the chamber without beam can be estimated from the data to about  $7^\circ \text{C}$ . In the presence of proton beam current the frequency behaviour depends on current intensity. At currents less than 50 mA the wire frequency changes are proportional to the beam current while at higher currents probably the electromagnetic disturbances also have influence on the frequency/temperature by absorbing some modes.

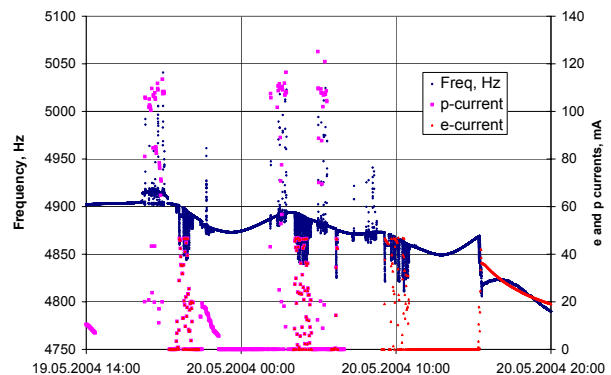


Figure 1: Dependence of VWS frequency on time in park position. Available values of proton beam and electron beam currents are also presented.

Conclusion: Even at a distance of  $6.7 \sigma$  from the proton beam the VWS has a sensitivity of about 1 Hz/mA.

### Scanning

The main mechanism of heat transfer is the thermal conductivity along the wire. The thermal equilibrium time  $\tau$  can be roughly estimated from the equality of the power scattered due to thermal conductivity  $(4\lambda S(T - T_0))/l$  ( $T$  is the temperature in the middle of the wire,  $\lambda$  is the coefficient of thermal conductivity,  $S$  and  $l$  are the cross-section and length of the wire) and power, necessary to maintain the wire at given temperature  $\rho S l c (T - T_0)/(2\tau)$  ( $\rho$  is the wire material density,  $c$  is the thermal capacity). From this equality we obtain  $\tau = c \rho l^2 / 8 \lambda$ . For beryl-bronze wire of total length 36 mm this time is about few sec. In these experiments the scanning was done at speed 0.5 mm/sec.

Before the scans some vertical and horizontal corrections of the beam position at the scanner were done.

Fig. 2 shows a scan started at a distance of 40 mm from the vacuum chamber center. Two scintillators with photo-multipliers PM1 and PM2 were installed in the

# DIGITAL BEAM POSITION MEASUREMENT AT GSI-SIS AND CERN-PS

A. Galatis, A. Peters, GSI, Darmstadt, Germany  
 J. Belleman, Uli Raich, CERN, Geneva, Switzerland  
 A. Zoubir, Darmstadt University of Technology, Germany.

## Abstract

New, digital BPM techniques needed in hadron machines, accelerating beams with fast varying frequencies, are to be presented. The role of analog electronics is reduced to signal amplification and attenuation as well as bandwidth limitation. This paper explores approaches for the position evaluation of acquired signals, suggesting systems for "free running" estimation as well as machine timing dependent methods. For accurate determining of the transversal bunch position, a good integration window estimation is needed. Two filtering methods will be introduced for this purpose, median and FFT filtering, both methods detecting peaks at bunch signal starting and ending points. Parallel to those a digital PLL approach is discussed in [1].\*

## PROBLEM DEFINITION

Beam position measurement and monitoring has a significant role in beam diagnostics. It can allow better controlling and regulation of the beam and can be used for estimating global feedback mechanisms. Both need a fast and accurate estimation for obtaining better results. Different approaches have been summarized in [2]. The problem is classified into two different tasks, hard- and software.

### Hardware demands:

In order to have sufficient sample data points, while taking into account even short bunches of 30ns FWHM length, a sampling speed of 125MSa/s will be used. ADC resolution has to be large enough to be able to realize observations of transversal position movement in the order of 0.1mm. This fact and considering calculated signal dynamics of the SIS100, a resolution of 14 bit will be needed. The first processing will be done inside an FPGA, which will produce bunch integral data. Due to the high sampling rate and the resulting very short processing time while running the FPGA at sampling speed, complex calculations have to be made off-line and proposed software solutions for first data processing have to be as time efficient as possible to allow bunch-by-bunch resolution. After pre-processing, data rates will decrease to  $h \cdot f_{REV}$  ( $h$  being the machine harmonic). In order to also be able to use the hardware setup as a fast digitizer to record full acceleration cycles, sufficient RAM has to be provided.

\* This project is part of the EU-RP6 SIS100 design study, collaborating members of this subtask being CERN-AB, GSI-SD, I-Tech, TUD and FZ-Jülich.

### Software demands:

Fast, online calculation of bunch signal integrals and centre of charge position should be achieved. Since the information primarily needed is the integration over a single bunch and not over all recorded data points, the algorithms determining the limits of a bunch structure will have to be running at full ADC sampling speed. This paper addresses only the software part of the described problem.

## PROBLEM SOLUTIONS

As mentioned, integration windows have to be estimated in order to have fixed boundaries on bunch signals. For obtaining those windows, efficient algorithms for online calculation have to be developed. Two methods for determination will be discussed below.

### Method 1: Median Filtering

Median filtering introduces a method using a window of  $N$  samples length. Data is filtered according to

$$y(n) = \frac{x(n)}{|\text{median}(x(n) + \dots + x(n+N))|}$$

The filter smoothes the signal form, filtering out peaks and noise, allowing better estimation of the starting and ending points of a bunch. The variable length of the window indicated by  $N$  can be modified to get better results. Since this method is strongly dependent on the used filter window length, different lengths have been tested, with a good estimation level achieved for a length of 16 samples, even for poor SNR. In order to get less falsely detected bunch signals a version will be tested, which adapts the filter window length according to the revolution frequency.

### Method 2: FFT calculation and interpretation

The FFT method implements a function that detects variations in the high frequency parts of signal spectra, which correspond to bunch signals emerging from baseline. A short-time FFT (DFT) is taken at consecutive parts of the signal. We again define windows at which we calculate the FFT. We expect to see a rise towards the higher frequency band in a transition from the baseline level to a bunch signal. From the general FFT we can get:

$$\begin{aligned} x(k) &= \frac{1}{N} \sum_{n=1}^N X(n) e^{2\pi i(n-1)(k-1)/N} \\ &= \frac{1}{N} (X(1)e^0 + X(2)e^{2\pi i(n-1)/16} + \dots + 0) \end{aligned}$$

All  $X(n)$  for  $n > 2$ , when using only two data points, are equal zero. It is obvious that for certain  $X(n)$  ( $X(n)$  being

# DESIGN OF A FAST ORBIT FEEDBACK FOR SOLEIL

N. Hubert, L. Cassinari, J.C. Denard, A. Nadji, L. Nadolski, D. Pédeau  
SOLEIL, Gif-sur-Yvette, France

## Abstract

SOLEIL is a third generation light source under construction. Great care is taken at all levels of the machine design in order to reach beam stability at the micrometer level. In particular, a fast global closed-orbit feedback is foreseen for suppressing remaining beam vibrations up to 100 Hz.

The correction uses the computing resource of 120 BPM electronic modules, distributed around the storage ring. Each BPM module includes a powerful FPGA that in addition to its specific BPM task leaves enough room to embed a part of the fast feedback correction algorithm.

All the BPM data (including XBPMs in the future) have to be broadcasted to the 120 modules in order to compute the correction. Broadcasting the data is expected to be fast (around 20 us), thanks to eight multigigabit transceivers per module, and fast links between them. The architecture of the dedicated network is flexible enough to keep the feedback system functional even with a few disabled BPMs.

The correction is applied to 46 dedicated air-core correctors in each plane at a rate of 8 kHz. Simulations will be performed in order to optimize the system in the bandwidth of interest to the machine users.

## INTRODUCTION

A third generation light source like SOLEIL has very tight orbit stability requirements. The level of the oscillations of the photon beam must not exceed one tenth of the beam size (see table 1) Great care is taken at all levels of the design to meet these requirements, from building foundations to girders design. The remaining beam motion will be suppressed by global orbit feedback. It is composed of a slow orbit feedback (SOFB) correcting slow beam position drifts and a fast orbit feedback (FOFB) for short term stability. This paper presents the present status of the FOFB system.

Requirements (um)	Long Section	Medium Section	Short Section	Dipole
H	28	18	39	6.2
V	1.7	0.8	0.8	2.5

Table 1: Photon beam stability requirements in each plane for each kind of sources.

## SYSTEM COMPONENTS

Both feedback systems use the position measured by the same 120 BPMs in order to compute their correction with a Single Value Decomposition (SVD) algorithm. The SOFB applies its correction at a maximum rate of 10 Hz to 56 correctors in each plane (secondary coils in

sextupoles). Those correctors are installed over aluminum vacuum chambers, which limit the correction frequency to ~30 Hz due to eddy currents. For the FOFB, dedicated air-core correctors are installed over the bellows next to the BPMs of the straight sections (fig. 1). Those bellows are in stainless steel and the frequency cut off is greater than 1 kHz.

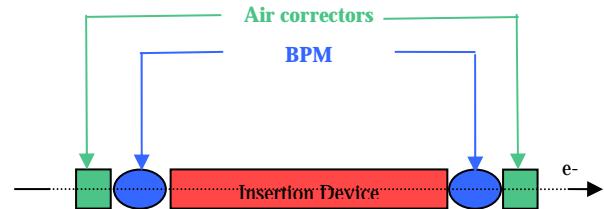


Figure 1: Location of the air correctors on the straight sections. Air correctors are effective in vertical and horizontal planes.

The system is composed of 120 BPMs modules, 46 air correctors in each plane with their power supplies.

Our BPMs are equipped with new electronics modules developed by Instrumentation Technologies [1], [2]. Those modules are based on FPGA technology with high speed communication ports. The large amount of resources of the FPGA allows us to embed the algorithm of correction in the module. In addition to calculating the beam position, the BPM modules perform all the processing of the FOFB. The algorithm computation is distributed on the modules around the storage ring, each one calculating the corrections for its dedicated corrector that is 1/46<sup>th</sup> of the algorithm.

Our power supplies are not yet ordered. They will house 16 bits DACs, power supplies and amplifiers. The command will come directly from a BPM module via its serial RS 485 link.

## NETWORKING

### Topology

A large amount of data has to be transmitted to all BPM modules as they all need the 120 positions to compute the correction. The high sampling rate of the correction, up to 8 kHz, requires a dedicated network.

The processing is distributed on the modules, and each module has eight multigigabit transceivers. A ring topology for this dedicated network is the most convenient.

This architecture is presented in figure 2. The BPMs are grouped in 16 cells (7 or 8 modules per cell). Two modules in each cell are carrying out the interface between their own cell and the others. In each cell, the 7

# NEW SINGLE SHOT BEAM POSITION MONITOR OF THE GSI HIGH ENERGY TRANSFER LINE

J.Schölles, W. Kaufmann, GSI, Darmstadt, Germany

## ABSTRACT

In the near future, single bunch handling with intensities from  $10^7$  up to  $3 \cdot 10^{12}$  charges/bunch and minimum lengths of 30ns (FWHM) are expected at the GSI high energy transfer line. Thus, the demand of an accurate real-time position monitoring is mandatory. At the moment, a recently developed amplifier optimised for the best common mode amplification covers a dynamic range from nearly -80dBm up to +20dBm and a bandwidth of 200MHz. To gain the required dynamic range of around 130dB, an improvement of the amplifiers will be necessary. The data acquisition shall be done by commercial DSOs which have a sample rate of 2GS/s on each of the four channels for every PU. This DSO based solution is cheap in comparison to the usage of other available sampling units. The data transfer from the DSOs to the operating staff is foreseen via Ethernet. Amplifier controlling and position calculation happens at the control centre with LabVIEW. First results measured at the GSI synchrotron will be presented.

## INTRODUCTION

The purpose of the new single shot BPM electronics is to monitor the position of the injected beam in the high energy beam transfer line (HEBT) and help tuning of machine parameters like the right kicker-timing for fast extraction. Due to the wide dynamic range the development of a complete new PU-electronics was necessary to fulfil the following requirements:

- Dynamic range  $10^7$  to  $3 \cdot 10^{13}$  charges/bunch
- Bandwidth 1MHz-200MHz
- Common mode gain matching better than 0.1dB for each PU-plate pair
- Utilisation of commercially available hardware

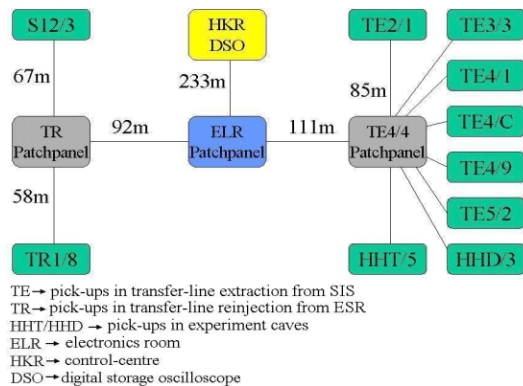


Figure 1: Former setup of the HEBT pick-ups without position measurement capability

A well matched common mode gain for each PU plane is very important for accurate position estimation. Within the scope of the rf-amplifier development it was necessary to find a solution for gain matching. The chosen amplifier concept enables the possibility of digital adjustment of the gain in retracted condition. At the moment there are nine broadband position pick-ups, distributed over the HEBT (and one in the SIS18), installed to supply position information, see Fig.1 for the setup. PUs and infrastructure (rf-signal cables and control-signal-cables) are taken over from a former system that did not fit the needs. The system worked only in a master-mode, an individual parameter based range switching was not possible. Due to the use of electro-mechanical-relays the system did not work reliably for longer times. The next section reports the new system concept and the further development of the remaining hardware. First measurements with a new rf-amplifier will be presented.

## SINGLE BPM-SYSTEM

The basic principle (see Fig.2) of the new system is the use of digital storage oscilloscopes for data acquisition instead of conventional A/D-converter-cards. This concept was taken over from the NEWSUBARU-accelerator in Japan [1].

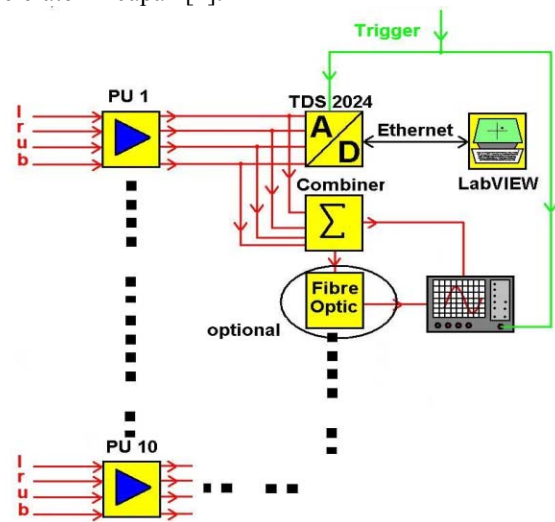


Figure 2: BPM-Overview

This is at the moment a cheap alternative to commercial high speed samplers. The Tektronix TDS 2024 DSO with 2GSa/s, a bandwidth of 200MHz and an 8bit vertical resolution complies the requirements for this project. Since signal magnitudes from  $\mu$ Volts up to several Volts from the given broadband-PU (aperture: 100mm x 50mm)

# DIRECT MEASUREMENTS OF SPACE-CHARGE-POTENTIAL IN HIGH INTENSITY H<sup>-</sup> BEAM WITH LASER BASED PHOTO NEUTRALIZATION METHOD

S. Lee<sup>A)</sup>, T. Tomisawa<sup>B)</sup>, H. Akikawa<sup>B)</sup>, Z. Igarashi<sup>A)</sup>, S. Sato<sup>B)</sup>, T. Toyama<sup>A)</sup>, A. Ueno<sup>B)</sup>,  
 Y. Kondo<sup>B)</sup>, M. Ikegami<sup>A)</sup> and K. Hasegawa<sup>B)</sup>

<sup>A)</sup> KEK, Tsukuba, Ibaraki, 305-0801, Japan

<sup>B)</sup> JAERI, Tokai, Naka, Ibaraki, 319-1195, Japan

## Abstract

Laser wire scanner is considered as the most promising method for profile measurements in high intensity H<sup>-</sup> beams [1]. In order to demonstrate the feasibility of laser wire scanner, a Q-switched Nd:YAG laser (1064nm) diagnostic system has been developed in Japan Proton Accelerator Research Complex (J-PARC) linac [2]. In this paper, first experimental results of laser based beam current profile and space-charge potential measurements in J-PARC medium energy beam transport line (MEBT1) are described.

## INTRODUCTION

Wire scanners are presently used to measure transverse beam profile in the J-PARC linac, and observed results agree with calculated rms widths within 20% differences [3]. However, measured beam intensity and pulse width has to be restricted by heat load limitations in the scanner wires. The interaction mechanism between thin wire and H<sup>-</sup> ions for various beam energies should also be investigated to clarify beam profiles. To avoid these limitations, the photo neutralization method with Nd:YAG laser has been developed as an available candidate for beam intensity profile monitor. Laser stripping technique is also considered as charge exchange procedure for Accelerator-Driven-System (ADS) in J-PARC [4]. An electron of H<sup>-</sup> beam can be stripped by fast and intense laser beam with non-destructively, and laser system have advantages of maintenance and radiation hardness in high intensity proton accelerators. The photo neutralization method is also expected as an advanced diagnostic technique to measure space-charge-potential in high intensity negative hydrogen ion beams. The kinetic energy of photo detached electron corresponds to the ion velocity and space-charge potential at stripped location.

## EXPERIMENTAL APPARATUS

The 0.5ms long, 30mA pulse beam in the MEBT1 consists of micro bunch of <0.5ns pulse width. The H<sup>-</sup> ion beam is accelerated by 324MHz radio frequency quadrupole linac (RFQ) up to the beam energy of 3MeV. Laser profile monitor system was installed on MEBT1 transport line and laser light is horizontally injected into the H<sup>-</sup> beam line and scanned across in the vertical direction (Fig. 1). Commercial Nd:YAG laser can produce pulse width of 20ns long, maximum pulse energy of 500mJ, wavelength of 1064nm at repetition rate of 25Hz. Laser beam size was formed to horizontal width of 6mm and height of 0.8mm at the H<sup>-</sup> beam line by a pair of 80mm focal length cylindrical lenses. A photomultiplier tube (PMT) observe the laser beam that passing through vacuum chamber after interaction with H<sup>-</sup> beam, to confirm laser injection timing, pulse width and optical alignment. Stripped electrons were deflected 90degree by a electromagnetic dipole and collected to a Faraday cup.

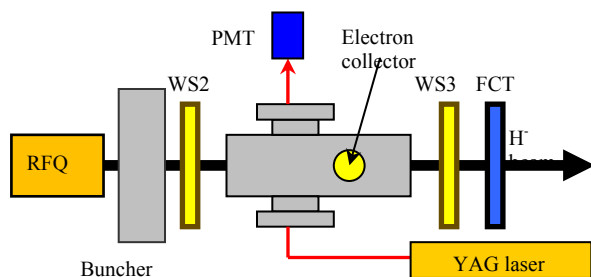


Fig.1: Schematic of laser profile monitor in MEBT1.

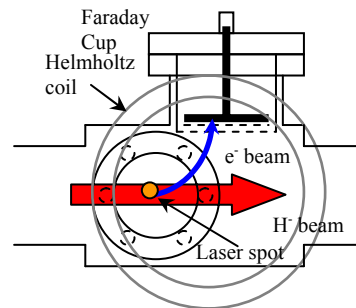


Fig.2: Layout of photo diagnostic box and Faraday cup.

The magnetic field required to deflect 1.63keV electrons is about 50G and its effect on the ion beam is negligible. In order to collect whole stripped electrons diffused by intense space charge, the sufficiently wide area collector plate have been prepared at the nearest location of downstream. The Faraday cup was also designed with electron repeller grid and electrostatic shield mesh (transmission ratio are both 56%, Au coated) in front of the detector. For a high current H<sup>-</sup> beam, Lorentz stripping and/or residual gas stripping can contribute to a significant amount of activation. It's also being a source of background in laser wire measurement. Although the high energy component of background electron can be neglected owing to the small cross section of

# PRESENT STATUS AND UPGRADE OF BPM SYSTEM IN THE PHOTON FACTORY

T. Obina<sup>#</sup>, T. Honda, K. Haga, M. Tadano, W. X. Cheng  
 KEK, 1-1 Oho, Ibaraki 305-0801, Japan

## Abstract

In the Photon Factory 2.5 GeV electron storage ring at KEK, the upgrade project of its straight sections is underway. In the project, we improve the beam-position monitors (BPMs) and the global orbit feedback system. New BPMs are designed and installed in the straight sections and the orbit stabilization system is improved. The effect RF phase modulation to the beam position fluctuation is also observed with turn by turn BPM.

## INTRODUCTION

The Photon Factory storage ring has been operating since 1982 as a dedicated synchrotron light source. The original beam emittance of 460 nm-rad was reduced twice with the major upgrade of the ring, namely, 130 nm-rad in 1987 and 36 nm-rad in 1997[1]. We started new upgrade project form 2002. Figure 1 shows an outline of the new upgrade project. Goal of this project is to equip new short straight sections and enlarge the existing straight sections[2,3]. The total number of straight section will increase from 7 to 13. The newly installed short straight sections plan to use for short-period and narrow-gap undulators.

In this project, two-thirds of the vacuum ducts those are used over 20 years will be renewed. We also install new quadrupole magnets which is shorter and stronger than the previous one. The replacement will be performed during the shutdown period beginning from Mar/2005.

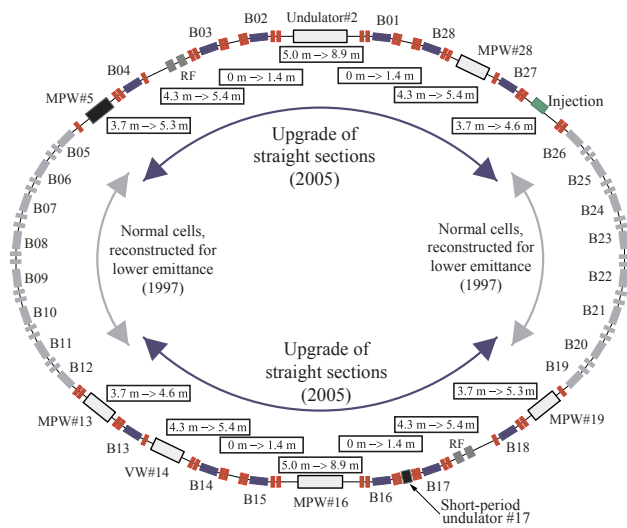


Figure 1: Outline of upgrade project of the straight sections. The arc-sections of the ring (normal cells) remain unchanged.

<sup>#</sup>takashi.obina@kek.jp

As a part of the project, we improve the beam-position monitors (BPMs), and the global orbit feedback system.

## IMPROVEMENT OF BPMs

We install a new arrangement of BPMs electrodes and increase the total number of BPMs. Figure 2 illustrates a cross sectional view of vacuum duct with arrangement of pick-up electrodes. Two different arrangements of the electrodes were used before, a 6-electrode type with BNC feedthroughs (left) and the 4-electrode type with SMA feedthroughs (right upper; type "A"). With the 6-electrode type BPMs, we use two electrodes in upon top and bottom for the detection of vertical position and four electrodes in the side to horizontal detection. With following reasons, we decided to remove 6-electrode type BPMs 1). We have no space to install the 6 electrodes BPMs. 2) 4-electrode type have enough sensitivity for horizontal and vertical. 3) Since we use switching circuit in front of the super-heterodyne detectors [4], we can decrease the readout time if the number of electrode reduced from six to four. We will use four electrodes arrangement for new BPMs.

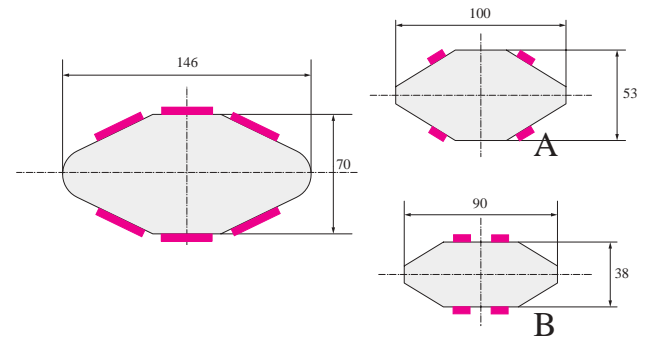


Figure 2: Cross-sectional view of the vacuum duct. The 6-electrode type (left) BPM at the normal cell section was replaced with the 4-electrode type "A" (right, upper) in 1997. We install the new type "B" (right, lower) in the straight section.

We designed a new 4-electrode type BPM as illustrated in Fig.2 (right bottom, type "B") for new vacuum duct of quadrupole magnets. We still have a type "A" in the existing section (from B05 to B12 and B19 to B26). The sensitivity for the vertical direction of type "A" is worse than that for the horizontal direction. The new type "B" has same sensitivity for both planes. We have 77 BPMs in total, and we will use 65 BPMs for the closed orbit measurement. Remaining 12 BPMs are used for feedback of insertion devices and diagnostics, for example, pickup for the bunch-by-bunch feedback system (longitudinal and transverse), turn-by-turn beam oscillation monitor and the phase space monitor.

# TEST OF NEW DIAGNOSTICS FOR BUNCH LENGTH MEASUREMENT

T. Perron, E. Plouviez, G. Naylor, K. Scheidt, ESRF Grenoble, France

## Abstract

Two new diagnostics for bunch length measurements have been recently tested at the ESRF. The first one is based on the spectral analysis of the visible light beam produced by a dipole. The beam is collimated at the input of a photodiode whose output is connected to a spectrum analyzer. The frequency signature is then equivalent to the longitudinal spectrum of the beam. The second device is based on two HF cavities, tuned at two different frequencies, and coupled to the beam wake fields. Their response to the beam passage gives the component of the beam spectrum at the two specified frequencies, from which the beam profile may be reconstructed. Results for these two devices will be presented and compared to measurements made with a streak camera in order to evaluate them. In particular, the reconstruction of the time profile from the information on frequency will be discussed.

## INTRODUCTION

For three years, an effort has been made at the ESRF to obtain the bunch length as an operational parameter. For this purpose, a streak camera is already available, and gives precise and reproducible results [1]. However, for reasons of risk of damage to the streak-Tube it is not feasible to operate the streak Camera in an un-manned and permanent mode.

The initial measurement bench is based on the time domain analysis of the visible light produced by a point like source located in a bending magnet [2]. It has shown to be a very practical diagnostic for wide large bunches and is already operational. Nonetheless, due to the reduced bandwidth (5 GHz) of this device, it is not meant to be operated for short bunches of the order of 15 to 20ps RMS.

We will present the test carried out on two new devices, one also using visible light but processing is done in the frequency domain using a 25GHz spectrum analyser, enabling measurements at low bunch currents, as well as for large bunches. The other diagnostic is based on two HF cavities measuring the components of the longitudinal beam spectrum at 10 and 16GHz. Bunch length can then be deduced assuming a Gaussian bunch shape. This device is only relevant for low current per bunch. Both diagnostics obtain information in the frequency domain, and the accuracy of the time domain reconstruction is an important issue, which will be discussed in detail.

## SET UP FOR MEASUREMENTS USING THE SPECTRUM ANALYSER.

For this measurement, the visible light beam is focused on the input of a 25GHz photodiode. The size of the active surface of the diode being rather small ( $25 \times 25 \mu\text{m}$ ), a lens with a short focusing length is used in order to get an

image of the source point as small as possible. The output of the photodiode is then directly plugged into a 20GHz 18dB RF amplifier. The amplified signal is processed by a 25GHz spectrum analyser. The resulting spectrum is corrected by the impulse response of the measurement chain. The impulse response drawn on figure 2 has been measured using a femto-second laser emitting at 980nm with a repetition rate of 80Mhz.

The schematic set up of the system is basic, care should be taken to avoid cables because of the high frequencies involved. In addition, the use of optical fiber is dangerous because of the chromatic dispersion they induce. It is possible to use them but the light beam should be filtered, resulting in a loss of input power. This was done for the measurements presented in [2], where input power was not an issue, but this is not the case for the spectrum method. The focusing of the visible light beam had to be done directly on the photodiode, without the help of optical fibers, making the focusing of the image on the optical sensor even more delicate. The set up is pictured on figure 1.

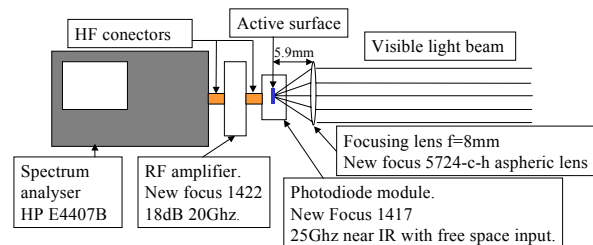


Figure 1: Experimental set up and component references.

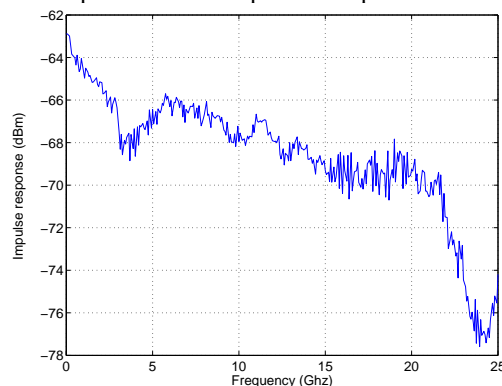


Figure 2: Spectrum of the impulse response of the measurement chain.

If the bunch has a Gaussian longitudinal profile with a standard deviation  $\sigma_t$ , the envelope of the spectrum also is a Gaussian with  $\sigma_\omega = 1/\sigma_t$ . To obtain the bunch length, a Gaussian fit of the spectrum envelope is performed, giving  $\sigma_\omega$ . A simple inversion then gives the RMS bunch length  $\sigma_t$ .

This analysis is made assuming a perfect Gaussian shape for the bunch, which is true for an electron bunch at

# DETAILED RESOLUTION STUDIES OF THE SYNCHROTRON RADIATION PROFILE MONITOR FOR THE HERA ELECTRON BEAM

G. Kube, R. Fischer, Ch. Wiebers, K. Wittenburg, DESY, Hamburg, Germany

## Abstract

For the measurement of the electron beam emittance at the proton–electron storage ring HERA (DESY) a monitor is used which is based on the direct imaging of visible synchrotron radiation from a bending magnet. In order to reduce the thermal heating of the light extracting beryllium mirror it is vertically offset. While the resolution of profile measurements by synchrotron radiation is already strictly limited by fundamental effects, the observation in this off-axis geometry modifies the measured vertical angular intensity distribution leading to an increased contribution of the diffraction limited resolution. In order to describe the resolution broadening effects calculations based on near field computation of synchrotron radiation have been performed with the code SRW [1]. The resulting wavefronts have been propagated through the optical elements of the monitor. Taking into account the calculated resolution broadening corrections the deduced beam emittances are in good agreement with the expected design values.

## INTRODUCTION

The precise determination of the beam emittance is essential for the understanding of luminosity in colliding beam experiments as the ones at HERA. While the emittance itself is not a directly accessible quantity, the beam width is usually measured from which the emittance can be calculated based on knowledge of beam optic parameters. For the measurement of the electron beam size at HERA a profile monitor is used which utilizes the visible part of synchrotron radiation (SR) from a bending magnet to form an image of the beam. The image resolution of this kind of monitor is affected by inherent effects like diffraction and depth of field.

In the vertical direction the resolution broadening is additionally increased due to off-axis observation, i.e. if a part of the radiation used for image formation is shielded. This is the case for the HERA monitor in order to reduce thermal heating of the light extracting mirror due to absorption of hard X-ray radiation which would result in an image deformation. However, by careful calculations of these resolution broadening contributions, the real beam size can still be derived.

The development of a model to describe these effects has turned out to be nontrivial. Attempts range from rules of thumb to quite elaborate models, see Refs. [2, 3, 4] and the references therein. In these works diffraction and depth of field are treated as independent processes and their broadening contributions are added together quadratically. A

more accurate approach is to calculate a Fraunhofer diffraction pattern that includes both the effects of diffraction and depth of field. This accounts for the fact that synchrotron radiation is not actually a spherical wave because of depth of field.

## PROFILE MONITOR SETUP

In luminosity operation the HERA electron beam energy is  $E = 27.6$  GeV. According to the beam optical design parameters, in this mode the beam should have a horizontal ( $1\sigma$ ) size of  $\sigma_x = 1175 \mu\text{m}$  and a vertical size of  $\sigma_y = 260 \mu\text{m}$ . The task of the optical system is to provide an image of the beam onto the chip of the CCD camera.

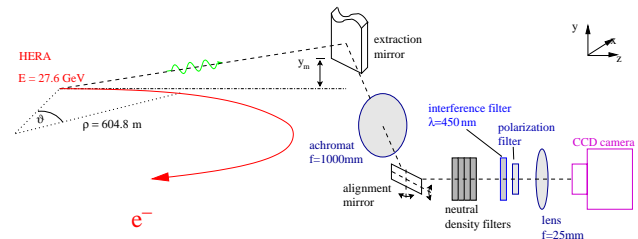


Figure 1: Schematic picture of the profile monitor setup.

In Fig. 1 a sketch of the monitor setup is shown. The emitted SR radiation is extracted out of the vacuum system by a mirror (thickness 4 mm, width 15 mm) which is located 6.2 m away from the central part of the bending magnet. The mirror surface has an inclination angle of  $45^\circ$  with respect to the  $xy$  plane, hence the light is reflected out perpendicular to the beam axis. An achromatic lens with focal length  $f = 1000$  mm, located about 6.5 m away from the source point, forms an image at a distance of 1.2 m. The resulting real intermediate image is then magnified by a second lens ( $f = 25$  mm) onto the chip of the CCD camera (JAI CV-M300E with  $768 \times 494$  pixels of size  $11.6 \times 13.5 \mu\text{m}^2$ ). The total magnification factor of the optical system is  $V = 0.55$ . The video output of the camera is fed to a commercially available 8 bit PCI framegrabber board (Data Translation DT3155) for digitalization and finally analyzed by a standard personal computer.

In order to minimize chromatic errors and to improve the diffraction limited resolution an interference filter (central wavelength 450 nm, FWHM 10 nm) is used together with a polarization filter. The neutral density filters serve to adjust the incoming light intensity to avoid saturation of the camera chip. The alignment mirror which is rotateable about the  $x$  and  $y$  axis allows to adjust the image onto the center of the CCD.

## WIRE SCANNERS IN THE UNDULATOR SECTION OF THE VUV-FEL AT DESY

P. Castro, H.-J. Grabosch, U. Hahn, M. Sachwitz, and H. Thom  
Deutsches Elektronen-Synchrotron DESY, Hamburg and Zeuthen, Germany

### Abstract

The design and implementation of wire scanners for the Vacuum Ultraviolet - Free Electron Laser (VUV - FEL) facility at DESY [1] is presented. In the undulator section of the VUV FEL a set of seven wire scanner stations determine the relative position of the electron beam within few  $\mu\text{m}$  and the absolute position related to the undulator axis with a precision better than 50  $\mu\text{m}$ . First results of beam trajectory and beam size measurements along the undulator section are shown.

### INTRODUCTION

Wire scanners have been in use for many years in accelerator facilities in order to measure the profile and the position of particle beams [2-4]. The basic working principle of wire scanners is shown in figure 1. A fork equipped with thin wires (10 – 50  $\mu\text{m}$ ) passes the electron beam. The beam interaction with the wires produces high energetic radiation which is detected by scintillation counters. Simultaneously monitoring of the wire position allows the measurement of beam profile, and position. Constant wire velocities of up to 1 m/sec (fast scan mode) are needed to scan powerful particle beams.

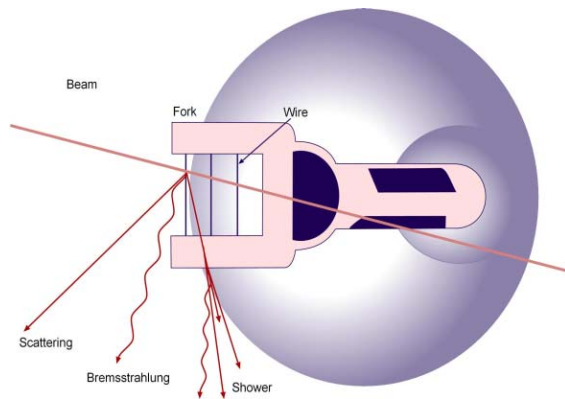


Figure 1: Working principle of the wire scanner. Secondary particles are created when the wire passes through the electron beam.

The VUV FEL at DESY [5] is a 30 m long permanent magnet undulator structure with seven integrated wire scanner stations. The system is part of a test linac operated in superconducting technology. The FEL light (down to a wave length of a few nm) is created by Self Amplified Spontaneous Emission (SASE). The SASE effect takes place when the electron and photon beam overlap better than 50  $\mu\text{m}$  over the whole undulator

length. Critical alignment parameters for this interaction are:

- Alignment ( $< 50 \mu\text{m}$ ) of the electron beam trajectory to the magnetic center of the undulator.
- Electron beam parameters as beam position and beam emittance.

To measure these alignment parameters in the undulator section of the VUV FEL special wire scanners were developed [6].

### TECHNICAL LAY OUT OF THE WIRE SCANNER

The essential features of the wire scanner are the stroke of 48 mm combined with high position accuracy (few  $\mu\text{m}$ ) over a working range of 30 mm. A scanning speed of 1 m/sec has to be realized to avoid destruction of the wire in multi bunch mode operation. In this case the electron beam with up to 7200 bunches within 800  $\mu\text{sec}$  (at 10Hz) will heat up slowly passing wires and destroy them. Three thin wires (10  $\mu\text{m}$  carbon, 10  $\mu\text{m}$  and 50  $\mu\text{m}$  tungsten) are clamped between the two teeth of a ceramic fork with a spacing of 10 mm. The linear movement of the fork is based on a slot winding cylinder transforming the rotation of a stepping motor into a linear motion. The cam of the slot winding cylinder uses the transfer function of a Besthorn-sinuide. The interaction between the wire and the electron beam takes place in the linear speed range of the transfer function. The position of the wires is measured on axis with an incremental length gauge with a resolution of 0.1  $\mu\text{m}$ .

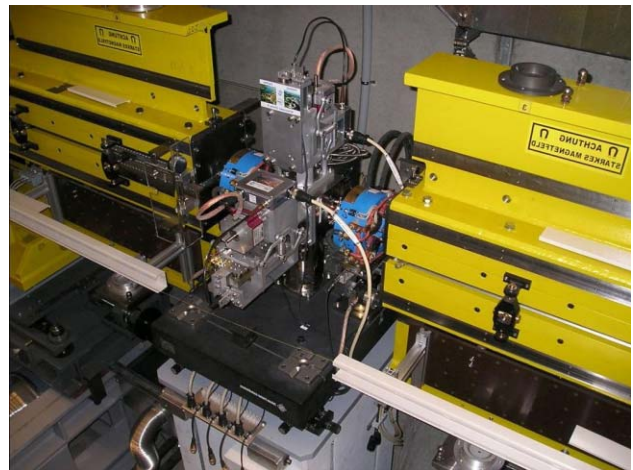


Figure 2: A wire scanner station between two undulators.

# IRRADIATION CONTROL OF THE “SPIRAL” TARGET BY MEASURING THE ION BEAM INTENSITY VIA A FAST CURRENT TRANSFORMER

P. Anger, C. Doutressoulles, C. Jamet, T. André, W. Le Coz, E. Swartvagher, M. Ozille  
 Grand Accélérateur National d'Ions Lourds (GANIL), Caen, France  
 e-mail : anger@ganil.fr

## Abstract

In order to obtain a more precise control on the irradiation of the targets of the “SPIRAL” installation, a new criterion of safety must be respected. To control this latter, an AQ system has been put in operation and more specifically a new device has been set up in order to measure the ion beam intensity and to calculate the number of particules per second. This value can then be integrated over time. This device consists of two Fast Current Transformers integrated in a mechanical unit placed in a vacuum chamber. These sensors reproduce the image of the pulsed beam at 10MHz and we take from the amplified signal of each sensor, the amplitude of the 2nd harmonic. Each one of these amplitudes is detected by a Lock-in Amplifier, which is acquired via a real time industrial controller. The intensity is calculated by the Fourier series relation between the amplitude of the 2<sup>nd</sup> harmonic and the average intensity. These equipments can be remotely tested by integrating a test turn on the sensors. They are redundant. The accuracy of measurement is estimated taking into account the variation of beam, of the environment and of the installation

## INTRODUCTION

The SPIRAL unit generates a radioactive ion beam by irradiating an ECS “Ensemble Cible-Source” (Target-Ion Source) with a high energy ion beam. GANIL is a facility submitted to approval, and the irradiation mode of targets is regulated by the safety authorities. At present, the target irradiation is limited by a safety criterion of 15 days of use, independently of the irradiating beam characteristics (ion species, power and risks linked to the operation of the accelerators). A request for modification of this criterion has been formulated to the safety authorities. The maximum irradiation time authorised should depend on the irradiating beam type and of its intensity, the new criterion being that the total number of ions received by the target (integrated flux) should not exceed a certain level, function of the radiological risk.

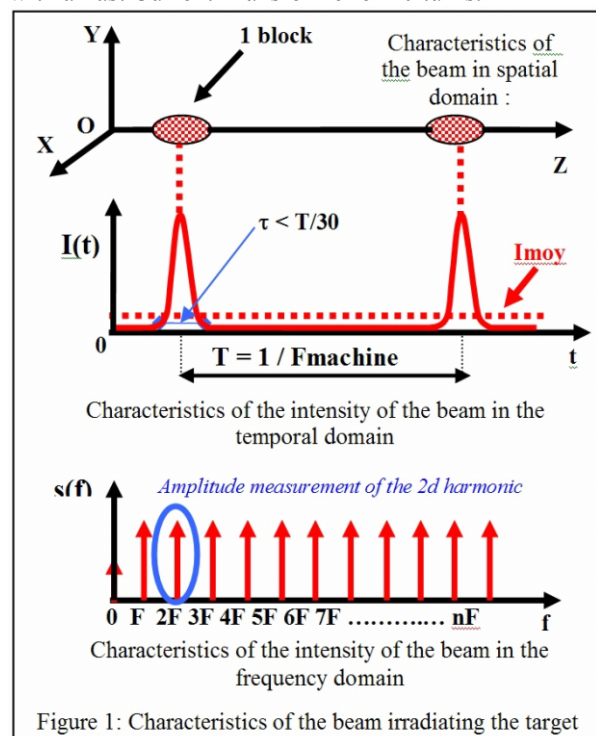
In order to control this new criterion, the CICS project (Contrôle de l'Irradiation de la Cible de SPIRAL) (Irradiation Control of the SPIRAL Target) has been issued: it will require a measurement system and a reliable control of the beam intensity which will, at any time, show both the instantaneous and the integrated beam intensity for each target. The intensity means the number of ions per second.

## DESCRIPTION OF THE SYSTEM

The system consists of two sensors measuring the intensity of the primary beam irradiating the ECS (Target- Ion Source) and returning an electric signal proportional to the intensity. A dedicated chain of measurement will handle the signal of each sensor so that they can be digitized by a computing system. This dedicated and autonomous computing system will be able to test the two instrumentations and handle any malfunctions. Using an user interface, this computing system will receive the necessary information from the primary beam, the identification of the ECS and the new criterion in order to measure the intensity of the beam, calculate the number of particles per second and integrate the number of ions stopping in the target. The computing system records the data related to the irradiation of each ECS on two reliable and permanent data carriers. It cuts off the beam either when a malfunction occurs or when the target has received the maximum dose (new safety criterion).

## PRINCIPLE OF THE MEASUREMENT OF THE BEAM INTENSITY

The beam intensity is obtained by measuring the magnetic field generated by the pulsed beam (fig.1) with a Fast Current Transformer of 10 turns.



# SPATIAL AUTO-CORRELATION INTERFEROMETER WITH SINGLE SHOT CAPABILITY USING COHERENT TRANSITION RADIATION

Daniel Sütterlin<sup>1</sup>, Volker Schlott<sup>1</sup>, Hans Sigg<sup>1</sup>, Daniel Erni<sup>2</sup>, Heinz Jäckel<sup>3</sup>, Axel Murk<sup>4</sup>

<sup>1</sup> Paul Scherrer Institute, CH-5232 Villigen, Switzerland

<sup>2</sup> Lab. for Electromagnet. Fields and Microwave Electronics, ETHZ, CH-8092 Zürich, Switzerland

<sup>3</sup> Institute of Electronics, ETHZ, CH-8092 Zürich, Switzerland

<sup>4</sup> Institute of Applied Physics, University of Berne, CH-3012 Berne, Switzerland.

## Abstract

The polarization dependent intensity distribution of CTR emission has been theoretically and experimentally studied at an optical beam port downstream the 100 MeV SLS pre-injector LINAC. Based on these analyses, a spatial interferometer using the vertically polarized lobes of coherent transition radiation (CTR) has been designed and installed at this location. A successful proof of principle has been achieved by step-scan measurements using a Golay cell detector. The single shot capability of this bunch length monitor is demonstrated by electro-optical correlation of the spatial CTR interference pattern with a Nd:YAG laser pulse.

## EMISSION CHARACTERISTICS OF CTR

Step-scan interferometer measurements, such as Martin-Puplett Interferometers offer excellent frequency resolution. One of their major drawbacks however is that a full measurement often takes minutes and averages over many electron bunches. Therefore, the unique emission characteristics of long-wavelength CTR is used to design a novel interferometer producing a spatial auto-correlation of the CTR pulse allowing the determination of the power spectrum in a single-shot. In the following an analytic formalism is presented describing the emission process of CTR.

The result derived by Ginzburg and Frank [1] is valid only for the optical part of the emitted radiation and/or for infinite target diameters. At long wavelengths the transversal extent of the electron field impinging onto the target screen is usually considerably larger than the target dimension. Hence, a model for the emission characteristics of long-wavelength transition radiation has been developed for a finite target screen that is rotated by 45° with respect to the electron trajectory [2,3]. In such a configuration, the metallic target screen acts as a source aperture for the emitted TR. In our formalism the magnetic field of the relativistic electron is inducing a surface current in the thin metallic target, from which the vector potential representation of the radiated field is acquired. When calculating the components of the resulting electrical and magnetic fields a further formalism has been introduced that provides accurate approximations for both cases the far-field and the radiating near-field. A complete description of the proposed analysis will be published elsewhere [3].

The simulated horizontal radiation pattern as depicted in Fig. 1 clearly reproduces the expected angular broadening with increasing wavelengths of the two-lobed emission profile. The asymmetry only occurs in the horizontal direction and vanishes for short wavelengths where our formalism converges with the Ginzburg and Frank model.

As displayed in Fig. 1 the simulations are in good agreement with the corresponding measurements c) and d) at the SLS LINAC. The underlying power spectrum used to model the broadband CTR excitation was measured with a Martin-Puplett interferometer. The discrepancies particularly in the wings of the radiation pattern can be attributed to deviations in the power spectrum (associated to different electron bunches), to the finite detectors size, and the additional diffraction at the vacuum port.

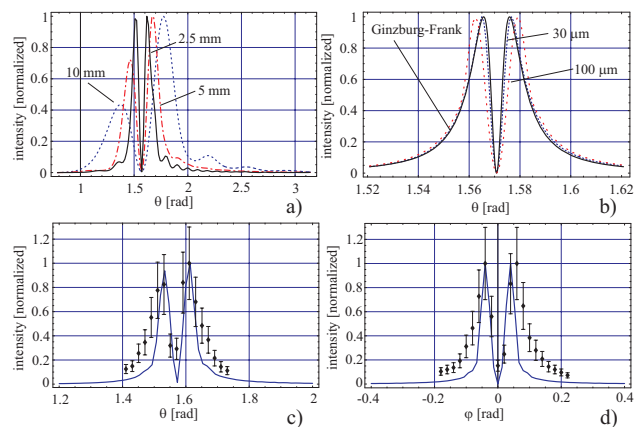


Figure 1: Calculated CTR radiation pattern (single electron of 100 MeV) at a spherical distance of  $R = 300$  mm for a finite target screen with  $r = 28$  mm; a) for millimeter wavelengths; b) for wavelengths in the FIR regime; c) measurements of the horizontal emission pattern for horizontal polarization; and d) measurements of the vertical emission pattern for vertical polarization. The simulations (solid line) are in good agreement.

## SPATIAL INTERFEROMETER

Based on above theoretical and experimental analysis effective optics for the spatial interferometer has been designed. Due to the asymmetry in the horizontal emission pattern, we selected to use the vertical polarized component of the emitted CTR using a wire grid

# A NEW TV BEAM OBSERVATION SYSTEM FOR CERN

E.Bravin, S.Burger, G.F.Ferioli, G.J.Focker, A.Guerrerro, R.Maccaferri  
 CERN, Geneva, Switzerland

## Abstract

Beam observation, emittance measurements and initial beam steering, are often achieved using scintillating or OTR (optical transition radiation) screens. In the CERN accelerators complex, this system is known as the BTV or MTV system. It consists of an observation camera, an illumination device and a vacuum tank provided of a view port containing the radiator.

More than 100 such equipments, in several different flavours, are installed in the CPS complex, another 50 in the SPS complex and another 50 will be installed in the upcoming LHC.

The newly developed electronics hardware consists of a single VME 64x card. This card is capable of controlling: all the different types of positioning mechanism for the screens, the adjustment of the illumination intensity, the different types of cameras (i.e. CCD or Vidicon tube) and the positioning of optical filters in front of the camera. Apart from the analogue video signal the card provides as output also the digitized image.

A preserie of this new electronics has been installed and tested during the tests of the LHC beam transfer line TI8 last autumn. The production of 300 cards is now underway. These cards will be used for the complete renovation of the MTV system of the CPS complex[1] and for the installations in LHC and its transfer lines.

In this contribution the new system is described with particular emphasis on the new VME card. The performances and limitations are also presented.

represent the basic of the system. The type of radiator depends on the type of beam (sensitivity, dynamic range, linearity and temperature issues) and on the type of measurement to be done. To cope with the problem of the dynamic range of the beam, filters can be used in front of the camera.

The complexity of this system arises mainly from the variety of equipments that were installed over the past 25 years. Now, thanks to the recent unification of different accelerator departments of CERN and to the development of new devices for LHC, all new installations of BTV and MTV systems are made following a standard design, which simplified layout is shown in figure 2. For the new mechanical designs too, as many parts as possible are reused, in particular, all the 50 new BTVs in LHC will share the same type of mechanism. The problem of the many existing different devices is however much reduced now with the installation of the new control hardware.

## SYSTEM OVERVIEW

Figure 1 shows the principle of a TV beam observation system (BTV or MTV), where a radiator screen, attached to an insertion device, an illuminator and a camera

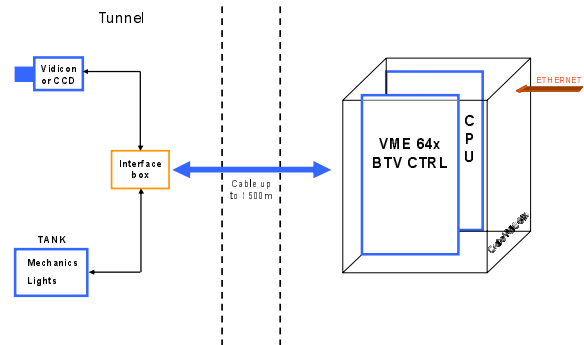


Figure 2: Layout of the new BTV/MTV hardware control system.

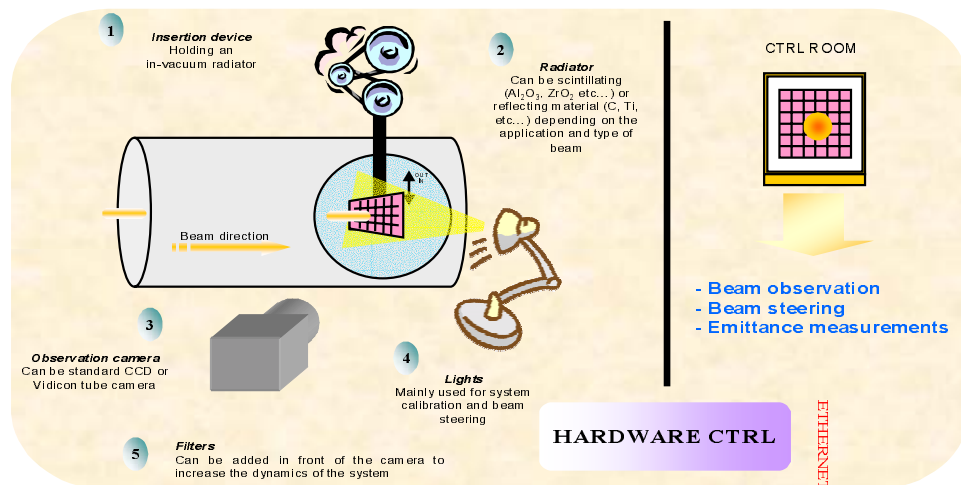


Figure 1: Principle of a BTV or MTV system.

# A PROBLEM IN RF SWITCHES OF MULTIPLEXING BPM SYSTEM

T. Fujita, S. Sasaki, M. Shoji and T. Takashima

JASRI/SPring-8, 1-1-1 Kouto, Mikazuki-cho, Sayo-gun, Hyogo 679-5198, Japan

## Abstract

At SPring-8, we have been developing a new detection circuit for beam position measurement with a resolution of submicron and a measuring interval of a few milliseconds with high stability. In the circuit, a multiplexing method using RF switches is employed in order for a drift of the circuit to be canceled. To achieve design performance, the switches must have following properties: a short switching time, high repeatability and long lifetime. During the evaluation of components for the new detection circuit, we found that some RF switches made of GaAs had a problem that the output signal changed for a few m dB for seconds after the switches were turned on. A few m dB, which is 1/10000 in voltage ratio, corresponds to a beam position error of a few microns in SPring-8. Such position error is out of the required specifications. We investigated several kinds of RF switches and decided to adopt a CMOS RF switches as the multiplexer. In this paper, we report switching properties of several RF switches and demonstration of beam position measurement using the switches.

## INTRODUCTION

We have been developing new detection circuit for COD measurement. The position resolution and the repetition rate of measurement required for the circuit is submicron and hundreds of cycles per second, respectively. Furthermore, a long-term stability of the micron to sub-micron is required. Recently, parallel processing circuits for COD measurement for the sake of high measurement repetition tend to be employed [1, 2, 3], however, we have adopt a multiplexing method, in which four beam signals from one BPM head are multiplexed with RF switches and detected with one detection circuit, in order to increase the long term stability and to reduce the signal amplitude dependence of the detection circuit.

In order to achieve fast repetition of measurement with the multiplexing method, short switching time is required for RF switches. In addition, for the purpose of high stability on beam position measurement, high repeatability of RF switches is required.

Now, we are checking performance of prototype of the circuit. Total performance and that of the circuit downstream of the RF switches will be reported after installation and commissioning. In this paper, we report effect which arises from characteristics of RF switches.

## PROTOTYPE

Fig. 1 is a block diagram of prototype of the developing circuit. Three BPMs (total twelve beam signals) are mul-

tiplexed with a 12:1 RF switch. After a frequency component of acceleration frequency, which is 508.58 MHz at SPring-8, in the pick-up signals is down-converted to 250 kHz IF frequency, the down-converted signal is digitized with 1MSPS-ADC for 1 ms. The digitized signal is processed with DSP and sent to control system. Thus three BPM data can be obtained every 12ms. When signal from a signal generator of 508.58 MHz is fed to the circuit without RF switches, i.e. BPMs and RF switches in Fig. 1 are replaced with signal generator and power divider, we can obtain the position resolution of 0.2  $\mu$ m in standard deviation.

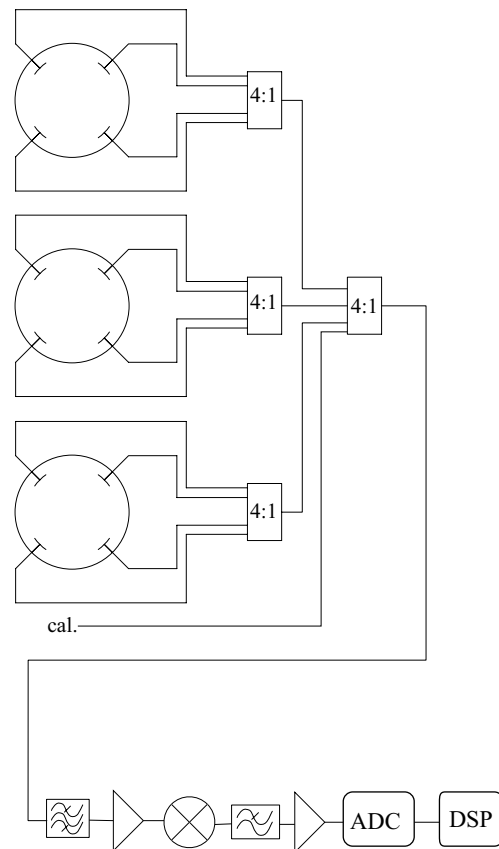


Figure 1: Block diagram of the developing circuit.

## SWITCHING TIME

During initial phase of the circuit design, we planned to adopt RF switches made of GaAs. When we measured signal from signal generator with a prototype of the detection circuit equipped with GaAs multiplexer, we observed an unexpected behavior. As shown in Fig. 2, obtained beam position changes asymptotically for a second after

# DESIGN OPTIMIZATION OF AN EMITTANCE MEASUREMENT SYSTEM AT PITZ \*

L.Staykov<sup>†</sup>, DESY Zeuthen, Germany;

## Abstract

The photo injector test facility at DESY Zeuthen (PITZ) has been built to test and to optimize electron sources for Free Electron Lasers (FEL's). In order to study the emittance conservation principle, further acceleration is required. To increase the electron beam energy up to 30 MeV, a booster accelerating cavity is under commissioning [1]. With this upgrade, the projected normalized transverse emittance less than 1 mm mrad is expected from beam dynamics simulations. To measure such small emittance, an upgrade of the existing Emittance Measurement SYstem (EMSY) is required. EMSY uses the slit mask technique to determine the beam emittance. In this paper, considerations on the physics of the system as well as results from GEANT4 simulations are given. The expected signal to noise ratio, the resolution of the system, and the energy deposition in the slit-mask are presented. EMSY is under construction at INRNE Sofia. Installation and first results are expected by the end of this year.

## INTRODUCTION

The careful optimization of the electron source at PITZ has shown that it is possible to achieve small emittance for 1 nC bunch charge. Upgrade on the facility including installation of accelerating booster cavity will increase the energy of the electron beam to about 30 MeV. This requires upgrade of the present Emittance Measurement SYstem (EMSY) Fig. 1. The layout of PITZ is shown on Fig. 2. The electrons are extracted from a photo cathode based RF gun. The minimum beam emittance of  $\sim 0.84 \pi \cdot \text{mm} \cdot \text{mrad}$  expected from the simulations could be achieved by further beam acceleration.

The setup of the emittance measurement system used at PITZ (Fig. 1) is typical for slit measurements. The system consists of two orthogonal actuators which can be inserted separately to penetrate the beam in order to take images or to cut beamlets in the beam transverse planes. The beamlets are observed at some distance  $L$  downstream and the normalized emittance  $\varepsilon_n$  is calculated using the standard formula (Eq. 1).

$$\varepsilon_n = \beta\gamma \cdot \sqrt{\langle x^2 \rangle \cdot \langle x'^2 \rangle - \langle x \cdot x' \rangle^2}. \quad (1)$$

Here  $\langle x^2 \rangle$  and  $\langle x'^2 \rangle$  are the rms dimensions of the beam in the so called trace phase space where  $x' = \sqrt{\langle p_x^2 / p_z^2 \rangle}$  represents the rms divergence of the beam. The rms beam

size is measured on an OTR or YAG screen at the position of the slits along the beam axis. The divergence is obtained by analyzing the profiles of the beamlets produced from the slits which drift some distance  $L$  downstream where the spatial distribution of the beamlets corresponds to the local divergence,  $x'$  can be derived from the size of the beamlet using the formula in Eq. 2.

$$x' = \sqrt{\frac{\langle x_b^2 \rangle}{L^2}}. \quad (2)$$

Here  $x_b$  is the rms size of the beamlet on the screen after distance  $L$ . The  $\beta\gamma$  is measured using a dispersive arm after EMSY.

## EMSY LAYOUT

In general EMSY consists of two orthogonal actuators perpendicular to the beam axis which are holding the components which are inserted in the beam line. Stepper motors are provided to move separately each one of the four axes which give the precise spatial positioning and orientation of the components. On each of the actuators, either an YAG or OTR screen is mounted to observe the beam distribution. A single and a multi slit masks are mounted consecutive to take samples from the transverse phase space of the electron beam. A CCD camera is placed to observe the screens. EMSY was designed and manufactured jointly of Sofia Institute for Nuclear Research and Nuclear Energy and DESY Zeuthen in the period 2000-2001.

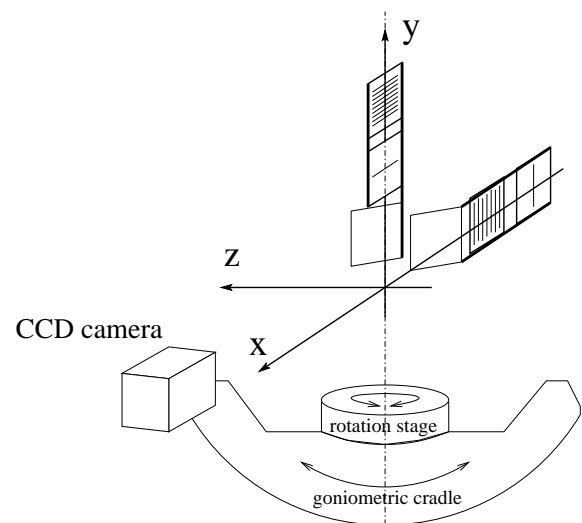


Figure 1: Layout of EMSY.

In the optimization process the components of the existing EMSY were modeled using GEANT4 [2] for the in-

\* This work has partly been supported by the European Community, Contract Number RII3-CT-2004-506008, and by the 'Impuls- und Vernetzungsfonds' of the Helmholtz Association, contract number VH-FZ-005.

<sup>†</sup> Presenting author, e-mail: lazaraza@ifh.de

# PROFILE MONITORS BASED ON RESIDUAL GAS INTERACTION \*

P. Forck, A. Bank, T. Giacomini, A. Peters

Gesellschaft für Schwerionenforschung GSI, Darmstadt, Germany, p.forck@gsi.de

## Abstract

The precise determination of transverse beam profiles at high current hadron accelerators has to be performed non-interceptingly. Two methods will be discussed based on the excitation of the residual gas molecules by the beam particles: First, the beam induced fluorescence (BIF) where light is emitted from the residual gas molecules (in most cases  $N_2$ ) and observed with an image intensified CCD camera. Secondly, by detecting the ionization products in an Ionization Profile Monitor (IPM) where an electric field is applied to accelerate all ionization products toward a spatial resolving Micro-Channel Plate. The signal read-out can either be performed by observing the light from a phosphor screen behind the MCP or electronically by a wire array. Methods to achieve a high spatial resolution and a fast turn-by-turn readout capability are discussed.

## INTRODUCTION

Various methods for the transverse profile determination are used, most of them are based on energy loss of the beam particles in matter or on nuclear reactions at a target material. But for high current hadron beams, non-intercepting methods are preferred to prevent the risk of material melting by the large beam power deposition. The diagnostics must be non-intersecting in order to monitor the undisturbed properties of a beam stored in a synchrotron at any time during the cycle. Even in a pulsed LINAC it might be important to have access to possible time varying processes during the macro-pulse. Two types of non-destructive methods are described here, based on atomic collisions between the beam ions and the residual gas within the vacuum pipe. These methods are: The detection of single photons from excited levels of the residual gas atoms or molecules by **Beam Induced Fluorescence (BIF)** and the direct detection of ionized residual gas ions or electrons at an **Ionization Profile Monitor (IPM)**. In particular IPMs are installed at most hadron synchrotrons and storage rings, but due to the various beam parameters at different laboratories no 'standard realization' is available. The basic features for both methods are discussed and their applicability are compared.

## BEAM INDUCED FLUORESCENCE

In most LINACs and transfer-lines  $N_2$  dominates the residual gas composition. Due to the electronic stopping

\* Partly funded by INTAS under Ref. No. 03-54-3931 and by European Union under EU-FP6-CARE-HIPPI

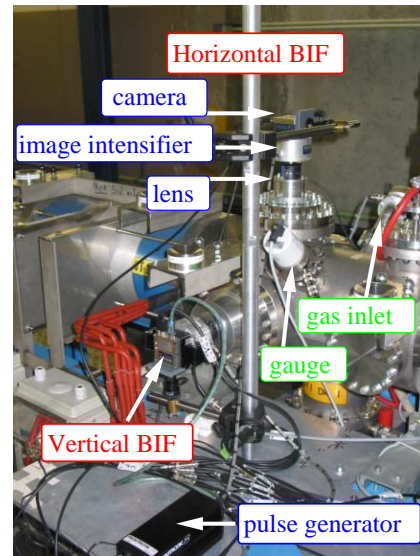


Figure 1: The installation of BIF station at GSI [6].

power the molecules are ionized and with a certain probability left in an excited state. A strong fluorescence in the blue wavelength range  $390 \text{ nm} < \lambda < 470 \text{ nm}$  is generated by a transition band to the  $N_2^+$  electronic ground state ( $B^2\Sigma_u^+(v') \rightarrow X^2\Sigma_g^+(v'') + \gamma$ , for vibrational levels  $v$ ), having a lifetime of about 60 ns [1]. Tests with other gases e.g. Xe were performed, but in this case a lower photon yield in the optical wavelength range was reported [2].

The low amount of photons can be detected and amplified using an image intensifier. This commercially available device consists of a photo cathode to transform the photons into electrons and amplifies them by a spatial resolving MCP electron multiplier. It is followed by a phosphor screen to create again photons, which are finally monitored by a CCD camera. A single primary photon can be amplified to yield  $10^4$  to  $10^7$  detectable photons on the CCD. The photon amplification depends on an adequate choice for the image intensifier components: Various types of photo-cathodes are available offering a different sensitivity with respect to the photon wavelength interval, see e.g. [3]. In general, a photo-cathode sensitive to longer wavelength results in a larger dark current. The photo-electrons can be amplified by a single MCP with typically  $10^3$  electron-multiplication or a double MCP assembly (Chevron configuration) with typically  $10^6$ -fold multiplication. Due to the enlarged distribution of the secondary electrons on several channels at the second MCP, the light spots on the phosphor screen are about a factor 3 larger compared to a single MCP. Depending on the application the required light detection threshold has to be balanced

# BEAM DIAGNOSTICS AT THE HIGH POWER PROTON BEAM LINES AND TARGETS AT PSI

R. Dölling, R. Rezzonico, P.-A. Duperrex, U. Rohrer, K. Thomsen, R. Erne, U. Frei, M. Graf, U. Müller, Paul Scherrer Institut, Villigen-PSI, Switzerland

## Abstract

The protection of beam lines, targets and target windows from proton beam powers of 0.13 MW (@72 MeV) and 1.1 MW (@590 MeV) is based on beam loss monitors, current measurements at collimators and 4-sector apertures as well as the measurement of the current transmission. The new targets also use harps or an optical observation of the thermally emitted light from a metal sieve in front of the target. Online beam centering using inductively coupled position monitors is needed for continuous operation. Wire profile monitors are used temporarily for setup and tuning. The high radiation background requires radiation hard devices, shielding, a suitable handling of the components and remotely positioned electronics.

## INTRODUCTION

High power proton beams of 590 MeV are produced at PSI using two consecutive cyclotrons. The beam current has increased over the years to 1.9 mA. After the passage of the graphite targets M and E for meson production, the remaining ~1.3 mA of beam is transported to the spallation neutron source "SINQ", which uses a solid target of stainless steel and lead. Beam is delivered for

~4800 hours per year for ~400 users [1]. A liquid Pb-Bi target "Megapie" is scheduled for 2006 and an additional beam line with a high power target "UCN" for ultra cold neutron production should start operation in 2007.

Melting of beam line/cyclotron components by missteered beam can occur within 10 ms @590 MeV or 1 ms @72 MeV (depending on the beam diameter). Such an event could cause 2 to 300 days of shutdown for replacement, repair or remanufacturing of components, since many built-in parts are not easily accessible or deeply buried under densely packed shielding. Furthermore, there are no spare parts for many components, and sometimes there is a lack of documentation, drawings and the knowledge of exact dimensions. Melting of the Megapie target and window by an overly concentrated beam could also cause a long shutdown. This can occur if the beam misses Target E, while the beam will then not be scattered, resulting in an increase of current density at the target and window by a factor ~25, which will melt after ~170 ms. Hence, redundant systems are needed for the fast (<1 ms) generation of interlocks. Therefore, the detector signals are evaluated in the readout electronics and interlock signals are hard wired to the control system.

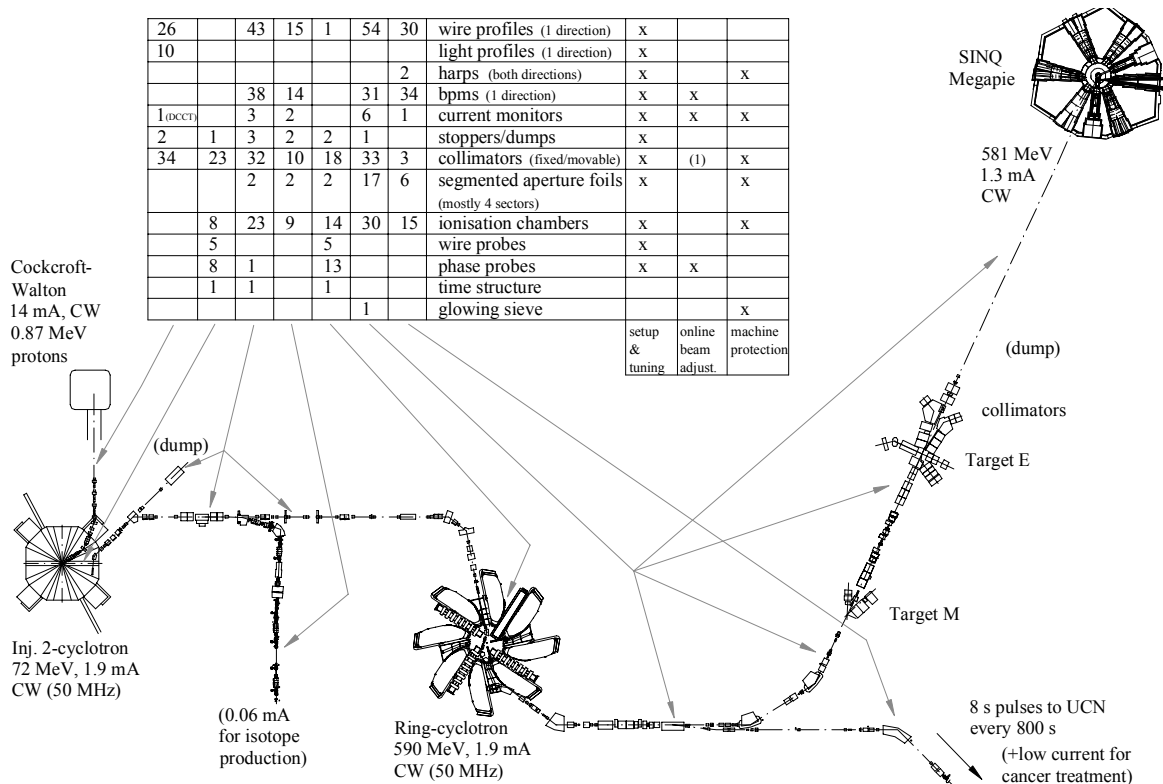


Figure 1: Overview of high power proton facility and diagnostics used.

# BEAM STABILITY IN SYNCHROTRON LIGHT SOURCES\*

Glenn Decker

Advanced Photon Source, Argonne National Laboratory

Argonne, IL 60439, USA

## Abstract

Numerous third-generation light sources are now in a mature phase of operation, and several new sources are under construction. Submicron beam stability is being achieved routinely at many of these light sources in terms of both AC (rms 0.1 - 200 Hz) and DC (one week drift) motion. This level of stability is a necessary condition for the success of x-ray free-electron lasers such as the Linac Coherent Light Source (LCLS) at Stanford or the European XFEL project. The different methods for addressing this problem at different laboratories— involving various combinations of passive noise identification and suppression, feedback, and feedforward— together with accomplishments to date will be discussed.

indications of what will be expected for future light sources such as x-ray free-electron lasers and energy recycling linacs.

Shown in Table 1 are a set of high-level parameters for the world's operational third-generation light sources (as of June, 2005), defined to be dedicated storage rings having natural emittance below 20 nm-rad. The essential things to notice are that the particle beam tends to be flat, with horizontal beam size  $\sigma_x$  in the range of a few hundred microns, but with vertical beam size  $\sigma_y$  below ten microns in many cases. Since beam stability requirements are typically stated as a fraction like 5 or 10 percent of beam size in a given frequency band, it is clear that submicron stability is a common requirement. The vertical angular divergence of these particle beams is at

Table 1: Properties of Operational Third-Generation Synchrotron Light Sources.

	Energy (GeV)	Horizontal Emittance (nm-rad)	Vertical Emittance (pm-rad)	$\sigma_x$ (mm)	$\sigma_y$ (mm)	Top-up
SPring-8	8	6	14	390	7.5	yes
APS	7	2.5	25	271	9.7	yes
ESRF	6	4.0	30	380	14	planned
SPEAR-3	3	12 / 18	60 / 90	350 / 430	25 / 31	planned
CLS	2.9	15	200	326	30	planned
Pohang LS	2.0 / 2.5	12.1 / 18.9	12 / 19	350 / 434	22 / 27	no
SLS	2.4	5	40	86	6	yes
ELETTRA	2 / 2.4	7 / 9.7	< 70 / 97	241 / 283	15 / 16	planned
ALS	1.5 / 1.9	4.2 / 6.75	200 / 150	240 / 310	27 / 23	planned
BESSY-II	1.72	6	180-240	290 / 76	27 / 17	planned

## INTRODUCTION

In the past ten years, there has been a remarkable increase in the number of accelerator facilities dedicated to the generation of synchrotron radiation. An indicator of this is the recent launch of the web site [lightsources.org](http://lightsources.org) [1], where 59 separate synchrotron radiation facilities around the world are now listed. The light source beam stabilization field is similarly reaching a mature phase, as evidenced recently by a series of international workshops on beam orbit stabilization [2,3]. Numerous excellent articles have been written on the subject of beam stability in synchrotron light sources [4,5]. The emphasis here will be on trends in third-generation light sources, with

the few microradian level, approaching the diffraction limit for many of these machines. At the Advanced Photon Source (APS), the goal for vertical pointing stability is to limit beam motion to less than 220 nanoradians rms in a frequency band ranging from 0.016 Hz (i.e., one minute) to 200 Hz, while the long-range pointing stability goal is 0.5 microradians p-p, for time scales extending from one minute to one week.

Beam stabilization efforts in general must account for motions in all six phase-space dimensions, on time scales ranging from the bunch repetition rate up to months. Not only beam centroid motion, but also beam size and even higher-order moments of the phase-space particle distribution must be considered. While historically beam stabilization has been defined in terms of the source, i.e., the particle beam properties, it is becoming clear that many properties of the photon beam cannot be directly controlled using particle beam diagnostics alone. As a

\*Work supported by U.S. Department of Energy, Office of Basic Energy Sciences, under Contract No. W-31-109-ENG-38.

# DETECTION OF HARD X-RAYS IN AIR FOR PRECISE MONITORING OF VERTICAL POSITION & EMITTANCE IN THE ESRF DIPOLES

B.K. Scheidt, ESRF, Grenoble, France

## Abstract

The un-used X-rays produced in each of the 64 ESRF dipoles are absorbed in so-called crotch absorbers at the end of the dipole. With 40mm of Copper + 5mm of Steel only 250uW/mrad (out of total power fan of 154W/mrad) traverse the absorber. About 20% of these ~170KeV energy X-rays are converted by a 0.5mm thick Cadmium Tungstenate (CdWO4) scintillator into visible light that is collected and focussed by simple optics on to a commercial CCD camera. This compact monitor operates in air and is situated just behind the crotch chamber. Knowing the small vertical divergence of the 170KeV photons and the distance of the source-point to the scintillator, it is possible to calculate precisely the vertical electron beam size at this sourcepoint. The light yield is enough to measure at >1KHz frequency, with a sub-micro-meter resolution of the beam position, thereby also constituting a powerful tool for beam stability measurement in the vertical plane. The principle, the practical realisation and the results obtained with a prototype since Jan.2005 will be presented.

## X-RAYS TRAVERSING THE CROTCH

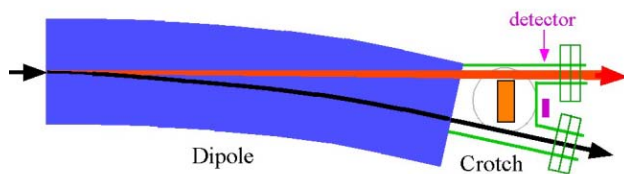


Figure 1: Position of the detector in air just behind crotch

Only 10% of the synchrotron light generated by the ESRF dipole ( $B=0.86T$ ,  $E=6GeV$ ) is accepted for possible passage into an X-ray beamline's front-end. The other 90% are dissipated directly by a crotch absorber (fig.1). The dipole's spectral flux characteristics (fig.2 & 3) show,

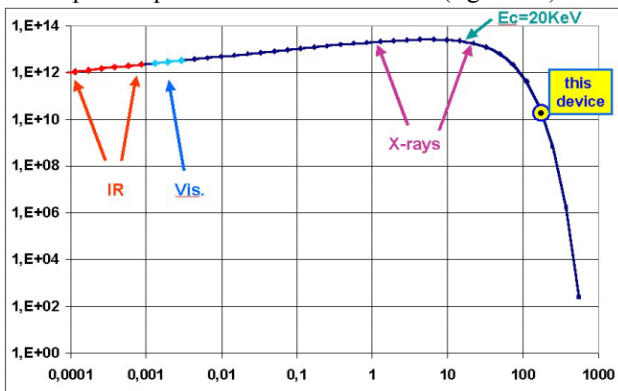


Figure 2: Dipole spectral flux (photons/sec 0.1%bw mrad)

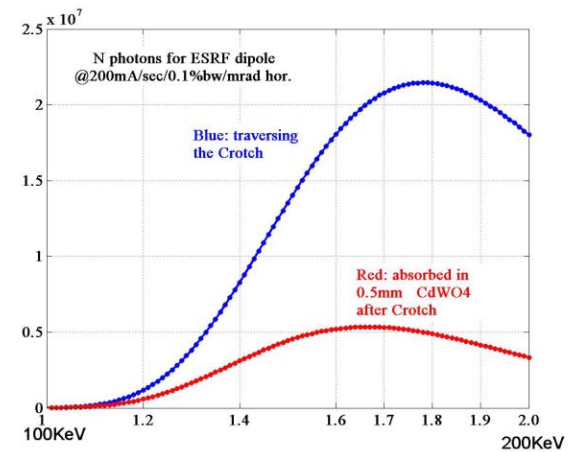
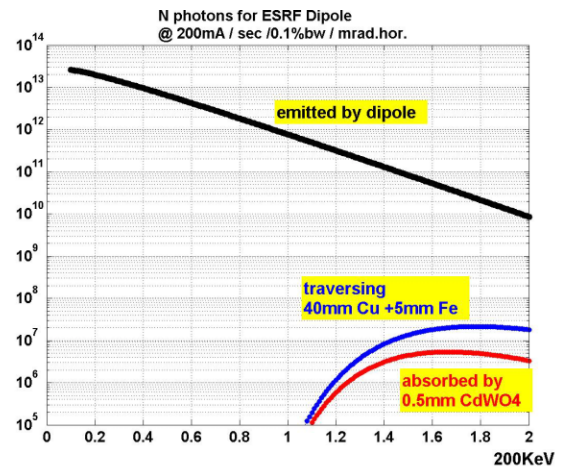


Figure 3: A spectrum of X-rays emitted by the dipole, entering the air and absorbed in the CdWO4 scintillator

with respect to 1-20KeV photons typically used for scientific work on a beamline, a reduced intensity of ~3 orders for the 150-200KeV range. The latter are attenuated another factor of ~3 orders by their 40mm path through the copper crotch absorber and 5mm through the steel vacuum chamber. Nevertheless, the fraction that enters the free air after the crotch chamber is still of an intensity of ~2E7 photons per second and per mrad horizontal angle in a 0.1% bandwidth at 200mA current.

The blue curve in the lower graph of fig.3 with a linear scale shows a sort of bandpass shape that is determined at the left-side by the increasing copper attenuation to lower energy photons, and on the right side by the slope of decreasing flux for higher energy photons.

## X-RAYS DETECTED BY SCINTILLATOR

Cadmium Tungstenate (CdWO4) is a high-Z crystal of nearly 8gr/cm3 density. [1] Thanks to its mechanical hardness it can be manufactured and polished to a

# THE X-RAY BEAM IMAGER FOR TRANSVERSAL PROFILING OF LOW-EMITTANCE ELECTRON BEAM AT THE SPRING-8

S. Takano\*, M. Masaki, and H. Ohkuma

Japan Synchrotron Radiation Research Institute, SPring-8, Hyogo 679-5198, Japan

## Abstract

The X-ray beam imager (XBI) at the accelerator diagnostics beamline I of the SPring-8 is briefly described. It has been developed for transversal profiling of the electron beam of the SPring-8 storage ring. It comprises a single Fresnel zone plate (FZP) and an X-ray zooming tube (XZT). The spatial resolution is 4  $\mu\text{m}$  ( $1\sigma$ ), and the time resolution is 1 ms. The field of view is vignetting-free and is larger than  $\phi 1.5$  mm. With the XBI, we have successfully observed the profiles of the electron beam having vertical emittance smaller than 10  $\text{pm}\cdot\text{rad}$ .

## INTRODUCTION

The SPring-8 is a third generation synchrotron light source operating since 1997. To observe the transverse profiles of the electron beam of the 8 GeV storage ring, we planned the XBI [1]. Our goal is the emittance diagnostics of the SPring-8 with resolution better than 1  $\text{pm}\cdot\text{rad}$ . The design targets of the XBI are 1) spatial resolution ( $1\sigma$ ) in the micron range, 2) time resolution of 1 ms, and 3) vignetting-free field of view larger than  $\phi 1$  mm on the coordinates of the electron beam. We have constructed the XBI at the accelerator diagnostics

beamline I (BL38B2) of the SPring-8 storage ring. The details of the XBI and the results of the measurements will be described elsewhere [2]. In this paper, we give brief descriptions of the XBI and some of the results obtained.

## THE X-RAY BEAM IMAGER (XBI)

The schematic layout of the diagnostics beamline I is shown in Fig.1. It has a bending magnet light source with an critical photon energy of 28.9 keV. The optical system of the XBI is shown in Fig.2. All the components of the XBI are in the optics hutch of the beamline. The XBI is based on a single FZP and an XZT. An X-ray image of the electron beam moving in the bending magnet is obtained by the FZP. To avoid the effect of the chromatic aberration of the FZP, monochromatic X-rays are selected by the double crystal monochromator. A 4-jaw slit is used to determine the horizontal width of the white X-ray beam incident on the monochromator to avoid unwanted heat load to the crystals. The magnification factor of the FZP is 0.274. We use an XZT to enlarge the reduced X-ray image of the electron beam. The observing photon energy of the XBI is 8.2 keV, which was determined by considering the

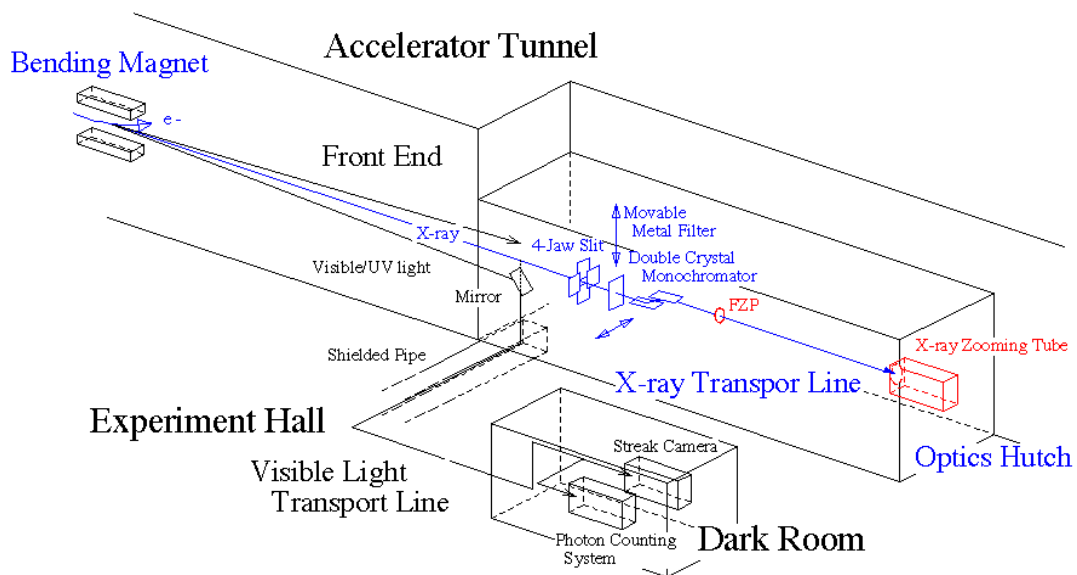


Figure 1: Layout of the SPring-8 accelerator diagnostics beamline I (BL38B2).

\* Email: takano@spring8.or.jp

## **PHOTON COUNTING MEASUREMENT IN SINGLE BUNCH OPERATION IN UVSOR-II ELECTRON STORAGE RING**

A. Mochihashi, K. Hayashi, M. Hosaka, M. Katoh, J. Yamazaki, UVSOR, Okazaki  
Y. Takashima, Nagoya University Graduate School of Engineering, Nagoya

### *Abstract*

In single-bunch operation in electron/positron storage ring for SR light source, it is very important to always keep good single-bunch purity because undesirable spurious bunches can disturb experiments with pulsed SR light. Even though only one main bunch is injected and stored initially, however, spurious bunches can be generated in RF-buckets following the main bunch and gradually grow. Such phenomenon has been understood as a result of Touschek effect in the main bunch; namely, electrons which gain larger momenta than RF-bucket height by scattering process between electrons in the main bunch and go out of the original RF-bucket can be captured again in the following bucket\*. We have observed impurity bunches in single-bunch operation in UVSOR-II electron storage ring by using photon counting method which has enough dynamic range to observe both the main bunch and the impurity bunches simultaneously. With the method, we have measured growth of the single-bunch impurity with time and tried to discuss Touschek effect in UVSOR-II.

**NO SUBMISSION RECEIVED**

# BUNCH BY BUNCH CURRENT AND LIFETIME MEASUREMENTS AT DAΦNE

A. Stella, G. Di Pirro, A. Drago, M. Serio, INFN-LNF, Italy

## Abstract

A dedicated system, based on digital sampling of beam signals with a commercial oscilloscope, has been developed to measure bunch by bunch current in the DAΦNE collider. It provides an automated tool to equalize bunch filling patterns in the main rings. Individual bunch current and lifetime are simultaneously computed from the sampled data, collected at a 4Hz rate and provided via ethernet to the accelerator control system to control individual bunch injection. System hardware and software data processing are reported, together with performance and results of the measurements obtained during DAΦNE operation.

## INTRODUCTION

In the electron-positron collider DAΦNE, the two symmetric rings can be filled with different patterns of maximum 120 bunches, spaced by 2.7ns and with a typical charge of  $1 \div 10$ nC. Storage of an equal charge in each bunch is crucial to optimize the luminosity.

By monitoring beam induced signals from wide band pickups the less charged buckets are selected for the next cycle of injection in order to obtain an even fill pattern.

This system provides to the accelerator control system an automated tool to perform this task; it is routinely used during the machine runs, being very useful and effective to maintain the average luminosity high and to increase the collider efficiency.

## HARDWARE

Sum signals from two beam position monitors (BPMs) installed in the electron and positron ring, are connected to a digital sampling oscilloscope Agilent Infinium 54832B (4GS/s real time sampling rate, 1GHz bandwidth) [1], through a 60m long coaxial cable (Andrew Heliax FSJ-50).

Electrodes used as pickups are of the *button* type with capacitance  $C_b=3.5$ pF showing a high pass frequency response. The transfer impedance is that of a time differentiator for frequencies  $f \ll 1/(2\pi R_0 C_b)=910$ MHz and of a resistor in the upper frequency range [2].

Each bunch induces a bipolar pulse signal in the button electrodes, whose peak to peak amplitude is proportional to its current. The system bandwidth, including the cable, is such that the peak-to-peak voltage is proportional to the bunch charge irrespective of the bunch length: in our case rms bunch length is less than 200 ps under all conditions.

The bunch pattern of the stored beam current will result, at the end of coaxial cables, in trains of pulses attenuated and stretched by the transfer function of the cable (Fig.1).

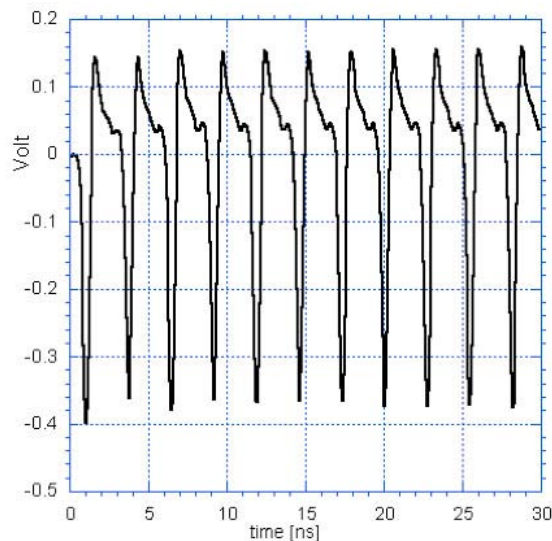


Figure 1: Detail of raw BPM signal waveform.

Due to the lack of DC response of the pickups, the resulting signals display also a significant drift of the base line which must be taken into account during data processing.

The digital oscilloscope samples the whole train of pulses both for electron and positron beams, with a 1GHz analog bandwidth (Fig. 2).

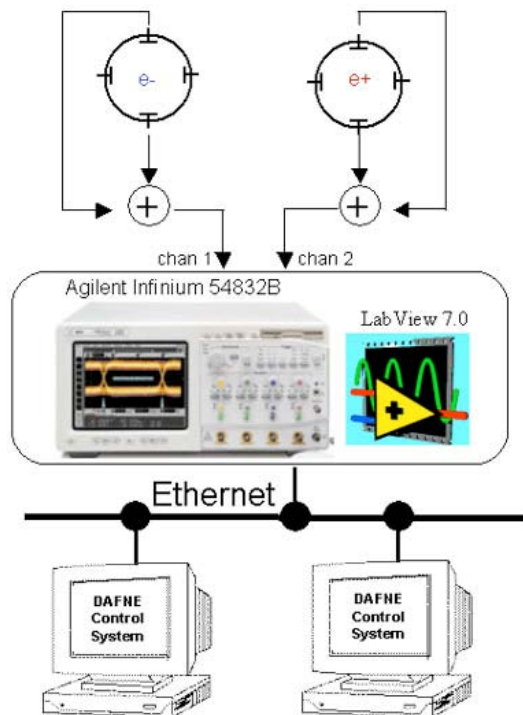


Figure 2: System block schematic.

# THE RENOVATION OF THE ISOLDE INSTRUMENTATION

Gerrit Jan Focker, Enrico Bravin, Stéphane Bart Pedersen, CERN, Geneva, Switzerland

## Abstract

The ISOLDE [1] instrumentation [2] is mainly based on mechanical scanners, wire-grids and faraday-cups. Additional items are the “fixed needle beam scanner” (FNBS), the tape-station and a device called the “fast faraday cup”. The control system for these devices is being redesigned and reimplemented in order to be integrated in the standard control system of the CERN accelerators complex. While some devices will still be controlled with “usual” standards (VME), the tape-station and the wire-grids will be controlled using industrial PLC’s. In fact, recently, the automates have become fast enough for these applications. This article will describe the different developments in the control electronics, the improvements of the devices themselves and will finish with a short peek at future projects.

## SCANNERS

The mechanical scanners as are used at ISOLDE were initially (1992) controlled by a “front-end computer” (FEC) running on DOS [3].

In 1998 a more intelligent electronic card containing an ADC and local memory to store the data was installed. This card was controlled via a 1Mb/s RS422 from a PC, running Windows NT and programmed in Visual Basic. In 2004 this system was ported to Windows XP.

This system is now being ported to the standard CERN control system based on VME and using a slightly improved version of the RS422 card. The front-end software is ready and this upgrade will be finalised as soon as the console-software is ready.

## WIRE-GRIDS

### Choice of Design

The main part of this article is however about the new controls of the ISOLDE wire-grids as it is based on a (for us) new technique. That is to say it is a new technique for taking data. The previous system was based on an obsolete front-end computer running DOS and should be integrated into the standard CERN control system. Adapting the existing electronics with its ISA-bus interface seemed too difficult and we had to look for an alternative. Siemens has in its Simatic program an ADC that has a 52 s conversion time, which is fast enough to read out the wire-grids. They also have a module called “Boolean Processor”, which is an independently running programmable logic device with a time-resolution of 10 s, good enough for controlling the track-and-hold timing and the integration time of the amplifiers which sit on an external chassis. The use of industrial controls is not new to us; the ISOLDE vacuum-controls were already controlled by Simatic somewhere in the eighties. But using them to replace a PC or VME Front-End Computer for data taking is new to us. It should be noted that it is not possible to use Simatic for the ISOLDE scanners as the Simatic-ADC is far too slow for this purpose.

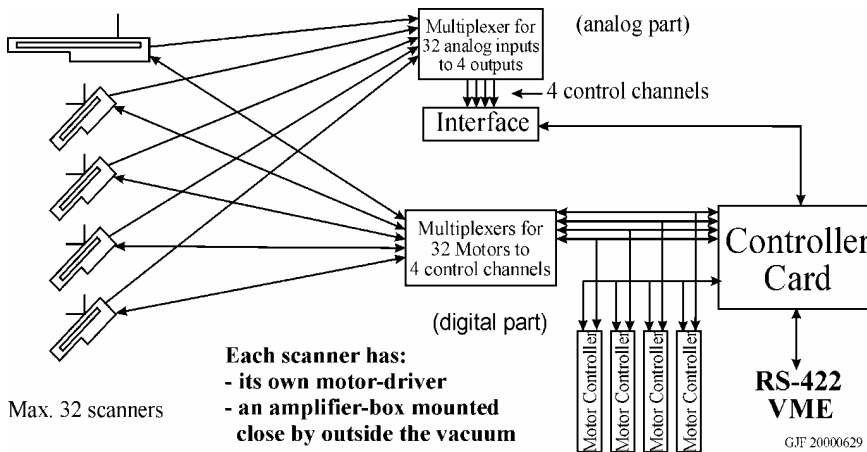


Figure 1: Block-diagram of the ISOLDE Scanner-system

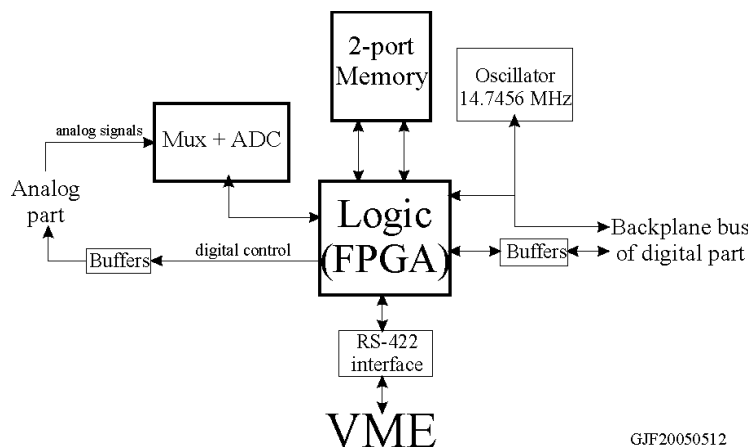


Figure 2: Block-diagram of the RS-422 controller card

## **BEAM PROFILE MEASUREMENTS BY USING WIRE DETECTORS IN J-PARC**

H. Akikawa, K. Hasegawa, T. Ohkawa,  
JAERI, Ibaraki-ken

H. Hiroki, Y. Kondo, H. Sakaki, S. Sato, M. Tanaka, A. Ueno, H. Yoshikawa,  
JAERI/LINAC, Ibaraki-ken

Z. Igarashi, M. Ikegami, S. Lee, K. Nigorikawa, T. Toyama,  
KEK, Ibaraki

J. Kishiro,  
JAERI/J-PARC, Tokai-Mura, Naka-Gun, Ibaraki-Ken

### *Abstract*

Beam intensity profiles are measured by wire detectors in high intensity proton accelerator J-PARC linac, RCS and MR. A single wire scanner is developed and examined for 20mA, 3 MeV  $H^-$  beam in KEK linac. Flying wire methods are also planned for RCS and MR commissioning. In this paper, basic design and preliminary experimental results are discussed.

**NO SUBMISSION RECEIVED**

# LINAC AND TRANSFER LINE BEAM POSITION MONITOR AT ELETTRA

S. Bassanese, M. Ferianis, F. Iazzourene, ELETTRA, Trieste, Italy  
V. Verzilov TRIUMF, Vancouver, Canada.

## Abstract

A Beam Position Monitor (BPM) system, based on Log Ratio detectors (Bergoz LR-BPM), has been designed, built and commissioned at ELETTRA. Currently, the system is installed on the ELETTRA Linac and Transfer Line and it is integrated in the ELETTRA control system. The system is being used to monitor the trajectory along the Transfer Line; in the Linac, it monitors and controls the Linac beam stability. Furthermore, the Transfer Line BPMs are integrated in the program TOCA for the correction of the trajectory and the optimisation of the injection efficiency. The paper describes the system and the measurements performed both in laboratory and on the ELETTRA electron beam. Future possible applications of the LR-BPM system for the upgraded ELETTRA Linac, to be used for the new seeded FEL source, are here briefly presented.

## INTRODUCTION

The old BPM system for the Linac and Transfer Line [5] based on a two GPIB-controlled oscilloscope acquisition system and multiplexer system, has been upgraded.

The system has been developed for the new ELETTRA full energy injector [1] composed by a 100 MeV Linac and a 3Hz cycling Booster synchrotron, up to 2.5GeV. The system will be used for the measurement of the beam position along the Linac and the two new Transfer Lines; it will be integrated in the beam trajectory feedback system for the optimization top up operation.

The single shot acquisitions can be averaged to improve the resolution for the trajectory's optimization. For the injection efficiency evaluation instead, a single shot charge measurement is required.

The main specifications of the system are the acquisition of the position with a resolution of less than 100  $\mu\text{m}$  in a circular vacuum chamber, 40 mm diameter; the minimum beam charge goes down to 50pC, both in single bunch and multi bunch mode.

The theoretical sensitivity [2] of a Log Ratio BPM can be calculated with the following formula referred to Figure 1 and calculated for the dimensions of the actual linac to storage ring transfer line.

$$20\text{Log}_{10}\left(\frac{A}{B}\right) = yS_y \cong \frac{160}{\text{Ln}(10)} \frac{\sin\left(\frac{\phi}{2}\right)}{\phi} \frac{y}{r} = \frac{160}{\text{Ln}(10)} \frac{\sin\left(\frac{\pi/4}{2}\right)}{\pi/4} \frac{1}{22.65} = 1.495\text{dB/mm} \quad (1)$$

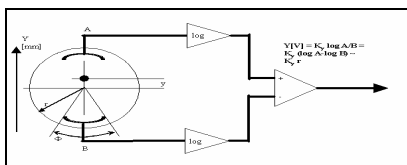


Figure 1: Log Ratio Principle of operation

## SYSTEM DESCRIPTION

The system is based on the Bergoz Log Ratio Beam Position Monitor (LR-BPM) electronic board, fitted with sample and hold module to acquire position and charge. Each electronic board can process signals either from orthogonal or rotated pick-ups (user configurable). Two analog outputs, for the x and y position, generate a signal of  $\pm 2\text{V}$ . A third analog output gives a signal (sum of logs) the area of which is proportional to charge [3].

There is also a digital output which detects a beam passage, to be used for triggering the A/D converter. The LR-BPM boards are housed in a 19" 3U RF shielded chassis (provided by Bergoz) including 2 power supply units and up to 16 BPM stations, connected to the pick-ups on the rear panel. A custom connection board collecting signals from four BPM stations has been developed to route signals to the A/D converter boards. The A/D converters adopt a CAEN V265 (8 ch.) charge integrating converter and two INCAA VD10 8 ch. 16 bit differential A/D converter. The timing signals to operate the system are provided by a CAEN V462 dual gate generator. All the VME boards are controlled by a Motorola VME5100 CPU, running a server application integrated in the ELETTRA control system, via RPC protocol. Each BPM station, equipped with a CPU, a dual gate board, a charge integrating converter, and two A/D converter boards can manage up to 8 groups of BPM. A group of BPM shares a LR-BPM front-end, and two A/D converter channels via four RF multiplexers that connect the LR-BPM input to each selected pick-up.

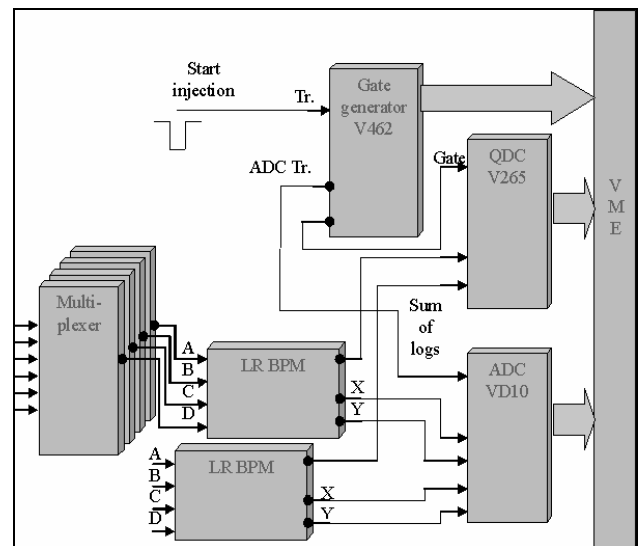


Figure 2: System layout

# FIRST TESTS OF THE MACHINE PROTECTION SYSTEM FOR CTF3

D. Belohrad, CERN, Geneva, Switzerland

## Abstract

CTF3, the test facility for the CERN Linear Collider study, is supposed to be operated at intensities and energies which may cause harm to the machine. For this reason there is a need for a machine protection system (MPS). The aim of the article is to describe the preliminary version of this system and to show first results measured in the CTF3 machine at the end of the 2004 running period.

The MPS is based on comparison of particle losses to a given threshold. As the MPS is required to stop the beam production within 1.5µs beam train pulse, very fast response needs to be achieved. Due to that, the losses are evaluated in real time as an amplitude attenuation of the beam current measured at two consecutive wall current monitors (WCM). When losses exceed given threshold, the beam-stop information is transmitted to the CTF3 gun interlock system. This causes inhibition of the beam production within the currently produced beam train. Manual actions are needed in order to recover from the beam-stop state of the MPS.

## INTRODUCTION

The MPS protects the CTF3 machine against the consequences of lossy transfer of the particles from CTF3 linac source to PETS, intermediate dumps or spectrometer lines. The system is supposed to recognize two types of losses:

- small repetitive losses, where the loss measured between two consecutive sensors doesn't exceed ~10% of nominal intensity
- a fraction of beam pulse train lost locally

The first case mentioned doesn't damage machine, but it raises personnel radiation hazard. In this case MPS should either decrease or stop the beam production in order to

lessen radiation. The response of the MPS to this particular case is not time critical, thus it can be implemented in the software. In the second case, the LINAC source beam production must be stopped inside the present pulse as there is a great risk of damaging the equipment. For this case a very fast response of the system is necessary. For both cases the recovery procedures must be applied and manual actions are needed in order to recover from the beam-stop state.

## DESCRIPTION OF THE SYSTEM

### Choice of Sensor

With respect to the beam parameters (electron beam of 1.5µs pulse length bunched at 3GHz and accelerated in a Linac working in fully loaded mode, repetition time max. 20ms) and required parameters of MPS, the sensor must satisfy following criteria:

- The intensity measurements must be available at maximum possible places.
- The bandwidth and dynamic range of intensity signal measured must be sufficient to follow fast beam intensity changes and to achieve reasonable precision of the intensity measurement.
- Usage of one measurement device type is advantageous.

A good candidate for the sensor is a wall current monitor (WCM) [1], which is commonly used to observe the time profile of the particle beams. Its high-frequency cut-off reaches 10GHz and the measuring devices are approximately equidistantly spaced in the machine each 10 to 15 metres. As we want to measure the beam intensity instead of observe the internal structure of the beam, we use the output of the WCM's integrator (signal compensated for residual droop of WCM). It provides a

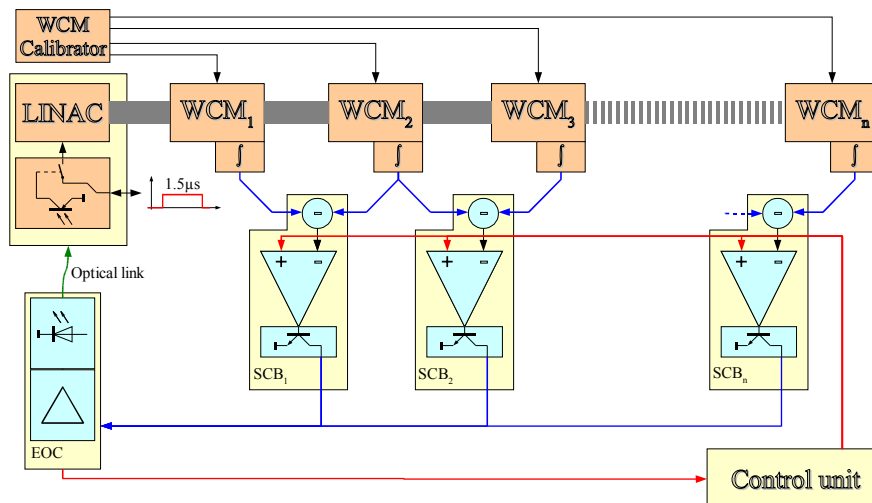


Figure 1: Simplified block schematic of MPS for CTF3

## LEIR BEAM INSTRUMENTATION

C. Bal, E. Bravin, S. Burger, C. Dutriat, M. Gasior, T. Lefevre, F. Lenardon, P. Odier, U. Raich, L. Søby, J. Tan, G. Tranquille, C. Vuitton, CERN, Geneva, Switzerland

### Abstract

The Low Energy Ion Ring (LEIR) is central to the “Ions for LHC” project. Its role is to transform a series of long low intensity ion pulses from Linac 3, into short high density pulses, which will be further accelerated in the PS and SPS rings, before injection into LHC. To do so the injected pulses are stacked and phase space cooled using electron cooling, before acceleration to the ejection energy of 72 MEV/u. This note describes different types of instruments which will be installed in the LEIR ring and transfer lines.

### INTRODUCTION

In addition to proton operation, the LHC machine will run a few weeks per year with ions to provide collisions for heavy ion experiments. The lead ion intensities achievable with the former ion accelerator chain were far below the needs for LHC, and it has been decided to convert the previous Low Energy Antiproton Ring (LEAR) into a low energy ion ring, dedicated to accumulate and cool ions, in order to reach the required beam brilliance for LHC. The installation of the LEIR machine is underway and commissioning will start soon. A typical LEIR cycle is shown in Figure 1. At the end of each multi turn injection of 200 $\mu$ s of PB<sup>54+</sup> the beam is electron cooled and stacked. After 4-5 injections the beam is bunched and accelerated to the ejection energy, where two bunches of 4.5  $10^8$  ions each are created and transferred to the Proton Synchrotron (PS). The main machine parameters are resumed in Table 1.

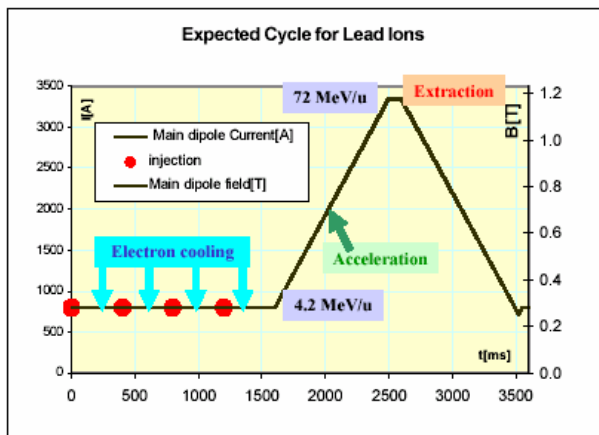


Figure 1: A typical production cycle.

Table 1: LEIR parameters.

Circumference	78.54m
Relativistic beta	0.095-0.37 <sup>1</sup>
Energy	4.2-72 MeV/u
Rev. Frequency	0.36-1.41 MHz
Q <sub>H</sub> , Q <sub>V</sub>	1.82, 2.72
Intensity range	2E8-2E11 Charges
Injection pulse	200us 50uA
Ejection bunch	2* 200ns 50mAp
Vacuum	10 <sup>-12</sup> Torr
Bake out temp.	300 °C

### INJECTION LINES

The injection line from LINAC3 consists of 3 segments: ITE, ETL which is common with the ejection line and the IE line just before the ring, see Figure 2.

#### Position

A total of 10 scintillating screens and cameras (MTV's) will be installed in the LEIR transfer lines. Seven are used to steer the injected beam, from which four can also be used at ejection.

Heavy ions at low energy are stopped within a few  $\mu$ m and all the energy is deposited in a very small volume. Different types of screen materials were tested in Linac3 [2], in order to find a material capable of withstanding this energy deposit. The material often used in high energy accelerators Al<sub>2</sub>O<sub>3</sub>, showed degradation and reduced sensitivity after a few hours of beam. ZrO<sub>2</sub> for which a degradation of the material was visible, showed no reduction in sensitivity, and has been chosen as screen material.

A new MTV electronics hardware, consisting of a single VME 64x card, has been developed. This card is capable of controlling: all the different types of positioning mechanism for the screens, the adjustment of the illumination intensity, the different types of cameras (i.e. CCD or Vidicon tube) and the positioning of optical filters in front of the camera. Apart from the analog video signal the card provides also the digitized image.

#### Intensity

Three old transformers will be re-used and installed in the ETL and EI lines refurbished with new magnetic shielding and water cooling system according to the PS standard model. New front end electronics have been

<sup>1</sup> Will be extended to 0.9 for light ions, but not before 2009.

# HARDWARE SIMULATION KIT FOR BEAM INSTRUMENTATION

Arkady Likhovitskiy, Danil Kortchaguin, JINR, Dubna, Russian Federation  
Michael Ludwig, CERN, Geneva, Switzerland

## Introduction

For beam instrumentation front-end software consolidation in the CERN-PS AB-BDI-SW section has launched a campaign in collaboration with the Joint Institute for Nuclear Research (JINR) in Dubna (Russia). This consolidation is to a large extent re-engineering of legacy front-end software of the running CERN-PS machine. This raises the following issues: standardization, simulation of non active timing events, simulation of non available hardware, and backward compatibility. This paper describes a beam instrumentation hardware simulation, which is used to develop, test and validate instrumentation software, which are disconnected from the real hardware and machine timings.

## CONSOLIDATION

The aim of this consolidation is to replace instrumentation servers in our front-end computers (FECs) which have reached the end of their lifecycle after more than a decade by completely re-engineered instrument servers for the LHC Injector chain. Directly affected are 15 FECs for beam current measurements hosting in total 279 devices and 8 FECs for beam position measurements with 357 devices, all of which are “24h/7d” mission critical. The new servers have to cover all functionality of the existing software, provide a high degree of backward compatibility in order to avoid software incompatibility in the client application layer, and provide subscription, structured properties, a data subset selection mechanism, object oriented design and code generation using graphical design tools. All these new features are needed to satisfy the increased demands of the LHC era. New servers are test-deployed and validated on a per-FEC basis under operational conditions with beam in dedicated software machine development sessions: this is normally the first time a new server runs with real hardware.

## CONSTRAINTS

### Standard Framework

The Front-End Software Architecture (FESA) framework [1] is the new framework which is used to overcome the current diversity in the LHC injector chain front end equipment software domain and pave the way towards LHC for efficient development, diagnostic and maintenance in this area. All data retrieving and processing is going through two types of actions: real-time (RT) actions and communication (COMM) actions. RT actions are scheduled according to timing maps and manage control and acquisition data flows between the

hardware and a common shared memory region called FESA device. COMM actions are scheduled according to users’ requests and transmit data to client applications.

### Instrument Functional Model

An instrument server generally performs many acquisitions from different hardware modules at different moments during the production of a type of a beam\*, processes them according to the logic of the measurement and then publishes the results for each type of beam separately†. The result data must be available and consistent for at least the duration of one cycle (of a given type), so that the application client can pick it up before it is overwritten by the next cycle of the same type.

### Backward Compatibility

FESA is not fully backward compatible with the present control system (referred to as **general modules GM**) and existing naming conventions [1]. The GM type software clients are interfaced to FESA using a system of special GM classes for each instrument which connect to a set of FESA properties for this instrument (FESA2GM adapter). Each GM class provides full inheritance to the GM super classes at the same time. Thereafter, the GM-specific communication channels: local GM access in the FEC, the common middleware servers (CMW) and the remote procedure calls (RPC) servers can be used transparently. Correspondence maps between old and new properties and devices, which provide also many-to-one relationships, are used to overcome naming incompatibilities and to regroup devices in the re-engineered instruments.

## STANDARDIZATION

In the context of the consolidation project [3] we deal with a lot of hardware module types and different coding principals. At the same time there are no common patterns to standardize and simplify hardware module calls as the FESA does with an instrument design. This requires finding some solution to provide an abstraction as a standardized approach to HW interaction design in FESA, including instrument simulation. The abstraction has to solve the following issues:

- Support a vastly heterogeneous structure of equipment and coding technologies present in CERN.

\* A beam is produced during a cycle. A sequence of several (usually different) cycles forms a supercycle.

† The results are multiplexed in pulse-to-pulse (=cycle) modulation (PPM) slots of the device memory.

# ACCURACY OF THE SPS TRANSVERSE EMITTANCE MONITORS

F. Roncarolo, B. Dehning, C. Fischer, J. Koopman, CERN, Geneva, Switzerland

## Abstract

A campaign of studies and measurements has been carried out with the aim of establishing the SPS transverse profile monitors resolution, reproducibility and accuracy. The studies regarded systematic dependencies of the SPS Wire Scanner (WS) monitors on the operation setups and on the beam parameters, like beam intensity, bunch spacing and beam size. The emittance increase due to multiple Coulomb scattering during the linear WS operation has been measured and compared with the theoretical model prediction. Numerical simulations estimate the errors introduced by the limited resolution of the imaging systems and by excessive electronic noise of the detectors. The experimental measurements have been carried out with a wide range of beams, from the low intensity pilot bunch to the LHC nominal beam. At first the different SPS WS are compared during simultaneous measurements. The SPS IPM vertical profiles have been compared to the WS while tracking the beam emittance from 26 to 450 GeV. The IPM resolution improvements from 2003 to 2004 are pointed out.

## WS MEASUREMENTS

The CERN SPS is equipped with ten WS monitors (five for each transverse plane) mounting  $30\ \mu\text{m}$  diameter Carbon wires. Four of them are based on a mechanism that drives the wire *linearly* along a direction orthogonal to the beam trajectory with a maximum speed of  $1\ \text{m/s}$ . The remaining six monitors are based on a rotational mechanism which drives the wire at a maximum speed of  $6\ \text{m/s}$ . All the WS measurements presented below were carried out with two or three instruments simultaneously, with a time jitter of  $1\ \text{ms}$ . For all the plots and tables which will be presented hereafter, the emittances are intended at one sigma and normalized to the beam energy.

### Linear WS Calibration

The result of the simultaneous operation of two linear WS (measuring the vertical beam size) during seventeen SPS cycles is shown in Fig. 1. Each time slot (horizontal axis on the plot) refers to one cycle and consequently to the injection of new particles that do not necessary have the same emittance as in the previous cycle. Two scans per cycle are performed with each instrument: at  $t = 0.5\ \text{s}$  after the protons injection the wires move in a forward direction (*IN scan*, from the bottom to the top of the beam pipe) and at  $t = 1.5\ \text{s}$  they move backward (*OUT scan*). Both instruments detect a systematic emittance increase during

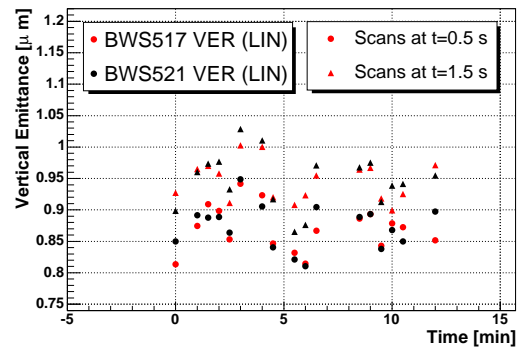


Figure 1: Comparison between two linear WS during simultaneous measurements with TOTEM beam injected every 30 s in the SPS and circulating at 26 GeV for 4.5 s.

the two scans. This is due to Coulomb scattering between the beam and the wire material, the OUT scan detects the emittance increase generated by the IN scan [3].

The standard deviation of the measured emittance increase, divided by  $\sqrt{2}$  (since the increase is detected by two scans), assesses the monitors *repeatability*. In terms of beam size the repeatability results in 6 and  $10\ \mu\text{m}$  for the considered instruments. The mean value of the differences between the emittances measured by the two linear monitors determines the relative WS *accuracy*. The relative average difference results well below 1% of the small vertical emittance characterizing the measured beam ( $\approx 0.9\ \mu\text{m}$ ).

### Cross Calibration Between Linear and Rotational WS

The three rotational WS monitoring the vertical beam size have been operated in synchronization with a linear device (labelled 517V) used as a reference. Table 1 and Fig. 2 summarize the comparisons, including the one between the two linear WS described in the previous paragraph. The IN and OUT scans are analyzed separately and in the table  $\mu$ ,  $\sigma$  and  $\sigma_\mu$  are the differences mean value, standard deviation and error on the mean ( $= \sigma/\sqrt{N_m}$ ) over  $N_m$  measurements. The figure also refers to the "IN/OUT correction".

A post-processing of the values of the wire position during the rotational WS operation is in fact necessary. The measured angular position of the wire is projected on the transverse coordinate by an algorithm. A systematic error in the angular position arises from a low pass filter used to reduce the electronic noise on the potentiometer. Such filter introduces a delay in the time domain between the measured and the real angle, which results in an opposite

# SRAM-BASED PASSIVE DOSIMETER FOR HIGH-ENERGY ACCELERATOR ENVIRONMENTS

D. Makowski, M. Grecki, B. Świercz, A. Napieralski, DMCS, Łódź, Poland  
 B. Mukherjee, S. Simrock, DESY, Hamburg, Germany

## Abstract

This paper reports on a novel Non-Volatile Random Access Memory (NVRAM)-based neutron dose equivalent monitor (REM counter). The principle of this device is based on the radiation effect initiating the Single Event Upsets (SEUs) in high density memories. Several batches of NVRAMs from different manufactures were examined in various radiation environments, i.e.  $^{241}\text{Am-Be}$  ( $\alpha, n$ ) and Linear accelerator, produced radiation fields. A suitable neutron moderator was used to enhance the detector's sensitivity. Further experiments were carried out in a linear accelerator VUV-FEL. A separate batch of SRAM was irradiated with  $^{60}\text{Co}$ -gamma source risen up to a dose of about 1.1 kGy. The proposed detector could be ideal for a neutron dose measurement produced by a high-energy electron linac, including synchrotron and Free Electron Laser (FEL) facilities.

## INTRODUCTION

During the operation of high energy linear accelerators bremsstrahlung gamma and photoneutrons are produced [1]. Both gamma and neutrons pose a real threat to electronic devices installed in an accelerator tunnel. Therefore radiation measurement plays a crucial role to assure the reliable operation of accelerators. A large number of gamma detectors is currently available [2]. One can use photomultipliers, ionization chambers, scintillation counters and semiconductor-based dosimeters. Conversely to gamma, neutrons are uncharged particles, that have only a few interactions with matter, thus their detection is much more complicated than gamma. Neutrons are only detectable through measurements of secondary particles or a secondary phenomena [2, 3]. Superheated emulsion (bubble) and thermoluminescent (TLD) dosimeters can be used for sensitive neutrons measurement. Superheated emulsion dosimeters have a flat-response characteristic, however require an arduous bubble-counting process. TLD must be calibrated before the measurement.

The pulsed generation of neutrons in the high gamma background is difficult to measure. Gamma radiation has always an influence on the measured neutron fluence [2]. Only bubble dosimeters are able to measure neutrons fluence without gamma interaction.

Radiation present in linear accelerators, like the VUV-FEL or Linac II located at DESY, is produced because of the unwanted collision of the electronbeam with high Z materials in the beam line [1]. The amount of gamma is a few orders of magnitude higher than the neutrons' dose.

## PRINCIPLE OF NEUTRON DETECTION

The basic idea of the SRAM-based dosimeter is to count the number of SEU induced in the memory during the measurement. SEU can be generated only by charged particles, which have relatively high Linear Energy Transfer (LET). Neutrons can be only detected from the secondary charged particles generated in the material (e.g.  $\alpha$ , protons) [7].

The presented passive dosimeter uses Non-Volatile Random Access Memory instead of the classical SRAM device as a dosimeter, which is depicted in Fig. 1. SRAM devices

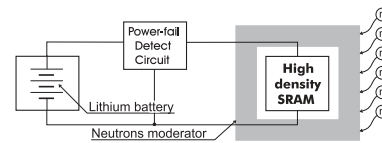


Figure 1: NVRAM-based neutron detector

cooperate with a lithium battery that provides a supply voltage when the memory is disconnected from the main power. An additional power supervisory circuit was implemented to detect a sudden disconnection from the main supply voltage and reconnect a back-up battery to avoid the accidental memory data corruption.

SEU in SRAM are generated by thermal neutrons which generate alpha particles present in accelerators, [5, 7]. Alpha particles have very high LET [7]. The energy is deposited along the ionising particle track, therefore electron-hole pairs are created. SEU is generated in the SRAM chip when a critical charge is deposited near the drain electrode of the MOS transistor [2]. The standard SRAM cell, presented in Fig. 2, consists of six MOS transistors, however only four are used to store a binary value. Solely, disabled transistors  $T_2$  and  $T_3$  are sensitive to SEU effect.

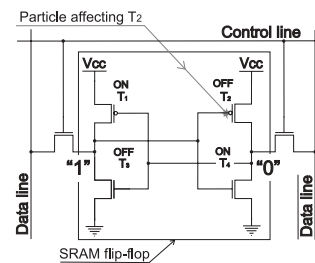


Figure 2: A single SRAM cell affected by ionising particle

The number of SEU induced in SRAM chips is proportional to the neutron fluence [3, 5]. However, the applica-

## BEAM POSITION MONITOR FOR THE J-PARC MAIN RING SYNCHROTRON

T.Toyama\*, D.Arakawa, Y.Hashimoto, S.Lee, T. Miura, H.Nakagawa, KEK, Tsukuba, Ibaraki,  
Japan  
N.Hayashi, R.Toyokawa, JAERI, Tokai, Ibaraki, Japan

### Abstract

A BPM system has been developed for the J-PARC Main Ring Synchrotron. A diagonal-cut 'electrostatic' pick-up and a processing circuit with an analog amplifier, attenuator, filter and ADC are adopted. The system expects no active devices in the tunnel to avoid radiation damage. The system aims at a position accuracy of  $\pm 0.1$  mm. The test using whole system except a cable at the KEK-PS shows good system performance with the position resolution better than  $\pm 20$   $\mu\text{m}$ . The position accuracy will be attained with careful installation and beam based calibration.

### INTRODUCTION

J-PARC 50 GeV Main Ring Synchrotron will feed  $3.3 \times 10^{14}$  protons per pulse (typically in 3.6 s), corresponding to an average current of 12.4 - 12.8 A and a peak current of 41.3 - 220 A as shown in Table 1[1]. Main features of this machine are: (1) high intensity, (2) main frequency components are localized less than a few 10 MHz, (3) a beam size is large both in transverse and longitudinal. To fit these characteristics the following design principle is adopted: (a) electrostatic pickup with diagonal-cut cylinder for linear response to the position, (b) no active devices (semiconductors) will be installed in the tunnel.

Signal processing is performed using a 14 bit - 80 MSPS ADC with 10 MHz LPF. The data acquisition and module control will be accomplished using a control software tool-kit, EPICS, in principle. Large data will be exceptionally handled with ftp [2]. The dynamic range of the system should meet the following conditions: (1) initial beam commissioning will be done with 1/100 of the design intensity [3], (2) the peak beam current is expected as 41 - 220 A.

The precise position measurements and COD correction is crucial to prevent beam losses at the injection flat

Table 1: Parameters of the 50 GeV MR

Parameter		Unit
Peak beam current	41.3 - 220	A
Average beam current	12.4 - 12.8	A
Speed of the beam	0.9712 - 0.9998	
Bunch length	360 - 67	ns
Bunching factor	0.3 - 0.058	
Revolution frequency	186 - 191	kHz
RF frequency	1.67 - 1.72	MHz

\*takeshi.toyama@kek.jp

bottom [4]. Therefore the goal is set at the position accuracy of  $\pm 0.1$  mm and the resolution of  $\pm 10$   $\mu\text{m}$ . The alignment between the quadrupole and BPM pair will be achieved by making use of beam based calibration.

### BPM PICK-UP

Electrostatic pickup with diagonal-cut cylinder is adopted because of its linear response to the position [5]. One BPM set consists of one horizontal and one vertical electrode pairs (Fig. 1). The electrodes and chamber are made of stainless steel, SUS316L and the SMA coaxial vacuum feed through is made of SUS316L brazed with alumina ceramics. The electrodes are supported and insulated with small ceramic block positioned in grooves of the inner surface of the chamber. The coupling impedance is very small. The electrode capacitance is  $\sim 210$  pF.

Calibration of the position response is going on with a copper wire of  $\phi 0.4$  mm and the position resolution of  $\pm 10$   $\mu\text{m}$ . The linear position response, deviation of less than 0.1 mm within  $r < 40$  mm was obtained. The lower cut-off frequency was  $\sim 17$  MHz (Fig. 2), which differentiates the beam signals. The frequency response of the position sensitivity:

$$\kappa = (L-R)/(L+R)/x$$

is plotted in Fig. 3, where  $L$  and  $R$  are the output voltage from the left and right electrodes,  $x$  is the horizontal displacement of the wire. Reduction of position sensitivity  $\kappa$  at  $f > \sim 5$  MHz is considered due to capacitive coupling between the opposite electrodes. The calculation with this assumption agrees with the measured data (Fig. 4) [5]. This will not affect the COD measurement because the detection frequency is the RF frequency,  $\sim 1.4$  or  $\sim 3.4$  MHz.

The wire calibration will be planned for all pickups in this year. Overall position offset relative to the quadrupole center will be identified by beam-based calibration.

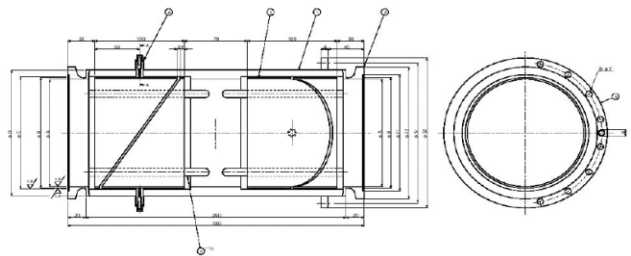


Figure 1: Drawing of the pick-up.

# FIRST STEPS TOWARDS THE INTEGRATION OF PHOTON BEAM POSITION MONITOR SIGNALS INTO THE SLS FAST ORBIT FEEDBACK

T. Schilcher, M. Böge, B. Keil, R. Kramert, J. Krempaský, P. Pollet, V. Schlott,  
Paul Scherrer Institute, Villigen, Switzerland

## Abstract

So far, photon beam position monitor (PBPM) signals at the SLS are mainly used to verify the performance of the fast orbit feedback (FOFB), which is based on RF BPM position readings. Additionally, a slow high level PBPM feedback compensates systematic effects of the digital BPM electronics. The development of a new PBPM signal processing electronics allows the synchronization of the PBPM signals with the 4 kHz sampling rate of the FOFB. Subsequent integration of the photon beam position data into the FOFB system will be achieved by signal distribution through fibre optics links (Rocket I/O) based on the generic VME PMC carrier board (VPC) and on mezzanine receiver modules on the FOFB DSP board. The integration of PBPM signals based on the new electronics concept is explained.

## INTRODUCTION

User operation of the SLS requires the reproduction and stabilization of a defined reference orbit within 1/10th of the electron beam size. In addition, the growing number of insertion devices (IDs) with their needs to change the gaps transparently to all other users and the increasing sensitivity of the experiments demanded a fast orbit feedback system (FOFB) to stabilize the beam to the required level. Such a FOFB has been foreseen at the design stage of the SLS [1] to correct orbit perturbations in the relevant frequency range up to 100 Hz to provide  $\mu\text{m}$  orbit stability. After the commissioning phase [2] the FOFB has replaced the former high level based slow orbit feedback in November 2003. Table 1 summarizes the improvements of the

Table 1: Integrated beam position temporal rms values with FOFB off and on measured at the tune BPM. The values are normalized to the beta function  $\beta_{x/y} \approx 12/17$  m and reflect the situation for fixed ID settings.

FOFB	horizontal		vertical	
	off	on	off	on
1–100 Hz	0.83 $\mu\text{m}$	0.38 $\mu\text{m}$	0.40 $\mu\text{m}$	0.27 $\mu\text{m}$
100–150 Hz	0.08 $\mu\text{m}$	0.17 $\mu\text{m}$	0.06 $\mu\text{m}$	0.11 $\mu\text{m}$
1–150 Hz	0.83 $\mu\text{m}$	0.41 $\mu\text{m}$	0.41 $\mu\text{m}$	0.29 $\mu\text{m}$

beam stability at the SLS with the FOFB running compared to the situation without feedback. The values still contain the noise contribution of the DBPM system, which has been measured to be  $<0.13 \mu\text{m}$  within the bandwidth up to 100 Hz.

In addition to the digital RF BPMs (DBPM), photon beam position monitors (PBPM) are important tools for beam-line and machine diagnostics. Several PBPMs have been installed and commissioned at the SLS [3]. They feature high resolution in the range of  $0.5 \mu\text{m}$  rms ( $<0.5$  Hz bandwidth). Due to the long lever arm PBPMs are excellent devices to judge the electron beam stability at the location of the photon beam source point beyond the resolution of any RF BPM. Moreover, PBPMs measure the photon beam movement and therefore allow to discriminate perturbations caused by the electron beam from those caused along the beam-line up to the experimental station. However, position measurements with PBPMs are subject to systematic effects like background radiation from the bending magnets, changes in the ID radiation spectrum during gap changes (for ID PBPMs) and/or varying PBPMs blade response due to thermal effects. Therefore, these systematics of PBPMs have to be understood for the desired ID settings before any conclusion can be drawn from their readouts. At the SLS, the in-vacuum undulators of two protein crystallography (PX) beam-lines and the wiggler of the material science (MS) beam-line are mostly operated at fixed gap positions. The PBPMs at the mentioned beam-lines are well understood and calibrated.

## PBPM FEEDBACK ALGORITHM

If PBPM readouts are calibrated they can be integrated into the global orbit correction scheme. The underlying PBPM feedback algorithm changes the orbit reference of the DBPMs adjacent to the IDs in such a way to keep the photon beam position constant at the PBPMs. If only one PBPM is available, the photon beam position change is compensated by a pure angle variation of the orbit at the source point. Eq. 1 allows to calculate the reference change of the two DBPMs 1 and 2 ( $d_1, d_2$ ) adjacent to the ID for a desired reading of the PBPM (see Fig. 1).

$$\begin{pmatrix} d_1 \\ d_2 \end{pmatrix} = \frac{1}{a} \begin{pmatrix} -c_{\alpha_x} \cdot l_1 \\ c'_{\alpha_x} \cdot l_2 \end{pmatrix} \cdot x_1 \quad (1)$$

The factors  $c_{\alpha_x}, c'_{\alpha_x}$  translate the purely geometrical offsets for an asymmetrical bump to the required offsets at the location of the DBPMs for a given optics. In case of two available PBPMs, the corresponding necessary angle and offset change can be calculated according to Eq. 2. Similar as in Eq. 1 the factor  $c_x$  allows to map a geometrical transverse shift to the necessary transverse offsets at the DBPMs for a given optics. In both cases, the calcu-

## INVESTIGATION OF PHOTO NEUTRALIZATION EFFICIENCY OF HIGH INTENSITY H<sup>-</sup> BEAM WITH Nd:YAG LASER FOR J-PARC

T. Tomisawa, H. Akikawa, K. Hasegawa, Y. Kondo, H. Oigawa, S. Sato, A. Ueno  
JAERI/LINAC, Ibaraki-ken

M. Ikegami, S. Lee, T. Toyama, I. Zenei  
KEK, Ibaraki

### *Abstract*

The photo neutralization method with Nd:YAG laser for negative hydrogen ions has been considered as an available candidate for beam intensity profile monitor and charge exchange procedure for Accelerator-Driven-System (ADS) in J-PARC. An electron of H<sup>-</sup> beam can be stripped by fast and intense Nd:YAG (1064nm) laser with non-destructive, and laser system have advantages of maintenance and radiation hardness in high intensity proton accelerators. In this paper, an experimental set-up and preliminary results of photo neutralization method for linac H<sup>-</sup> beam in KEK DTL1 are described.

**NO SUBMISSION RECEIVED**

# INVESTIGATION OF PHOTO NEUTRALIZATION EFFICIENCY OF HIGH INTENSITY $H^-$ BEAM WITH ND:YAG LASER IN J-PARC\*

T. Tomisawa, H. Akikawa, S. Sato, A. Ueno, Y. Kondo, H. Oigawa, T. Sasa and K. Hasegawa  
JAERI, Tokai, Naka, Ibaraki, 319-1195, Japan

S. Lee, I. Zenei, T. Toyama and M. Ikegami, KEK, Tsukuba, Ibaraki, 305-0801, Japan

## Abstract

The photo neutralization method with Nd:YAG laser for negative hydrogen ions has been expected as an available candidate for the transverse beam profile measurement. The fraction of photo detached electron can also be used for charge exchange procedure to extract very low power proton beam for Transmutation Experimental Facility in J-PARC. The laser system has advantages of maintenance and radiation hardness in high intensity proton accelerators. In order to establish the low power beam extraction system and beam profile monitor, the photo neutralization efficiency must be surveyed in practical beam line with high intensity  $H^-$  beam. In this paper, an experimental set-up and preliminary results of photo neutralization method for intense  $H^-$  beam in J-PARC MEBT1 are described.

## INTRODUCTION

The J-PARC linac aims to provide high intensity negative hydrogen ion beams of peak current 50mA, kinetic energy 181/400MeV, pulse width 0.5mA and repetition rate 25Hz [1]. The goal of 133 kW beam power and hand-on maintenance will place significant demands on the performance and operational reliability of accelerator diagnostics systems. Beam diagnostics system is required to verify proper transverse focusing and matching of the magnetic focusing lattice of the linac. The transverse beam profile is one of the most important parameter for beam commissioning and/or tuning, and currently measured by single wire scanner in linac [2]. However, the interaction mechanism between thin wire and  $H^-$  ions for various beam energies should also be investigated to clarify beam profiles. The photo neutralization method with Nd:YAG laser has been considered as an available candidate for beam intensity profile monitor. The photo neutralization technique is also expected as a beam extraction method for Transmutation Experimental Facility (TEF) in J-PARC [3]. The laser charge exchange method is an essential technique to extract very low power and narrow pulse width proton beam from intense  $H^-$  beam as shown in Fig.1.

Thus, the neutralization efficiency should be investigated experimentally. This paper reports the development of a laser based beam profile monitor system. The MEBT1 beam diagnostic system to measure photo neutralization efficiency is also described in detail.

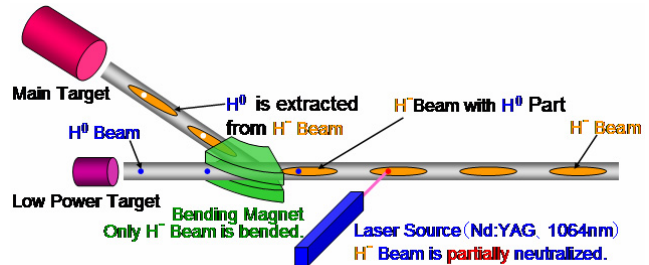


Figure1: Schematic view of low power beam extraction

## EXPERIMENTAL SET-UP

The experimental device is composed of ion source, RFQ, MEBT1 and the laser system. A photo interaction chamber of laser profile monitor was installed in the MEBT1 (Fig. 2).

### Ion Beam Line:

0.5ms long, 30mA pulse beam in the MEBT-1 consists of micro bunch of <0.5ns pulse width. The  $H^-$  ion beam is accelerated by 324MHz radio frequency quadrupole linac (RFQ) up to the beam energy of 3MeV.

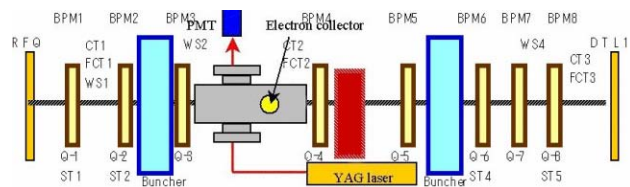


Figure 2: Laser profile monitor in MEBT1

### Laser System:

Commercial Nd:YAG laser can produce pulse width of 20ns long, maximum pulse energy of 500mJ, wavelength of 1064nm at repetition rate of 25Hz. Laser beam size was formed to horizontal width of 6mm and height of 0.8mm at the  $H^-$  beam line by a pair of 80mm focal length cylindrical lenses. Stripped electrons were deflected 90degree by an electromagnetic dipole and collected to a Faraday cup.

## THE LHC BEAM LOSS MONITORING SYSTEM'S REAL-TIME DATA ANALYSIS CARD

C. Zamantzas, B. Dehning, E. Effinger, G. Ferioli, G. Guaglio, R. Leitner  
CERN, Geneva, Switzerland

### Abstract

The BLM (Beam Loss Monitoring) system has to prevent the superconducting magnets from being quenched and protect the machine components against damages making it one of the most critical elements for the protection of the LHC. The complete system consists of 3600 detectors, placed at various locations around the ring, tunnel electronics, which are responsible for acquiring, digitising, and transmitting the data, and surface electronics, which receive the data via 2km optical data links, process, analyze, store, and issue

### ANALYSIS CARD (BLMTC)

The data analysis card is based on the general purpose PCB that was implemented for the whole instrumentation group, named DAB64x [3]. It is comprised from an Altera Stratix™ [4] FPGA, an Altera MAX™ CPLD [5] for power-on configuration and VME functionality, and three SRAM memories. The functionality of the system is realised by using different firmware on the FPGA and CPLD devices, and different mezzanine cards that can be placed on either of the six general-purpose connectors.

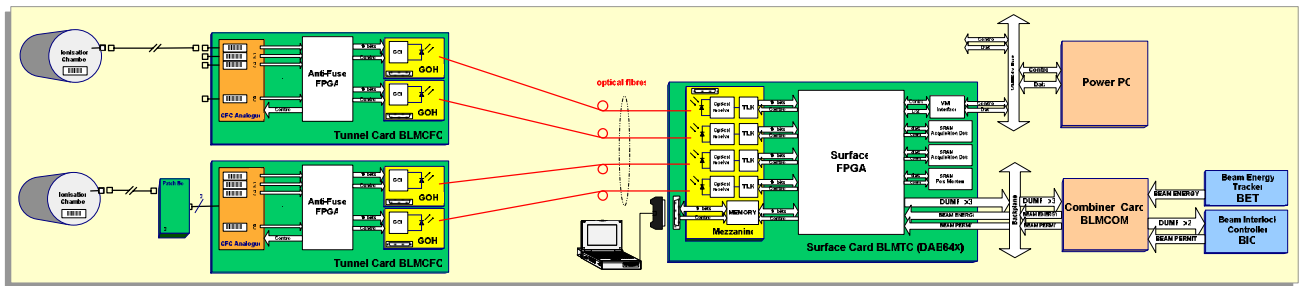


Figure 1: Overview of the complete BLM System for the LHC.

warning and abort triggers. At those surface units, named BLMTCs, the backbone on each of them is an FPGA (field programmable gate array) which treats the loss signals collected from 16 detectors. It takes into account the beam energy and keeps 192 running sums giving loss durations of up to the last 84 seconds before it compares them with thresholds uniquely programmable for each detector. In this paper, the BLMTC's design is explored giving emphasis to the strategies followed in combining the data from the integrator and the ADC, and in keeping the running sums updated in a way that gives the best compromise between memory needs, computation, and approximation error.

### INTRODUCTION

Around 3600 *Ionization Chambers* are the detectors of the system. A set of up to 8 of them can be connected to each of the tunnel cards. In those tunnel cards, called *BLMFCs*, the digitisation of the detector signal is done by using *CFCs* (current-to-frequency converters) and *ADCs*. An *Anti-Fuse FPGA* [1] acquires the digitised data and transmits them at the surface using the *GOLs* (*Gigabit Optical Links*) [2]. There, the data analysis cards, named *BLMTCs*, receive those data. The surface *FPGA* will analyse by keeping a history of those data and decide whether or not a dump request should be initiated. Each surface card receives data from 2 tunnel cards, which means that it can treat up to 16 channels (see Fig.1).

The BLM mezzanine card [6] includes all necessary components for the four gigabit optical receivers and a Mbit of Flash memory for system specific data.

### PROCESSES RUNNING IN THE FPGA

The surface FPGA has 41,000 LE (logic elements), 615 user I/O pins, and 400KBytes of internal memory as available resources for the system to be built from.

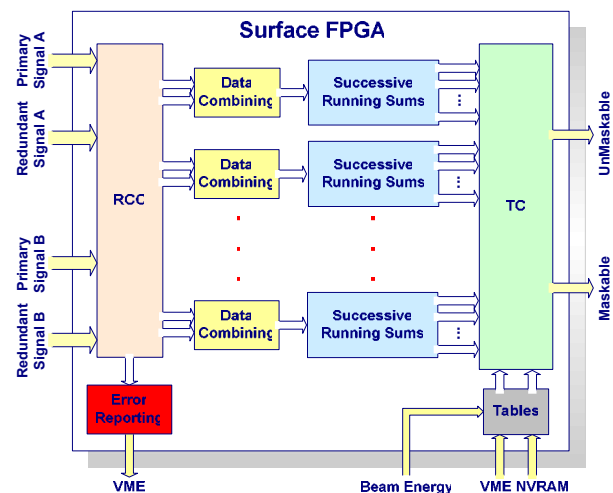


Figure 2: Block diagram of processes related to data analysis running in the surface FPGA.

# THE DIGITAL CAMERA APPLICATION IN THE TAIWAN LIGHT SOURCE

C. H. Kuo, Y. T. Yang, J. Chen, S. Y. Hsu, D. Lee, K. H. Hu, C. J. Wang, K. T. Hsu

NSRRC, Hsinchu 30076, Taiwan

## Abstract

Digital camera has been adopted for the booster, storage ring and transport-line diagnostic recently at the Taiwan Light Source. The system provides low image distortion transmission over long distance. The system is integrated with control system. Each screen monitor equip with a digital camera. These screen monitors are used for beam profile measurement and help injection condition optimization. Wider dynamic range and highly flexibility of the digital gated camera provide various functional enhancements. System configuration and present status will be summary in this report.

## INTRODUCTION

Using a fully digital camera has two major advantages over analog CCD camera. First, the A/D conversion is performed closer to the CCD/CMOS sensor, keeping the amount of electronic noise to a minimum degree. Once the digitized signal is immune to noise, we can implement long haul (10 m ~ 10<sup>3</sup> m) applications in accelerator researching field. Various long hops solution is supported by the IEEE1394A/B interface. Noise immunity and isolation provided by this solution must be welcome in the accelerator environment. Second, unlike analog camera systems, digital systems do not suffer from pixel jitter. Each captured pixel value corresponds to a well-defined pixel on the CCD/CMOS chip. The IEEE1394 interface is a hot swappable and self-configuring, high performance serial bus interface that is capable of 400 Mbit/sec data transmission and will be enhanced to 3.2 Gbit/s for next generation products. The interface support asynchronous (guaranteed delivery) and isochronous (guaranteed bandwidth and latency) data transfers. By using digital IEEE1394 camera system [1,2], we are able to eliminate the frame-grabber stage of processing and directly transfer data at maximum rates of 400 MB/sec. IEEE1394 general purposed CMOS cameras (Prosilica CV640, 659 x 494 by 4.65 μm square pixels) [1] were chosen for screen monitor application. Progressive scan interline CCD camera (Q-Imaging QICAM, 1392 x 1040 4.65 μm square pixels) [2] are used for synchrotron radiation monitor with 12-bit digital output. There is no frame grabber or additional power supply required. Frame rates of up to 100 fps can be achieved with adequate binning and ROI selection.. Intensify gated CCD camera are also used for low light applications.

Imaging applications in the accelerator community are most often utilized to measure beam profile and interference fringes. The beam profile may convert form fluorescence, various optical diagnostics [3]. Usually,

fluorescence screen/OTR and synchrotron light source radiation monitor is used to measure size of beam profile in order for performance optimization, routine operation, and various beam physics studies in the accelerator. This tool has been useful for characterizing properties of electron beam analysis. For example, the beam emittance is calculated from the measured beam size.

## SYSTEM STRUCTURE

There are about fifteen IEEE-1394 cameras [4] were installed for the screen monitor of the transport line and storage ring. All of these cameras are distributed in a large area beyond copper wire can cover, three to four near-by cameras are grouped and connected to central hub by IEEE-1394B fiber link for long distance transmission. To simply cabling, multiple nearby cameras are cascading together. Only one camera is active in the cascading chain, transmission bandwidth is shared by all cameras in cascading when system is initializing. All screen monitor are controlled by one computer. Since only one camera is used, the main bus bandwidth in used by only camera. Synchrotron radiation monitor for the booster synchrotron and storage ring are stand alone station to acquire image and to do analysis.

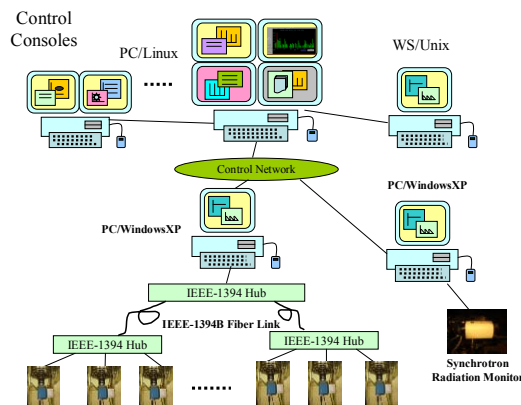


Figure 1: Topology of the IEEE-1394 camera installation.

The copper cable is suffered for longer distance transmission especially near the pulse magnet power supplies. Data stream is deteriorated sharply by the operation of pulse magnets for the cameras nearby. The camera may hang and need power reset to assume its operation occasionally. After this problem was identified, the topology of the camera array has been changed slightly to ensure the reliable operation of the whole system. Camera radiation damage is similar with analog

# RESONANT STRIP LINE BPM FOR ULTRA LOW CURRENT MEASUREMENTS

M. Dehler,

Paul Scherrer Institut, CH-5232 Villigen PSI, Switzerland

e-mail: Micha.Dehler@psi.ch

## Abstract

Proton beams used in proton therapy facilities like PROSCAN have extremely small currents of an order of nanoamperes, which create a challenge for a precise beam position measurements due to their extremely low signal level and subsequent bad signal per noise ratios. For suitable power levels with these currents, pickups need to have a high shunt impedance, something, which is difficult to design for wide band devices. So for a new strip line BPM design, the coupling of the signal outputs to the electrode was deliberately mismatched to create a resonance at the second harmonic of the RF frequency at 145 MHz. The optimum Q-factor to use is given by the coupling between the BPM electrodes leading to a Q of 50, an overall shunt impedance of 2.9 kOhms and power output levels of an order of -120 dBm at the design current of 1 nA. A prototype of the device has been manufactured, first measurement results will be presented.

## INTRODUCTION

The PROSCAN project at PSI aims at the development and construction of a dedicated facility for proton therapy. It consists of a supra conducting 250 MeV cyclotron built by ACCEL Instruments GmbH and will allow the treatment of interior tumors with protons [1].

Due to the extremely small beam currents, the conventional measurement of position and beam profile using ionization chambers must be performed outside vacuum, which limits its application [2]. Furthermore the measurement always introduces some degradation of the beam due to its intrusive character. To overcome these restrictions, it was decided to adapt the design of the strip lines in the SLS transfer lines, which have increased signal levels due to a non conventional resonant layout and so are more suitable for low current measurements. Adding a low noise RF front end and a sophisticated digital receiver should allow a performance suitable for PROSCAN.

With bunch trains in the order of seconds, the signal to be measured is essentially mono frequent and the bandwidth of the system can be chosen at convenience. The design current is 1 nA, for minimum interference and crosstalk a center frequency twice of the RF frequency of 72.7 MHz was defined. A further requirement was to have 100 mm clear space for the beam.

## BASIC DESIGN CONSIDERATION

The central figure of merit in a beam position device is the obtainable signal to noise ration. With the position de-

pendent difference part of the signal  $\Delta$  and the independent sum part  $\Sigma$ , the beam offset computed from these signals can be written as

$$x = C \frac{\Delta}{\Sigma}, \quad (1)$$

where  $C$  is the inverse device sensitivity. Linearizing the equation with respect to the sum gives

$$x \approx C \left( \frac{\Delta}{\Sigma_0} - \frac{\Delta}{\Sigma_0^2} \delta \Sigma \right),$$

so that one can get the statistical variance of the position reading as

$$\sigma_x^2 = C^2 \frac{\sigma_\Delta^2}{\Sigma_0^2} \left( 1 + \frac{\sigma_\Sigma^2}{\Sigma_0^2} \right) \quad (2)$$

With the sum signal noise  $\frac{\sigma_\Sigma}{\Sigma_0}$  typically being small, the optimum device has a high sensitivity (low factor  $C$ ), low noise in the difference signal (mostly determined by thermal noise) and high signal levels  $\Sigma_0$ .

One option for the BPM would be to use a pair of cavities as a BPM, one using a dipole resonance to procure the position dependent signal and monopole resonant cavity for the sum signal. The Q factors and so the bandwidth could be optimally adapted to the beam spectrum. The problem with this would have been the relatively high temperature variations in the measurement location, which would have led to frequency drifts and subsequent accuracy problems. So it was decided to go for a strip line design, which has been designed in a similar way already used for the transfer lines of the swiss light source (SLS).

A conventional strip line design, as shown in the upper part of figure 1, consisting of strip line shorted on one side and perfectly matched to the output coupler, has a FIR pulse response consisting of two peaks giving a transfer impedance of

$$Z_T = \frac{U_{out}}{I_{beam}} = jZ_l e^{-j\omega\tau} \sin \omega\tau$$

with  $\tau = l/c$  as the electrical strip line length and  $Z_l$  the characteristic impedance of strip line and coupling. The first idea of changing the characteristics consists in introducing a deliberate mismatch by lowering the strip line impedance  $Z_s$  with respect of that of the coupler. The transfer impedance becomes

$$Z_T = Z_l \frac{1 + e^{-2j\omega\tau}}{1 + Z_l/Z_s + e^{-2j\omega\tau}(1 - Z_l/Z_s)}.$$

The method has two drawbacks, the first having to realize mechanically very low characteristic strip line impedances

# TURN-BY-TURN AND BUNCH-BY-BUNCH DIAGNOSTICS AT NSRRC

K. H. Hu, Jenny Chen, C. J. Wang, Y. T. Yang, Demi Lee, C. H. Kuo, K. T. Hsu

NSRRC, Hsinchu 30076, Taiwan

## Abstract

Turn-by-turn and bunch-by-bunch diagnostic systems were set up to support various studies. The beam oscillation signals were detected by transverse and longitudinal bunch signal detectors, and were digitized by a transient digitizer or oscilloscope. The signal data thus obtained were analyzed to extract information concerning the bunch oscillation on a turn-by-turn and bunch-by-bunch basis. The analytical results of this study are summarized herein.

## INTRODUCTION

Turn-by-turn and bunch-by-bunch store beam parameters are useful in many studies [1]. Parameters which can be extracted for the data include the filling pattern, multi-bunch oscillation modes, ion instability, pseudospectrum growth and instability damping time. In this study, a system with this capability was setup up for measurement and analysis. Similar system have been set up and proved useful in many accelerator institutes. We set up the system accompany with the development of multi-bunch feedback system. Current effort is to improve the system to support study beam stabilities improvement.

## SYSTEM DESCRIPTION

The turn-by-turn and bunch-by-bunch diagnostics are based upon transient digitizers. Time domain diagnostic tools with transient capability are useful for studying the multi-bunch instability and turning of a multi-bunch feedback system. A transient digitizer and feedback electronics are applied to record the bunch-by-bunch and turn-by-turn beam signal as shown in Fig.1. The digitizer acquires data from a transverse bunch oscillation detector and a longitudinal bunch phase detector [2]. The CompuScope 82G digitizer [3] was specified for this study because it provides a friendly application development environment (SDK for LabVIEW and MATLAB). Simple MATLAB scripts were applied to access transient digitizer hardware to enable capture data. These scripts were designed to be easily integrated with analytical scripts. The system supports transient domain data capture. A trigger signal and a feedback switch was used to capture the transient signal for 30 msec for all bunches without decimation.

Intensity gated CCD cameras with an IEEE-1394 interface were also set up to observe the oscillation of bunches. Single turn observation was performed to observe longitudinal stability of the stored beam. The cameras support triggering by revolution clock, adjustable exposure time and multiple exposure are supported.

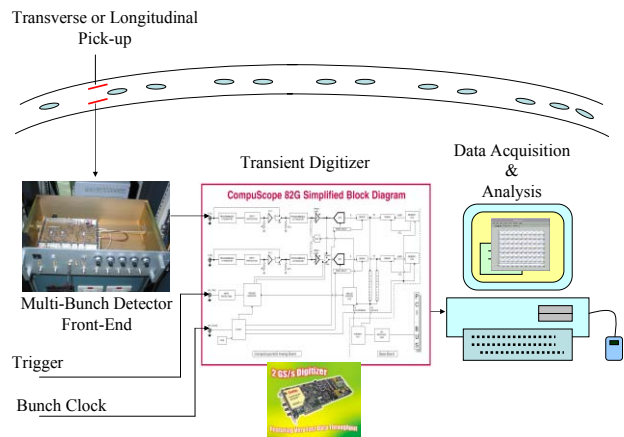


Figure 1: Transient signal capture system.

## TIME DOMAIN DIAGNOSTIC

The acquired data can be arranged according to bucket address and bunch ID to reconstruct the individual bunch oscillation. Fig. 2 illustrates the captured data. The oscillation of each bunch is illustrated in Fig. 3. This study aims to use the proposed system to measure growth time and damping accompany with the multi-bunch feedback system.

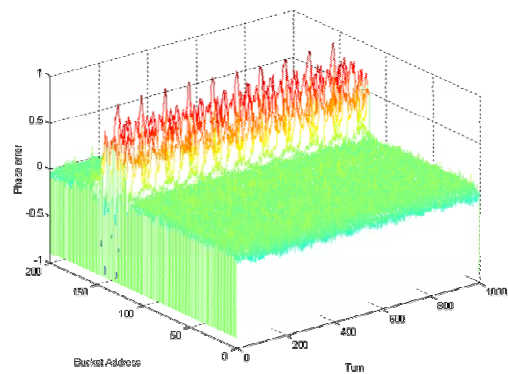


Figure 2: Turn-by-turn and bunch-by-bunch signal captured.

# BPM SYSTEM AND ITS DEVELOPMENT FOR THE STORAGE RING OF NSRRC

Jenny Chen, K. H. Hu, Y. T. Yang, C. J. Wang, C. H. Kuo, Demi Lee, K. T. Hsu

NSRRC, Hsinchu 30076, Taiwan

## Abstract

About 60 BPMs were installed in the storage ring of an NSSRC. High precision closed orbits were measured by Bergoz's MX-BPMs. Data were acquired by multi-channel 16-bit ADC modules. The orbit data was sampled every millisecond. Fast orbit data were shared by reflective memory network to support fast orbit feedback. The Averaged data were updated to control database at a rate of 10 Hz. Turn-by-turn beam position signals were processed by several Bergoz's log-ratio BPMs and recorded by a transient digitizer to support various beam physics study. Digital BPMs were installed at the storage ring to improve the BPM system functionality at the storage ring, supporting routine operation and study of beam physics. A preliminary test of Instrumentation Technologies' Libera digital BPM is ongoing. The system structure, software environment and performance of the BPM system are summarized in this report.

## INRODUCTION

The storage ring of an NSRRC is a 1.5 GeV synchrotron light source. Orbit stability and multi-bunch stability are both very important for user service. The storage ring consists of six super-period triple-bent achromatic lattices. Multi-bunch instability was eliminated using the SRF cavity and multibunch feedback systems. Eight BPMs one wiggler, two conventional undulators (U5 and U9), one elliptical polarised undulator (EPU5.6), one superconducting wavelength shifter and one superconducting multi-pole wiggler were installed in each section. Extra BPMs were installed at the upstream and downstream the insertion devices to guarantee micro-level stability, except thermal, water flow measure. A BPM and orbit feedback system is essential to guarantee good orbit performance, especially when operating the undulator gap change and the EPU phase during an experimental scenario.

## MULTIPLEXING BPM SYSTEM

A total of 58 button-type BPMs were installed. The orbit signal was process with Bergoz's MX-BPM [1]. The measured performance was around one micron for a 10 Hz orbit update rate. All MX-BPMs were synchronized externally with a common clock source to avoid the alias effect resulting from synchrotron sideband. To achieve  $\mu\text{m}$  level stability, the ambient environment of the BPM electronics was also monitored. The control system interface of the MX-BPM system and its relationship with corrector control and orbit feedback is illustrated in Fig.

1. The BPM server VME crate acquired orbit data every 1 msec. These fast orbit data were shared with an orbit feedback VME crate and a corrector control VME crate with a dedicated reflective memory network. The average slow orbit was updated to control the database every 100 msec. The orbit feedback node read the fast orbit data and compared them with the reference orbit data to execute the control rule, locking the orbit into in-loop BPMs. A typical orbit in a user shift is illustrated in Fig. 2. The beam position can be maintained at the  $\mu\text{m}$  level by an orbit feedback system even when undulator parameters are changed.

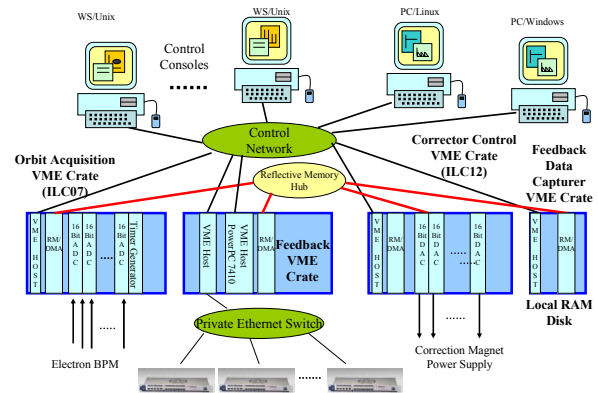


Figure 1: Software environment for BPM data access.

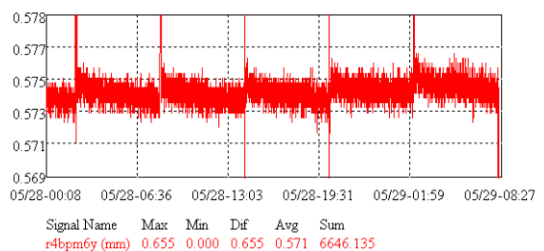


Figure 2: Typical long term beam position measured by in-loop MX-BPM, root mean square is less than 1  $\mu\text{m}$  by the help of orbit feedback loop.

## LOG-RATIO BPM

To measure the turn-by-turn beam position, several Bergoz's log-ratio BPM processors [1] were installed at the storage ring accompany with a digitizer to capture the turn-by-turn beam position data. The digitizer was clocked by the machine revolution clock, and triggered by the timing system to synchronize with the external excitation source. The system support mechanism has

# DIAGNOSTICS FOR THE 1.5 GeV TRANSPORT LINE AT THE NSRRC

K. H. Hu, Jenny Chen, C. J. Wang, Demi Lee, C. H. Kuo, Y. T. Yang, K. T. Hsu

NSRRC, Hsinchu 30076, Taiwan

## Abstract

Electron beams at 1.5 GeV were extracted from a booster synchrotron and transported via a transport line and injected into a storage ring. This booster-to-storage ring transport line was equipped with stripline beam position monitors, integrated current transformers, fast current transformer and screen monitors. Commercial log-ratio BPM electronics were adopted to process the 500MHz bunch signal directly. The position of the passing beam was digitized by VME analog interface. An integrated current transformer was applied to measure the transmission efficiency. Screen monitors were used to support routine operation. This study summarizes the system architecture, software tools and performance of the BTS diagnostic system.

## INTRODUCTION

A 1.5 GeV electron beam was extracted from a booster synchrotron and transported via a 70 m long transport line before being injected into a storage ring. Various diagnostic devices were installed along the transport line, as illustrated in Fig. 1. These devices included seven stripline type beam positions monitors, three integrated current transformers (ICT) [1], a fast current transformer (FCT) [1] and seven screen monitors. Commercial log-ratio beam position monitor (LR-BPM) electronics [1] were adopted to process the 500MHz bunch signal directly. The passing beam position was digitized by VME analog interface. The transmission efficiency was measured by an integrated current transformer. Screen monitors were applied to support routine operation. Several test screen monitors equipped with a short decay time, a YAG:Ce scintillator and an optical transition monitor with an aluminium file were also installed for various R&D tests.

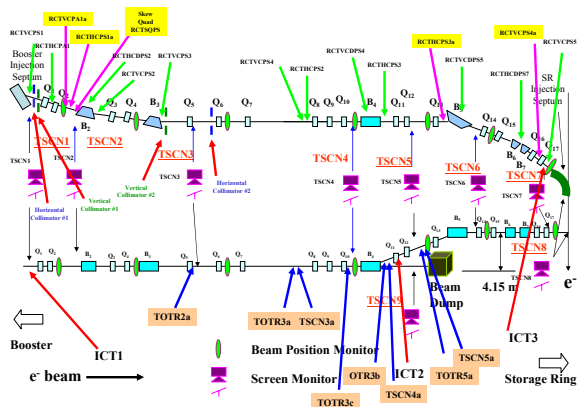


Figure 1: Transport line diagnostic devices layout

## BEAM POSITION MONITOR

Seven stripline type BPMs were installed in the transport line to measure the beam trajectory, as shown in Fig. 2. The stripline was mounted on the circular vacuum chamber with a 63 mm inner diameter. The stripline was 10 mm wide and 150 mm long. The beam intercept angle was around 10°. Each BPM had a sensitivity was about 1 dB/mm near the beam pipe centre.



Figure 2: Stripline type beam position monitor

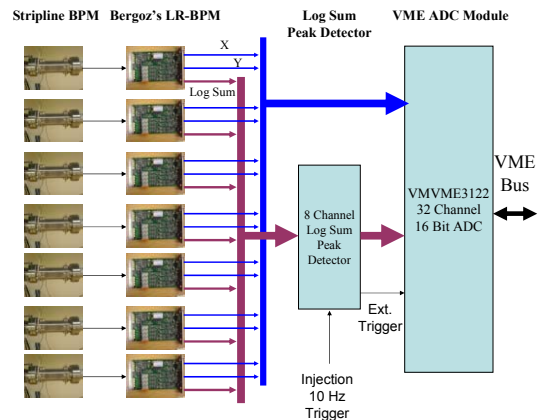


Figure 3: Data Acquisition System for the BTS LR-BPM

Log-ratio BPM electronics were used to measure the beam position in the BTS of the NSRRC [2]. The log ratio processor was a two-channel device. This module consisted of a low-pass filter, a band-pass filter, a log-ratio amplifier and sample & hold (S&H) circuits. The S&H circuits were a timing control circuit, and a position and an intensity signal processing circuit. The transport line beam position data acquisition system, with a 32-channel, 16-bit VME ADC module acquired data from seven LR-BPMs, is illustrated in Fig. 3. The S/H position data are held on the on the LR-BPM module, and a log

# TOWARDS A ROBUST PHASE LOCKED LOOP TUNE FEEDBACK SYSTEM

Rhodri Jones, CERN, Geneva, Switzerland

Peter Cameron, Yun Luo, Brookhaven National Laboratory, Upton, NY 11973, USA

## Abstract

Attempts to introduce a reliable tune feedback loop at RHIC (BNL) [1] have been thwarted by two main problems, namely transition crossing and betatron coupling. The problem of transition crossing is a dynamic range problem, resulting from the increase in the revolution content of the observed signal as the bunch length becomes short and from the fast orbit changes that occur during transition. The dynamic range issue is being addressed by the development of a baseband tune measurement system [2] as part of the US LHC Accelerator Research Program (US-LARP). This paper will focus on the second problem, showing how a phase locked loop (PLL) tune measurement system can be used to continuously measure global betatron coupling, and in so doing allow for robust tune measurement and feedback in the presence of coupling.

## INTRODUCTION

There are two main difficulties associated with utilizing a PLL tune measurement and feedback system in the presence of coupling. The first arises from the fact that in a coupled machine the excitation from one plane shows up in the other. A PLL therefore has the possibility to become confused regarding which signal is associated with a given measurement plane, which causes problems for both PLL measurement and tune feedback.

The second difficulty arises when a tune feedback system tries to maintain the tunes at their 'set' tune values in the presence of coupling. When the coupling amplitude becomes larger than the difference in the unperturbed tunes (the value of the tunes for a completely decoupled machine), then no amount of quadrupole adjustment can diminish this minimum tune split and restore the tunes to their desired 'set' values. This again leads to a breakdown in the tune feedback loop.

As these obstacles to tune measurement and feedback became evident at RHIC, the need for improved coupling measurement became clear, and the PLL was re-configured to permit measurement of the projections of both eigenmodes in both planes. The excellent quality of the data obtained by this method motivated the development of a proper formalism [3, 4] for its interpretation.

## MEASUREMENT OF COUPLING PARAMETERS USING A PLL TUNE TRACKER

This section will discuss the use of a phase locked loop tune tracker to measure the betatron coupling amplitude and phase.

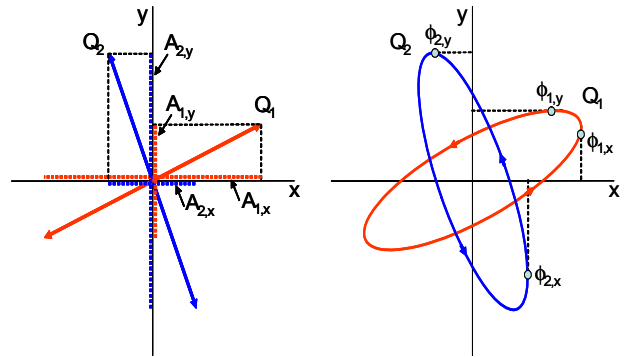


Figure 1: Schematics showing the two eigenmodes rotated with respect to the horizontal and vertical planes due to coupling.

## Equations of Interest

For a linearly coupled circular accelerator the observed displacement on turn  $n$  in the horizontal ( $x$ ) and vertical ( $y$ ) planes are a combination of the projections of two eigenmodes (see e.g. [3]). This is illustrated in Fig. 1 and can be expressed as

$$\begin{cases} x(n) = A_{1,x} \cos(2\pi Q_1 n + \phi_{1,x}) + A_{2,x} \cos(2\pi Q_2 n + \phi_{2,x}) \\ y(n) = A_{1,y} \cos(2\pi Q_1 n + \phi_{1,y}) + A_{2,y} \cos(2\pi Q_2 n + \phi_{2,y}) \end{cases} \quad (1)$$

The eigenmode frequency of Mode 1 is denoted by  $Q_1$ , while  $A_{1,x}$  and  $A_{1,y}$  represent the amplitudes of this mode in the horizontal and vertical plane respectively. Similarly  $\phi_{1,x}$  and  $\phi_{1,y}$  represent the phases of this mode in the horizontal and vertical plane respectively. The same notation applies for Mode 2.

Using Hamiltonian perturbation theory in the absence of intentionally strong local couplers, it is possible to define the following relationships [3]

$$\begin{cases} r_1 = \frac{A_{1,y}}{A_{1,x}} = \sqrt{\frac{\beta_y}{\beta_x}} \cdot \frac{|C^-|}{2\nu + \Delta} \\ r_2 = \frac{A_{2,y}}{A_{2,x}} = \sqrt{\frac{\beta_y}{\beta_x}} \cdot \frac{|C^-|}{2\nu + \Delta} \end{cases}, \begin{cases} \Delta\phi_1 = \phi_{1,y} - \phi_{1,x} = \chi \\ \Delta\phi_2 = \phi_{2,x} - \phi_{2,y} = \pm\pi - \chi \end{cases} \quad (2)$$

Here  $\Delta$  is the difference between the fractional part of the unperturbed tunes,  $\beta_{x,y}$  the beta functions at the

# BEAM LOSS POSITION MONITOR USING CERENKOV RADIATION IN OPTICAL FIBERS

W. Goettmann, F. Wulf, HMI, Berlin, Germany

M. Körfer\*, DESY, Hamburg, Germany

J. Kuhnenn, FhG-INT, Euskirchen, Germany

## Abstract

The VUV FEL in TESLA technology at DESY provides Giga-Watt output power in laser pulses. The SASE single pass Free Electron Laser (FEL) has been developed for high-brightness user applications. At the design parameters the average power of the electron beam is about 72 kW. To avoid vacuum breakdown and high radiation levels caused by electron losses a machine protection system is required. Collimators are installed upstream of the radiation sensitive undulators [1]. However, the proper operation of the collimator system needs to be measured with a beam loss monitor. Conventional radiation sensor systems are not suited for the VUV-FEL undulators, because of the restricted free space in the undulator gap. A Beam Loss Position Monitor (BLPM) based on Cerenkov light in optical fibers allows real time monitoring of loss location and loss intensity. Electrons with energies above 175 keV generate Cerenkov light during their penetration of the optical fiber. The fast response of the Cerenkov signal is detected with photomultipliers at the end of the irradiated fibers. The reconstruction of the particle loss trace in 3 space dimensions became possible with four sensors.

## INTRODUCTION

Since September 2004, the VUV-FEL has been in operation and will soon be used by synchrotron radiation users. The accelerator consists of an rf-laser gun, the acceleration modules, each containing eight 9-cell superconducting (SC) cavities, two bunch compressors, collimators and a 30 m long permanent magnet undulator section comprising six 4.5 m long undulator units. The final electron beam energy is 1.0 GeV. Dark current electrons caused by field emission from the normal conducting rf gun and generated in the first acceleration module are transported along the beamline. Electrons outside the phase space acceptance of the accelerator will be lost anywhere. Moreover, the electron bunches suffer unavoidable beam emittance growth from space charge effects in the gun and bunch compressors.

Lost electrons hit the vacuum chamber and create a shower of secondary particles. These showers penetrate an optical fiber and generate Cerenkov radiation. Using four parallel sensors radial to the vacuum pipe along the section of interest the electron loss traces can be determined in transversal and longitudinal direction. Thus

a Beam Loss Position Monitor BLPM is used at the VUV-FEL for online analysis of particle losses. During machine commissioning and routine operation the online optimisation of collimator efficiency and studies concerning electron losses are performed.

## CERENKOV RADIATION

Cerenkov radiation is emitted whenever charged particles pass through dielectric matter with a velocity exceeding the velocity of light in the medium (fiber). Cerenkov emission is immediately generated by recombination effects in the material. The response time is negligible compared to light propagation time in the fiber or rise time in photomultiplier electronics. The intensity of Cerenkov light increases inverse to the cube of the wavelength. Consequently, in the visible spectrum the blue colour dominates.

The propagation of Cerenkov light in the fiber depends on the particle shower geometry, particle and fiber properties. The shower angle with respect to the fiber axis and the shortest distance (Stoss-Parameter) between particle trajectory and the center of fiber cross-section are important for the coupling of Cerenkov light into the fiber. The modelling of Cerenkov-effects in fibers is documented in [2-5]. For electrons, the lowest energy for emitting Cerenkov light in pure quartz fibers ( $n=1.46$ ) is about 175 keV. The opening angle of Cerenkov radiation in the fiber scales with the energy of non-relativistic electrons. Above 6 MeV electron energy the light intensity is given only by the number of electrons hitting the fiber and their path length inside the material.

## BEAM LOSS POSITION MONITOR

Some publications about fibre optic radiation monitoring systems for accelerators based on the generation of Cerenkov light by relativistic charged particles appeared recently [6-9]. Using one fiber, a particle loss trace can be detected only within a small radial angle. Using four (or more) parallel fibers in equidistant radial space, similar to the arrangement of beam position monitor (BPM) sensors, the loss trace can be measured in transverse and longitudinal dimensions. The Cerenkov light is detected with photomultipliers (PMT's) at the end of the sensor fibers. The response of the PMT is monitored with a fast scope (ACQIRIS-Card). Measuring the time of light propagation in the fiber by

\* corresponding author: markus.koerfer@desy.de

# BEAM POSITION MONITOR AND KICKER FOR THE SPRING-8 TRANSVERSE BUNCH-BY-BUNCH FEEDBACK

T. Nakamura, JASRI/SPring-8, Mikazuki-cho, Hyogo, Japan

## Abstract

A high-resolution beam position monitor and a wideband kicker for the SPring-8 transverse bunch-by-bunch feedback system are developed. To avoid the increase of effective emittance by unwanted kicks by a feedback driven by noise, the monitor is designed to have high position resolution of the order of micro meters for single pass of 0.25nC bunch by adopting shorted stripline structure. Also a kicker for the feedback and the experience of those are described.

## INTRODUCTION

A transverse bunch-by-bunch feedback is in operation to suppress the instabilities in the SPring-8 storage ring. The parameters of the ring are shown in a Table 1. The vertical emittance is small and the beam size at the feedback is 9 $\mu$ m(rms). The allowable amplitude (rms) of the motion driven by the feedback should be less than 10% of that and is  $\sim 1 \mu$ m.

Table 1. Parameters of the SPring-8 Storage Ring

Energy	E	8 GeV
Average Current	I	100 mA
RF Frequency	f <sub>RF</sub>	508.58 MHz
Harmonics	h	2436
Bunch current at multi-bunch operation (2000 bunches)	I <sub>b</sub>	0.24 nC
Revolution Period	T <sub>0</sub>	4.8 $\mu$ s
Emittance / Coupling	$\epsilon / \kappa$	6.6 nm / 0.2 %
Beta function <sup>†</sup>	$\beta_H / \beta_V$	25 m / 6 m
Beam size <sup>†</sup>	$\sigma_H / \sigma_V$	400 $\mu$ m / 9 $\mu$ m
Beam Pipe Radius (elliptic shape)	r <sub>H</sub> / r <sub>V</sub>	45 mm / 20 mm
Transverse Radiation Damping Time	$\tau_\beta$	8.3 ms
Feedback Damping Time	$\tau_{FB}$	$\sim 1$ ms

<sup>†</sup> : Values at BPMs and kickers for feedback

## REQUIREMENT FOR BPM

### Effective Emittance Degradation by Noise

The analysis of the effect of the random error/noise in measured beam position signal on the beam quality is performed. This shows that the random error drives a feedback and kicks a beam and increases the effective emittance with the relation as

$$\sigma_x = \sqrt{\epsilon\beta} = \sqrt{\frac{T_0\tau}{\tau_{FB}}} \sigma \quad (1)$$

where,  $T_0$  is a revolution period and  $\tau$  and  $\tau_{FB}$  are a total damping time with feedback and other effects and a damping time only with feedback, and  $\sigma$  is the rms position resolution of a BPM. This relation shows that the increase of the effective emittance is larger for larger ring and faster feedback damping. And the bunch charge of the ring at multi-bunch operation is smaller than the other rings and the vertical size of beam pipe also larger, the requirement on the resolution of BPM is more severe.

### Position Resolution

The relation in Eq.1 is  $\sigma_x = 0.07 \sigma$  for the SPring-8 feedback of which damping time is 1ms. The vertical beam size (rms) is 9 $\mu$ m, hence, the requirement for the vertical position resolution of the BPM is 13  $\mu$ m for one pass of 0.24 nC bunch if the allowable degradation of the beam size is less than 10%.

From the result of the button type BPMs for C.O.D. measurement[2], shows that the resolution of the button type BPM is one order smaller than requirement.

### Carrier Frequency

For the ease of the handling, the RF acceleration frequency, 508.58MHz, is chosen as the carrier frequency. A 933MHz Bessel type low pass filter is inserted to the signal from the monitor to reject unnecessary higher frequency signals.

## POSITION MONITOR

To fulfill the requirement, we developed a new monitor for the feedback. The design of the monitor is performed with MAFIA.

### Shape

A shorted stripline type monitor is adopted to obtain higher voltage signal to fulfill the requirements described in previous section. The shape of the BPM is shown in Fig. 1, 2 and 3.

Its advantages over button type BPMs are

- (1) compact : It is difficult to make large button type BPM because of its complicated structure.
- (2) easy to fit to elliptical shape of the beam pipe of the ring.

Disadvantage over stripline type is that its impedance seen from ports is zero by shorted structure, while the impedance of stripline is matched to cables. This makes a unwanted signal to feedback.

### Independent in Horizontal and Vertical

To make RF signal processing stage simple, a pair of stripline electrodes are placed horizontally and vertically

# LOW ENERGY HIGH BRILLIANCE BEAM CHARACTERIZATION

J. Bähr, DESY, Zeuthen, Germany

## Abstract

Low energy high brilliance beam characterization plays an important role for electron sources and injectors of Free Electron Lasers (FELs) and electron linear accelerators as for example the future ILC project. The topic is discussed basing on solutions of the PITZ facility (Photo Injector Test facility Zeuthen) which are compared with methods applied at other facilities. The properties of an electron beam produced at a laser driven rf-gun is mainly influenced by characteristics of the laser beam and the electron gun itself. Therefore aspects of diagnostics will be discussed for the laser, laser beam line and gun as well. The main properties of the electron beam are transverse and longitudinal phase space and emitted charge. Measurement of transverse beam size and position, transverse emittance, charge and longitudinal phase space will be discussed in detail. At PITZ the measurement of the longitudinal phase space is based on a correlated measurement of the momentum spectrum and the temporal characteristics of the electron bunch.

## INTRODUCTION

Low energy high brilliance beam characterization will be discussed at the example of PITZ (Photo Injector Test facility Zeuthen) [1] at DESY. PITZ is a dedicated facility for the optimization of electron sources for FELs. The energy range of PITZ1 (until fall 2004) was 4.5 MeV, the energy range of PITZ2 [2] just under commissioning will increase to 30 MeV in 2005-2006. The nominal bunch charge is 1 nC. The discussion of the characterization will cover mainly the transversal phase space, the longitudinal phase space and charge as well. Further diagnostics topics as the characterization of processes at the cathode and in the electron gun, the relative phase between laser and rf and properties of the photocathode laser beam will be discussed shortly as well. Further examples of

diagnostics of other facilities will be discussed in the momentum range up to 130 MeV/c. The production and characterization of polarized beams is not matter of this paper.

## PITZ

The sketch of the beam line of PITZ1 is shown in fig.1. The facility consisted of three sections: the cathode section, the gun section and the diagnostics section. PITZ1 was dismantled in the beginning of 2005. The upgrade, PITZ2, is under commissioning now and will be completed in several steps until end of 2006. Fig. 2 shows schematic of the beam line of PITZ2.

The electron source of PITZ is a normal conducting 1.5 cell laser-driven rf-cavity. The rf-frequency is 1.3 GHz. The active cover of the photo cathode is Cesium Telluride. Main topics of the upgrade for PITZ2, are the use of a booster cavity to demonstrate the emittance conservation principle [3] and the increase of the field gradient in the gun to improve the electron emittance from the beginning. The diagnostics beam line will be essentially extended.

## TRANSVERSE PHASE SPACE

### Beam Size and Beam Position

The characterization of beam position and beam size is a standard task at every particle accelerator. There are invasive and non-invasive devices in use:

- Fluorescence screens (e.g. YAG)
- Optical Transition Radiation (OTR) screens
- Beam position monitors (BPM)
- Wire scanners

The YAG (Yttrium-Aluminium garnet) transforms part of the beam energy in visible light. This light is usually imaged on the sensor of a TV-camera. Two kinds of YAG

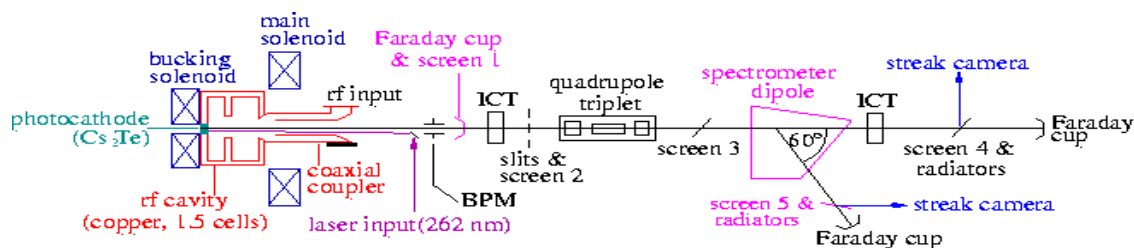


Figure 1: Schematic of PITZ 1.

# HIGH SENSITIVITY TUNE MEASUREMENT BY DIRECT DIODE DETECTION

M. Gasior, R. Jones, CERN, Geneva, Switzerland

## Abstract

The fractional part of the betatron tune for a circular accelerator can be measured by observing beam oscillations on a position pick-up. In frequency domain the betatron frequency is seen as sidebands on either side of the revolution harmonics. Usually beam signal pulses from the pick-up are very short with respect to the revolution period, resulting in a broadband spectrum. Classical tune measurement systems filter out just one of the betatron sidebands. As a consequence, most of the betatron energy is lost and only a very small fraction remains for further processing. This paper describes a new method, referred to as Direct Diode Detection (3D). It is based on the idea of time stretching beam pulses from the pick-up in order to increase the betatron frequency content in the baseband. The 3D method was recently tested in the CERN SPS and PS, BNL RHIC and FNAL Tevatron machines. Results from all these machines [1, 2, 3, 4] show that this method can increase the betatron signal level by orders of magnitude as compared to classical systems, making it possible to observe tunes with no explicit excitation. Frequency resolution in the order of  $10^{-5}$  and amplitude sensitivity in the order of 10 nm has been achieved with this very simple hardware.

## 3D PRINCIPLE AND THE HARDWARE

The crucial part of a 3D-based tune measurement system is the peak detector. Two such detectors connected to opposing electrodes of a beam position pick-up (PU) (see Fig. 1) yield the amplitude modulation envelope of the beam signals. Such signals, depicted in Fig. 2, are superimposed on a DC voltage related to the bunch amplitude (revolution frequency content). The signal difference, shown in Fig. 3 for single bunch in the machine, contains almost the whole bunch modulation amplitude, with a DC component related to the beam offset from the centre of the pick-up. Since the DC content can be easily suppressed by series capacitors, most of the corresponding revolution frequency ( $f_r$ ) background can be removed by the peak detectors before the first amplifying stage. In Fig. 4 the  $f_r$  attenuation characteristic is shown assuming single bunch in the machine, which is the most difficult case to deal with. For a detector time constant  $\tau = R_f C_f$ , which is larger than the machine revolution period  $T = 1/f_r$ , the suppression of the revolution line goes as  $4\tau/T$  [1]. This makes it possible to obtain  $f_r$  attenuation in the order of 50 dB for  $\tau \approx 100$ , which is easily achievable in practice.

The 3D circuit in Fig. 1 can be also understood as two sample-and-hold blocks, sampling bunch signals close to their maxima at the bunch repetition rate, downmixing the wideband bunch spectrum into the baseband.

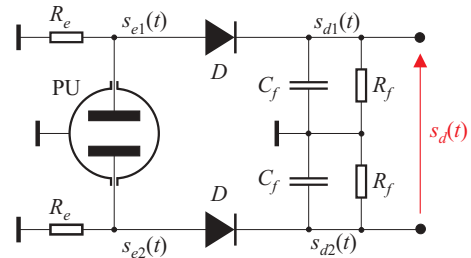


Figure 1: Direct Diode Detection principle.

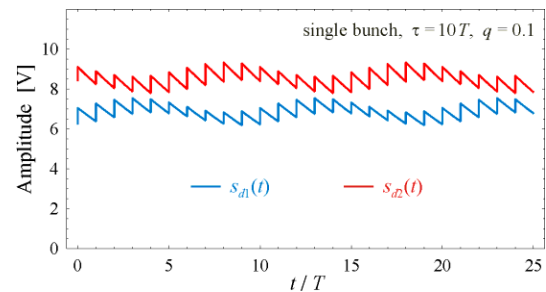


Figure 2: An example of peak detector voltages.

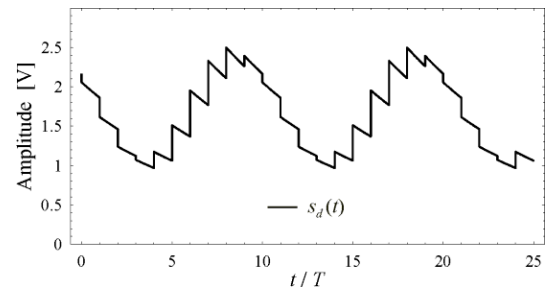


Figure 3: Difference of the signals in Fig. 2.

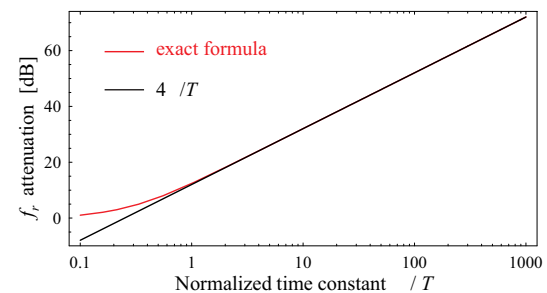


Figure 4: 3D circuitry revolution frequency attenuation.

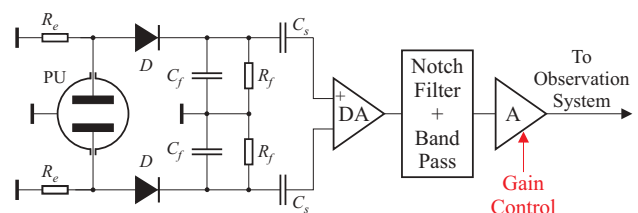


Figure 5: Block diagram of a 3D-BBQ system.

# RADIATION TESTS ON SOLID STATE CAMERAS FOR INSTRUMENTATION

S. Hutchins, M. Facchini, E. Tsoulou, CERN, Geneva, Switzerland

## Abstract

Technological advances in solid state camera design have provided a wider choice of equipment for beam diagnostics, but following simulations of the expected radiation environment in the LHC knowledge of their radiation tolerance was required. Several cameras have been progressively exposed to a 60MeV proton beam and their performance degradation monitored. Following these results, further simulations have been carried out on the level of shielding needed to ensure satisfactory operation in the LHC.

## OBJECTIVES

Previous experience with CCD based cameras has shown that the performance degrades with as little as 10Gy, which limits the areas in which they can be used and imposes the use of local radiation shielding[1]. It will be very difficult to provide shielding in the LHC, given the high energy of the secondary particles, which are generated by the interaction of the beam with residual gas in the vacuum chamber.

## Resolution and Contrast

In order to get quantifiable data on the degradation of the sensors a simplified testing method was used. Rather than using resolution test targets to establish the Contrast Transfer Functions [2] at each radiation test point, a checker-board pattern was used as the target.

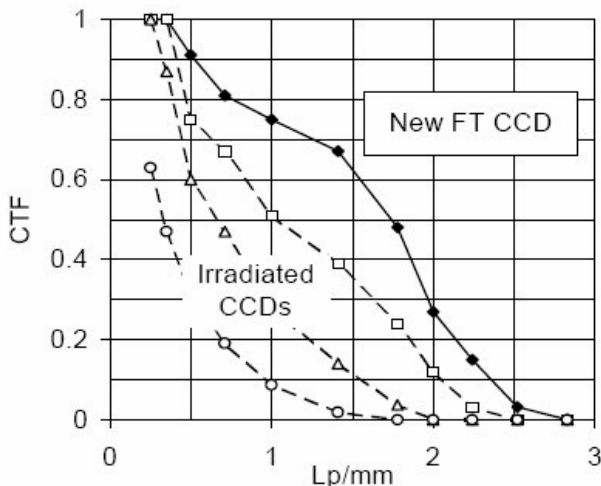


Figure 1: Contrast Transfer Function

It is assumed that the main effect of radiation damage is the loss of contrast, so that by ensuring that each square would correspond to many pixels on the sensor, problems of single pixel damage, optical resolution and speckle

would be avoided. Sensors having different pixel sizes can be tested with the same equipment, each pixel in the stored bitmap image would be analyzed and a histogram produced for each radiation level, to show the loss of contrast due to radiation effects. The cameras were also to be tested under operational conditions so that Single Event Upsets (SEU's) could be noted and the risk of damage due to the devices being powered was of interest.

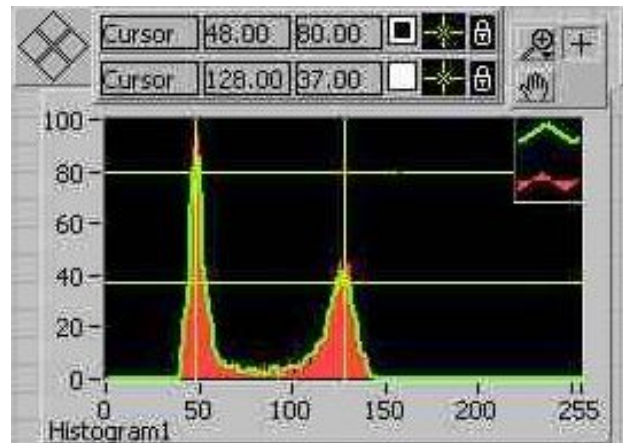


Figure 2: Histogram of pixel brightness for an area of the checkerboard pattern

## Radiation Damage

Any semiconductor device operating in a radiation field can undergo degradation due to radiation damage effects. Energetic particles incident on the semiconductor bulk lose their energy to ionising and non-ionising processes as they travel through a given material. The ionising processes involve electron-hole pair production and subsequent energy deposition (dose) effects. The non-ionising processes result mainly in displacement damage effects, i.e. displaced atoms in the detector bulk and hence defects in the semiconductor lattice like vacancies and interstitials.

The solid state arrays use a structure of metal-dielectric-semiconductor that makes them sensitive to ionising radiation due to energy deposition in the gate dielectric and displacement damage in the semiconductor substrate.

Ionization effects refer to the transient effects due to energy deposition in the gate dielectric and silicon bulk. The gate dielectric in the CCD imagers is usually a silicon oxide. 3.6 eV for the silicon and 17-18 eV for the silicon oxide are needed in order to create an electron-hole pair. Electron-hole pairs are created all along the charged particle track, which may be trapped in the silicon oxide or the silicon oxide/silicon interface, swept away by the applied electric field or recombine. The processes taking place are quite fast (in the picosecond range) and depend